ELUCIDATING THE MECHANISM OF PROTEIN AGGREGATION AND CONFORMATIONAL STABILITY OF SOME PROTEINS

THESIS

SUBMITTED FOR THE AWARD OF THE DEGREE OF

Doctor of Philosophy

IN

BIOTECHNOLOGY

BY

JAVED MASOOD KHAN

INTERDISCIPLINARY BIOTECHNOLOGY UNIT
ALIGARH MUSLIM UNIVERSITY
ALIGARH - 202002, (INDIA)

2013

INTERDISCIPLINARY BIOTECHNOLOGY UNIT
ALIGARH MUSLIM UNIVERSITY, ALIGARH-202 002 (INDIA)
Phone : 0091-571-272388
Fax: 0091-571-2721776
E-mail: alg_btisamua@sanchamet.in

Certificate

This is to certify that the thesis reported herein entitled **"ELUCIDATING THE MECHANISM OF PROTEIN AGGREGATION AND CONFORMATIONAL STABILITY OF SOME PROTEINS"** has been carried out by **Mr. Javed Masood Khan** under my guidance and supervision. The work presented herein is suitable for the award of **Doctor of Philosophy** degree in **Biotechnology** of Aligarh Muslim University Aligarh.

16/4/13

Aligarh

Dr. Rizwan Hasan Khan
Supervisor

Declaration

I hereby declare that the thesis entitled "ELUCIDATING THE MECHANISM OF PROTEIN AGGREGATION AND CONFORMATIONAL STABILITY OF SOME PROTEINS" embodies the work carried out by me.

Javed Masood Khan
Senior Research Fellow of Council of Scientific and Industrial Research,
Interdisciplinary Biotechnology Unit,
Aligarh Muslim University,
Aligarh 202002 India

Dedicated

To

My Parents

&

Maternal Uncle

TABLE OF CONTENTS

Chapter 3

Hydrophobicity Alone can not Trigger Aggregation in Protonated Mamalian Serum Albumins

Chapter 4

Elucidating the Protective Effect of Sodium Dodecyl Sulphate on Serum Albumins Against Urea and Temperature at Low pH

Chapter 5

Monomeric Banana Lectin at Acidic pH Overrules Conformational Stability of Its Native Dimeric Form

ABSTRACT

Protein folding process is an extensively studied topic. Folding of proteins is vital for performing various biological functions. Therefore, understanding the mechanisms by which protein fold is an important issue in current proteomic era. These folded proteins are stabilized by various covalent and non-covalent interactions and can be denatured by denaturant, surfactant, change in pH and temperature. *In vivo* mis-folding of proteins occurs because of change in environmental conditions or due to mutations that lead to the exposure of hydrophobic residue and aggregation. These aggregates are deposited at various part of central nervous system and other organs hence causing development of human diseases including Alzheimer, Parkinson, Prion, Huntington and type II diabetes etc. In view of above in the first part of review we have focused on protein folding mechanisms, factors that affect the protein folding and stability under *in-vitro* and *in-vivo* conditions. The second part is devoted to protein aggregation mechanisms and detection of the aggregates and its morphology by using different dyes. The pros and cons of dyes are also discussed. Additionally, we have uncovered the mechanisms by which negatively charged surfactants and lipids induce amyloid fibril formation.

Chapter 1

Sodium dodecyl sulphate (SDS), an anionic surfactant that mimics some characteristics of biological membrane has also been found to induce aggregation in proteins. The present study was carried out on 25 diverse proteins using circular dichroism, fluorescence spectroscopy, dye binding assay and electron microscopy. It was found that an appropriate molar ratio of protein to SDS readily induced amyloid formation in all proteins at a pH below two units of their respective isoelectric points (pI) while no aggregation was observed at a pH above two units of pI. We also observed that electrostatic interactions play a leading role in the induction of amyloid. This study can be used to design or hypothesize a molecule or drug, which may counter act the factor responsible for amyloid formation.

Chapter 2

Different proteins have different amino acid sequences as well as conformations, and therefore different propensity to aggregate. Electrostatic interactions have an important role in the aggregation of proteins as revealed by our previous report (Khan et al. PLoS One 2012, 7, e29694). In this study, we designed and executed

experiments to know the role of charge variations on protein during the events of protein aggregation with lysozyme as a model protein. To impart positive and negative charge on protein we incubated lysozyme at different pH values, which were below and above the pI of lysozyme (~11). Negatively charged SDS were used to antagonize positive charges on the lysozyme at the respective pH values. We examined the effect of pH variations on SDS-induced amyloid fibril formation of lysozyme using method such as far-UV CD, Rayleigh scattering, turbidity measurements, dye binding assays and dynamic light scattering. We found that sub-micellar concentrations of SDS (0.1 to 0.6 mM) induced amyloid fibril formation of lysozyme in the pH range 10.0-1.0 and the maximum aggregation was found at pH 1.0. The morphology of aggregates was fibrillar in structure, as visualized by transmission electron microscopy. Isothermal titration calorimetry studies demonstrated that fibril formation is an exothermic reaction. To our current understanding on the mechanism of aggregation this study demonstrates the crucial role of electrostatic interactions during amyloid fibril formation. Conclusively, we propose the mechanistic model of protein aggregation through this study. The model proposed here will help in designing molecules that can prevent or reverse the amyloid fibril formation or the aggregation.

Chapter 3

Many proteins form amyloid fibril which is associated with several neurodegenerative diseases such as Alzheimer's, type II diabetes and dialysis-related amyloidosis. In this study different serum albumins were used at pH 3.5 below two units of pI (pH 5.5) to examine the role of negative charge and hydrophobicity in amyloid fibril formation. In this context three anionic surfactants viz SDS, SDBS and AOT were taken, bearing same negative head but different hydrophobic tail. The propensity of SDS, SDBS and AOT to form amyloid fibril were investigated by using turbidity, Rayleigh light scattering measurements, ThT and Congo Red dye binding assays, dynamic light scattering as well as by far-UV CD methods. At submicellar concentrations (0.5-2.5 mM) of SDS and SDBS amyloid fibril were formed in all albumin taken in this study while at higher concentration amyloid fibril formation was completely inhibited. Interestingly AOT promotes amyloid fibril formation up to 11 mM without any inhibition as SDS and SDBS does. The amyloid induced by SDS, SDBS and AOT have fibrilar morphology as confirmed by Congo Red, ThT and also visualized by

transmission electron microscopy. Albumins surfactant interaction was exothermic as confirmed by isothermal titration calorimetry (ITC). At lower concentrations of SDS and SDBS electrostatic interaction play the major role while at higher concentration only hydrophobic interaction were found effective. In case of AOT electrostatic interaction persists even at higher concentration of detergents. From the turbidity, Rayleigh light scattering and dynamic light scattering it was concluded that the order of amyloid induction was more in AOT followed by SDBS and least in SDS. Similar studies were performed at pH 7.4 approximately above two units of pI and no amyloid fibril were noticed it may be due to electrostatic repulsion. From this study we have concluded that the negatively charged surfactant induced amyloid fibril formation in serum albumins with the help of electrostatic and hydrophobic interaction. Beside this study performed pH above two units of pI confirmed that hydrophobic interaction alone can not induce aggregation in serum albumins.

Chapter 4

The effect of sodium dodecyl sulphate (SDS) on human, bovine, porcine, rabbit and sheep serum albumins were investigated at pH 3.5 by using various spectroscopic techniques like circular dichroism (CD), intrinsic fluorescence and dynamic light scattering. In the presence 4.0 mM SDS the secondary structure of all the albumins were not affected as measured by CD but fluorescence spectra reveled 8.0 nm blue shift in emission maxima.We further checked the stability of albumins in the absence and presence of 4.0 mM SDS by urea induced unfolding at pH 3.5. In the absence of SDS, urea unfolds secondary as well as tertiary structural elements of the albumins at very low concentrations (~2.0 M) but in the presence of 4.0 mM SDS urea was unable to unfold even up to 9.0 M. Thermal stability of albumins were also checked under similar condition. The albumins were very less stable at pH 3.5 with decrease in *Tm* values 54 °C to (HSA), 57 °C (BSA, PSA),59 °C (SSA) and 63 °C (RSA) but in the presence of 4.0 mM SDS, the *Tm* was increased to 74 °C (HSA), 75 °C (BSA), 70 °C (PSA, SSA) and 75 °C (RSA). From this study it was concluded that SDS is showing a protective effect against urea as well as thermal denaturation of albumins. This behavior may be due to electrostatic as well as the hydrophobic interaction of SDS with albumins. Further we have proposed the mechanism of action of urea. We have proposed that urea interacted with proteins directly when proteins are in charged

form. Indirect interaction may be taking place when the environment is more hydrophobic.

Chapter 5

Banana lectin (BL) is a homodimeric protein categorized among jacalin-related family of lectins. The effect of acidic pH was examined on conformational stability of BL by using circular dichroism, intrinsic fluorescence, 1-anilino-8-napthalene sulfonate (ANS) binding, size exclusion chromatography (SEC) and dynamic light scattering (DLS). During acid denaturation of BL, the monomerization of native dimeric protein was found at pH 2.0. The elution profile from SEC showed two different peaks (59.65 ml & 87.98 ml) at pH 2.0 while single peak (61.45 ml) at pH 7.4. The hydrodynamic radii (R_h) of native BL was 2.9 nm while at pH 2.0 two species were found with R_h of 1.7 and 3.7 nm. Furthermore at, pH 2.0 the secondary structures of BL remained unaltered while tertiary structure was significantly disrupted with the exposure of hydrophobic clusters confirming the existence of molten globule like state. The unfolding of BL with different subunit status was further evaluated by urea and temperature mediated denaturation to check their stability. As inferred from high C_m and ΔG values, the monomeric form of BL offers more resistance towards chemical denaturation than the native dimeric form. Besides, dimeric BL exhibited a Tm of 77 °C while no loss in secondary structures was observed in monomers even up to 95 °C. To the best of our knowledge, this is the first report on monomeric subunit of lectins showing more stability against denaturants than its native dimeric state.

Acknowledgments

Undoubtedly, no task can be accomplished without the blessing of Allah. Whatever I am today, it is all because of His blessing. It is not possible for me to write their gratefulness in words.

The success and final outcome of this thesis required lots of guidance and assistance from many people and I am extremely fortunate to have got this all along the completion of my thesis work. Whatever I have done is only due to such guidance and assistance and I would not forget to thank them.

First and foremost, I would like to express my sincere and profound gratitude to my mentor ***Dr. Rizwan Hasan Khan*** *for introducing me into the area of "protein aggregation, protein folding and stability" and offering his dexterous guidance. His scientific acumen strong determination, excellent knowledge and immense valuable ideas have been vital for me to take up this work. During our association of approximately five years, He always supported me with, his constructive criticism and words of encouragement. He always praised my abilities to make me feel comfortable. It's really proud to have mentor like him. I respect his vast knowledge, vision and advised for the subject which always reflected in this study. I have been lucky to work under his unique guidance that develops a sense of sincerity, tackle the harsh situation and self confidence. Sir, I am very much thankful to you from the bottom of heart, without your aboriginal guidance this journey would not have been possible. I wish take as an opportunity to thank Saba Aapa for his dua.*

I wish to acknowledge our former coordinator Prof. M Saleemudin Saheb and present coordinator Dr. Asadullah Khan Saheb for providing all the support, facilities and excellent environment during the course of study.

I wish take as an opportunity to thank all the faculty members of the Interdisciplinary Biotechnology Unit (IBU) particularly Dr. Hina Younus, Dr. Ejaj and Dr. Sehar Waris for their help whenever required. I also thank Dr. Parveen Salahuddin, Mr. Syed Faisal Maqbool, Mr. Lal Mohd. Khan, Mr. Aqtedar Husain,

Mr. Amir Ali, Mr. Ramesh Chandra, Mr. Islam Khan, Mr. Mohd. Nasir, Mr. Chandra Pal, Mr Mashkoor, Mr. Asharf, Mr. Rajendra and Mr. Rajesh for their help and cooperation whenever needed.

I would like to thank Dr. Samudrala Gourinath from School of Life Sciences, Jawaharlal Nehru University, New Delhi, India, for his valuable help for exposure of various techniques.

I am extremely grateful for the opportunity to have had Prof. Kabir-ud-Din as a collaborator. I would like to express my very great appreciation to Prof. Kabir-ud-Din for his valuable and constructive suggestions. I also wish to acknowledge for his esteemed guidance and constant encouragement throughout the study. I have learned so many things during this journey, thank you sir. A very special thanks to all the lab members of Prof. Kabir-ud-Din Shaeb lab they have supported me a lot.

How can I forget the Lab where I have spent approximately five years, the most precious time of my life which I have bestowed to the thesis.

In the electrifying environment of the lab, how this golden time passed away, I have not felt. It is my heartiest thanks to all my seniors who always enthuses me and supported me all the way. Thank you ***Priyankar Bhai and Sadaf Appa*** *for your valuable suggestion, help, encouragement and guidance in optimizing the protein folding, unfolding and protein aggregation and biophysical studies. My respect and thanks to one of my senior* ***Ejaz Bhai*** *for his great suggestion to join one of the esteemed lab of AMU and work with Dr. Rizwan Hasan Khan. I will never forget your contribution. I am extremely grateful for your brotherly affection, support and guidance. Thanks also extended to Ankita Didi, Dr. Aabgeena Aapa and Dr. Tashfeen Bhai for their help and support. Apart from seniors, I heartily acknowledge the help and cooperation which I received from my juniors. Words fail me to express my appreciation for their support and help in IBU thank you Sumit, Atiya, Iftekhar, Rehan, Mohshin, Mashi and Parvez. I would like to acknowledge my MSc. Juniors for their moral support and motivation, which drives me to give my*

best, thank you Raghib, Fatima, Bharat, and most affectionately Sah Kamranur Rehman.

I sincerely acknowledge the assistance of my seniors apart from my lab Mr. Anis, Mr. Akram, Mr. Atif, Ms. Barira, Mr. Meraj, Mr. Faraz, Mr. Khalid, Mr. Shazi, Mr. Ajaj, Mr. Mahroof, Ms. Hafiza, Ms. Nishat and Mr. Shehpar for making my stay in IBU a memorable experience.

A special thanks to all the research scholars of IBU for their moral support.

I would also like to extend huge, warm thanks to Afsheen, Taqi, Samreen, Amin Mir, and Dr. Nuzhat Gull Aapa for their great support and encouragement.

A special thanks to ***Mohd. Owais (micro) Shakir Bhai and Shaharyar,*** *I have spent many cherished moments in the journey of the thesis which will be enduring throughout my life. I would like to thank my friend Dr. Malik Abdul Rub, Dr. Basher, Dr. Sajid, Dleep, Both Azam Bhai (micro), Dr. Nazam Bhai, Dr. Shaigan, Afaque Bhai, Amir Bhai, Dr. Imran, Dr. Shafique Bhai, Vinod Kumar Chaturvedi and Yaga Paul for a healthy discussion on scientific and many more issues and celebrating the several events together. I wish to thank my other colleagues and friends apart from AMU, Dr. Sharfuddin, Prof. Arif, Mohd. Arif, Faisal, Hafiz, Irfan, Fareed and Maaz. I would not forget to remember our Jamia Hamdard seniors,* ***Dr. Firdaus Bhai, Dr. Jeelani Bhai, Dr. Shadab Bhai, Dr. Meraj Bhai, Dr. Babu Bhai , Dr. Rashid Bhai and Usama Bhai*** *for their unlisted encouragement and moreover for their timely support till the completion of our PhD. Work. A special thanks to my best friend* ***Wasid and Naseem*** *together we have spent grateful moments and still, these will be continuing throughout my life. I wish to thank my Hamdonian seniours and friends, Mumtaz, Shams Bhai, Monis, Zahid Bhai, Shafat, Rehan, Wasil Bhai, Dr. Gauhar Bhai, Latif, Bashir, Irtiza, Ashaque, Devashiash, Tanu, Mehboob Bhai, Dr. Minhaz Bhai, Hina Maam, Ishreena Maam, Dr. Farha Khan, Khalid Bhai, Prateek, Adarsh, Zaheer, Abrar, Rajesh, Shakeel, Praveen, Rabbani, Rupesh, Subhanjan, Atul, and Arif for their morla support.*

It is not possible for me to express gratitude to my parent in words. Ammi and Abba huzoor you are the best parent in the world. This is all your dua whatever I have achieved, and I can achieve anything with your dua Insha-allah. It is my sincere gratitude to my mamu Merajuddin and Azhruddin Khan who has accomplished all my wishes, always supported and encouraged me. I am highly thankful to my brothers (Junead, Ubaid, Aavesh, Owais), sisters (Nazma and Nazreen), cousin (Aarish, Guddu Bhaiya, Ahmad, Arshad, Ashraf, Afzal) and nephew (Samshad, Mehboob, Babli and Anam) for their love, encouragements and supports.

I am highly indebted to my wife and Son who borne (Huzifa M Khan (DOB 23.01.2013 at 2.55 am). Hina khan Yusufzai thank you very much for your encouragement, affection and support. I am also thankful to my father-in-law and his family members for his love support and encouragements.

I am also thankful to department of biotechnology and council of scientific and industrial research for their financial assistance during the tenure of doctoral studies.

"PROUD TO BE AN ALIG"

Javed Masood Khan

ABBREVATIONS AND SYMBOLS

%	percentage
α	alpha
λ	lambda
λmax	wavelength maximum
=	equal to
ANS	1-anilino-8-naphthlene sulfonic acid
AOT	bis-(2-ethyl 1-hexyl) sulfosucccinate
BL	banana lectin
BSA	bovine serum albumin
CD	circular diichroism
CR	Congo Red
DLS	dynamic light scattering
Fd	fraction denaturation
FI	fluorescence intensity
GdnHCl	gunidine hydrochloride
h	hour
HSA	human serum albumin
ITC	isothermal titration calorimetry
kDa	kilodalton
K_{sv}	Stern-Volmer constant
mg	milligram
MG	molten globule
min	minute
ml	milliliter
mM	milimolar
MRE	mean residue elipticity
N	native state
n	number of amino acids
nm	nanometer
°C	degree centigrade

PSA	porcine serum albumin
R	gas constant
R_h	hydrodynamic radii
RLS	Rayleigh light scattering
RSA	rabbit serum albumin
SDBS	sodium dodecylbenzene sulfonate
SDS	sodium dodecyl sulphate
s	second
SSA	sheep serum albumin
TEM	transmission electron microscopy
ThT	thioflavin-T
Tm	temperature mid point of transition
Trp	tryptophan
Tyr	tyrosine
β	beta
ΔG	standard free energy
Θ	theta
µl	microlitre
µM	micromolar

INTRODUCTION

A Journey from Protein Folding to Misfolding: Detection of Amyloid, Role of Surfactants and Lipids in Amyloid Fibril Formation

Protein folding:

The process of protein folding is the ability of a denatured, unstructured polypeptide chain to form highly structured functional conformational states, that is secondary, super-secondary, tertiary, and quaternary structures through non-covalent and covalent interactions (Anfinsen, 1972). For the proper functioning of proteins, protein has to be folded into specific conformation. As Anfinsen has shown in his seminal work that proteins can fold spontaneously from the denatured state to the native state if urea is dialyzed out to neutral pH (Anfinsen, 1973). Protein folding plays vital roles in various biological functions in the cell. Most of the secretory and membrane proteins are folded in the endoplasmic reticulum (ER) and where post-translational modification takes place in an energy dependent manner (Naidoo, 2009). Proteins are correctly folded and assembled in the ER prior to transport to the cell surface or other intracellular organelles. The folded form of proteins is thermodynamically more stable at physiological conditions (Dobson, 1998). The proper folding of proteins is critically important for performing cellular activities but sometimes proteins do not fold correctly because of the complex cellular environments in which it is present. Last 50 years has witnessed great advancement in understanding protein folding process through experimental, theoretical and computational approaches (Lindorff-Larsen et al., 2005, Fersht, 2008, Dill et al., 2008). The protein folding has three related but separate issues (Dill et al., 2008). First thermodynamics issue, second kinetics and third prediction of protein native structures (Ferreon and Deniz, 2011). Presently, the question arises that how does a protein fold? Several models of protein folding have been proposed. They are based on theoretical considerations or phenomenological constructs and computer simulation. Molecular dynamics (MD) simulations give a detailed description of each step of protein folding and unfolding processes which may be comparable with the experimental data of protein folding and unfolding(Finkelstein, 1997).

Framework model:

This model was proposed by Ptitsyn (Ptitsyn, 1994). He suggested that the folding of protein occurs in a stepwise manner. According to this model, the secondary structure formed first followed by tertiary structures.The details of this model include formation of fluctuating segments of secondary structures first which eventually come close together and become compact and finally assembled into the tertiary structure. Ribonuclease A is a good example of this model.

Hydrophobic collapse model:

According to this model of protein folding, hydrophobic amino acids repell water molecule in doing so these hydrophobic amino acids are forced to come close to each other stabilized by hydrophobic interaction and consequently gives rise to the hydrophobic collapse structure upon which higher order structure are built up.Hydrophobic interaction are infact fast interaction in comparison to any other non-covalent interaction (Kauzmann, 1959). Experimentally, it is the most acceptable model for folding kinetics of many globular proteins including myoglobin, alpha-lactalbumin, barstar and staphylococcal nuclease.

Nucleation–condensation growth model.

The nucleation-condensation model is similar to framework and hydrophobic collapse models. According to this model the linear polypeptide chain of proteins forms secondary and tertiary structures simultaneously and finally proteins become folded. According to this model long range hydrophobic interactions are formed in a transition state and are stabilized by transient secondary structure (Fersht, 1997). Chymotrypsin inhibitor (CI2) is a first protein which follows nucleation - condensation model (Itzhaki et al., 1995).

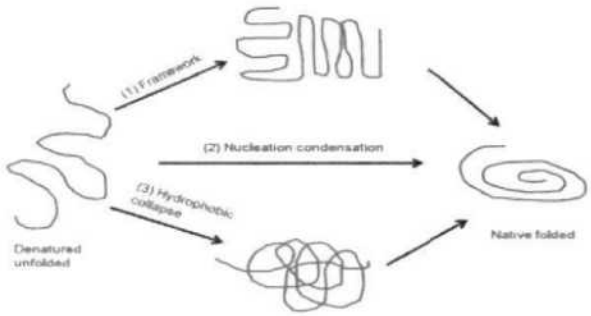

Figure 1. Schematic presentation of protein folding models

Folding funnel model:

A unified model of protein folding based on the effective energy surface of the polypeptide chain for understanding the self organization of a protein, is termed "folding funnel model" and it describes the folding process in terms of energy landscape and a folding funnel (Wolynes et al., 1995). Protein folding is viewed to consist of progressive organization of ensembles of partially folded structures that arise through multiple routes. According to this new view, to fold, a protein navigates with remarkable ease through a complicated landscape (Figure 2.). At the top of the funnel, there is a competition between maximization of entropy in protein that keeps the protein in random coil state and minimization of enthalpy that drags the protein towards the bottom of funnel. Many unfolded proteins are found on the brim of funnel therefore the energy and entropy are maximum on the brim of the funnel. The apex of funnel contains native folded proteins where energy and entropy are minimum and space intervening between the brim and the apex of the funnel lies(Laughlin et al., 2000). Towards the bottom of the folding funnel, the number of protein conformations decrease as does the entropy. The steeper the slope, faster will be the folding process. The downhill bias of the energy landscape is sufficient to drive random coil into folded structure in a reasonable time period of folding. Folding proceeds one amino acid at a time in no particular order through an unlimited continuum of undefined intermediates and paths (Rumbley et al., 2001). One of the very attractive features of "folding funnel" model is that it brings together many of the earlier conceptual models of folding. These models can now often be seen as special cases of a unified general mechanism of folding that describes behavior of all protein molecules. However, characterization of folding intermediate still remains central issue for solving protein folding problem.

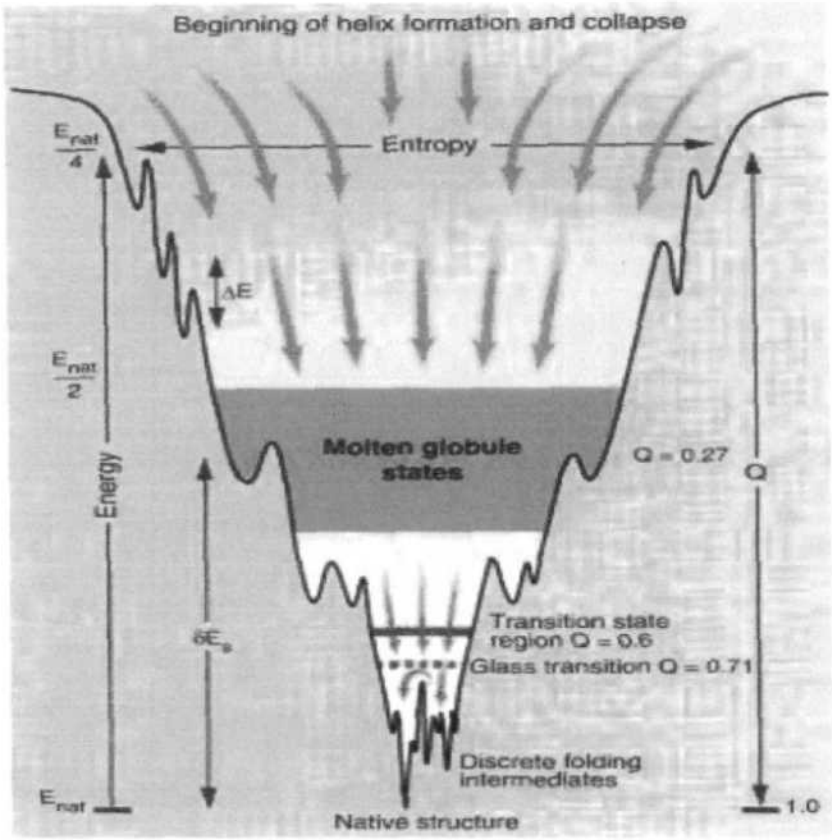

Figure 2. Schematic two-dimensional presentation of the folding funnel. Width of funnel presents the entropy, depth represents the energy. Q is the fraction of native contacts for each collection of states.

Mechanism of protein folding:

Understanding the mechanism of protein folding is a central problem in structural biology and modern protein physics. Two different mechanisms have been proposed for the folding of small single domain molecules (i) diffusion-collision model (DC) (ii) nucleation-condensation model (NC). In DC model, the protein folding proceeds *via* a series of intermediates formation. In this model, secondary structure are formed first followed by tertiary structure (Karplus and Weaver, 1976).The NC model proposes formation of folding nucleus first and after this significant portion of protein structure collapse. This model is not a rate limiting steps (Fersht, 1995). According to the atomic level description of chymotrypsin inhibitor 2 (CI2) folding, it was noticed that at denatured state some of the hydrophobic clusters near the main chain are inconsistent with fluctuating native helical structure. From this description, it was concluded that the protein might appears to fold in a two-state manner (Daggett and

Fersht, 2003). In a hierarchic folding model, the folding starts with the structure which is local in sequence as well as possess very minor stability. Due to interaction taking place in between these structures, leads to formation of intermediate with increasing complexity and finally attains native conformation. In non-hierarchic folding processes the tertiary structures are not only stabilized by local structure (Baldwin and Rose, 1999). Hierarchic folding is the most acceptable model because it is too much tractable both conceptually and computationally. The folding of multimeric proteins has a biological significance because majority of proteins exist as protein-protein complexes. These multimeric proteins fold in various ways, some follow two-state mechanism from native dimer to unfolded monomer whereas the other follow three-state transition which is unfolded, with stabilization of dimer or monomer intermediate and native state (Rumfeldt et al., 2008). Human fibroblast growth factor (hFGF-1) and some other proteins are example of multimeric proteins which follow three states mechanism (Englander, 2000, Samuel et al., 2001). The dimeric protein factor for inversion stimulation (FIS) has a monomeric or dimeric intermediate during the protein folding and unfolding equilibrium denaturation (Hobart et al., 2002).

Protein Folding in Cell:

Nascent proteins are transported from the secretory pathways through membranes of endoplasmic reticulum (ER). The protein enters in the lumen of ER with the help of proteinacious pore known as "translocon" (Johnson and van Waes, 1999). The translocated proteins which are in unfolded state assemble into their native conformation by subsequent steps of folding in the ER. For this, the organelle maintains an inventory of raw materials, enzymes, and chaperones needed for proper protein folding and modification (Hebert and Molinari, 2007, Anelli and Sitia, 2008). In the oxidizing environments of ER, some proteins like molecular chaperon and folding enzymes are mainly responsible for proper folding, post-translational modification and oligomerization of the proteins (Gething and Sambrook, 1992). The formation of hydrogen bond and burial of hydrophobic residues facilitates a final state of folding. The N-linked glycosylation takes place in ER (Rutkevich and Williams, 2011). Intra and inter-molecular disulfide bonds are formed co-translationally in the ER before entering their C-terminal regions of the nascent proteins (Chen et al., 1995). Disulphide bonds are usually formed between adjacent cysteines when the

proteins consist of autonomously folded domains (Braakman et al., 1991). Disulfide bonds can also stabilize a protein by reducing the entropy of an unfolded state (Feige MJ, 2010).

Protein folding in molecular crowding environment:

Generally, the cellular environment is highly concentrated with macromolecules which limit the polypeptide chain folding and movement (Zhou et al., 2008). Folding in the complex cellular environment hinders the molecular motion of protein. Smaller protein has less translational diffusion rates in the macromolecular crowding and macromolecular networks of the cytoplasm because intermolecular interaction is a main driving factor which reduce the mobility of proteins (Kumar et al., 2010, Nenninger et al., 2010). Molecular crowding also alters viscosity of the cytoplasm which is an important factor that influences folding rate and mechanism of protein folding (Hagen, 2010).

Protein folding with the help of chaperons:

There are many proteins in the cell that help other proteins to acquire their native and biologically active conformation. These proteins are known as molecular chaperones which posses high affinity for unfolded or partially unfolded state of the proteins for proper folding. The molecular chaperones also play an important role in the defense mechanism by preventing improper association of exposed hydrophobic residues of non-native proteins thereby inhibit the protein aggregation (Frydman, 2001, Hartl and Hayer-Hartl, 2002). Molecular chaperones act as a folding catalyst. Molecular chaperones are divided into two distinct groups one occurs in prokaryotes and endosymbiotic organelles called as a group I chaperones and other is found in archae and eukaryotic cells called as group II chaperones (Ellis, 1997, McClellan and Frydman, 2001). GroEL is molecular chaperone found in Escherichia coli belongs to group I chaperone. It consists of 14 identical subunits and ring-shaped cofactors GroES. The role of GroES is to deattach the GroEL from the cavity and provide a folding chamber to assist proper folding (Sigler et al., 1998). In eukaryotes, the group II chaperones such as TCP-1 ring complex (TRiC) and the thermosome occur in archea are multimeric complexes possessing either eight or nine different subunits per ring (Valpuesta et al., 2002). Two types of intramolecular chaperons were found such as type I intramolecular chaperone that helps in the tertiary structure formation of

particularly the N - terminal sequence while type II intramolecular chaperones are involved in the quaternary structure formation (Chen and Inouye, 2008). The example of a type I intramolecular chaperons are subtilisin: a serine protease from *Bacillus subtilis*. Other proteases such as α-lytic protease, carboxypeptidase Y, cathepsin L, aqualysin I, proteinase A, procaricain, the prohormone convertase Kex32 and thermolysin which work as a type I intramolecular chaperones (Groves et al., 1996, Shinde et al., 1997, Zuhl et al., 1997, Kervinen et al., 1999). Type II chaperones are somatostatin II, cathepsins D, L, G and myeloperoxidases, their propeptides contain putative sorting signals, however in acetylcholine esterase in *Pichia pastoris* and proteinase B from *Streptomyces griseus*, they adapt the extent of protein that is secreted (Mitra et al., 1998, Garwicz et al., 1998, Andersson et al., 1998).

Protein Stability:

The term stability of a protein is defined as a protein that retains conformation and function. To elucidate the forces involved in protein stability, we first look towards physical and chemical forces that contribute to protein stability. The proteins are stabilized by various non-covalent and covalent interactions. The non-covalent interactions are as follows (i) Hydrogen bonding (ii) van der Waals interaction (iii) Electrostatic interactions (iv) Hydrophobic interaction

Hydrogen Bonding:

The hydrogen bond is formed when an electronegative atom interacts with a hydrogen atom bound to other electronegative atom. The distance between hydrogen bonded atoms like NH·····O is around 2.99 A^0 in an α-helix and 2.91 A^0 in a β-sheet (Baker and Hubbard, 1984). Approximately one amino acid residue form 1.1 hydrogen bonds when they become folded. The most prevalent backbone hydrogen bonds around (68.1 %) between >C=O·····H-N< and between side chains >C=O and >N-H approximately (10.9 % and 10.4 %) (Stickle et al., 1992). In an amide transfer reaction the negative ΔH and negative ΔS represent amide interaction with aqueous urea which is enthalpically favorable and entropically unfavorable. Thus, from these observations it can be said that the amide-urea interaction is specific and occur by hydrogen bonding (Zou et al., 1998).

van der Waals interaction:

van der Waals forces are driven by inducing electrical interactions between two or more atoms or molecules that are very close to each other. van der Waals interactions

are extremely short range, weak interactions resulting from transient induced dipoles in the electron cloud surrounding an atom. Atoms in close proximity can contribute ~0.4-1.2 kJ mol^{-1} per interaction. A van der Waals interaction strengthens hydrophobic interaction because non-polar atoms are especially favored in this type of interaction. van der Waals interaction contribution to protein stability is small.

Electrostatic Interaction:

The electrostatic interaction occurs between two oppositely charged groups. Thermophilic proteins are mostly stabilized by electrostatic interactions in comparison to mesophilic proteins. Similarly, antigen-antibody interactions are mainly stabilized by electrostatic interactions. Further, rigid part of the surface of protein is stabilized by electrostatic interactions. Thus, electrostatic interaction plays an important role in the stability of proteins. The protein-protein complex formations, molecular recognitions, conformational adaptabilities, stability and function of proteins all require mediation of electrostatic interaction. Computer simulation is one of the important methods to predict the electrostatic interaction but the intermolecular interaction should be in the range of 4-5 nm otherwise the intermolecular interaction determination is not possible (Hünenberger, 2001). On the basis of structural and mutational study, it has been reported that the protein-protein association is also stabilized by electrostatic interaction. In protein-protein interactions charged and polar residues are present at protein-protein interface which enhance complex stability (Sheinerman et al., 2000). The short-range electrostatic interactions (salt bridges) are shaped by proximity of joining the oppositely charged residues in native protein structures (Kumar and Nussinov, 2002). Four Glu residues of designed disulfide-linked leucine zipper AB(SS) are involved in an ion paring in which two are destabilizing (-5.6 kJ mol^{-1}) and other two are stabilizing (+3.8 kJ mol^{-1}) which interacts with positively charged histidines at the C-terminal of AB(SS) (Marti and Bosshard, 2003).

Hydrophobic Interaction:

Hydrophobic interaction is main driving forces for stabilizing the native structures of proteins (Dill, 1990). In hydrophobic interaction, hydrophobic groups of protein does not contact with water but contact with each other and thereby they stabilize the protein conformation. Generally, hydrophobicity of a given compound can be

determined by measuring the free energy transfer (ΔG_{tr}) of a compound from an aqueous to non-aqueous solution and *vice versa*. If ΔG_{tr} values are positive,this means the molecules prefer an aqueous environment. The forces operating between the hydrophobic groups are generally weak but have a great propensity to repel the water molecules. The contribution of individual amino acid residues to the stability of proteins can be determined by hydrophobicity scales which are obtained from oil-to-water free energy transfer experiments. From these experiments it was concluded that the contribution of hydrophilic residues to the stability is insignificant or negative compared to hydrophobic residues (Pace, 2001). In a small protein villin headpiece (VHP) subdomain (0.6 ± 0.3 kcal/mole per –CH2– group), hydrophobic interactions contribution is less than in large protein VIsE (1.6 ± 0.3 kcal/mol –CH2– group) isolated from Borrelia burgdorferi (Pace et al., 2011).

Factor affecting protein stability under in-vitro conditions:

Conformational stability of proteins can be determined by denaturing the proteins using different methods like pH, temperature, chaotropic agents, surfactants etc.

(i) pH effect:

The acid-base features of proteins are regarded as stabilization and destabilization of native structure by protonation/deprotonation which affects both physical and chemical properties of proteins (Wang, 1999). A proteins electrostatics state is decided by pH only. At isoelectric point (pI) the number of positive and negative charges are equal. At pH below the pI, the proteins acquire a positive charge on the surface while at pH above pI, proteins acquire negative charge on the surface. The intermolecular repulsion between the positively charged groups leads to unfolding of the proteins (Goto et al., 1990). Generally, proteins at extreme pH become unfolded and might form aggregate due to exposure of hydrophobic residues (Chi et al., 2003a). The ion channel protein CL1C1 was exploited as pH sensor, the sensor could be histidine or glutamine residues with pKa values that comes in neutral pH range (Legg-E'silva et al., 2012). The fusogenic property of wild type glycoprotein B can be changed under acidic pH suggesting that glycoprotein B conformational change is directly linked to fusion activity of virus (Roller et al., 2008). Low endosomal pH is required for the penetration of herpes simplex virus (HSV) envelop proteins into the cell which is accompanied by conformational changes(Nicola et al., 2003). The

apomyoglobin B (apoMb) undergoes three-step unfolding transitions at acidic pH 4.0 to generate an intermediate state. Under acid-denaturation three types of conformational states were observed (1) native-like state, N', which is similar to native state; (2) acid unfolded state (UA) which may retain somewhat more secondary structure than the corresponding Gdn-HC1-denatured protein; an acid-denatured state, the A state, that is relatively compact and exhibits a high level of secondary structure and minimal tertiary structure (Fink et al., 1994). The four Trp residues of recombinant hepatic stimulator substance (rhHSS) were exposed at pH 7.4 and wavelength maximum was found at 342.4 nm. At acidic pH (pH 4.0) wavelength maximum blue-shifted and maximum blue shift of 7.6 nm was noticed at pH 2.0. The blue-shift occurred under acidic conditions probably because of the shielding of Trp residues (Yang et al., 2007). The pH dependence change in ΔG^{H2O} values signifies the involvement of electrostatic interactions which make a significant contribution to the conformational stability of the protein. Similar unfolding behavior was observed for other RNase (Kumar et al., 2011).

(ii) Effect of temperature:

The temperature is one of the best sought method to understand the protein folding and unfolding pathways (Liu et al., 2005). Generally, most of the proteins become denatured in the temperature range 50 to 80 °C and nature of denaturation is specific for each protein. The 3-D structure of proteins is stabilized by non-covalent interactions such as ionic interaction, hydrogen bonds, and hydrophobic interactions but after heat treatment all of these interactions are lost and protein becomes unfolded or denatured. The thermal denaturation curves are characterized by broad transitions (Brooks, 2002). Protein stability can be measured directly using calorimetric methods, and indirectly by the Gibbs free energy change estimated from transition curves from native to the unfolded state (Nicholson and Scholtz, 1996). Thermal induced unfolding of small peptides are less cooperative than single domain proteins. The *Tm* of proteins is defined as the temperature at which half of the protein becomes unfolded. It is also used to compare the conformational stability of proteins (Patel et al., 2010). Generally, folded protein becomes unfolded upon heat treatment without occurence of intermediates but in some cases intermediate states were found during this transition. Upon thermal unfolding of lipase protein (Lip1) from Candida at pH 7.0-8.6 contents of secondary structure i.e. the α-helix decreased while at pH 5.5 an

increase in secondary structure content was observed. From these observations it can be said that it is the changes in pH that only bring the modification of enzyme secondary structure not the thermal stability (Fucinos Gonzalez et al., 2011). γ-glutamyltranspeptidase from G. *thermodentrificans* is a thermostable enzyme and also exhibits excellent halotolerant properties because very small red shift was observed in the presence of 2.8 M NaCl while upon addition of 4.0 M NaCl the red shift was not noticed even at 97 °C. So it was concluded that salt provides thermal stability because of the interaction occurring between negatively charged side-chain residues of the proteins with surrounding positive ions (Pica et al., 2013). The phosphoserine aminotransferase (EhPSAT) from an enteric human parasite entamoeba histolytica is a holo-enzyme that has a higher *Tm* value in comparison to apo-form because of electrostatic interaction (Mishra et al., 2011b).

(iii) Effect of Urea:

Urea is a small hydrophilic molecule that acts as a strong denaturant of proteins, but its molecular mechanism of denaturation is still controversial (Sagle et al., 2009, Berteotti et al., 2011). In urea induced protein denaturation, the protein-protein and protein-water contacts are replaced by protein-urea interaction and both hydrophobic as well as hydrophilic residues assest in unfolding process (Das and Mukhopadhyay, 2008). Available literature suggests that urea acts in a two ways (i) by directly interacting with proteins *via* hydrogen bonding and electrostatic interactions, or interact directly with the amino acids through more favorable van der Waals attractions (ii) by indirectly interacting it disturbs the position of water molecules and change the activity coefficient of solvent environment and finally weakens the hydrophobic interactions of protein (England et al., 2008, Sagle et al., 2009, Yang and Gao, 2010). If urea interacted directly with water so what types of forces are involved whether electrostatic or Van der Waals is still controversy (O'Brien et al., 2007). In recent research, sufficient evidence has accumulated which support direct mechanism that is urea interacted directly with a backbone of protein via hydrogen bonding and electrostatic interactions with charged and polar side chains exclusively (Chen et al., 2007, Zhou et al., 2011). Before water, urea penetrates to hydrophobic core and preferentially binds to all the regions of proteins. Eventually hydrogen bonds are formed between urea carbonyl and backbone amides of protein thereby leading to destruction of intrabackbone hydrogen bonds which ultimately unfold the protein

(Hua et al., 2008). Recently, it has been found that the protein-protein interaction occurs in water but not in the presence of urea (Das and Mukhopadhyay, 2009). At lower concentrations, NaCl shows strong salting-out property while urea shows salting-in property. Salting effect is enthalpy-driven in the presence of both urea and NaCl (Li et al., 2012). The urea and alkyl urea derivatives have a free (-NH) moiety which is directly involved in hydrogen-bonding with bovine serum albumin and consequently leads to unfolding (Kumaran and Ramamurthy, 2011). Ste11 is a dimeric protein which is found in the mitogen-activated protein kinase (MAPK) cascade, it follows a two-state unfolding in presence of urea. At 5.0-5.5 M urea concentration, both native and unfolded protein exists together while global unfolding occurred at a 6.0 M urea concentration. From these results it is evident that the hydrophobic residues of the dimeric interface are actively involved in maintaining the structural integrity and stability of the Ste11 proteins (Bhunia et al., 2008).

(iv) Effect of Guanidine Hydrochloride (GdnHCl) :

GdnHCl is widely exploited to check the conformational stability of monomeric and multimeric proteins by equilibrium unfolding methods (Wojciak et al., 2003, Ahmad et al., 2005). GdnHCl induced unfolding of monomer of human serum albumin (HSA) showed it follows a single step in unfolding while multimeric proteins or enzymes unfolding are multistep process with the stabilization of partially folded intermediates (Muzammil et al., 2000, Jaenicke and Lilie, 2000). The p*K*a of GdnHCl is about 11; below the pH 11 the GdnHCl is ionized into Gdn^+ and Cl^- and these ions affect the stability of proteins and enzymes. Most recent studies suggest that GdnHCl stabilizes the proteins at sub-denaturing concentration through charge-charge interactions (Ibarra-Molero et al., 1999, Bhuyan, 2002). For example the thermostability of RNase T was observed in the presence of 0.1-1.0 M NaCl or 0.1 M GdnHCl and it increased the *T*m, the possible explanation is that the stabilization of Na^+ and Gdn^+ by interaction with negatively charged amino acids of RNase T1(Mayr and Schmid, 1993). GdnHCl is currently best denaturant because it unfolds the proteins at lower concentration than any other chemical denaturants.

(v) Effect of surfactants:

Many physiochemical and conformational phenomena are regulated by protein-surfactant interaction (La Mesa, 2005). The interactions between protein and surfactant have been exploited for many years in various fields including biological,

industrial, cosmetics and pharmaceutical systems (Bathaie et al., 1999, Taheri-Kafrani et al., 2010). It is well established that when detergents bind strongly to proteins, conformational changes takes place (Lu et al., 2005). Many surfactants are used in protein unfolding like anionic, cationic, hydrophobic and zwitterionic (Ohnishi et al., 1998, Mir et al., 2010). The anionic surfactant sodium dodecyl sulphate (SDS) is the most common surfactant used in protein unfolding (Santos et al., 2003, De et al., 2005, Mahanta et al., 2009). The SDS induced protein denaturation shows that at very low concentration, only monomer of SDS binds to the high affinity sites producing structural changes which is very small but at higher concentration micelles bind around the proteins and expands the protein molecules. The negative part of SDS forms electrostatic interaction with positively charge residues of proteins (Oellerich et al., 2003). If the proteins lysyl side chain is fully deprotonated, the SDS head is unable to bind to protein due to loss of electrostatic interaction therefore only hydrophobic interaction participate (Bhuyan, 2010). The tail of SDS interacts with a apolar site of proteins and the nature of interaction is hydrophobic. The hydrophobic tail of SDS played an important role in protein denaturation (Otzen, 2002). SDS below CMC increases the secondary structure formation and stabilizes the structure of heynein isolated from medicinally important plant *Ervatamia heyneana* but beyond the CMC it becomes unfolded (Prasanna Kumari and Jagannadham, 2011).

Protein Misfolding and aggregation:

Protein misfolding and aggregation are very alarming problems. The misfolding of proteins occurred by the interaction of unfolded protein molecules which acquires various structural organizations (Markossian and Kurganov, 2004). Some of the misfolded proteins tend to form aggregates and their deposition at various part of central nervous system and other organs leads to different types of human diseases including Alzheimer, Parkinson and type II diabetes etc. Protein aggregation occurs at every stage of development and it is very less understood, in some study it is found that the non-native structures of proteins are very prone to form aggregates (Cromwell et al., 2006). On the basis of morphology, the aggregation of proteins is divided into two types (i) amorphous aggregates (ii) amyloid fibril. Amorphous aggregates show granular structure lacking ordered structure as viewed by electron microscopy (Temussi et al., 2003, Vetri et al., 2007, Morell et al., 2008). However, amyloid fibrils are highly ordered and repetitive structures where all polypeptides adopt a common

fold. Amyloid fibrils are threadlike aggregates that form repetitive β- sheet structure oriented perpendicular to the fibril axis. This structure is known as cross β-structure (Wang et al., 2008). The amyloid fibrils are associated with many neurodegenerative diseases such as Parkinson's, Alzheimer's, Creutzfeldt–Jakob disease, type II diabetes, and bovine spongiform encephalopathy (Chiti and Dobson, 2006, Toyama and Weissman, 2011).

Mechanism of Protein Aggregation:

There are several mechanisms of protein aggregation which are shown in (Figure 3) They are not mutually exclusive. Infact more than one mechanism occurs for the same protein . In the first mechanism reversible, association of the native monomer occurs. According to the first mechanism, the folded surface of one monomer has multiple sticky patches or complementary patches that help in association with other complementary monomer and leading to the formation of oligomers (Chiti and Dobson, 2009). In the second mechanism, aggregations occur in association of conformationally altered monomers. However, the native monomers have a very low propensity to reversible associate. These native folded monomer becomes partially unfolded at lower pH, high temperature, chemical denaturant and in the presence of organic solvents. These partial unfolded monomers link to other partially unfolded monomer through exposed hydrophobic residues and consequently form aggregates (Raso et al., 2005). In the third mechanism chemical modification such as oxidation of methionine, deamidation, or proteolysis of monomers creates a new sticky patch on the surface of proteins or changes the charge thereby it decreases the electrostatic repulsion between monomers and increase association (Hermeling et al., 2006). Fourth mechanism is nucleation controlled aggregation. According to this mechanism, aggregation is a common mechanism for formation of visible particulates or precipitates (Chi et al., 2003b). In this mechanism, the native monomer has a low propensity to form small and moderately-sized oligomers. If the aggregate of sufficient size oligomer is produced it is called "critical nucleus". This nucleus further forms a large species which get converted into mature fibril. During this process a lag phase occurs which is required for proper growth of aggregate (Chi et al., 2005). The last mechanism to be explored is surface induced aggregation. In this mechanism aggregation process starts with binding of the native monomer to the surface. In the

case of air-liquid interface that binding would probably be driven by hydrophobic interactions, but electrostatic interactions might also be involved.

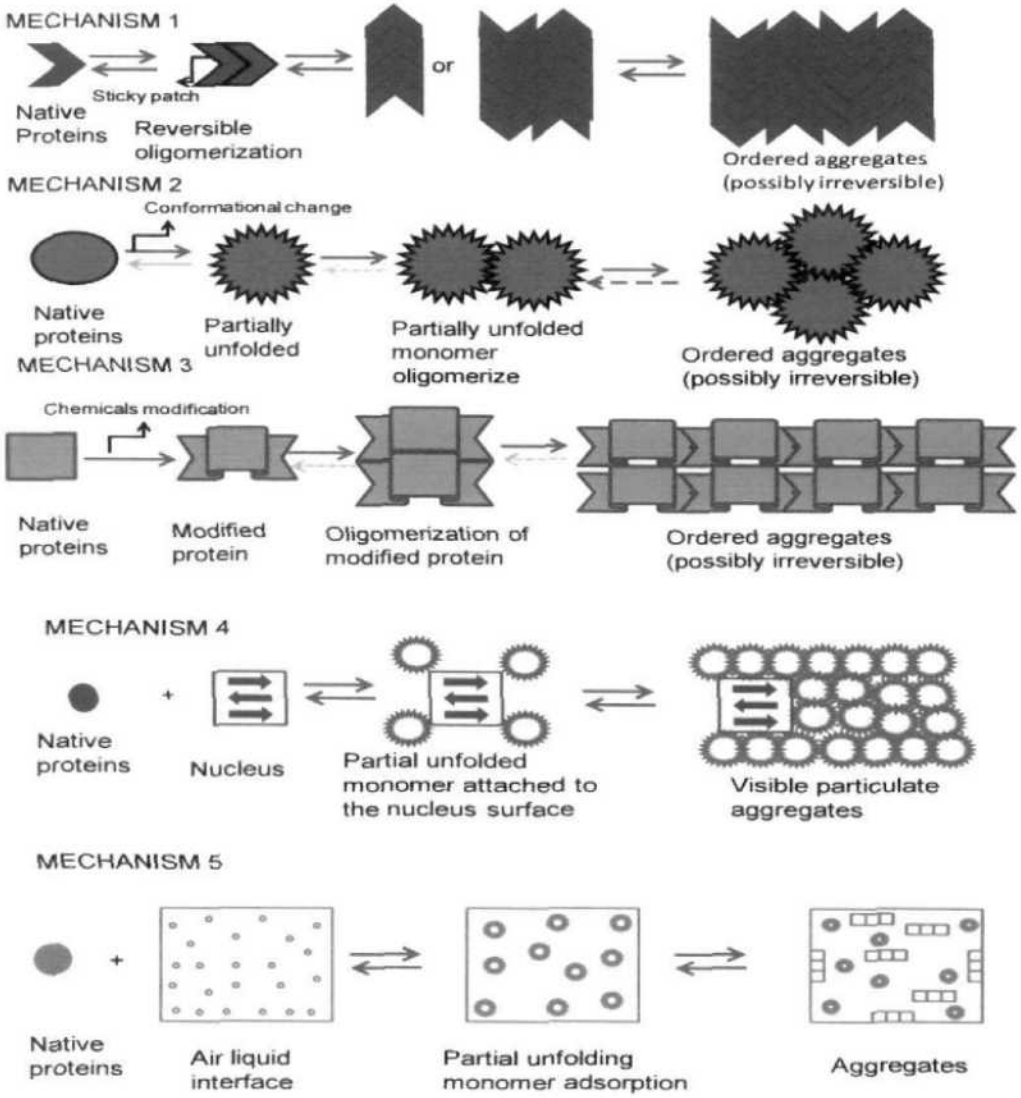

Figure 3. Mechanism of protein aggregation a graphical presentation.

Structure of Amyloid fibril:

Several types of amyloid structures are known so far and they are shown in Figure 4. In the electron microscope, amyloid fibrils appear in various shapes like straight fibril, unbranched strands of 80-120 Å in width and highly variable length reaching to micrometers (Jaroniec et al., 2002, Makin et al., 2005). Sometimes fibrils are twisted in shape and have bundles of protofilaments structure of 20-30 Å in diameter. There are two general observations of amyloid fibrils. First, amyloid fibrils are more stable than native states. Second amyloid fibril motifs are capable of joining many

polypeptide sequences which are native like. Amyloid fibrils show cross-β sheet structure while the native proteins possess secondary structure like α-helix, β-sheet and random coil. At the atomic level different types of amyloid fibril models have been proposed in past. These models are refolding model, natively disorder model and gain-of-interaction model (Makin and Serpell, 2005, Nelson and Eisenberg, 2006). In the refolding model the native proteins are converted into fibrils. For this conversion protein must unfold and then refold. The fibril structure is defined by backbone hydrogen bonding in almost all proteins. The side chain amino acids are unimportant but content of amino acids influences the rate of fibril formation. The proteins have parallel β-sheet structure (Jimenez et al., 1999, Fandrich et al., 2001, Jimenez et al., 2002). The natively disordered model has certain feature in which, proteins have very poor order structure in the native state and this unordered polypeptide gets stuck and form cross β-sheet spine structure (Krishnan and Lindquist, 2005, Ritter et al., 2005). In the third model, the conformational change was found in the limited region of the native proteins and thereby expose a previously inaccessible surface. The newly exposed surface gets stuck to the other molecules and form a mature fibril. In this model the structure of native proteins is not disturbed but forms fibril (Elam et al., 2003). The solid-state NMR has contributed a lot to understand the amyloid fibril structure.Because of large size, low solubility and noncrystalline nature of amyloid it is difficult to explore by other techniques (Tycko, 2006). Recently crystalline forms of amyloid fibrils were determined by X-ray diffraction (Sawaya et al., 2007). A β (1-40) peptide fibril is made up of two protofilaments and each filament is 5 nm long regions of β-sheet structure. This type of pairing occurs via tightly packed interfaces, reminiscent of the recently reported story zipper structures (Sachse et al., 2008). The cross-β spine consists of many β-sheets, and each β-sheet is formed from extended strands of the segment stabilized by hydrogen bonding (Sawaya et al., 2007).

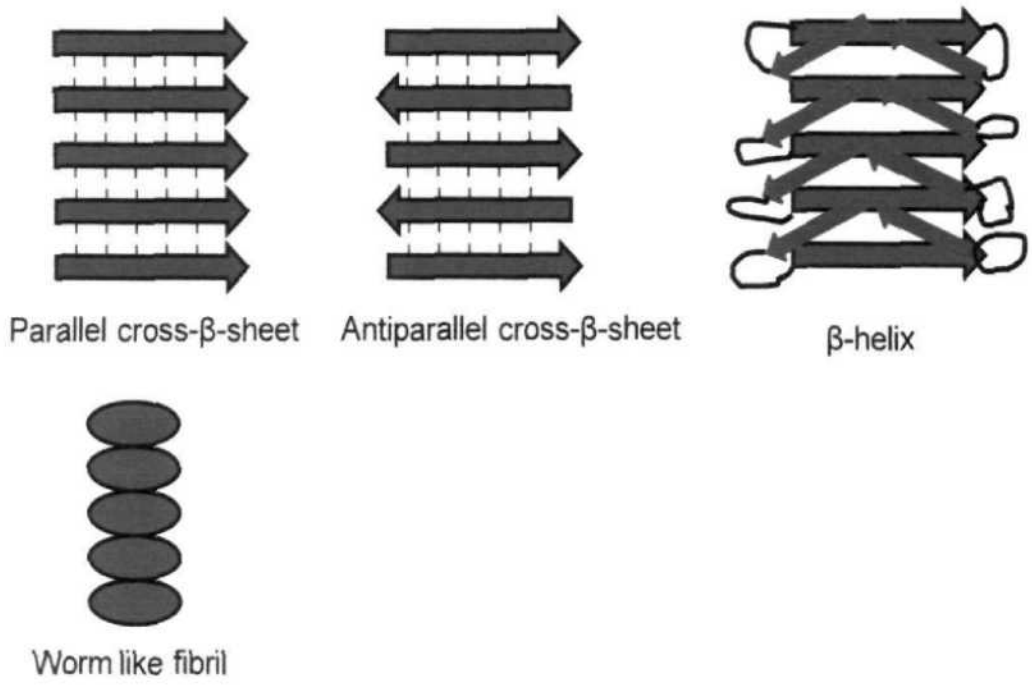

Figure 4. Structures of amyloid fibril

Role of intermediates in fibril formation:

Partially unfolded states of proteins are important precursors in amyloid fibril formation (MacPhee and Dobson, 2000, Chiti et al., 2002, Uversky and Fink, 2004). It is very difficult to trap and characterize these partially unfolded states at physiological conditions because they are transiently populated on the fibrillation pathway. The partially unfolded states of a protein produced under high temperature, high pressure, low pH or moderate concentrations of organic solvents exhibit more propensity to aggregate as shown in Figure 5. (Lansbury, 1999, Zerovnik, 2002). Under these conditions protein hydrophobic residues are exposed and these exposed residues interact with each other and form mature amyloid. These partially unfolded states facilitate intermolecular interaction including electrostatic interactions, hydrogen bonding and hydrophobic interactions which help in oligomerization and fibrillation (Dobson, 2001, Zerovnik, 2002). Partially unfolded states are also generated by mutation and theses states are rapidly converted into a mature fibrilar form (Nielsen et al., 2001a). In many reports, it was found that the amyloid fibrils are formed when the native structure of folded proteins is destabilized but the noncovalent interactions are still in favor (Krebs et al., 2000, Ramirez-Alvarado et al., 2000). β-lactoglobulin

aggregation follows two-step; in the first step oligomeric intermediate (di, tri, and tetramer) are formed and in the second step these oligomers associate to form mature amyloid fibrils (Croguennec, 2004). The intermediate oligomers of *β*-lactoglobulin are covalently linked by intermolecular disulphide bonds and by electrostatic interaction in the presence of salt (NaCl). The electrostatic interaction and intermolecular disulphide bonds coexisted in amyloid fibril because of reduction of repulsive forces due to shielding of charge on the surface of intermediate oligomers (Schokker, 2000). Due to three mutations in α-spectrin SH3 domain, the strand β1 becomes totally unfolded and most of the hydrophobic core residues are highly exposed to solvent. From the docking simulation studies it was found that intermediate comprising β1 strand has a strong capability to dimerize and form amyloid (Krobath et al., 2012). The β2 microglobulin becomes unfolded at acidic pH but some residual structures still persist and these structures are stabilized by clustering of hydrophobic residues. Ultimately, these exposed residues serve as seeds for the extension of amyloid fibrils (Yanagi et al., 2012).

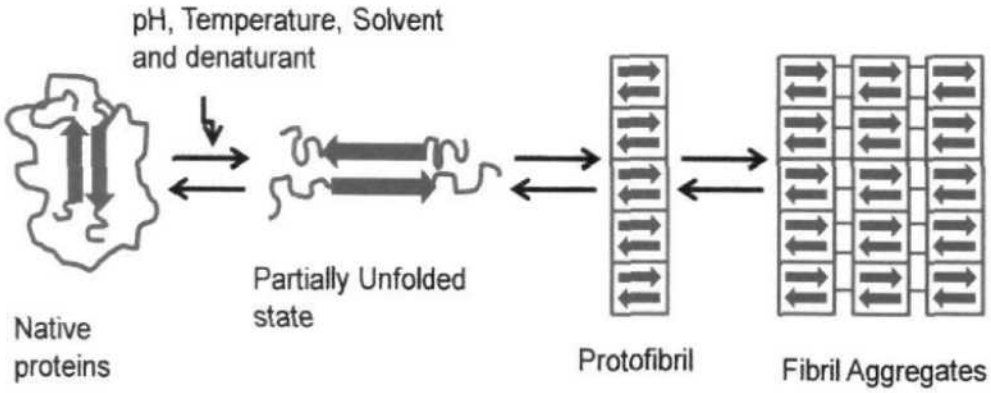

Figure 5. Role of partially unfolded state in amyloid fibril a schematic presentation.

Nucleus dependent Amyloid fibril formation:

Many amyloid fibrils are formed *via* a nucleation-dependent mechanism (Nielsen et al., 2001b, Sabate et al., 2003, Bhak et al., 2009). In this mechanism the proteins monomer are converted into a fibrillar structure *via* rapidly populated aggregation nucleus (Naiki and Gejyo, 1999). Two steps are involved in the formation of fibril structures as shown in Figure 6.First step involves a slow nucleation called lag phase in which monomers are joined together to form oligomer nucleus. The nucleus is in

the highest energy state but is thermodynamically unfavorable. Second is elongation phase which starts by further addition of monomers and ultimately mature fibril are formed. This fibril is thermodynamically favorable (Harper and Lansbury, 1997, Kelly, 2000). In nucleation process, the length of lag phase can be shortened by change in pH, salt ions, temperature, mutation, protein sequence and therefore the length of the whole process is decreased(Modler et al., 2003, Pedersen et al., 2004). Sometimes amyloid fibril formation process procedes without lag phase and does not require nucleus (Serio et al., 2000, Vilasi et al., 2011). Further, in presence of certain mutations the length of the lag phase can be reduced but nucleation is not rate-limiting factors for amyloid fibril formation (Fezoui and Teplow, 2002).

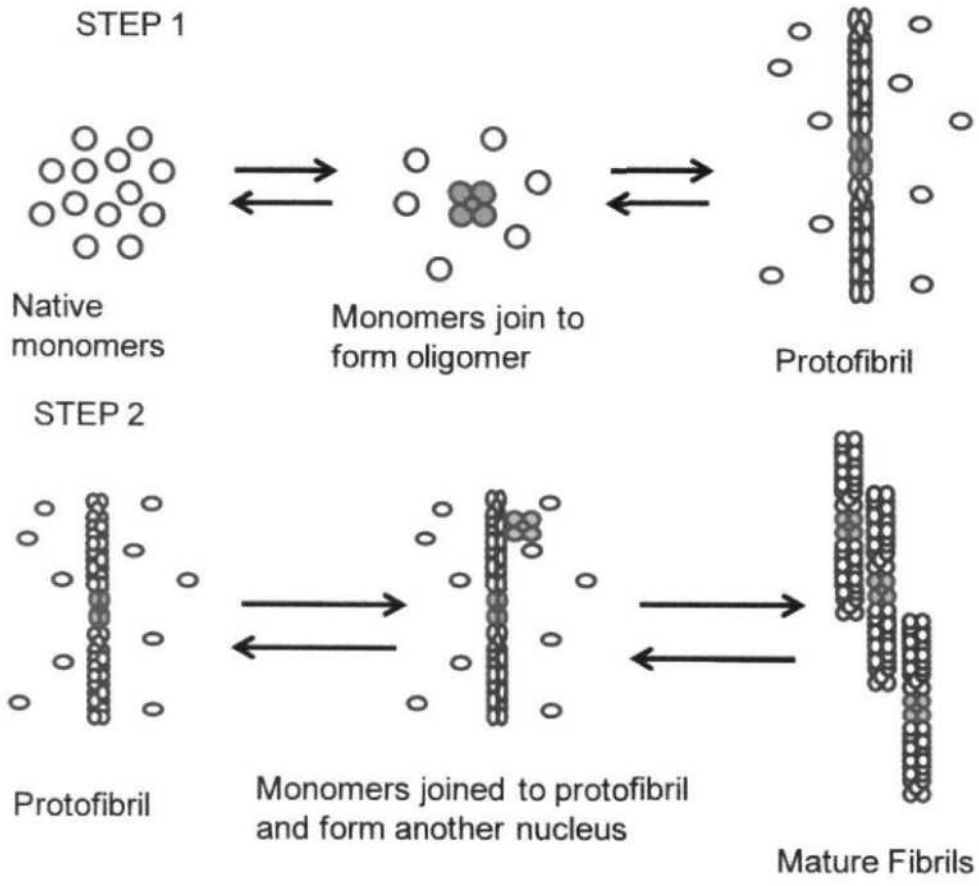

Figure 6. Nucleus dependent amyloid fibril formation an illustration

Dye used for amyloid detection:

Many dyes are used for the detection of amyloid fibril (Volkova et al., 2007, Ahn et al., 2012, Vus, 2012). Among them Thioflavin T (ThT) and Congo Red (CR) are

widely used. These dyes are very good molecular probes for the identification of amyloid fibrils and also help in understanding the mechanism of amyloid fibril formation.

ThT binds to amyloid:

ThT, a benzothiazole dye; usually binds and forms a highly fluorescent complex with amyloid and amyloid-like fibrils (Gessel et al., 2012, Sulatskaya et al., 2012, Robbins et al., 2012). ThT is highly soluble in water and has a moderate affinity to fibrils (Groenning, 2009). ThT binds various fibrils such as exposed β-sheet edges, an extended β-sheet surface, as well the laminated "steric zipper" interface between the β-sheets and cross-β sheet architecture (Wu et al., 2008). This cross-β structure has a specific arrangement of side chains that are called "cross-strand ladders". These cross-strands ladders are made up of repeating side-chain interactions running across β-strands that are parallel to the long axis of the fibril (Biancalana et al., 2008). The mechanism of ThT binding is well illustrated in Figure 7. The critical micelle concentration (CMC) of ThT is 4.0 μM in water. At above the CMC these molecules self assembled in water and enhance the fluorescence intensity (Khurana et al., 2005). The minimal size required for ThT binding is at least five channel or more β-strands of a flat β-sheet surface (Wu et al., 2009). From the isothermal titration calorimetry (ITC) results it was found that ThT has two binding sites in insulin amyloid fibrils and 0.1 moles of dye binds per mole of insulin in fibril form. In a study it has been found that the binding capacity of ThT remains unaffected by pH, but the affinity was lowest at acidic pH (Groenning et al., 2007). In solution, the benzylamine and benzathiole ring of ThT rotates freely at low energy barriers and rotation occurs because of carbon-carbon bond. Due to rotation the excited photon is quenched causing low fluorescence emission. In case of amyloid fibril the rotation is immobilized and ThT binding site is locked thus leading to enhancement of fluorescence emission (Biancalana and Koide, 2010). ThT does not bind to wild-type peptide self-assembly mimic (PSAM) because it contains charged or polar amino acid residues on its surface. It has been suggested that ThT requires hydrophobic residues particularly aromatic amino acids for interaction (Biancalana et al., 2009). From the molecular dynamic simulations study the binding mechanism of ThT to neutral analog 2-(4′-methylaminophenyl benzothiazole [BTA-1] and model protofibrils showed that two binding sites are located one at the grooves of the β-sheet surface and other at the

ends of the β-sheet (Wu et al., 2008). However, there is one drawback in using ThT in that it binds to non amyloid structures as well such as P-site of human Acetylcholinesterase (De Ferrari et al., 2001),(Harel et al., 2008).

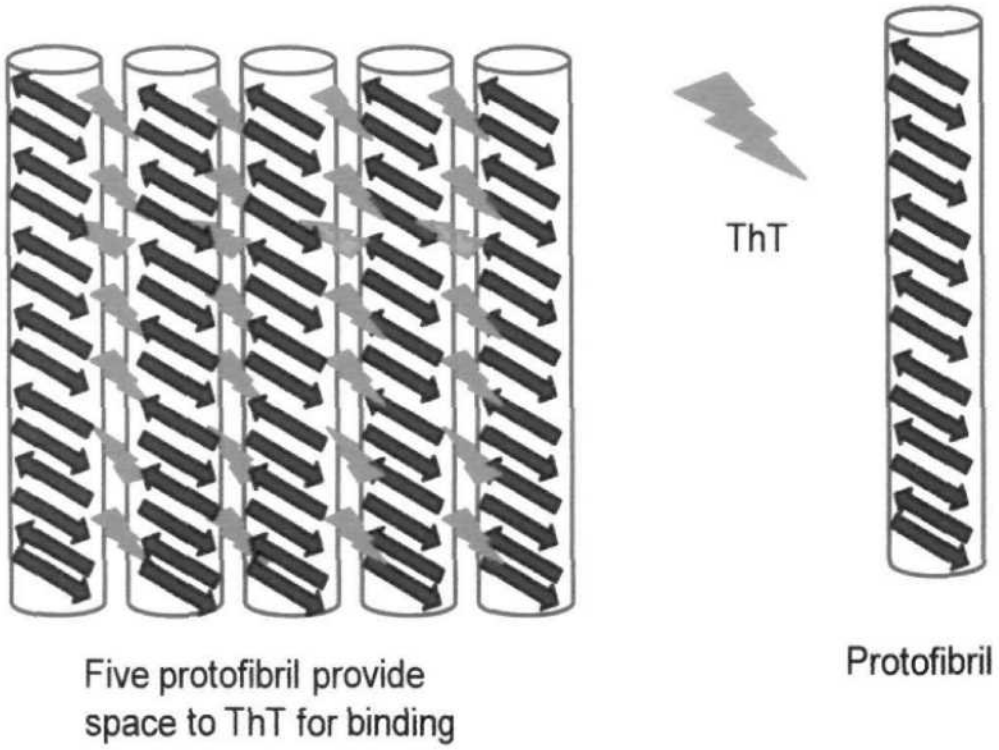

Figure 7 Mechanism of ThT binding to amyloid fibril a schematic presentation

Congo Red (CR) binding to amyloid:

CR is commonly used as a histological stain and is amyloid specific dye. CR is a symmetrical linear molecule and its chemical name is 3,3′-[(1,1′-biphenyl)-4,4′-diylbis(azo)] bis-(4-amino-1-naphthalene acid) disodium salt. It contains two hydrophobic phenyl rings at the center which is attached through diazo bonds to two charged naphthalene moieties. These charge groups are sulfonic acid and amine groups. The mechanism of interaction of CR with amyloid fibrils is not well understood. Generally, it is believed that CR binds to cross β-pleated sheets of fibrils (Klunk et al., 1989). Upon binding to amyloid fibril, a change in the absorbance maximum occurred and the wavelength is red shifted from ~490 to ~540 nm and increased the apple-green birefringence and dichroism under polarized light (Khazaei et al., 2012). On the basis of CR structures the binding is believed to occur through hydrophobic benzidine centers and negatively charged sulphate and positively

charged amino acids residues of protein (Turnell and Finch, 1992, Roterman et al., 2001). CR interacts with amyloid in two possible ways. CR molecules are highly specific for β-sheet and bind along the fibril axis and proposed mechanism is that it intercalates in between antiparallel β-pleated sheets of amyloid fibrils by aromatic stacking and binding is electrostatic because of negatively charged sulphate groups of CR and positively charged amino acid residues of proteins (Klunk et al., 1994, Roterman et al., 2001). The second method is highly specific for β-strand. In this method CR intercalates between two β-strands in the antiparallel β-sheets (Carter and Chou, 1998). Sometimes CR is directly inserted between the two neighboring β-strands only after fibril formation but this is a problem because it has to overcome large energy barrier by breaking the main-chain/side-chain hydrogen bonds between neighboring strands. In another way CR binds at the end of β-sheet which is sandwiched by another β-strands (Wu et al., 2007). CR is not only specific for β-sheets structure but also for various other secondary structures like α and α/β and β configurations (Khurana et al., 2001, Sereikaite and Bumelis, 2006). CR also induces aggregation or amyloid fibril formation (Findeis, 2000, Rudyk et al., 2000). CR has dual behavior at lower concentration it accelerates the fibril formation but at higher concentration it inhibits the amyloid fibril formation (Esler et al., 1997, Piekarska et al., 2001). CR also binds to native or partially folded states of proteins (Inouye et al., 2000, Heegaard et al., 2000).

Nile Red:

Nile red is an uncharged, heterocyclic dye that is sparingly soluble in water but is highly soluble in organic solvents and shows less photosensitivity (Greenspan et al., 1985). It is a hydrophobic dye and its fluorescence maximum depends on the polarity of environments (Sackett and Wolff, 1987). Earlier this dye has been used as a red fluorescence probe for checking the aggregation state (Uversky and Fink, 2004, Sutter et al., 2007). Since the binding of ThT is afftected by pH at a low pH the fluorescence intensity is 10 fold decreased (Lindgren et al., 2005). Due to this limitation Nile red is used because it works well under acidic conditions but its main drawback is solubility. Free Nile red gives maximum emission peaks at 650 nm after excitation at 350 nm and when it binds to amyloid the emission maximum is blue shifted around 25 nm. The Nile red also binds to a molten globule of bovine carbonic anhydrase II (BCA II) and fluorescence is blue shifted as compared to lysozyme fibrils (Mishra et al.,

2011a). One major drawback in using this dye is that it not only interact with amyloid in tissue but also has high affinity for lipids (Mukherjee et al., 2007).

1-anilinonaphthalene-8-sulfonate (ANS):

ANS are broadly used *in vitro* to check the changes in protein conformation. ANS fluorescence is totally environment dependent, it is essentially nonfluoresent in water but it is highly fluorescent in presence of hydrophobic environments (Semisotnov et al., 1991). ANS binds to hydrophobic part of proteins and emits maximum fluorescence. Maximum fluorescence was observed when ANS binds to hen egg white lysozyme aggregates after 6 hours incubation (Kumar et al., 2008). The fluorescence intensity of ANS is also high when it binds to misfolded Aβ42 (Hadley et al., 2011). The rate of aggregation of hen egg white lysozyme was increased 10-folds when incubated with SDS at pH 9.2 and ANS fluorescence intensity was also increased more at pH 9.2 than at pH 7, 8, 9 and 10 (Jain et al., 2011).

Role of negatively charge surfactants and lipids in amyloid fibril formation:

Various negatively charged additives have also been used for the induction of amyloid fibril. These molecules are surfactants, lipids and glycosaminoglycans.

Negatively charge surfactant:

Sodium dodecyl sulphate (SDS) is negatively charged surfactant containing negatively charged head group and hydrophobic tail and it also mimics the structure of biological membranes. SDS interacts with proteins and changed both their secondary and tertiary structures (Reynolds and Tanford, 1970, Yonath et al., 1977). SDS is an anionic surfactant which has been widely used to induce the amyloid fibril (Reynolds and Tanford, 1970, Yonath et al., 1977, Yamamoto et al., 2004, Kihara et al., 2005). At low concentration of SDS, the natively folded β2-microglobulin monomer is converted into partially folded α-helix which further stabilized the fibril structure (Yamamoto et al., 2004). The positively charge surface of hen egg white lysozyme is neutralized in presence of SDS which leads to turbidity and the precipitation of the solution and this precipitation was reduced by raising the pH (Pirzadeh et al., 2006). The mechanism of SDS induced aggregation involves interaction of the negative charge head of SDS with the positive charge surface of

lysozyme and hydrophobic tail is inserted into the groove of protein where hydrophobicity is high (Moosavi-Movahedi et al., 2007). SDS induces amyloid fibril formation in beta 2-microglobulin protein through the nucleus dependent mechanism (Ohhashi et al., 2005). A monomer of beta 2-microglobulin protein was ultrasonicated in the presence of 0.5 mM SDS at pH 7.0 and the native structure of β2-microglobulin was destabilize which leads to oligomers formation (Kihara et al., 2005). SDS shows dual behavior such that at very low concentrations (0-0.1mM SDS) it induces amyloid fibril formation in hen egg white lysozyme while at higher concentrations (0.25-20 mM SDS) it inhibits the amyloid formation at pH 2.0. Thus, it is concluded that the SDS head group interacts with the oppositely charged surface of hen egg white lysozyme electrostatically (Hung et al., 2010). A secondary structural transition was also observed in Amyloid beta-peptide$_{1-42,}$ the α-helical content of protein was converted into β-sheet structure at the submicellar concentration of SDS (Sureshbabu et al., 2009). Studies have shown that below 2 mm SDS concentration the protein structure is extended and exposes the hydrophobic clusters which provide favorable condition for amyloid fibril formation (Ahmad et al., 2006). Recently, we have reported that SDS induces amyloid fibril formation in various proteins when the proteins pH was below two unit of their pI. Thus, major conclusion of this study is that at pH below pI protein becomes positively charged and interacted with the negative charge head of SDS while the hydrophobic tail repels the water molecules around the proteins and binds to exposed hydrophobic residue which ultimately leads to aggregation (Khan et al., 2012).

Lipid induced amyloid fibril formation:

Many processes inside the cell are dependent on lipid-protein interaction like signal transduction, intracellular transport, enzyme catalysis, energy conversion in the cell, antimicrobial defense, and control of membrane fusion (Lee, 2004, Palsdottir and Hunte, 2004). The general physiochemical properties of lipid protein-interactions are phase state, bilayer curvature, elasticity, surface charge and degree of hydration but it also depends on the chemical nature of lipid such as alkyl chain, which may be saturated/unsaturation and lipid head groups (Jensen and Mouritsen, 2004). All of these factors affect the protein conformation and provides suitable environments for the aggregation of proteins and peptides (Fernandez and Berry, 2003, Fernandes et al., 2003). Lipid bilayer works as catalyst for amyloid fibril formation and provides

appropriate environments for the orientation and conformational changes in proteins which assemble into protofibrillar and fibrillar structures (Sparr et al., 2004). The phosphatidylcholine (PC) vesicles containing anionic lipids 1,2-Dioleoyl-sn-glycero-3-(phospho-L-serine) sodium salt (DOPS) were incubated with IAPP proteins the fibril formation is increased markedly by the time $0\text{-}10^3$ seconds as compared to PC vesicles. This reflects that the interaction is strongly electrostatics (Sasahara et al., 2010).For example Aβ proteins possess positive charge which interact electrostatically with negatively charged phosphatidylinositol and gangliosides and thereby self associate into β-sheets (Choo-Smith and Surewicz, 1997, McLaurin et al., 1998). Similarly, phosphatidylserine (PS) as well as other acidic phospholipids maintain the low pH of the cell membranes due to their negative charged head which interact with the positive part of protein and forms protein fibers (Zhao et al., 2004). When amyloid-β peptide (Aβ) was incubated with 1-palmitoyl-2-oleoyl-*sn*-glycero-3-phosphocholine (POPC) possessing varying percentage of G_{M1} no amyloid fibril were detected but when peptide were interacted with pure POPC vesicles containing 5 and 10% of G_{M1} ,the marked increase in ThT-fluorescence was noticed whereas in presence of 20 % or 30% of G_{M1} the ThT-fluoresence intensity remains virtually unchanged (Chi et al., 2007). The interaction between Aβ and negatively charged lipids are electrostatic in nature (Chauhan et al., 2000). Amyloid-β peptide (Aβ) were also incubated with lipids monolayers which contains zwitterionic 1,2-dipalmitoyl-sn-glycero-3-phosphocholine (DPPC), cationic, 2-dipalmitoyl 3-trimethylammonium propane (DPTAP) and anionic lipids 1,2-dipalmitoylsn-glycero-3-[phospho-rac-(1-glycerol)] (DPPG).The data showed that only anionic lipids enhanced amyloid fibril formation because negative head of lipid electrostatically interacted with Aβ while other lipids did not form electrostatic interaction with Aβ because they lacked negative charge (Chi et al., 2008). The recombinant amyloidogenic light chain variable domain, SMA, strongly interacted with lipid vesicles which has 1,2-dipalmitoyl-sn-glycero-3-phosphocholine/1-palmitoyl-2-oleoyl-sn-glycero-3-phosphate (DPPC/POPA) and drastically hastened fibril growth due to electrostatic interaction (Meng et al., 2008).

In this thesis we had discussed the mechanism of protein aggregation by taking various types of proteins viz albumins, lysozyme etc. along with the stability issue of banana lectin as well as serum albumins.

CHAPTER 1

Adapted from: **PLoS ONE (2012) 7: e29694**

Sodium Dodecyl Sulphate (SDS) can be Utilized as an Amyloid Inducer: A Case Study on Diverse Proteins

1.1. Introduction:

While the majority of the proteins may acquire completely folded and functional conformation under *in-vivo* conditions, some of these undergo misfolding due to several reasons. It still remains unclear whether amyloid development is commenced by native state of proteins, partially or totally unfolded states. The amyloid formation is often linked to genetic mutations that can efficiently destabilize the native state, suggesting that a conformational change is the first essential step in amyloidogenesis (Rochet and Lansbury, 2000, Uversky and Fink, 2004). The partially unfolded states of a protein produced under high temperature, high pressure, low pH or moderate concentrations of organic solvents exhibit more propensity to aggregate. Due to several biological and environmental factors, the partially folded intermediates of proteins undergo α/β or β-sheet transition, a characteristic feature of amyloidosis. Amyloid formation is usually a pathogenic process where proteins undergo a conformational change and self-assemble into nonfunctional but toxic fibrils (Zerovnik, 2002). This process is linked with a wide range of human disorders such as Alzheimer's and Creutz-feldt-Jacob disease, senile systemic amyloidosis, type 2 diabetes and dialysis amyloidosis, etc. Amyloid fibrils are also formed in endogenous proteins where they perform normal functions. Hence the amyloid formation is not always harmful as evidenced from the simple to complex organisms (Chiti and Dobson, 2006, Fowler et al., 2006). Sodium dodecyl sulphate (SDS), an anionic surfactant having negatively charged head group and hydrophobic tail, mimics the structure of lipid molecules of biological membranes. SDS is often used as a denaturant that destroys protein's native conformation; it provides an anionic micellar interface that has been shown to accelerate the aggregation of Aβ (1-40) over a limited range of (low SDS) concentrations (Yagi et al., 2007). Understanding the nature of protein–surfactant interaction is of vital interest and allows us to gain insight into the binding mechanism between the two components and its consequent effect on protein structure and functions in the complex (Vasilescu M, 1999, Valstar A, 2000). Since the conditions required to induce aggregation vary from protein to protein, the objective of this study was to provide a simple legislative to induce protein

aggregation or amyloid formation with SDS by choosing appropriate pH conditions based on isoelectric point (pI). The aggregates so formed were studied using various spectroscopic as well as microscopic methods including circular dichroism, turbidity measurements, intrinsic fluorescence, Thioflavin T (ThT) binding and transmission electronic microscopy.

1.2. Materials and Methods:

1.2.1. Materials:

Human serum albumin [HSA], porcine serum albumin [PSA], bovine serum albumin [BSA], sheep serum albumin [SSA], rabbit serum albumin [RSA], ovalbumin [Oval], *Mucor javanicus* lipase [*M. Java*], lysozyme [Lyso], invertase [Invert], hemoglobin [Hb], glucose oxidase [GOD], gelatin, fetuin, concanavalin A [ConA], α-lactalbumin [ALA], cobra toxin [Cobra], *Candida rugosa* lipase [Cand], β-lactoglobulin [BLG], bovine liver catalase [BLC], α-amylase [Alp Amy], conalbumin [CA], chymopapain [Chymo], rat IgG [RIgG], asialofetuin [AFT] and SDS were purchased from Sigma Chemical Co. (St. Louis, MO, USA). Banana lectin [BL] was purified from banana pulp. All other reagents used were of analytical grade. Abbreviations used for particular proteins are mentioned adjacent to the name of each protein in parentheses.

1.2.2. Protein concentration determination:

The stock solutions of all proteins were prepared in neutral buffer. Protein concentration was determined with BCA (Bicinchoinc acid) kit as well as UV-Visible spectrophotometer (Perkin Elmer Lambda25). The concentration of each protein was taken to be 5.0 μM.

1.2.3. pH determination:

pH measurements were made using Mettler Toledo Seven Easy pH meter (model S20) serial no-1229505169, which is routinely calibrated by standard buffer. The pH of the buffer for each protein was set two units below and above its isoelectric points. Experiments were conducted in 20 mM of following buffers- pH 1.4 (KCl-HCl); pH 2.4, 2.5, 2.7, 2.94, 3.1, 3.2, (Glycine-HCl); pH 3.4, 3.65, 3.7, 3.9, 4.26, 4.69, 5.1, 5.4, 5.69, 5.8 (Sodium acetate); pH 6.4, 6.5, 6.7, 6.94, 7.1, 7.2, 7.4, 7.6, 7.7, 7.9, 8.4 (MOPS); pH 8.69, 9.1, 9.2, 9.69, 9.8 (Glycine-NaOH) and 12.4, 13.2 (KCl-NaOH) . All buffers were filtered through 0.45 μM syringe filters.

To avoid any complication due to micelle formation, the molar concentration of SDS was taken as 500.0 μM (0.5 mM) which is far less than its critical miceller concentration (CMC) in distilled water (8.0 mM). Before all spectrophotometric measurements, each protein (5.0 μM) was incubated in buffer containing 100-fold molar excess of SDS (500 μM) for 1 hour at 25 °C. The proteins at neutral pH as well as in buffer at pH below two units of pI, both devoid of SDS, served as control A and control B respectively. Similarly, SDS containing protein samples in the buffer at pH above two units of pI were taken as control C.

1.2.4. Rayleigh Scattering measurements:

Rayleigh scattering measurements were performed on a Hitachi F-4500 fluorescence spectrophotometer at 25 °C in a 1 cm path-length cell. Protein samples were excited at 350 nm and spectra were recorded in the range of 300-400 nm. Both excitation and emission slits were fixed at 10 nm. Data were plotted at 350 nm.

1.2.5. Turbidity measurements:

The turbidity of the all protein (5.0 μM) samples below two units of pI in the presence and absence of 500 μM SDS was monitored by UV absorbance at 350 nm using a Perkin Elmer UV/VIS spectrometer model lambda 25 in a cuvette of 1 cm path length. The measurements were carried out at 25 °C.

2.2.6. ThT binding assay:

A stock solution of Thioflavin T (ThT) was prepared in double distilled water. The concentration of ThT was determined using an extinction coefficient of 36000 $M^{-1}cm^{-1}$ at 412 nm. Protein (5.0 μM) samples at different pH values were incubated in 1:1 molar ratio of ThT (5.0 μM) for 30 minutes in a dark at 25 °C. The fluorescence of ThT was excited at 440 nm. The spectra were recorded from 450 nm to 600 nm and plotted at 485 nm. The excitation and emission slit width were both fixed at 10 nm. Spectra were also subtracted from appropriate blanks.

1.2.7. Circular dichroic (CD) measurements:

Circular dichroic measurements were performed on a JASCO spectropolarimeter (J-815). The instrument was calibrated with D-10-camphorsulfonic acid. All measurements were made at 25 °C with a thermostatically controlled cell holder attached to a peltier with Multitech water circulator. Spectra were collected with a

scan speed of 100 nm min^{-1} and a response time of 2 s. Each spectrum was average of three scans. Far-UV CD spectra were taken in the range of 200-250 nm range in a cell of 0.1 cm path length. All spectra were smoothed by the Savitzky–Golay method with 25 convolution width. The percent secondary structure content of alpha class proteins was calculated by K2d method.

1.2.8. Transmission Electron Microscopy (TEM):

Transmission electron micrographs were collected on JEOL transmission electron microscope operating at an accelerating voltage of 200 kV. Fibril formation was assessed by applying 6 µl of protein sample (5.0 µM) on 200-mesh copper grid (CF 200-Cu, lot no-110323) covered by carbon-stabilized Formvar film. Excess of fluid was removed after 2 mins and the grids were then negatively stained with 2 % (w/v) uranyl acetate. Images were viewed at 10000X.

1.3. Results:

1.3.1. Rayleigh Scattering and Turbidity measurements:

Fluorescence intensity (FI) at 350 nm is a sensitive probe to detect aggregation in proteins. The extent of light scattering in protein samples, pH below two units of pI, was measured in the absence and presence of 500 µM SDS. A marked increase in fluorescence intensity at 350 nm was observed in the samples incubated with SDS in buffer at pH below two units of pI (Figure 1.1). The increase in FI was more than five-fold for all proteins taken in the present study as compared to controls A, B and C suggesting the aggregate formation (Table1.1). (Santiago et al.). The possibility of pH dependent aggregation in proteins was ruled out by measuring the scattering at neutral pH (control A) as well as at pH below two units of pI (controls B). As can be observed from (Figure 1.1), only a slight increase in FI occurred in control B as compared to control A, implying that the impact of pH on aggregation appears to be far less than that of SDS. The turbidity measurements taken at 350 nm for protein incubated with 500 µM SDS at pH below two units of pI, also revealed significantly enhanced turbidity, thus giving further evidence in support of aggregate formation (Figure 1.2 and Table 1.1).

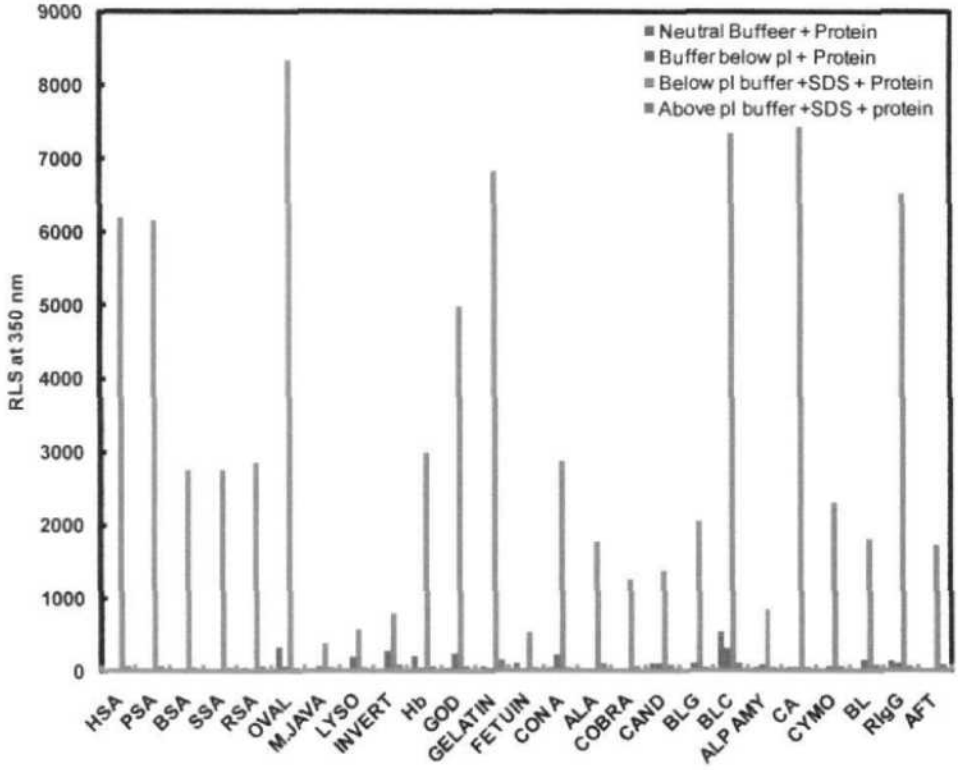

Figure 1.1. Effect of SDS on many proteins were seen by Rayleigh scattering measurements. Rayleigh scattering measurements at 350 nm in the absence as well as presence of 500 μM SDS at pH below and above two units of respective pI. Data at neutral pH + protein [dark blue], pH below two units of pI + protein [red], pH below two units of pI + 500 μM SDS + protein [light green], pH above two units of pI + 500 μM SDS + protein [purple]. The molar ratio of protein to SDS was 1:100.

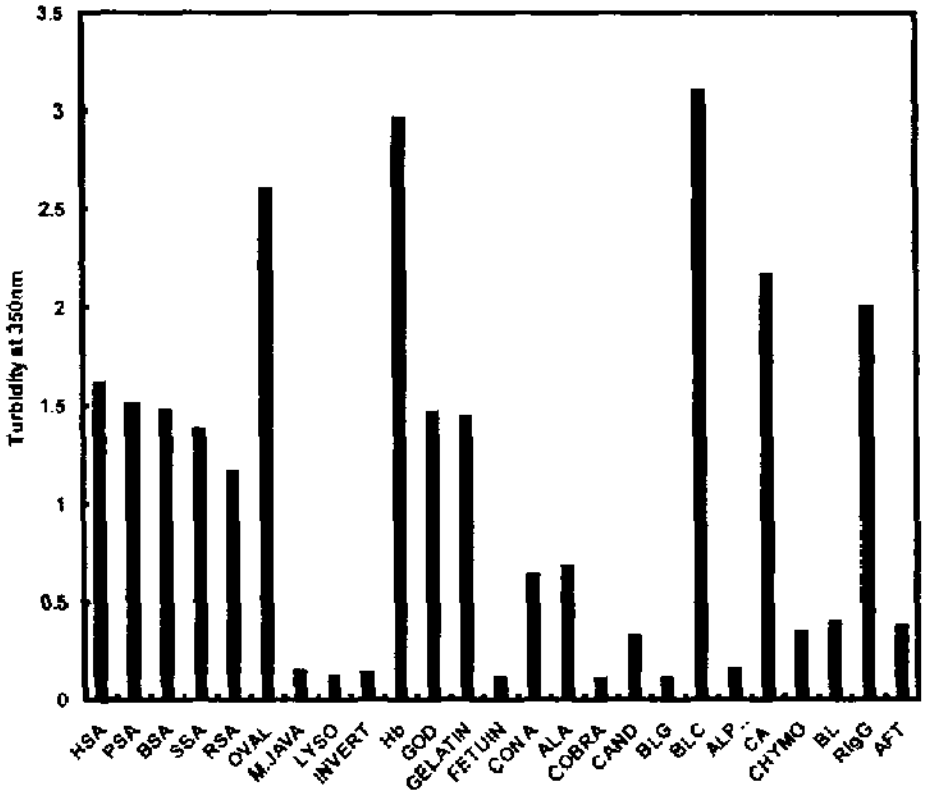

Figure 1.2. Aggregation behavior of all proteins in the presence of SDS was measured by Turbidity. The turbidity measurement of proteins at 350 nm pH below two units of pI in the presence of 500 μM SDS.

2.3.2. ThT binding studies:

ThT is a benzothiazole dye that exhibits enhanced fluorescence emissions upon binding to amyloid fibrils and does not bind to amorphous aggregates as well as non amyloid structures (Khurana et al., 2005). Thus, ThT binding assay was performed to characterize the nature of aggregates induced by SDS. Protein (5.0 μM) samples containing 500 μM SDS at pH below two units of pI revealed strong ThT binding as indicated by enhanced ThT the fluorescence intensity whereas little or no change that ThT fluorescence was noticed in controls A, B and C (Figure 1.3 and Table 1.1). The results confirm the formation of aggregates with fibrillar structure and thus, the possibility of amorphous aggregate formation was ruled out.

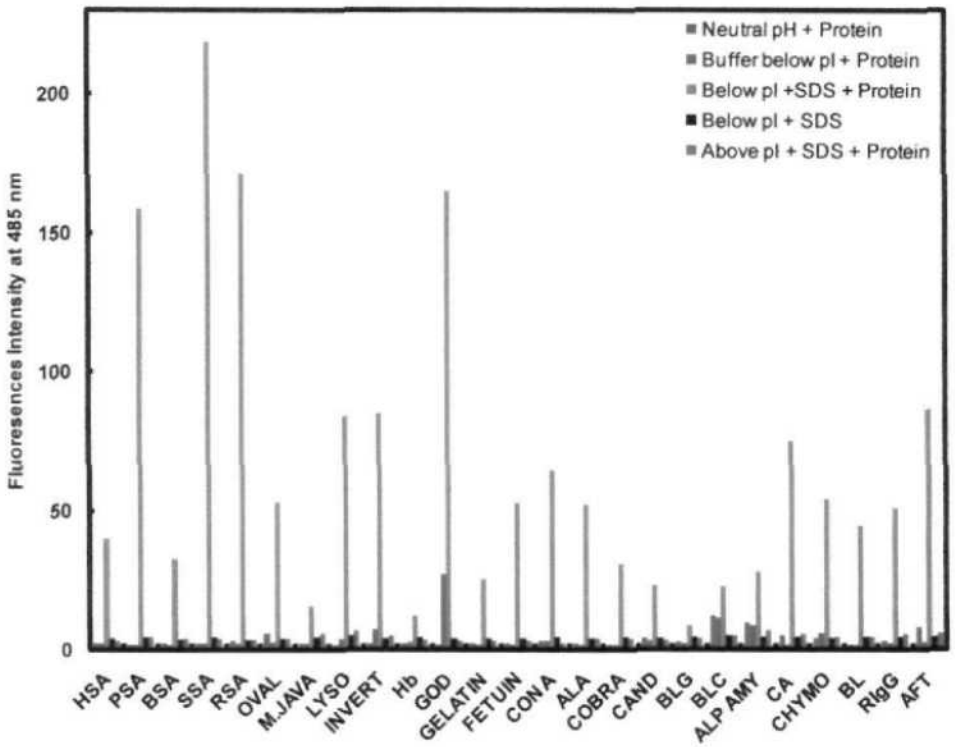

Figure 1.3. ThT dye binding to detect the amyloid fibril. ThT fluorescence intensity data at 485 nm at neutral pH + protein [dark blue], pH below two units of their pI + protein [red], pH below two units of their pI + SDS + protein [light green], pH above two units of their pI + SDS [purple], pH above two units of their pI + SDS + protein [black] The molar ratio of protein to ThT was 1:1.

Table 1.1. Spectroscopic properties of all proteins under various experimental conditions.

S. No.	Protein	pI	Rayleigh Scattering at 350 nm			Turbidity at 350 nm			ThT fluorescence intensity at 485 nm			
			pH below pI + protein	pH below pI + SDS + protein	pH above pI + SDS + protein	pH below pI + protein	pH below pI + SDS + protein	pH above pI + SDS + protein	pH below pI + protein	pH below pI + SDS + protein	pH below pI + SDS	pH above pI + SDS + protein
1	HSA	5.67	36.01	6191	61.22	0.01	1.62	0.01	2.17	39.80	4.24	3.12
2	PSA	5.89	27.38	6160	61.00	0.01	1.52	0.01	2.00	158.50	4.56	4.54
3	BSA	5.65	28.88	2754	59.00	0.01	1.49	0.01	2.02	32.90	3.84	3.99
4	SSA	5.63	30.10	2750	60.00	0.013	1.39	0.02	2.07	218.40	4.35	4.08
5	RSA	5.70	42.45	2860	72.00	0.01	1.18	0.01	2.43	171.20	3.60	3.68
6	Ovalbumin	4.50	68.47	8341	47.75	0.01	2.61	0.01	2.76	52.97	3.92	4.30
7	*M.javanicus*	5.90	75.86	386	45.00	0.01	0.16	0.01	2.04	16.11	4.42	5.88
8	Lysozyme	11.20	189.10	561	53.36	0.01	0.14	0.01	4.20	83.97	4.85	6.89
9	Invertase	3.40	268.20	793	78.00	0.01	0.16	0.02	7.33	84.78	3.96	4.79
10	Hemoglobin	7.10	56.41	2986	69.00	0.02	2.98	0.01	2.65	12.30	4.42	3.46
11	Glucose oxidase	4.94	249.30	4996	60.60	0.01	1.48	0.01	27.09	165.10	4.19	3.10

12	Gelatin	4.70	44.82	6828	146.80	0.01	1.45	0.01	1.94	25.38	4.10	3.23
13	Fetuin	5.21	25.77	532	59.16	0.01	0.13	0.01	1.89	52.75	3.92	3.23
14	Concanavalin A	5.43	222.60	2871	48.20	0.01	0.65	0.03	3.05	64.68	4.55	2.13
15	α- lactalbumin	4.40	31.31	1766	98.00	0.01	0.69	0.01	1.82	52.38	3.93	4.12
16	Cobra toxin	7.69	32.64	1250	74.00	0.01	0.12	0.01	1.98	30.69	4.55	3.98
17	*C.rugosa* lipase	4.70	101.10	1384	80.00	0.01	0.34	0.01	3.17	22.97	4.08	2.99
18	β-lacto globulin	5.20	109.40	2056	50.62	0.01	0.12	0.01	2.42	8.71	4.53	3.98
19	BLC	5.40	311.30	7349	111.00	0.02	3.11	0.01	11.22	22.63	4.80	4.79
20	α-amylase	5.90	85.83	843	46.86	0.01	0.17	0.01	8.77	28.07	4.35	6.89
21	Conalbumin	6.69	59.08	7433	51.66	0.02	2.17	0.01	1.96	75.02	4.33	5.44
22	Chymopapain	10.40	67.00	2309	69.00	0.01	0.36	0.01	5.90	54.04	3.98	4.34
23	Banana lectin	6.26	52.90	1812	78.00	0.01	0.41	0.01	1.77	44.37	4.49	4.57
24	Rat IgG	7.80	107.50	6525	63.00	0.01	2.01	0.01	2.42	50.82	4.37	5.46
25	Asialofetuin	5.10	36.23	1720	90.00	0.01	0.39	0.01	2.61	86.31	4.31	5.79

1.3.4. Secondary Structure Determination:

Far UV-CD was used to determine the secondary structure content of proteins. On the basis of secondary structure, several classes of proteins were used in the present study including α-class, β-class, α+β class and proteins with pronounced random coil conformation. α-class and α+β class proteins exhibit two negative peaks, one at 208 nm and other at 222 nm, while β-class proteins show single negative peak between 215 nm and 222 nm. Random coil proteins give single negative peak around 200 nm. The influence of SDS induced aggregates on secondary structure contents of all proteins remained unaltered in control samples A and B (Figure 1.4A and 1.4B). In the presences of 500 μM SDS, however, pronounced conformational changes were observed (Figure 1.4C). All α-class proteins acquired a single negative peak suggesting their transition into β-sheet conformation while proteins belonging to α+β class showed a gain in their β-sheet content. Similarly in β-class and random coil proteins, the negative elipticity reduced upon aggregation. The above secondary structure transitions are characteristic features of amyloid fibrils (Villegas et al., 2000) (Schmittschmitt and Scholtz, 2003, Moosavi-Movahedi et al., 2007). Table 1.2, summarizes the secondary structure content for only α-class proteins since K2d software is not sensitive enough for other classes of protein.

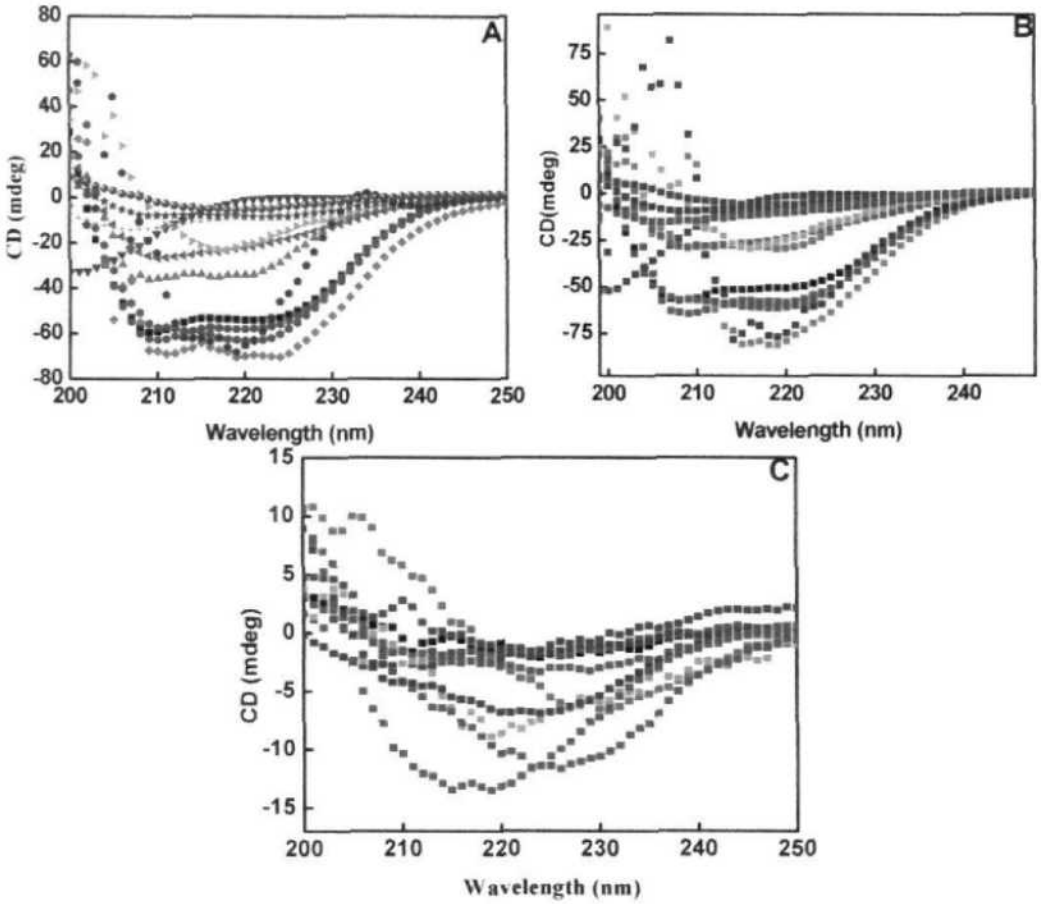

Figure 1.4. Secondary structural changes were monitored at different condition. Far-UV CD spectra of the proteins at [A] neutral pH, [B] pH below two units of their pI in absence of SDS, and [C] pH below pI in presence of SDS. Spectra are shown for HSA [black], RSA [red], GOD [green], Gelatin [blue], BLC [aqua], CA [pink], RIgG [yellow], Oval [dark green], Hb [dark blue], Invert [purple], BL [dark red], AFT [orange]. Some Spectra are omitted for sake of clarity. [The presecent of secondary structure contents for α-class protein was calculated by K2d methods].

Table 1.2. % Secondary structure content of the proteins in different experimental conditions.

Protein	pH 7.4			pH below pI			pH below pI+SDS		
	α-helix	β-sheet	RC	α-helix	β-sheet	RC	α-helix	β-sheet	RC
HSA	60	8	32	57	10	33	5	47	48
PSA	62	7	31	59	8	33	5	47	48
BSA	62	7	31	60	8	32	5	47	48
SSA	62	5	33	59	8	33	5	47	48
RSA	63	6	31	64	6	30	4	48	48
Ovalbumin	80	13	7	84	8	8	4	48	48
Lysozyme	41	15	44	43	22	35	4	48	48
Hemoglobin	60	5	35	61	5	34	4	44	48
Glucose oxidase	38	3	59	29	16	55	9	47	44
Conalbumin	36	21	53	27	19	54	5	47	48
Chymopapain	29	16	55	30	14	56	17	32	51
BLC	27	18	55	25	27	48	16	39	45
α-lactalbumin	25	24	51	17	34	49	12	41	47
Asialofetuin	12	40	48	19	31	50	18	38	54

1.3.5. Morphology determination by TEM:

The morphology of aggregates formed was further investigated using electron microscopy. In the past, several authors have reported amyloid induction in the presence of 500 μM SDS (Yamamoto et al., 2008, Hung et al., 2010). Proteins in respective below pI buffers were incubated with 100-fold molar excess of SDS for 1 hour and were subsequently examined. Fibriller structures resembling typical amyloid fibril were clearly noticeable in all protein samples (Figure 1.5). However, no fibril formation was detected in the samples without SDS (data not shown).

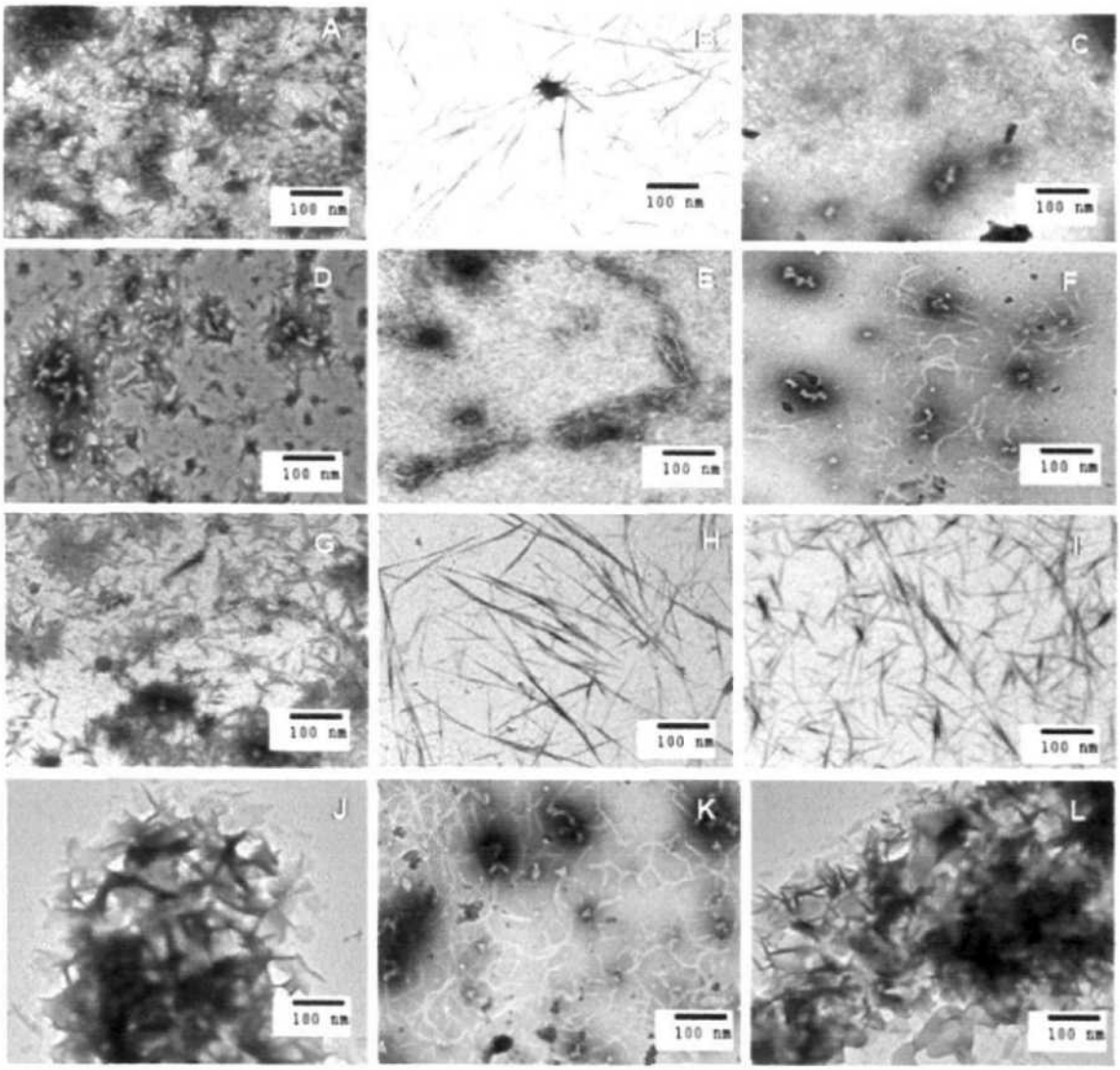

Figure 1.5. Morphology of aggregates were visualized by TEM. TEM images of 12 representative proteins showing amyloid fibrils in the presence of 500 μM SDS below two units of their pI. [A] AFT, [B] ALA, [C] BLC, [D] CA, [E] Cand, [F] Con A, [G] Gelatin, [H] GOD, [I] Hb, [J] HSA, [K] Oval, [L] RSA.

1.4. Discussion:

The aggregation of proteins in the presence of very low concentration of SDS has already been reported earlier but the role of pI in SDS induced aggregation has not yet been discussed (Stenstam A, 2001, Yamamoto et al., 2004, Ahmad et al., 2006, Hansted et al., 2011). The partially unfolded state of a protein produced under high temperature, high pressure, low pH and moderate concentration of organic solvents exhibits a tendency towards aggregation (Chiti et al., 2000, Ferrao-Gonzales et al., 2000, McParland et al., 2000). In the present study we have made an attempt to devise

a general approach to induce aggregation in proteins and explore the mechanism behind aggregation by anionic surfactant. It is well documented that proteins acquire net positive charge pH below two units of its isoelectric point. This results in electrostatic repulsion among charged moieties, leading to partial unfolding of the molecules and thus the exposure of hydrophobic patches. A convenient strategy to induce aggregation in such system requires neutralization of positive charge along with increased hydrophobic interactions. Both of these requirements can be successfully satisfied by an amphipathic detergent such as sodium dodecyl sulphate (SDS). SDS contains negatively charged polar head groups and a twelve carbon long non-polar hydrophobic tail. In general, the negatively charged head group of SDS interacts with positive charge developed on protein and the hydrophobic region makes contact with its protein counterpart by repelling the water molecules wrapped around the protein molecule. As a result, solute-solvent interactions are perturbed leading to the induction of aggregates (Pertinhez et al., 2002). In the present study, a total of 25 proteins belonging to different families and conformational classes were subjected to pH below two units of their respective pI followed by incubation with 100-fold molar excess of SDS (500 μM). Aggregation occurred readily in all proteins possibly due to neutralization of the positive charge (developed pH below two units of pI) and provision of favorable hydrophobic interaction by SDS, thus collapsing the molecules into aggregates. Furthermore, to investigate the leading forces behind the aggregation phenomenon, we conducted the same experiment at pH above two units of pI in the presences of 500 μM SDS. We, however, could not get aggregates under this condition possibly due to the development of net negative charge (above pI) which did not allow the interaction of negatively charged SDS head groups with the proteins because of charge-charge repulsion. These findings suggest the possible role of electrostatic interactions behind amyloid induction. Besides, the involvement of electrostatic interactions in aggregation it is also highlighted by the fact that the negatively charged group present in the polysaccharide chain of heparin and heparin sulphate of GAG enhances the aggregate formation in mAcP (Motamedi-Shad et al., 2009a). Similar findings have been reported by group of Shweta et al (Jain and Udgaonkar, 2010), where in the presence of anion, moPrP molecules becomes a worm-like fibrils because anion binds to opposite-charged proteins via neutralizing charge-charge repulsion. Studies have reported that the elimination of the terminal

charges of tetrapeptide KFFE and KVVE by acetylating the N-terminus and amidating the *C*-terminus appreciably reduced fibril formation. Similarly, fibril formation of KFFE and KVVE was more prominent in water than in phosphate buffer, demonstrating that charge attractions are important in fibril formation (Tjernberg et al., 2002). These findings suggest that electrostatic interactions play a major role in aggregation. The twelve carbon- long chain of SDS, however, is large enough to avoid the importance of hydrophobic interaction in the aggregation process. This is also proved by the fact that the detergent (MMPA) with longer hydrocarbon chain length (12-C) induces aggregation while those (MCPA) with shorter (6-C) alkyl chain are incapable in this regard (Hagihara et al., 2002). Furthermore, it has been shown that SDS (anionic) but not DTAC (cationic), SB12 (amphipathic) and TX 100 (non-ionic) surfactants interact with β2 microglobulin and promote the extension of fibril reaction [18]. All of these findings revealed that both electrostatic as well as hydrophobic forces are a prerequisite for all aggregation processes but electrostatic interactions plays a leading role. Figure 1.6. showed in a hypothetical model describing the present findings where proteins, when subjected to pH below two units of pI, acquire a net positive charge and become partially unfolded. In the presence of appropriate molar concentration of SDS, opposite charges are neutralized along with the provision of favorable hydrophobic interactions between non polar hydrocharbon tails of the SDS and hydrophobic patches of proteins leading to amyloid induction. However pH above two units of pI the protein molecules attain net negative charge forming N' state which exhibits resistance to aggregation towards SDS due to charge-charge repulsion.

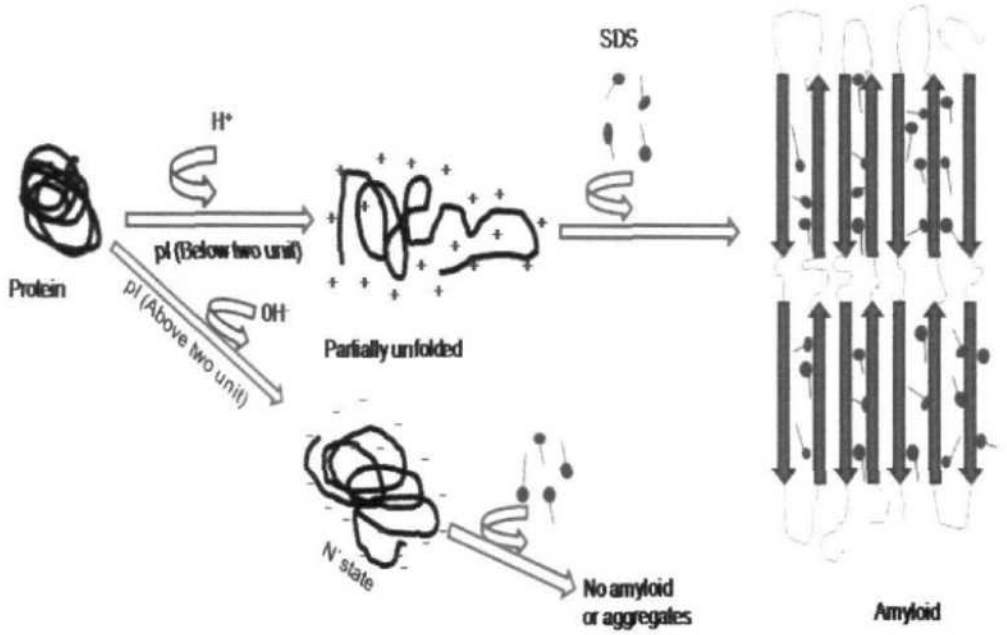

Figure 1.6. A hypothetical model for amyloid formation.

1.5. Conclusions:

In summary, the data presented here indicate that the SDS molecules have great potential to induce amyloid formation when proteins are in partially unfolded states (below two units of pI). Besides we found that for the formation of amyliod fibril both electrostatics as well as hydrophobic interactions are responsible but has former an upper hand. This study is also very helpful for those working in the area of solublization of misfolded proteins since it provides an easier approach to induce the aggregation. Further studies are required to elucidate the type of fibrils formed whether a cross-β, rigid, straight, spherulitic or worm-like structures.

CHAPTER 2

The Influence of Sodium Dodecyl Sulphate in Promoting Amyloid Fibril Formation in Hen Egg White Lysozyme as pH is Lowered from 11.0 to 1.0

2.1. Introduction:

Proteins require correctly folded conformations to show their biological function. Major diseases such as Alzheimer's, Parkinson's, Huntington's, Senile systematic amyloidoses, type II diabetes and many others are caused by the abnormal function of proteins through adoption of an incorrect conformation (Stefani and Dobson, 2003b, Luheshi et al., 2008, Uversky, 2008, Stefani and Dobson, 2003a). In addition to *in-vivo* studies, much *in-vitro* work has been performed to gain insight into the mechanism of amyloid formation. However, the detailed mechanism of amyloid formation is still under debate (Chiti et al., 2003). Under *in-vitro* conditions amyloid fibrils are generated by employing harsh conditions such as high temperature, high pressure, extreme acidic or alkaline pH and by the use of cosolvents, metal ions, lipid assemblies and surfactants (McParland et al., 2000, Uversky and Fink, 2004, Tougu et al., 2009, Bhattacharya et al., 2011, Simon M. Loveday, 2011). These conditions cause protein molecules to adopt partially folded conformations that facilitate fibrillation in a relatively short time. The characteristic features of amyloid structures are high β-sheet content, fibrillar morphology, enhanced ThT fluorescence intensity and Congo red birefringence (Dobson, 2004). In this context protein–surfactant interactions have been widely studied due to their applications in pharmaceutical, chemical, and cosmetic industries (Wang, 2005, Wang et al., 2011, Li et al., 2006). Anionic surfactants and particularly SDS are now widely used for amyloid fibril formation at different conditions (Sureshbabu et al., 2009, Andersen et al., 2009, Naidu and Prabhu, 2011). SDS-contains, a negatively charged head and a 12 carbon hydrophobic tail for which it is also said to mimic some characteristics of biological membranes. SDS can induce amyloid formation in proteins below its critical micellar concentration (CMC) and has ability to induce helical conformations in many proteins above its CMC (Rizo et al., 1993, Ahmad et al., 2006). The CMC of SDS in distilled water is around 8 mM. In our previous report we have shown how SDS induces amyloid in numbers of proteins when subjected to pH below their isoelectric point (pI) and demonstrated that fibril formation is determined mainly by electrostatic

interactions (Khan et al., 2012). The present study is aimed at exploring the response of protein conformation towards SDS upon varying pH from acidic to alkaline. We further investigate the role of charge in amyloid induction using several spectroscopic techniques complemented with calorimetry and microscopy. In this study, we took hen egg white lysozyme as a model protein. Researchers had studied lysozyme before, using different methods to understand the mechanism of protein aggregation (Frare et al., 2004, Holley et al., 2008, Morshedi et al., 2010, Liu et al., 2012). While some groups have shown amyloid induction in lysozyme by SDS under alkaline conditions, others have reported that SDS can also induce fibril formation in lysozyme in an acidic environment (Hung et al., 2010, Jain et al., 2011). However, thus far the detailed explanation for such behavior was not been discussed. Hen egg white lysozyme shares 60% homology with its human counterpart, which is involved in hereditary non-neuropathic systemic amyloidosis (Booth et al., 1997). Hen egg white lysozyme belongs to $\alpha+\beta$ class of protein and contain 129 amino acid residues, out of which nine are negatively charged while 17 are positively charged residues. It consists of two domains, residues 1–36 and 87–129 belong to an alpha domain, and residues 37–86 belong to a beta domain (Eyles et al., 1994). In this study we demonstrate how lysozyme aggregates in the presence of SDS and tried to elucidate the mechanism of amyloid fibril formation. pI of lysozyme is ~11.0 which makes it a good choice for studying the effect of pH variation on SDS induced aggregation.

2.2. Material and Methods:

3. Materials:

Hen egg white lysozyme, Thioflavin T (ThT), sodium dodecyl sulfate (SDS) and Congo red were purchased from Sigma Chemical Co. (St. Louis, MO, USA). All other reagents used were of analytical grade. Double distilled water was used throughout the study.

3.1. Methods:

2.3.1. Protein concentration determination:

A stock solution of 500 μM was made in 20 mM Tris-HCl buffer pH 7.4 and concentration was determined using a UV-Visible spectrophotometer (Perkin Elmer Lambda25) εM = 37970 M-1cm-1 at 280 nm. The stock of lysozyme was further

diluted 33.33 times in the respective buffer for the measurements and pH of sample did not change.

2.3.2. pH measurements:

pH was determined using Mettler Toledo Seven Easy pH meter (model S20) which was routinely calibrated with standard buffers. The experiments were performed in the pH range 13.0-1.0 with the following 20 mM buffers; KCl-NaOH (pH 13.0-11.0), Glycine-NaOH (pH 10.0-9.0), Tris-HCl (pH 8.0-7.0), Sodium Phosphate (pH 6.0), Sodium Acetate (pH 5.0-3.0), Glycine-HCl (pH 2.0) and KCl-HCl (pH 1.0). All buffers used in the experiments were filtered through 0.45 μm Millipore Millex-HV PVDF filter.

Before performing the turbidity, Rayleigh light scattering, ThT, Congo Red, DLS, Circular dichroism and TEM experiments the protein was incubated with a desired range of buffers at the 25 ^{o}C for 12 h followed by the addition of 20 fold molar excess of SDS (300 μM).

2.3.3. Turbidity Measurements:

Turbidity measurements were performed on a Perkin Elmer double beam UV-Visible spectrophotometer model lambda 25 in a cuvette of 1 cm path length. The turbidity of lysozyme (15 μM) sample incubated at different pH in the absence as well as the presence of 300 μM SDS was determined by monitoring the change in absorbance at 350 nm. All the samples were incubated for 12 hours before the measurements.

2.3.4. Rayleigh scattering measurements:

Rayleigh light scattering measurements were taken on a Hitachi F-4500 fluorescence spectrofluorometer at the 25 ^{O}C in a cuvette of 1 cm path length. The samples were excited at 350 nm and spectra were recorded from 300 to 400 nm. Both excitation and emission slit width were set at 5 nm. The lysozyme sample without SDS served as control. In each case lysozyme concentration was taken 15 μM. All the samples were incubated for 12 hours prior to measurements.

The kinetics of the aggregation process were studied in the presence of SDS at different pH on SHIMADZU RF 5301 PC fluorescence spectrophotometer by exciting the samples at 350 nm and recording the light scattering at 350 nm for 15 minutes. The excitation and emission slit widths were set at 1.5 nm. The lysozyme

concentration was 1.0 μM and SDS was 20 μM for kinetic studies in order to maintain the ratio of protein to SDS as1:20.

2.3.5. ThT binding assay:

A stock solution of ThT was prepared in double distilled water and filtered with 0.2 micron Millipore filter. The concentration of ThT was measured using molar extinction coefficient ε_M = 36000 $M^{-1}cm^{-1}$ at 412 nm. The protein samples (15.0 μM), in the absence as well as presence of 300 μM SDS, were incubated at different pH values for overnight. Post incubation, samples were supplemented with 15 μM ml^{-1} of ThT solution, and were further incubated for 30 minutes in the dark. The ThT was excited at 440 nm and spectra were recorded from 450 to 600 nm. The excitation and emission slit widths were set at 10 nm. The spectra were subtracted from an appropriate blank.

2.3.6. Congo Red (CR) binding assay:

A Stock solution of Congo red was prepared in double distilled water and filtered for further use. The concentration was determined using ε_M = 45000 $M^{-1}cm^{-1}$ at 498 nm. The protein concentration was taken 15.0 μM and incubated at different pH for overnight (~12 hrs). Aliquots of Congo Red (15.0 μM), were mixed with protein (15.0 μM), in the absence and presence of SDS in a molar ratio of 1:1 and kept for 15 min at 25 °C. The absorbance spectra (300-900 nm) of the resulting samples were recorded on UV-Visible spectrophotometer (Perkin Elmer Lambda 25) in a 1 cm path length cuvette.

2.3.7. Dynamic light scattering (DLS) measurements:

The change in aggregation behavior of lysozyme at different pH values was determined using DLS techniques. The R_h measurements were taken with a protein concentration of 70.0 μM at 830 nm by using DynaPro–TC–04 dynamic light scattering instrument (Protein Solutions, Wyatt Technology, Santa Barbara, CA) equipped with a temperature-controlled microsampler. All the solutions were filtered through 0.22 μm pore sized microfilter (Whatman International, Maidstone, UK). Measured hydrodynamic radius (R_h) was the average of 50 measurements taken at 25 ^{O}C. The mean R_h and polydispersity (P_d) were estimated, on the basis of an

autocorrelation analysis of scattered light intensity based on the translational diffusion coefficient, from the Stokes–Einstein equation:

$$R_h = \frac{kT}{6\pi\eta D_W^{25°C}}$$

where R_h is the hydrodynamic radius, k is the Boltzman's constant, T is the absolute temperature, η is the viscosity of water and $D_W^{25°C}$ is the translational diffusion coefficient. All the samples were incubated overnight prior to measurements.

2.3.8. Far-UV CD measurements:

The circular dichroic measurements were performed on a JASCO spectropolarimeter (J-815) with a thermostatically controlled cell holder attached to a peltier with multitech water circulator.

The experiments were carried out after 12 hours of incubation at 25 °C and spectra were scanned in the range of 200-250 mm in a cuvette of 0.1 cm path length. Each spectrum was an average of three scans. The spectra were smoothed by the Savitzky-Golay method with 25 convolution width. The results were expressed as mean residual ellipticity (MRE) in deg cm^2 $dmol^{-1}$ which is defined as:

$$\text{MRE} = \theta_{obs}\,(\text{mdeg})\,/10 \times n \times Cp \times l$$

where θ_{obs} is the CD in millidegree, n is the number of amino acid residues l is the path length of the cell in centimeters and Cp is the molar fraction of protein. The percent secondary structure was calculated by online K2d software. In all CD measurements the lysozyme concentration was invariably 15.0 μM.

2.3.9. Transmission Electron Microscopy (TEM):

TEM images were taken on Philips CM-10 transmission electron microscope operating at an accelerating voltage of 200 kV. The amyloid fibril formation was assessed by applying 6 μL of lysozyme (15.0 μM) containing 300 μM SDS on 200-mesh copper grid (CF 200-Cu, lot no-110323) covered by carbon-stabilized formvar film. Excess of fluid was removed after 2 min and the grids were then negatively stained with 2% (w/v) uranyl acetate. Images were viewed at 10000X. Before taking the image all the samples were incubated overnight.

2.3.10. Isothermal titration calorimetry (ITC):

The calorimetric measurements were taken on a titration calorimeter from Microcal (Northampton, MA) at the 25 ^{O}C in 20 mm buffer pH 11.0-1.0. Before running the experiment, all the solutions were filtered and degassed on Thermovac. The sample cell was filled with 70 μM lysozyme at the desired pH values while the reference cell contained respective buffers. SDS (7mM) was introduced a syringe while ensuring the removal of any trapped air bubbles. The titration experiments consisted of 28 injections of 10 μL each of duration 20 s with 2 s filter period and 180 s spacing between each injection. The stirring speed was 307 RPM. The analog input range was +/21.25 V and the reference power was set at 20 μcal s^{-1}. Control experiments were performed by titrating SDS into the same buffer to obtain the heats of ligand dilution.

3.2. Results:

3.2.1. Turbidity measurements:

The increase in absorbance of protein sample at 350 nm is a measure of turbidity which gives an idea about the extent of aggregation in the solution. In many reports, the change in absorbance was found to be due to the change in number and size of the protein-surfactant complexes (Mir et al., 2012, Bourgault et al., 2011). Figure 2.1A shows the change in turbidity of lysozyme at different pH values following incubation with or without 300 μM SDS. As can be seen the turbidity of the SDS+lysozyme increased with decreasing pH values and attained a maximum turbidity at pH 1.0. On the other hand, the turbidity of the control samples were insignificant and more or less same at all pH values. Suggesting that the SDS itself was not showing any turbidity at all the pH taken in this study. In Figure 2.1B similar pattern was obtained from, lysozyme versus varying concentrations of SDS, as monitored by absorbance at 350 nm. The maximum change in absorbance was found in the range of 0.1 to 0.6 mM of SDS concentration. Beyond this concentration the absorbance was dropped down. From this observation it can be concluded that SDS have strong capacity to induce aggregation in the concentration range of 0.1 to 0.6 mM. This is so because the interaction between SDS and lysozyme might be electrostatic and beyond this concentration hydrophobic interaction was highly favorable.

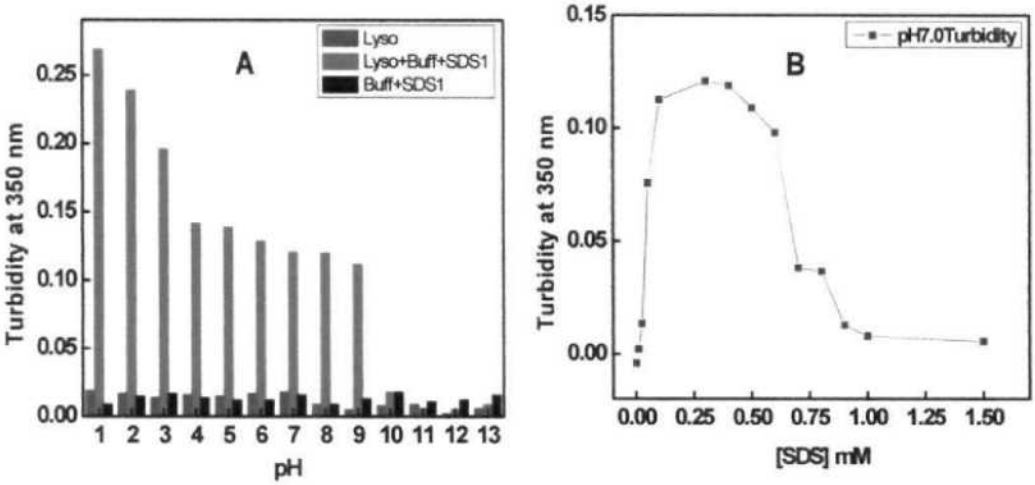

Figure 2.1. Influence of SDS to induced aggregation in lysozyme was seen at diffent pH. A. Turbidity of samples was measured by taking the optical density at 350 nm. Lysozyme (15.0 μM) was incubated in the absence (■) and presence of (■) 300.0 μM SDS at different pH for 12 hrs. The turbidity was also checked only in the presence of 300.0 μM SDS at different pH (■). Turbidity of lysozyme was also measured with respect to varying concentration of SDS at pH 7.0 at 25 °C (Figure 3.1 B).

2.4.2. Rayleigh light scattering:

The light scattering at 350 nm is another important parameter used to determine the extent of aggregation. The increase in the scattering at this wavelength is due to the rise in aggregation. The change in scattering at 350 nm of lysozyme, in the absence as well as the presence of 300 μM SDS, at different pH values is shown in Figure 2.2A. The results further supported the fact that lowering the pH promotes aggregation of lysozyme by SDS. Besides that, negative controls (samples at different pH values without SDS in it) showed negligible scattering suggesting that the aggregation was not pH dependent, but has been induced by SDS It is true that sometimes surfactants do make micelles or large particle in a solution on its own and shows scattering during the experiment. This can lead to erroneous readouts. This is why before performing the experiment, we made sure that up to 300 μM of SDS in solutions (of different pH values taken in this study) is not scattering any light on its own. In Figure 3.2B the maximum scattering was found in the range of 0.1 to 0.6 mM of SDS that's why we have chosen one particular concentration of SDS in all the pH studied.

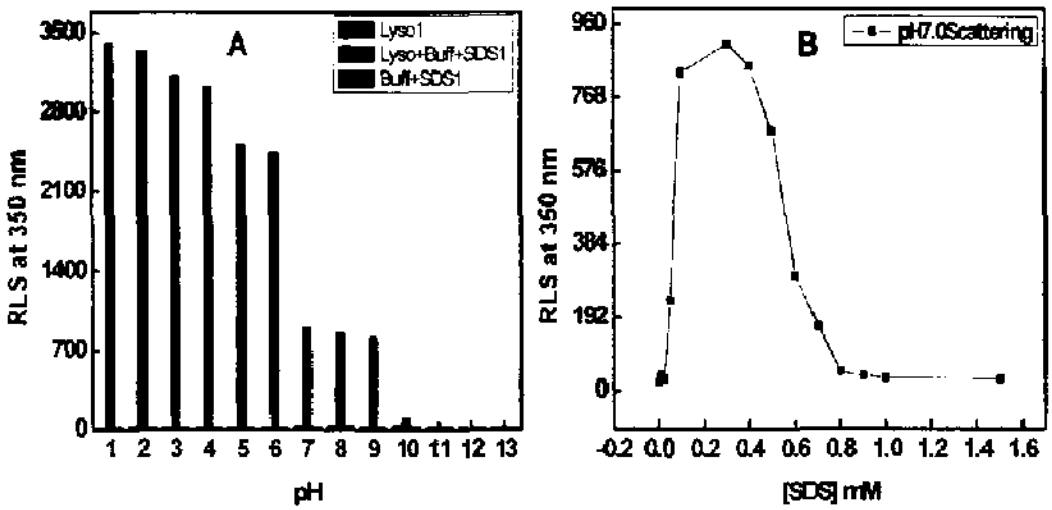

Figure 2.2. Aggregation of lysozyme was measured by Rayleigh light scattering (RLS). A. RLS of lysozyme at 350 nm were obtained in the absence (■), presence (■) of 300.0 μM of SDS at different pH. The RLS were also check only in the presence of 300.0 μM SDS at different pH (■). The change in RLS of lysozyme versus SDS in mM at pH 7.0 (Figure2B). Prior to measurements lysozyme (15.0 μM) was incubated at different pH in the presence of 300.0 μM SDS for 12 hrs.

2.4.3. Kinetics of aggregate formation:

The SDS-induced aggregation of lysozyme was also followed as a function of time at different pH values under the define condition as discussed earlier. The kinetics of lysozyme aggregation in the presence of SDS at pH 11.0 to 1.0 was studied by monitoring RLS at 350 nm. To make figure clear only few points are shown in Figure 2.3. At pH 11.0 in the presence of SDS no scattering was observed with respect to time while below pH 11.0 the scattering of light increased correspondingly with a maximum at pH 1.0 (Figure 2.3). The aggregation induced by SDS is without any lag phase. The aggregation was induced by SDS is without lag phase.

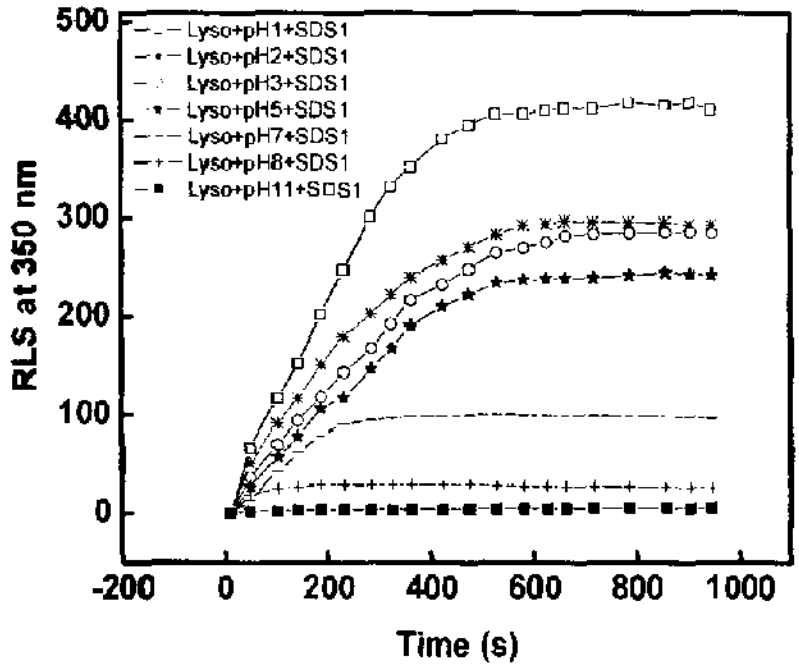

Figure 2.3. Kinetics of formation of amyloid fibrils followed by RLS fluorescence measurements. Kinetics of lysozyme were performed by Rayleigh light scattering (RLS) at 350 NM at different pH conditions in the presence of 20.0 μM SDS.

3.4.4. ThT binding assay:

We further checked whether the nature of aggregation induced by SDS is fibrillar or amorphous. For which we performed ThT binding assay where the SDS-induced aggregated lysozyme was incubated with ThT and nature of binding was analysed by measuring changes in the ThT fluorescence intensity. ThT is very commonly used as an amyloid detector as it is reported to bind specifically to the characteristic β-sheet structure of amyloid fibrils (Ahmad et al., 2009a, Sukenik et al., 2011). The ThT fluorescence spectra of lysozyme at different pH values, in the absence and presence of 300 μM SDS, are shown in Figure 2.4A. The binding of ThT to lysozyme in the absence of SDS was quite insignificant throughout the pH range, whereas in the presence of SDS a strong ThT binding was found in all the pH values as shown in Figure 2.4B. The ThT fluorescence intensity at 485 nm was markedly increased in the presence of 300 μM SDS when pH values were lowered from 11.0 to 3.0. A slight decrease in fluorescence intensity below pH 3.0 could be attributed to the charge-charge repulsion between positively charged protein as well as ThT. Similar ThT binding pattern was also reported below pH 3 (Khurana et al., 2005). We further

confirmed ThT binding whether it binds to SDS micelles or SDS induced amyloid fibril we took appropriate control. In this context ThT was not showing significant binding with SDS at different pH values data are shown in Figure 2.4C. The above results, suggested that SDS induces aggregates of fibrillar structure in lysozyme and aggregation increases with decreases in pH.

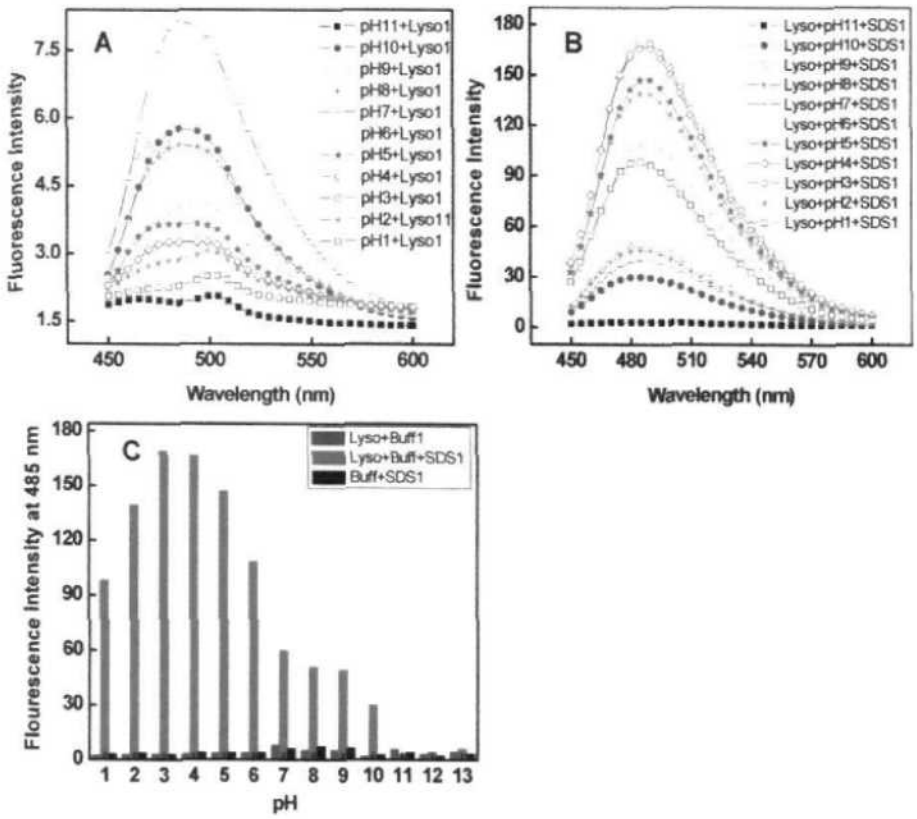

Figure 2.4. Amyloid fibrils formation was measured by ThT fluorescence. ThT fluorescence spectra of lysozyme (15.0 μM) in the absence (A) and presence (B) of 300.0 μM SDS at different pH. ThT fluorescence intensity of lysozyme at 485 nm as a function of pH in the absence (■), presence (■) of 300.0 μM SDS and also measured only in presence of 300.0 μM SDS at different pH (■) (C). Before the ThT experiments the ThT was incubated with aggregated and non aggregated samples for 30 min in dark.

2.4.5. Congo Red (CR) binding assay:

Since ThT also binds to the oligomer of the proteins we performed CR binding assay to corroborate our hypothesis (Carrotta et al., 2001, Groenning, 2010). Characterization of fibril formation in lysozyme was carried out through CR binding assay. CR is widely used to detect amyloid fibril (Nilsson, 2004). The results from the CR binding assay are shown in Figure 2.5A and 2.5B. The dye binding to protein in the absence of SDS showed a maximum absorbance at 495 nm. However in the presence of 300 μM SDS, the concentration at which fibrils are formed, the absorbance maxima were red shifted to 505 nm at pH 7.0 and to 509 nm at pH 5.0 The data showing shift at other pH values are shown in Table 2.1. These results confirmed the formation of characteristic fibrillar species and ruled out the possibility of mere oligomerization. The reason for this shift is that lysozyme becomes more compact that allows only hydrophobic interaction to take place with SDS at these pH conditions. Unfortunately, the assay could not be performed below pH 5.0 because CR changes colour under acidic condition.

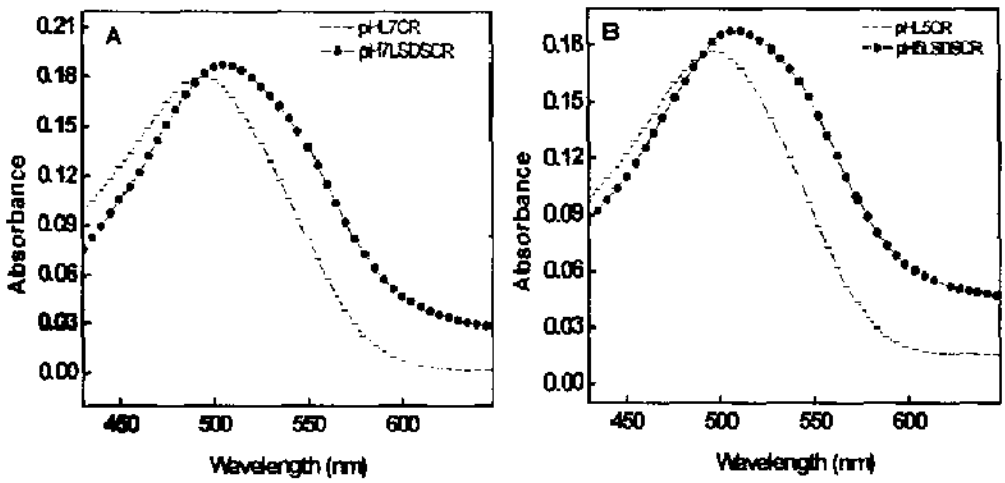

Figure 2.5. CR binding was performed to detect the amyloid fibril. The absorbance spectra of lysozyme obtained from CR binding assay at (A) pH 7.0 and (B) pH 5.0 in the absence (—) and presence (•) of SDS.

Table 2.1. Wavelength shift of lysozyme upon binding with CR at different pH.

pH	Shift in λmax (nm) of lysozyme	Shift in λmax (nm) of lysozyme + 300.0 μM SDS	Difference in λmax (nm) shift
11	496	489	7 (blue)
10	496	493	3 (blue)
9	498	503	5 (red)
8	496	505	9 (red)
7	495	505	10 (red)
6	495	505	10 (red)
5	497	507	10 (red)

3.4.6. Dynamic light scattering measurements:

DLS is a well exploited technique for monitoring the changes in the size of aggregates (Simpanya et al., 2008). It was thus used to determine the pH dependent changes in the size of SDS-induced aggregates in lysozyme (Figure 2.6, Table 2.2). It was found that the intensity of light scattered at 90° increased in the presence of SDS at all pH values studied below the pI of lysozyme. This observation further supports the conclusion that protein aggregates are formed. The increase in light scattering was less pronounced, when pH of the sample was close to pI indicating the inability of SDS to induce aggregation under such conditions (Table 2.2). In the absence of SDS at pH values from 11.0 to 1.0 the light scattering was more or less the same. However there was an increase in R_h value of protein under acidic pH which suggests partial unfolding of the molecule. The results from DLS experiments obtained at pH 7.0 and pH 3.0 are shown in Figure 2.4 and rest of the results are in Table 2.2. The R_h value of protein at pH 7.0 was 2.1 nm while at pH 3.0 it was increased to 3.0 nm. Upon incubation with 1400 μM SDS, two types of species were generated with size 2.8 nm & 54.5 nm at pH 7.0 and 5.3 nm and 154.9 nm at pH 3.0. This observation suggests that the larger aggregates were formed at lower pH.

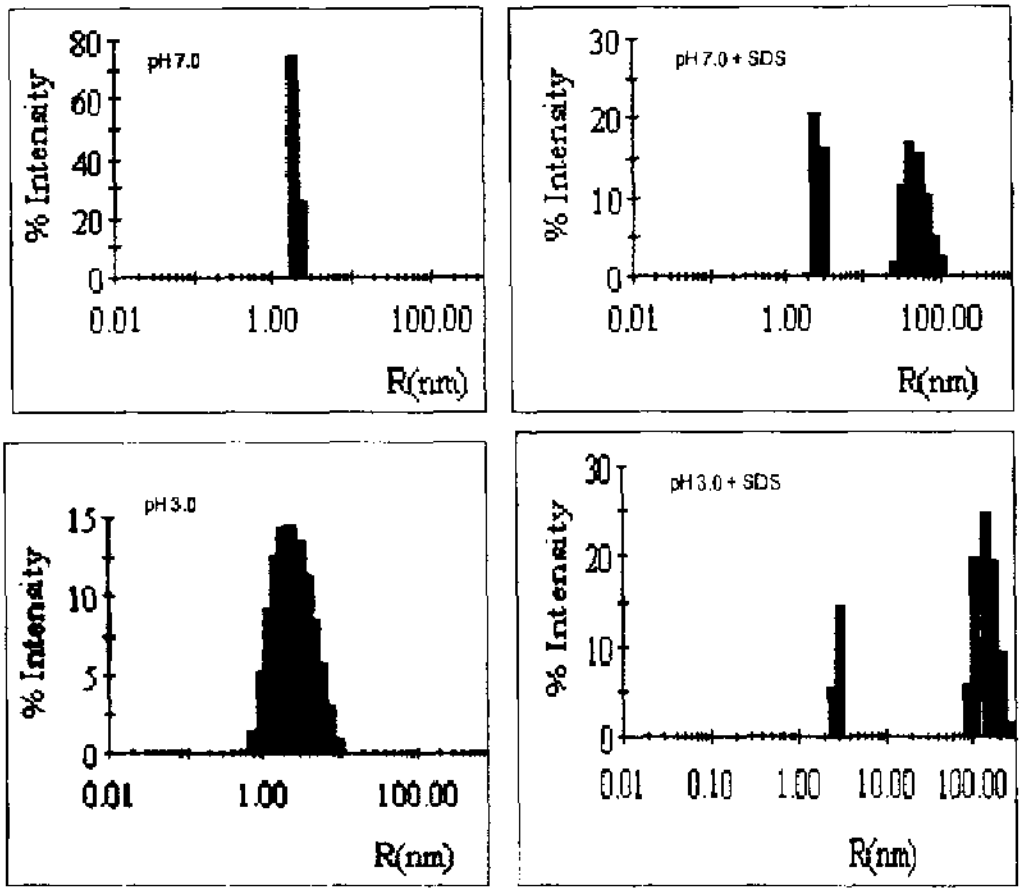

Figure 2.6. Hydrodynamic radii were measured to know the size of aggregates. Dynamic light scattering measurements performed to determine the hydrodynamic radii (R_h) of lysozyme (70.0 μM) in the absence and presence of 1400.0 μM SDS at pH 7.0 and pH 3.0 at 25 °C after 12 hrs incubation.

Table 2.2. Hydrodynamic radii of lysozyme under different conditions at 25 °C.

S.No.	Condition (pH)	Hydrodynamic radii (nm)
1	11.0	3.0 ± 0.1
2	11.0+SDS	2.0 ± 0.09
3	10.0	2.0 ± 0.1
4	10.0+SDS	2.0 ± 0.1, 9.0± 0.1
5	9.0	2.0 ± 0.1
6	9.0+SDS	3.0 ± 0.1, 41.0 ± 0.2
7	8.0	2.0 ± 0.1
8	8.0+SDS	3.0 ± 0.1, 49.0 ± 0.1
9	7.0	2.0 ± 0.1
10	7.0+SDS	2.0 ± 0.1, 54.0 ± 0.2
11	6.0	2.0 ± 0.1
12	6.0+SDS	3.0 ± 0.1, 71.0 ± 0.2
13	5.0	2.0 ± 0.1
14	5.0+SDS	3.0 ± 0.1, 79.0 ± 0.3
15	4.0	2.0 ± 0.1
16	4.0+SDS	3.0 ± 0.1, 112.0 ± 0.1
17	3.0	3.0 ± 0.1
18	3.0+SD	5.0 ± 0.2, 122.0 ± 0.2
19	2.0	3.0 ± 0.1
20	2.0+SD	5.0 ± 0.2, 144.0 ± 0.3
21	1.0	3.0 ± 0.2
22	1.0+SDS	5.0 ± 0.2, 150.0 ± 0.5

2.4.7. Circular dichroic measurements:

The change in the secondary structure of lysozyme (15 μM) was monitored at different pH values, in the absence and presence of 300 μM SDS, using far-UV CD method. Lysozyme belongs to α+β class of proteins and its far-UV CD spectra are characterized by two negative peaks centered around 208 nm and 222 nm (Arnaudov and de Vries, 2005). As shown in Figure 2.7A, in the absence of SDS the spectral features were retained throughout the pH range (11.0-1.0) studied, with some increase in ellipticity at low pH, owing to the formation of some secondary structure elements. When lysozyme was incubated with 300.0 μM SDS, the far-UV CD spectra showed two types of changes. From pH 11.0 to pH 10.0, the protein showed a considerable decrease in ellipticity probably due to loss of structure but the overall spectra quality remaining unchanged (spectra are not shown). On the contrary, the spectra of proteins below pH 9.0 exhibited a transition from α to β-sheet structure characterized by a single negative peak around 219 nm, which is a hallmark of amyloid formation

(Figure 2.7B). For the sake of clarity we have shown spectra at pH 1.0, 3.0, 5.0 and 7.0 as some spectra were overlapping each other. The secondary structure content of the lysozyme at different pH values was calculated by the K2d method and the results are listed in Table 2.3. As can be seen, a prominent increase in β-sheet content of protein, occurring below pH 10.0 in the presence of SDS, clearly suggesting aggregate have defined fibril structure.

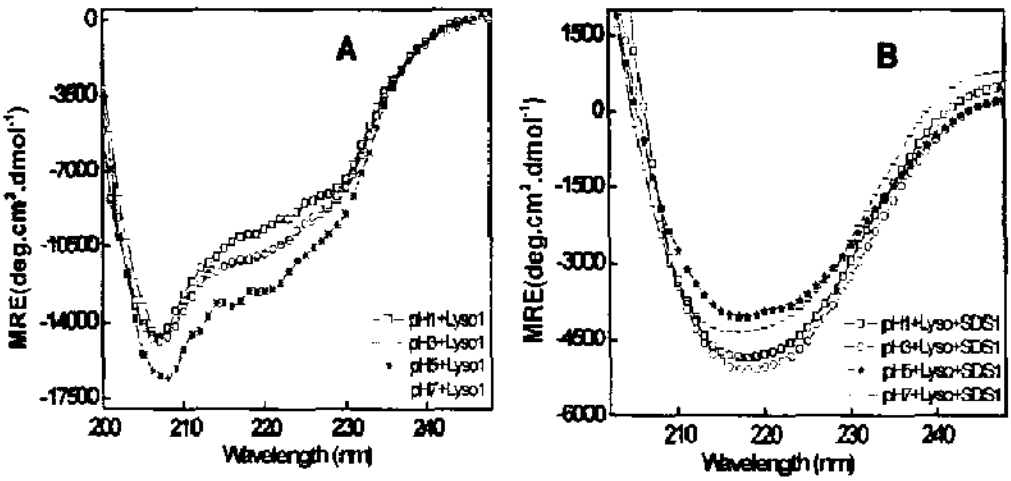

Figure 2.7. Secondary structural transition was measured by Far-UV CD. Far-UV CD spectra of lysozyme (15.0 μM) in the absence (A) and presence of 300.0 μM SDS (B) at pH 1.0 (-□-), 3.0 (-○-), 5.0 (-•-) and 7.0 (----) at 25 °C. Only selected spectra are showing in panel A and B because some spectra are overlapping. Prior to CD measurements the entire sample was incubated for 12 hrs.

Table 2.3. % secondary structure calculated by K2d method at different conditions.

pH	lysozyme			Lysozyme +SDS		
	% α-helix	% β-sheet	% random coil	% α-helix	% β-sheet	% random coil
11.0	40.0	18.0	42.0	45.0	23.0	31.0
10.0	44.0	23.0	33.0	45.0	23.0	31.0
9.0	43.0	22.0	35.0	20.0	45.0	35.0
8.0	44.0	23.0	33.0	18.0	44.0	38.0
7.0	44.0	23.0	37.0	13.0	42.0	55.0
6.0	45.0	23.0	32.0	15.0	35.0	50.0
5.0	45.0	23.0	31.0	5.0	48.0	48.0
4.0	45.0	23.0	33.0	5.0	47.0	48.0
3.0	44.0	23.0	33.0	4.0	48.0	48.0
2.0	44.0	23.0	33.0	4.0	48.0	48.0
1.0	42.0	21.0	36.0	4.0	48.0	48.0

2.4.8. Transmission electron microscopy:

The morphology of lysozyme aggregates was analysed by transmission electron microscopy (TEM). Prior taking the TEM image the lysozyme was incubated with 300 μM of SDS at pH below their pI for 12 hours. Fibril formation was observed at all pH values, we studied, below the pI of lysozyme in the presence of SDS. However, only four representative figures are shown (Figure 2.8). Mature fibrils were observed in all pH values. While in the absence of SDS, at pH below their pI, no significant fibril or aggregates were found (data not shown). Similar type of fibril structure was also found for other proteins as well (Harper et al., 1999, Motamedi-Shad et al., 2009b, Panza et al., 2010).

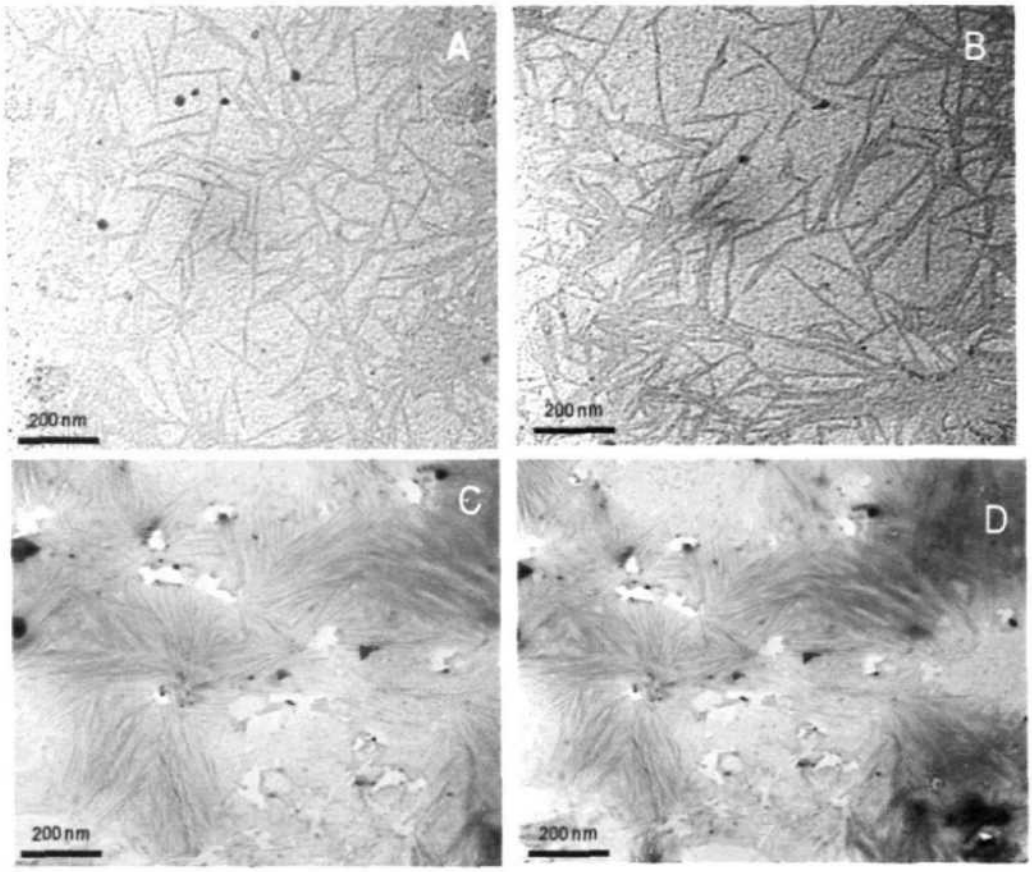

Figure 2.8 Morphology of aggregates were detected by TEM. TEM images of lysozyme (15.0 μM) in the presence of 300.0 μM SDS at pH 9.0 (A), pH 6.0 (B), pH 3.0 (C) and pH 1.0 (D). TEM images were taking after 12 hrs incubation.

2.4.9. Isothermal titration calorimetry:

When ligand binds to proteins the heat is released or absorbed. It is very difficult to understand the nature binding process, in-vivo, whether it is exothermic or endothermic. Therefore we study the binding process in-vitro using isothermal titration calorimetry. From the above spectroscopic results we found that lysozyme aggregates in the presence of 300 μM SDS, at different pH values. Here we used ITC to examine the type of interaction between lysozyme and SDS. In ITC experiments we injected 10 μl of 7 mM SDS, for 28 times into the reaction cell, which is filled with 70 μM lysozyme at the desired pH values. The ITC isotherms showed an exothermic peak when lysozyme was titrated with SDS pH below 10.0 (Figure 2.9). These exothermic peaks reveled us that binding between SDS and lysozyme is electrostatic. Similar type of exothermic peaks were also reported in some proteins at

pH 7.4 (Mitaben D. Lad, 2003). In control experiments heat released is very low. We further explore whether the interactions between lysozyme and SDS were strong or weak at different pH values (11.0-1.0). In the ITC measurements, a less exothermic heat was released at pH 11.0, while below this pH a continuous increase in exothermic heat was observed with maximum heat being released at pH 1.0. The possible explanation for low low heat released at pH 11.0 is that lysozyme becomes uncharged thereby SDS could not bind to it properly. However at lower pH value, lysozyme was protonated favoring negative part of SDS head to interact strongly and release more heat.

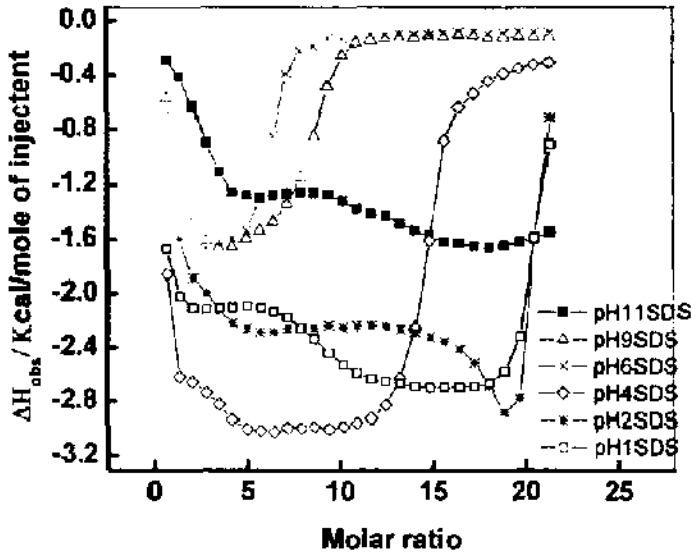

Figure 2.9. Heat released was measured by ITC. Plot of enthalpy change against molar ratio for titration of SDS with lysozyme at pH11.0 (-■-), 9.0 (-Δ-), 7.0 (-×-), pH 4.0 (-◇-), pH 2.0 (-*-) and pH 1.0 (- -).

3.3. Discussion:

Polypeptides and proteins have a generic property of forming amyloid fibrils, which originate from different parts of the protein (Chiti et al., 1999). The lysozyme was incubated at different pH values ranging from 13.0-1.0. The positive charge starts increasing on lysozyme pH below 11.0 and the maximum positive charge was found at pH 1.0. We observed that as the pH of sample was lowered below the pI of lysozyme, in the presence of SDS, the protein began to aggregate — as confirmed by turbidity, light Scattering, DLS and far-UV CD measurements. These results were also supported by the Wang *et al.*(2011), where lysozyme incubated with

phospholipids D6PC and D7PC, showed enhanced light scattering due to the formation of larger aggregates (Wang et al., 2011). The kinetics of aggregation process was measured by Rayleigh light scattering experiments; also the aggregation tendency of different conformations of lysozyme at varying pH values in the presence of SDS was determined. The rate of aggregation was so fast that no lag phase was observed at any of the pH conditions taken in this study. Similar results were obtained for amyloid formation in ApoMb where exponential growth was observed without lag phase (Correa and Ramos, 2011). In this context it is also reported that the amyloid fibril formation of N47A Spc-SH3 is a rapid process without any lag phase. In our case saturation took place within 1200 s, so we conclude that the process was fast and amyloid nuclei established early (Ruzafa et al., 2012). We used ThT binding assay to investigate whether aggregation was amorphous or fibrillar. We observed A continuous increase in ThT fluorescence intensity in the presence of SDS at pH below the pI of lysozyme suggesting that aggregates formed were amyloid fibrils. A slight decrease in ThT fluorescence intensity at pH 1.0 and 2.0 could be attributed to the fact that at acidic pH. The positively charge N-atom of a benzothiazole group of ThT repels the N-atom of Arginine and lysine of lysozyme that may not allow strong binding to the amyloid fibril due to charge-charge repulsion (Khurana et al., 2005). This notion is also supported by the observation that ThT binding to insulin filaments is greater in distilled water than at pH 1.6 (Zako et al., 2009). We further reconfirmed fibril formation of our protein by Congo red dye binding assay. Congo red binds strongly to parallel and antiparallel β-sheet region of the amyloid cross-β structures (Higurashi et al., 2005). The Congo red binding assay was performed to rule out the doubt of that binding to some non-amyloid structures, as it does occasionally. A noticeable red shift was observed at acidic pH indicating strong Congo red binding to protein corresponding to amyloid formation. These two dye binding experiments confirmed that aggregates of lysozyme being formed at all pH values below its pI and having well-ordered structures.

Further, we followed changes in the secondary structure of lysozyme in the presence of SDS at different pH. Generally amyloid fibrils have order β-sheet structure (Suzuki et al., 2011, Kardos et al., 2011). The lysozyme contains both α-helix and β-sheet structure at neutral pH. The α-helical content of lysozyme is converted into β-sheet after incubation with SDS at pH below the pI. Due to this

secondary structure transition we come into conclusion that the aggregate induced by SDS is having order structure which might be amyloid fibril. To confirm it further we also employed transmission electron microscopy to observe the morphology of aggregates. TEM image revealed aggregates formed by SDS is a typical fibrilar structure. It can be concluded that lysozyme exhibits a strong propensity to form amyloid in the presence of SDS at any pH below its pI and the size of the aggregates increases with the increase in positive charge on the protein (as pH moves down from pI).

In Figure 2.10, we have proposed a hypothetical model that explains how SDS induces aggregation in lysozyme. In our previous study, we discussed how SDS induces aggregation in proteins at pH below their pI. Since pI of lysozyme is 11.0, so below this pH the polypeptide will acquire net positive charge. The net charge on lysozyme from pH 11.0-1.0 was calculated using PROTEIN CALCULATOR v3.3 software (Table 2.4). As pH of the protein samples decreases below 10.0, the net positive charge on protein keeps on increasing due to protonation of carboxylate (-COOH) and amino ($-NH_3^+$) group of amino acid side chains. The negatively charged head group of SDS will neutralize more and more positively charged centers on the protein and therefore aggregation propensity as well as the size of aggregate increases accordingly. On the other hand, at pH above 10.0, the lysozyme develops a net negative charge on its surface, which will not bind to the negatively charged SDS due to charge-charge repulsion and ultimately no aggregation is observed.

Table 2.4. Estimated charge over pH range by "PROTEIN CALCULATOR v3.3" software.

S.No.	pH	Total Charge
1.0	11.0	-4.5
2.0	10.0	0.2
3.0	9.0	4.9
4.0	8.0	5.5
5.0	7.0	7.9
6.0	6.0	8.9
7.0	5.0	10.8
8.0	4.0	15.5
9.0	3.0	18.2
2.0	2.0	18.9
1.0	1.0	19.0

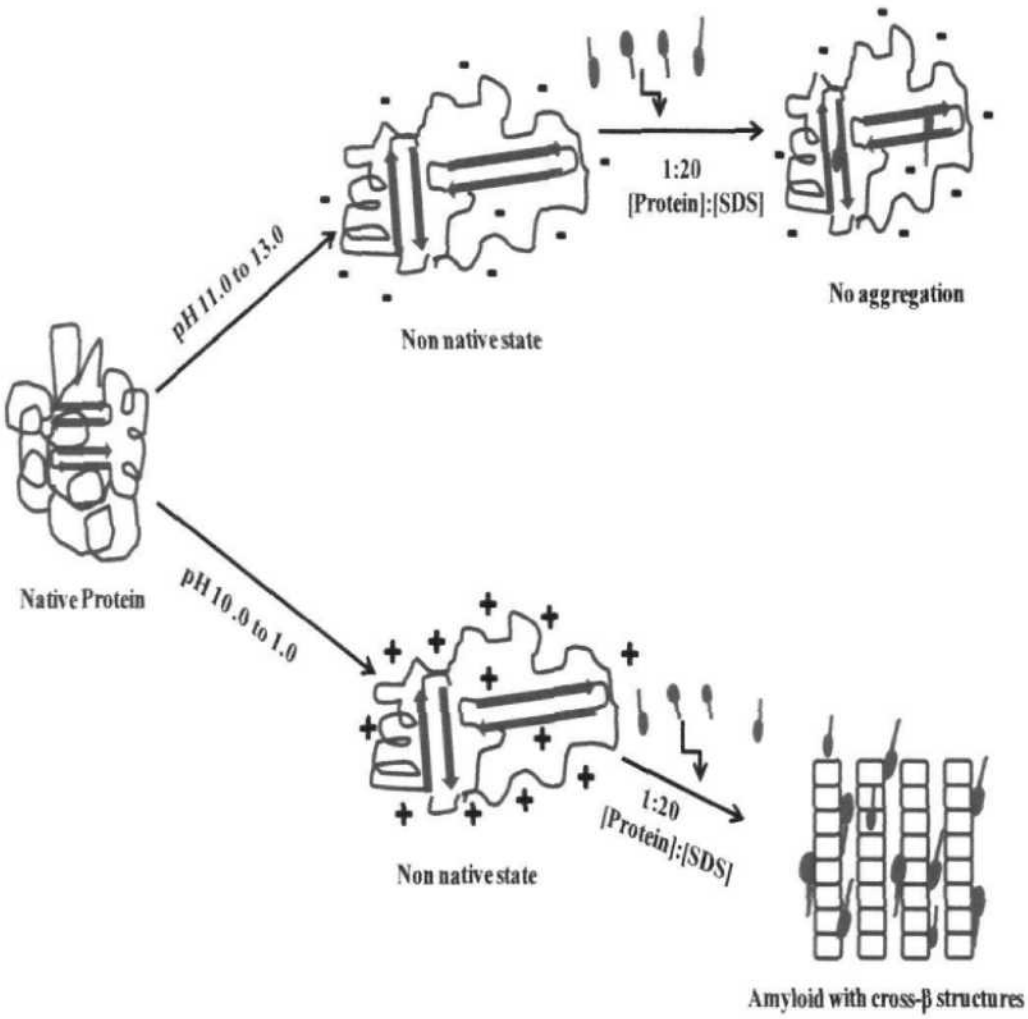

Figure 2.10. Schematic representation of effect of SDS on conformation of lysozyme below and above isoelectric point of protein.

3.4. Conclusions:

From this study it can be concluded that SDS induces aggregation in lysozyme pH below 11.0 and the aggregation propensity was maximum at pH 1.0 because net positive charge increases on lysozyme at lower pH and SDS interacts electrostatically with the oppositely charged surface of lysozyme and leads to assembly of protein into characteristic amyloid fibrils.

CHAPTER 3

Hydrophobicity Alone can not Trigger Aggregation in Protonated Mamalian Serum Albumins

3.1. Introduction:

Amyloid fibril formation is a specific form of protein self oligomerization. Amyloid fibril formation process which is known to be associated with several neuronal as well as non neuronal diseases. Amyloid formation is the results of improper protein folding, therefore partially unfolded conformations or fragmented part of precursor proteins are considered to be more prone to form amyloid fibrils (Uversky and Fink, 2004, Mishra et al., 2007). Considerable progress has been made in understanding the molecular mechanism of amyloid formation, however the comprehensive details of this phenomenon are still not known. Under in-vitro conditions, the fibrils can be generated by using a variety of conditions such as extreme pH, high temperature, high pressure and use of additives etc. (Kumar et al., 1996, Malisauskas et al., 2003, Arora et al., 2004, Kumar and Udgaonkar, 2009). Surfactants are one of the common additives that are employed for inducing amyloid formation. Among various surfactants, SDS is mostly used for this purpose (Necula et al., 2003, Barghorn et al., 2005). The in-vitro studies have provided several useful clues to explore the mechanism underlying amyloid fibril formation. In our previous report, we have demonstrated that SDS can induce aggregation in proteins of different origin at a pH below two units of their respective isoelectric point (pI) due to strong electrostatic interactions between a negatively charged head group of SDS and positively charged center of proteins but we did not explore the role of hydrophobic tail in details (Khan et al., 2012). It is well known that amyloid formation is the result of the complex interplay of both electrostatic as well as hydrophobic forces (Schmittschmitt and Scholtz, 2003, Izawa et al., 2012, Fukunaga et al., 2012, Ramakrishna et al., 2012). In order to emphasize the role of hydrophobic interaction in the formation of amyloid fibrils, we have sought to compare the amyloid inducing capability of three negatively charged surfactants viz sodium dodecyl sulphate (SDS), sodium dodecylbenzene sulfonate (SDBS) and sodium bis-(2-ethyl 1-hexyl) sulfosuccinate (AOT). All of the three surfactants contain single sulphate moiety on the head but differ in length of hydrocarbon tail. SDS contains 12 carbon long aliphatic tails while in case of SDBS and AOT the hydrocarbon tail contain 18 and 20 carbons respectively. The critical

micellar concenterations of theses surfactants are 8.0 mM for SDS, 2.5-4.0 mM for SDBS and 0.8 mM for AOT in distilled water. The protein chosen for carrying out present study were serum albumins viz human serum albumin (HSA), bovine serum albumin (BSA), porcine serum albumin (PSA), sheep serum albumins (SSA) and rabbit serum albumin (RSA). Serum albumins are α-helical globular proteins found in the circulatory system, particularly most abundant in plasma (60%) with an average concentration of 50 g L^{-1}. Their important function is to bind and transport fatty acids, drugs, metabolites and also maintain the colloid of osmotic pressure (Carter and Ho, 1994). The mammalian serum albumins show great similarity in terms of sequence, structure and function (Peters, 1996). They contain single polypeptide chain arranged into three domains (I, II, III) and adopt a heart shaped structure at physiological pH (Sugio et al., 1999). HSA and RSA contain one Trp residues while BSA, SSA and PSA contain two Trp residues. Apart from performing various important functions as mentioned above, albumins are known to form amyloid fibrils under different conditions and hence are well exploited for carrying out aggregation studies (Taboada et al., 2006, Vetri et al., 2007b, Xu et al., 2012).

In the present study, we have examined the effect of increasing concentration of SDS, SDBS and AOT, the surfactants having the same charge at the head but differing in the tail hydrophobicity. In this study we were also trying to know the role of charge and hydrophobicity in amyloid fibril formation of five serum albumins at pH below and above two units of their pI. For this we have employed various spectroscopic techniques as well as microscopy to check the fibril induction propensity of negatively charged surfactant with bearing different hydrophobic tail.

3.2. Material and Methods:

3.2.1. Materials:

Human serum albumin (068K7538V), Bovine serum albumin (110M166IV), Porcine serum albumin (094K7636), Sheep serum albumin (117K7540), Rabbit serum albumin (117K7565), sodium dodecyl sulphate (SDS), sodium dodecylbenzene sulfonate (SDBS) and sodium bis-(2-ethyl 1-hexyl) sulfosuccinate (AOT), Thioflavin T (ThT) and Congo Red (CR) were purchased from Sigma Chemical Co. (St. Louis, MO, USA). All other reagents were used of analytical grade.

3.2.2. Methods:

3.2.3. Protein concentration determination:

The stock solutions of proteins were prepared in 20 mM sodium phosphate buffer pH 7.4. The protein concentrations were determined spectrophotometrically using molar extinction coefficients, ε_m 35700 M^{-1} cm^{-1} (HSA), 43827 M^{-1} cm^{-1} (BSA), 43385 M^{-1} cm^{-1} (PSA and RSA) and 42925 M^{-1} cm^{-1} (SSA) at 280 nm on a Perkin Elmer (Lambda 25) double beam spectrophotometer. The mother stocks of every albumin were prepared in 20 mM sodium phosphate buffer with 200 μM concentrations and which is further diluted for experiments.

3.2.4. pH measurements:

pH measurements were carried out on Metler Tolado pH meter (seven easy S 20-K) using Exper "Pro3 in 1" type electrode. The least count of the pH meter was 0.01 pH unit. The protein samples were prepared in 20.0 mM sodium phosphate buffer pH 7.4. The buffers were filtered through PVDF 0.45 μm syringe filter (Millipore Milex-HV) before using experimental purpose.

3.2.5. Turbidity measurements:

The turbidity was measured in the absence and presence of varying concentration of surfactants (SDS, SDBS and AOT) at pH 3.5 and 7.4 by monitoring the change in turbidity at 350 nm on Perkin Elmer (Lambda 25) in cuvette of 1 cm path length. Before the turbidity measurements albumins were incubated with varying concentration of surfactatants for 12 hrs at both pH. The protein concentrations of albumins were kept 5 μM in all the samples

3.2.6. Rayleigh light Scattering measurements:

Rayleigh light Scattering experiments were performed on Hitachi spectrofluorometer (F-4500) at 25 °C in a cuvette of 1 cm path length. The samples were exited at 350 nm and spectra were recorded in the range of 300-400 nm. Plots between fluorescence intensity (FI) at 350 nm versus varying concentration of surfactants were plotted. The protein concentration in the entire sample was kept 5.0 μM. Both the excitation and emission slit width were set at 5 nm. Before performing the experiments, the albumins were incubated with surfactatnts for 12 hrs at pH 3.5 and 7.4.

3.2.7. Kinetic measurements:

Time kinetics studies were performed on a Shimadzu fluorescence spectrophotometer at 25 °C with a 1 cm pathlength cell. Light Scattering was measured after excitation the sample at 350 nm and emission was taken at 350 nm versus time in seconds. In time kinetics study albumins concentration was kept 0.1 μM and surfactant were taken 40 μM. The data were plotted between fluorescence intensity versus time in second and the data were fitted by origin 7. The albumin concentration was taken very low in kinetics study because limitation of instruments it can not detect the FI beyond 1000. For this purpose we maintained the protein surfactant ratio (1:400).

43.2.8. Thioflavin T (ThT) binding assay:

A stock solution of the ThT was prepared in double distilled water and its concentration was determined using a molar extinction coefficient 36000 $M^{-1}cm^{-1}$ at 412 nm. The protein samples (5.0 μM), in the absence as well as presence of varying concentration of surfactants (SDS, SDBS and AOT) were incubated for 12 hrs after that we added equimolar concentrations of ThT (5.0 μM) for 30 min in the dark. The ThT fluorescence spectra were recorded on Hitachi F-4500 fluorescence spectrofluorometer by exciting the samples at 440 nm and monitoring the emission in the range of 450-600 nm. Both excitation and emission slit width were fixed at 10 nm.

3.2.9. Congo Red (CR) binding:

The stock solution of CR was prepared in double distilled water and concentration was determined using a molar extinction coefficient 45000 $M^{-1}cm^{-1}$ at 498 nm. Albumins (5.0 μM) in the absence and presence of 2000.0 μM surfactants were incubated for 12 hrs. Then aggregated and non-aggregated sample was further incubated with Congo Red (5 μM) for 30 min in the dark. The absorbance spectra (200-900 nm) of the samples were recorded on Perkin Elmer (Lambda 25) UV-Visible spectrophotometer in a 1 cm path length cuvette.

3.2.10. Dynamic light scattering (DLS):

DLS measurements were done at 830 nm by using DynaPro–TC–04, equipped with a temperature controlled microsampler. Before performing experiments, all the solution was spun at 5000 rpm for 10 minutes and filtered through 0.22 μm pore size micro filter (Whatman International, Maidstone, UK) directly into 12 μl black quartz cell. Albumin concentration was 15.0 μM throughout the DLS measurements. Albumins

were incubated with 6000.0 μM of surfactants at pH 3.5 for 12 hrs. Protein surfactant ratio (1:400) was fixed through out the DLS measurements. Measured size was presented as an average of 50 scans taken at 25 °C. The data were analyzed by Dynamics 610.0.10 software at optimized resolution. The mean hydrodynamic radius (R_h) and polydispersity (P_d) were estimated on the basis of an autocorrelation analysis of scattered light intensity based on the translational diffusion coefficient, by Stokes–Einstein equation.

$$R_h = \frac{kT}{6\pi\eta D_W^{25°C}}$$

where R_h is the hydrodynamic radius, k is the Boltzman's constant, T is the absolute temperature, η is the viscosity of water and $D_W^{25°C}$ is the translational diffusion coefficient.

3.2.11. Circular dichroism measurements:

Circular dichroism measurements were carried out on JASCO spectropolarimeter (J-815). The instrument was calibrated with D-10-camphorsulfonic acid. All measurements were carried out at 25 °C with a speed of 100 nm min^{-1} and response time of 1 second. Far-UV CD spectra were collected in the wavelength range 200-250 nm in a cell of 0.1 cm pat length with a protein concentration of 5.0 μM in the absence as well as presence of varying concentrations of surfactants. Spectra were smoothed by the Savitzky - Gaolay method with 25 convolution width. The results were expressed as mean residual ellipticity defined as

$$\text{MRE} = \theta_{obs}\,(\text{mdeg})\,/10 \times n \times Cp \times l$$

where θ_{obs} is the CD in millidegree, n is the number of amino acid residues l is the path length of the cell in centimeters and Cp is the molar fraction of proteins. The percent secondary structure proteins was calculated by K2d method.

3.2.12. Isothermal titration calorimetry (ITC):

ITC measurements were performed on VP-ITC from microcal (Northampton, MA) U.S.A at 25 °C in 20.0 mM sodium acetate buffer at pH 3.5. The sample cell was filled with 15.0 μM serum albumins at pH 3.5 and reference cell contained respective pH 3.5 buffer. Titrations were carried out using desired surfactant at pH 3.5. Duration

of each injection was 20 seconds and time delay to allow equilibration between successive injections was 180 seconds. Stirring speed was 307 rpm and reference power was a 15 μ call s^{-1}. Control experiments were done to correct the data for that of dilution of ligand and buffer mixing. The heat signals from ITC was integrated using the origin 7.0 software supplied by microcal Inc.

3.3. Results:

3.3.1. Turbidity Measurements:

The turbidity of proteins was monitored at 350 nm in order to determine the aggregation behavior (Tian et al., 2012). The turbidity of five albumins in the presence of increasing concentration of SDS, SDBS and AOT concentration range 0.0-11.0 mM at pH 3.5 was examined. As shown in Figure 3.1, all the albumins gave maximum turbidity in the presence of 0.5-2.5 mM SDS and SDBS beyond which there were sharp decline in turbidity was noticed. On the other hand, in case of AOT, the turbidity of the sample began to increase from 0.5 mM concentration and reached a plateau around 1.0-11.0 mM, without any noticeable reduction in turbidity as observed form SDS and SDBS. This shows that aggregation increase from 0.5 mM to 2.5 mM of SDS and SDBS, while for AOT, aggregation pattern does not change up to 11 mM concentration. From the above observation two surfactants SDS and SDBS are showing dual behavior at lower concentration promoting aggregation because of electrostatic interaction between negatively charged head of SDS and SDBS but at higher concentration aggregation were not found due to increase in hydroiphobic interaction. In case of AOT only aggregation induction behavior was found. The turbidity of all albumins were also measured in the presence of all three (SDS, SDBS and AOT) surfatcatns at pH above two units of pI, pH 7.4 but no turbidity was noticed (data not shown). The surfactants unable to induce amyloid at pH 7.4 due to strong electrostatic repulsion between proteins and surfactants because both have a same charge.

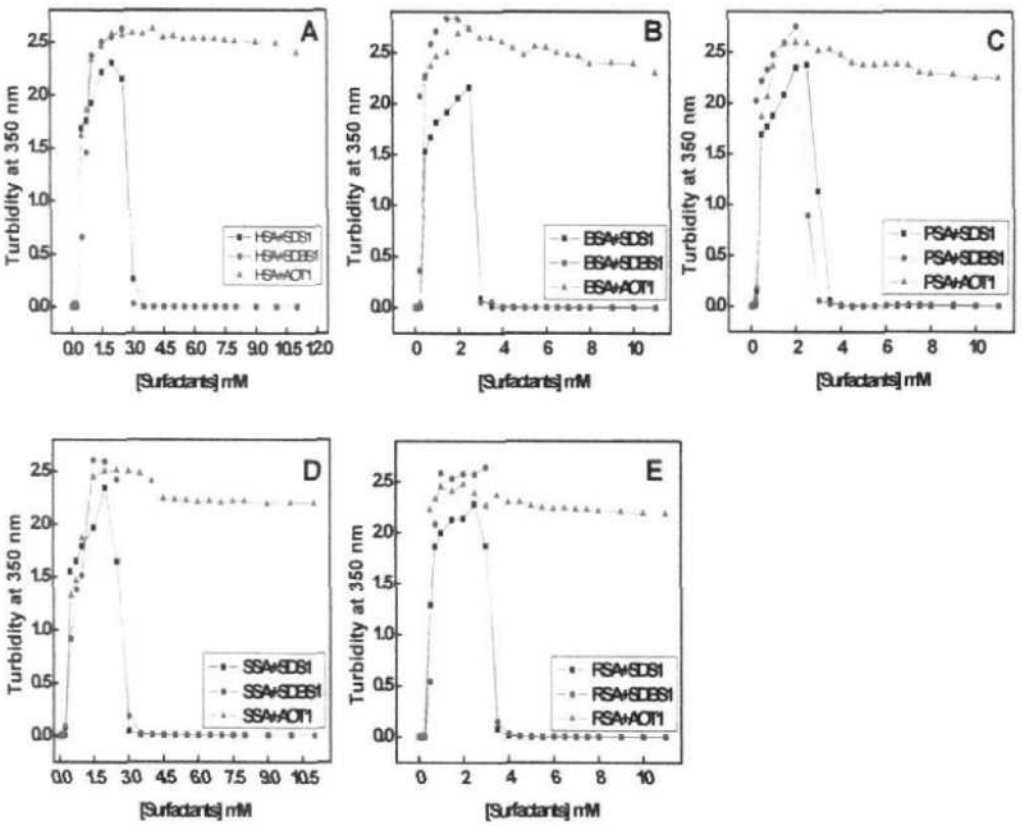

Figure 3.1. Turbidity of the sample was measured to detect the aggregation. Turbidity measurements of human (A), bovine (B), porcine (C), sheep (D) and rabbit (E) serum albumins at 350 nm were obtained in the absence and presence of varying concentration of SDS (-■-), SDBS (-●-) and AOT (-▲-) in 20.0 mM sodium acetate buffer at pH 3.5 at 25 °C. Albumins concentration was kept constant 5.0 μM ml^{-1} in all conditions in 20.0 mM sodium acetate buffer at pH 3.5 and experiments were performed after 12 hrs incubation.

3.3.2. Rayleigh light Scattering measurements (RLS):

The aggregation propencity of SDS, SDBS and AOT was further determined by RLS at 350 nm of albumin samples in the presence of increasing concentration of surfactants. The aggregation of proteins was measured by RLS is also reported earlier (Vetri and Militello, 2005, Mir et al., 2010b). The data thus obtained showing good agreement with that obtained from turbidity measurements. As shown in Figgure 3.2, light scattering at 350 nm for albumin samples containing SDS and SDBS showed maximum FI in between 0.5-2.5 mM concentration, while above 2.5 mM the intensity of scattered light decreased significantly and become almost negligible. On other hand

sample containing AOT exhibited an enhanced scattering which remained persistent up to 11.0 mM of surfactant. These results again demonstrated that aggregation were permoted in the concentration range 0.5-2.5 of SDS and SDBS respectively beyond which aggregation was suppressed. In the presence of AOT the aggregation was not suppressed even up to 11.0 mM concentration. The Turbidity and RLS results were demonstrated showed different patterns of aggregation in the presence of SDS, SDBS and AOT but in the presence of SDBS, AOT the turbidity and extent of light scattering is more in comparison to SDS because SDBS and AOT has a long hydrophobic chain.

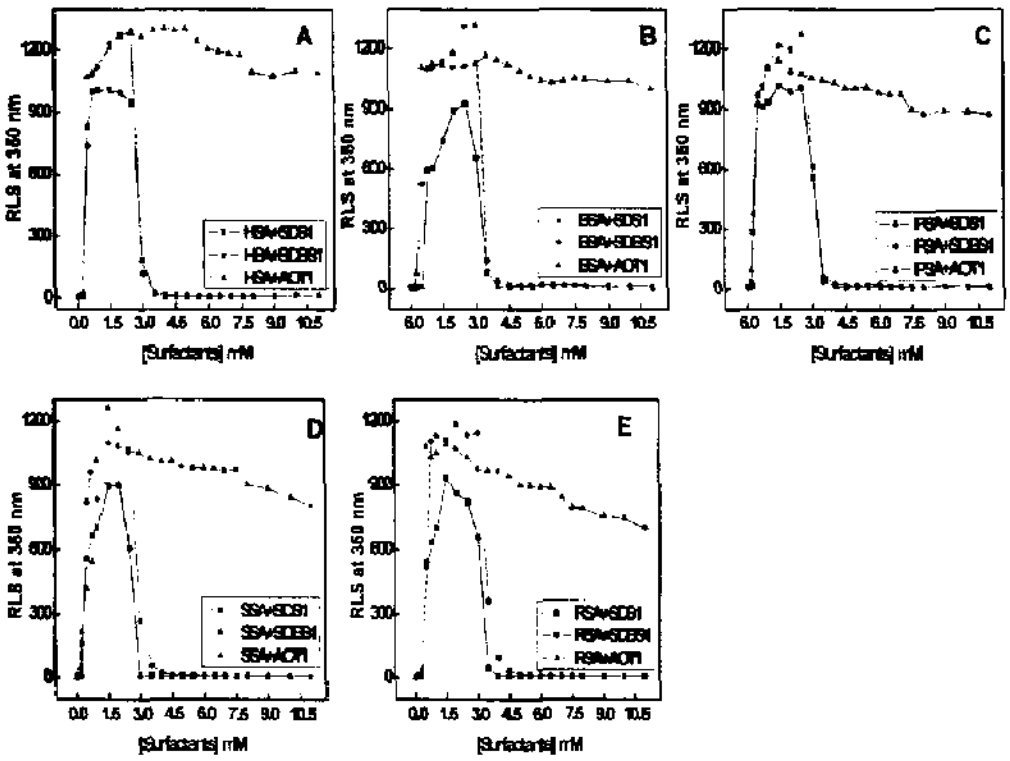

Figure 3.2. Aggregation of albumins was measured by Rayleigh light scattering (RLS). Rayleigh scattering measurements of human (A), bovine (B), porcine (C), sheep (D) and rabbit (E) serum albumins at 350 nm in the presence of increasing concentration of SDS (-■-), SDBS (-●-) and AOT (-▲-) in 20.0 mM sodium acetate buffer at pH 3.5 for 12 hrs incubation. The albumin concentrations were kept 5.0 μM ml^{-1} in all the samples.

3.3.4. Kinetics of surfactant induced aggregation by RLS:

The time dependent changes in aggregation of albumins at pH 3.5 in the presence of 40.0 μM SDS, SDBS and AOT were studied through light scattering measurements. The molar ratio of albumins and surfactant was fixed for 1:400. It can be observed that aggregation was induced in the protein by SDS, SDBS and AOT at a very fast rate and no lag phase could be detected shown in Figure 3.3. So, it suggested that aggregation reaction was not nucleus dependent. Similar kinetic behavior was also reported in human apolipoprotein (apo) C-II and Tau proteins (Ryan et al., 2011, Ramachandran and Udgaonkar, 2012). Further in case of AOT, saturation was achieved very fast while in case of SDBS the aggregation occurred at a relatively slower rate than AOT. In case of SDS the rate of aggregation was least among all surfactant as the log phase was prolonged. Also the extent of aggregation induced by the surfactant followed the order AOT>SDBS>SDS. The result shows that rate as well as extent of aggregation was greatly influenced by the chain length of the surfactants.

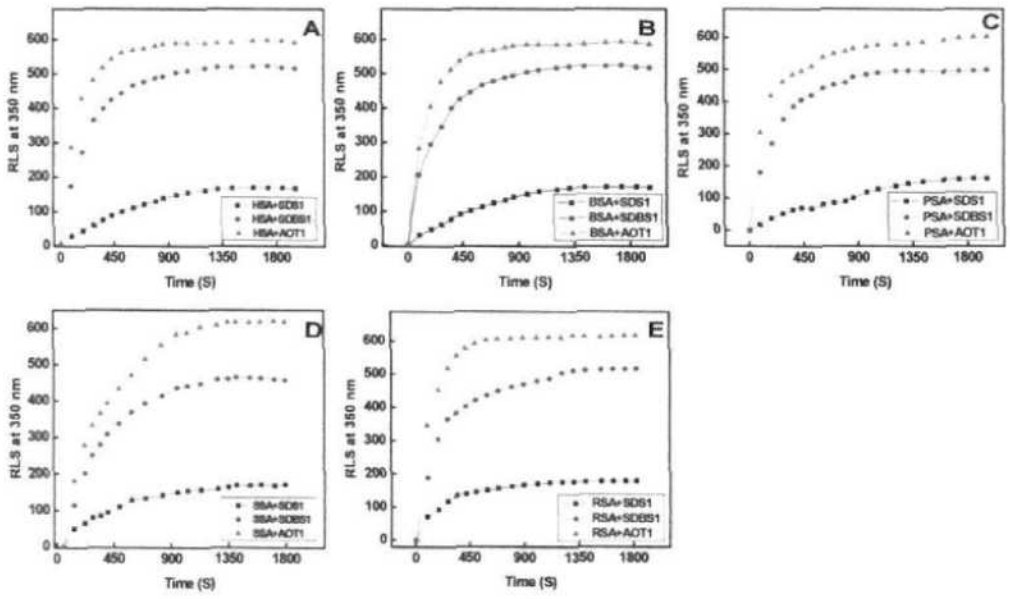

Figure 3.3. Kinetics of aggregation in albumins were monitored by RLS measurements. Time dependent change in aggregation was monitored by Rayleigh scattering measurements in human (A), bovine (B), porcine (C), sheep (D) and rabbit (E) serum albumins (0.1 μM ml^{-1}) in the presence 40.0 μM ml^{-1} SDS (-■-), SDBS (-●) and AOT (-▲-) at pH 3.5. The protein surfactant ratio was taken 1:400.

3.2.5. ThT binding assay:

ThT is an amyloid specific dye which is used to detect the presence of fibrillar aggregate in both tissues as well as in vitro samples. An enhanced ThT fluorescence is a characteristic of the amyloid fibrils (Touchette et al., 2010, Luo et al., 2012). ThT binding assays were performed to study the nature of aggregates induced by all the three surfactants in serum albumins at pH 3.5. A plot of FI at 485 nm versus varying surfactant concentration is shown in Figure 3.4. From the figure it can be seen that at lower concentration 0.5-2.5 mM of SDS and SDBS the ThT florescence of five albumins were enhanced significantly. Beyond 2.5 mM a marked reduction in FI occurred. The ThT fluorescence was negligible for sample containing 4-5 mM of SDS and SDBS. It is interesting to note that the FI was much higher in the presence of SDBS (18C) than that of SDS (12C), which suggests that SDBS is more efficient in inducution of order fibrillar structure than SDS. A very unique behavior was shown by AOT, in the presence of 0.5-2.5 mM AOT the ThT fluorescence intensity was lesser than that obtained for SDBS. However the FI did not decline as in case of SDBS and a considerable higher fluorescence could be observed at much higher concentration of AOT. The ThT binding data shows that aggregates formed have fibrillar structure and that chain length of the surfactant plays an important role in fibrillation of the serum albumins.

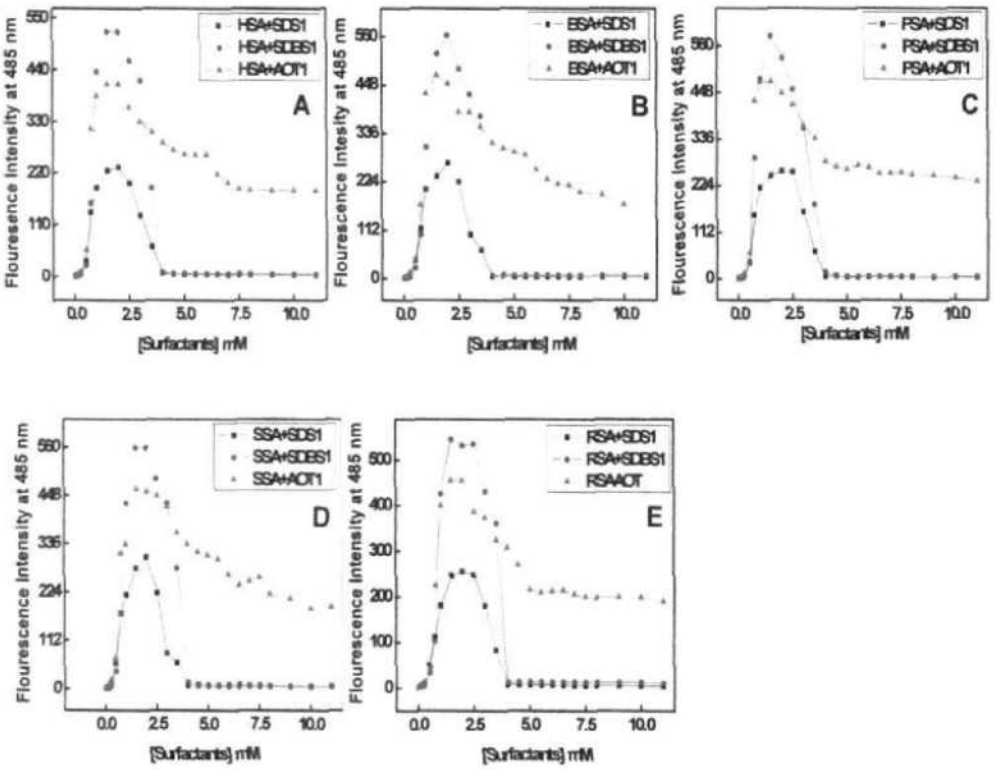

Figure 3.4. Amyloid fibrils formation in five albumins were measured by ThT fluorescence. The effect of hydrophilic head and hydrophobic tail of SDS (-■-), SDBS (-●-) and AOT (-▲-) on amyloid fibrillogenesis of human (A), bovine (B), porcine (C), sheep (D) and rabbit (E) serum albumins was measured by ThT fluorescence Intensity at 485 nm after excitation at 440 nm at pH 3.5. Prior to measurements the aggregated sample was incubated with ThT for 30 min in a dark. The protein concentration was taken in all cases 5.0 μM ml^{-1}. The protein ThT ratio 1:1 was fixed.

3.3.6. Congo Red (CR) binding assay:

The fibril formation of five albumins in the presence of 2000.0 μM ml^{-1} SDS, SDBS and AOT was further assessed by Congo Red (CR) binding assay at pH 3.5. CR is known to intercalate between β-sheets of fibril and produces a red-shift in the absorbance spectrum (Kim et al., 2003, Srinivasan et al., 2003). The CR absorbance spectra of five albumins with and without SDS, SDBS and AOT are shown in Figure 3.5. The spectra obtained in the absence of surfactant gave maximum absorbance at 503 nm. In the presence of surfactants i.e. SDS, SDBS and AOT, a prominent red shift in the spectra was observed. The shift in the absorbance maxima further indicates

that surfactant induced aggregates of albumins have β-sheet structure and are arranged into well defined fibrils.

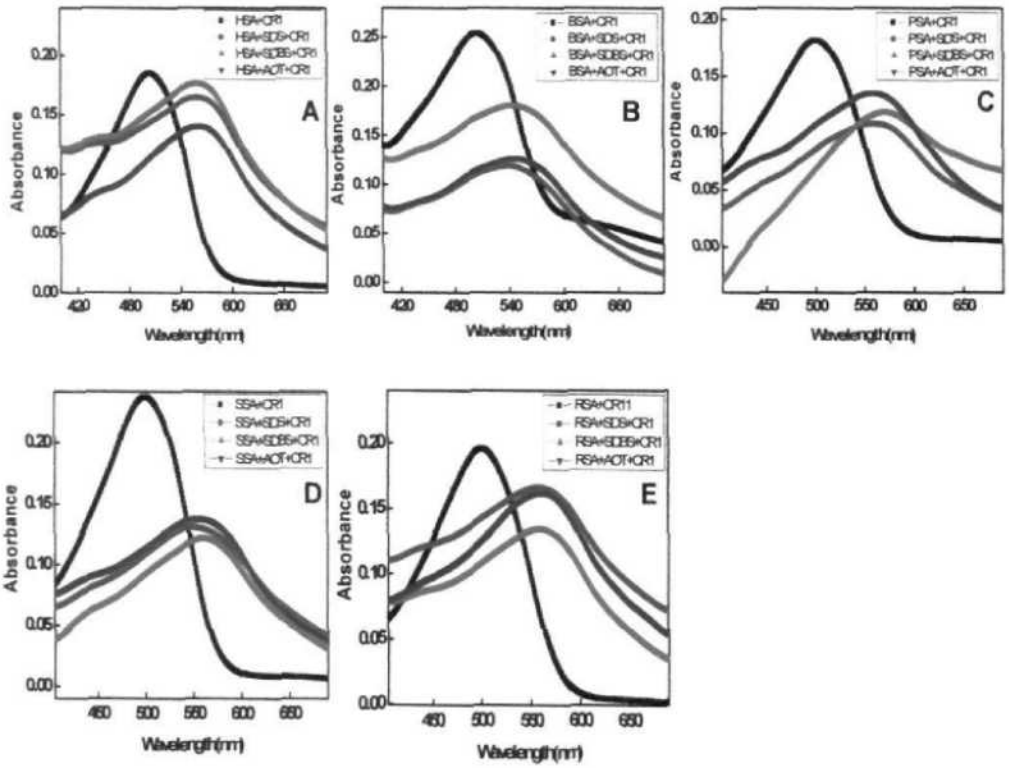

Figure 3.5. CR binding was performed to detect the amyloid fibril. Interaction of CR with aggregated and non aggregated human (A), bovine (B), porcine (C), sheep (D) and rabbit (E) serum albumins were seen. The spectrums of non-aggregated albumins are (black) and in the presence of 2000.0 μM ml^{-1} SDS, SDBS and AOT are red, green and blue (aggregated). The aggregated and non aggregated samples were incubated with CR for 30 min in a dark prior to measurements. Final concentrations of albumins were taken 5.0 μM.

3.3.7. Dynamic light scattering analysis (DLS):

DLS is a technique used to characterize the size of particle as well as to detect protein aggregates in a solution (Ahrer et al., 2003) (Kumar and Udgaonkar, 2009). The change in hydrodynamic radii of five albumins in their native state (pH 7.4), acid induced state at pH 3.5 and in the presence of 6 mM SDS, SDBS and AOT were studied by DLS (Figure 3.6). The R_h of albumins in their native state (pH 7.4) was found to be 3.8 nm (HSA, SSA) 3.4 nm (BSA, RSA), 3.6 (PSA). At pH 3.5, a slight increase in R_h was observed 4.0 nm (HSA, PSA and RSA), 3.8 nm (BSA) and 4.2

(SSA) owing to the loosening of protein structure under acidic condition. Upon incubation with surfactant a significant increased in R_h occurred which suggest the formation aggregated species. Table 4.1. summarizes the results obtained from DLS study.

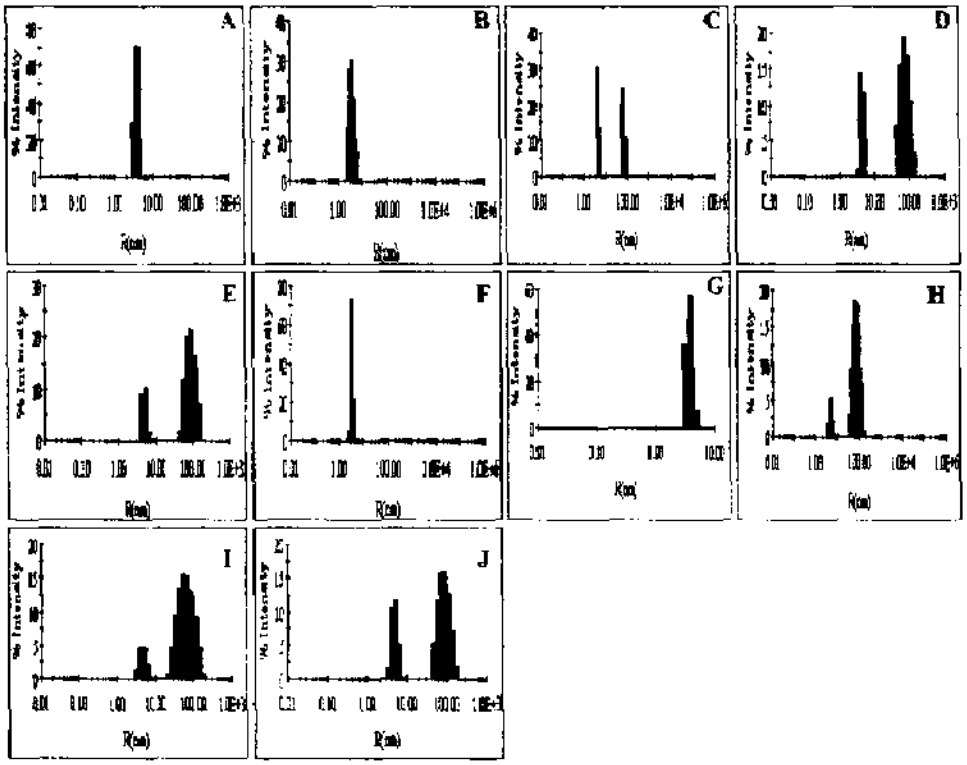

Figure 3.6. Hydrodynamic radii were measured to know the size of aggregates. The hydrodynamic radii of native human serum albumins 15.0 μM ml^{-1} (A), at pH 3.5 (B), in the presence of 30000.0 μM ml^{-1} SDS (C), SDBS (D) and AOT(E) and bovine serum albumin 15.0 μM ml^{-1} at pH 7.4 (F), at pH 3.5 (G) and in the presence of 30000.0 μM ml^{-1} SDS (H), SDBS (I) and AOT (J). Prior to measurements all the samples were incubated for 12 hrs.

Table 3.1. Hydrodynamic radii of all albumins at differcat conditions.

S.No.	Protein	R_h (nm)				
		Native	pH 3.5	SDS	SDBS	AOT
1	HSA	3.8	4.0	4.4, 69.3	4.4, 80.5	4.8, 92.6
2	BSA	3.4	3.8	4.7, 82.3	4.8, 72.8	4.9, 89.0
3	PSA	3.6	4.0	4.0, 82.3	4.1, 86.9	4.6, 83.5
4	SSA	3.8	4.2	4.4, 85.7	4.6, 90.8	4.8, 90.9
5	RSA	3.4	4.0	4.3, 89.0	4.9, 94.0	5.0, 94.7

3.3.8. Far-UV CD measurements:

Far-UV CD studies were carried out in order to study the effect of surfactant on the secondary structure of albumins at pH 3.5. As shown in Figure 3.7, far-UV CD spectra of five albumins at pH 7.4 and 3.5 exhibited two minima, one at 208 nm and other at 222 nm which is characteristics in the presence of α-helical structure, similar spectral behavior were also reported in other study (Mir et al., 2010a, Johnston et al., 2010, Ahmad et al., 2011). At 2.0 mM concentration of SDS, SDBS and AOT, the spectra of the albumins showed only a single negative peak which indicates the acquisition of prominence β-sheet structure in all the cases studied. The existence of β-sheet structure is a characteristic features of amyloid fibrils. The % α-helix to % β-sheet transition of all albumins at different concentration of surfactants were calculated by K2d software are shown in Table 3.2. The spectra of albumins in the presence of SDS and SDBS obtained beyond 2.5 mM was similar to the spectra of albumins at pH 3.5, which indicates the higher concentration of these surfactants inhibited conformational transition from α-helix to β-sheet structure. The AOT persists β-conformation even at higher concentration (11 mm) in all albumins. From CD results it can be concluded that SDS and SDBS are showing dual behavior in five albumins. But at higher concentration (beyond 3 mM) of SDBS the CD measurements will not be performed because it's showing high HT noise.

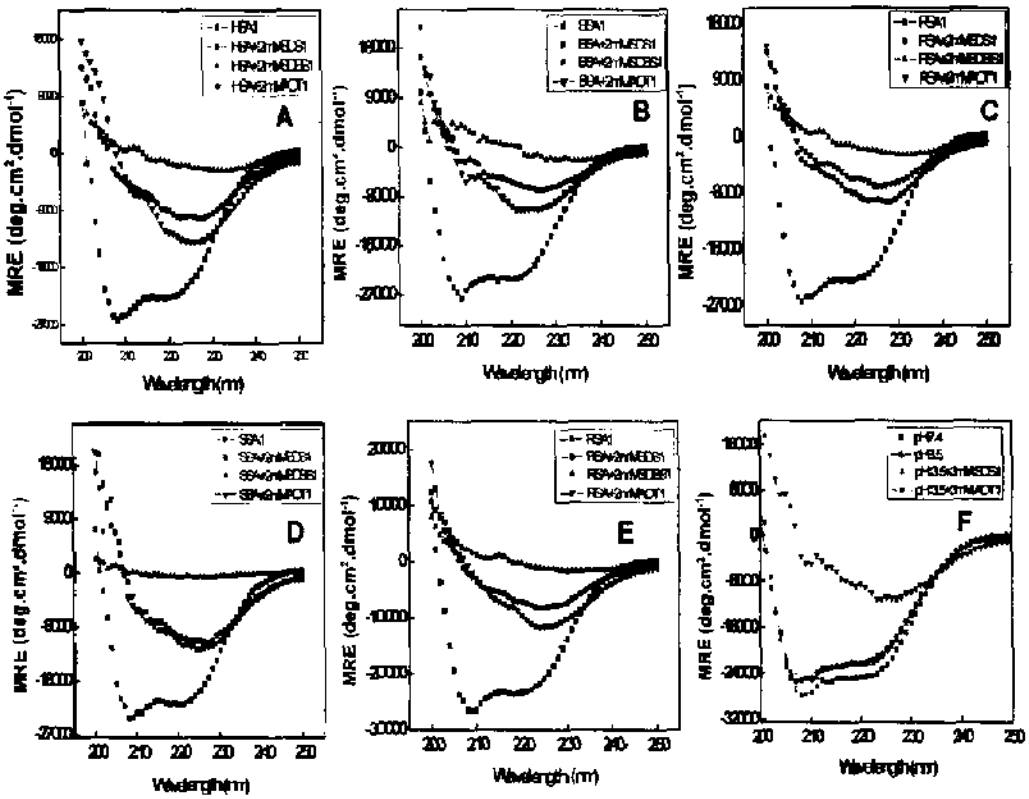

Figure 3.7. The secondary structure transition was measured by Far-UV CD. Far-UV CD spectra of human (A), bovine (B), porcine (C), sheep (D) and rabbit (E) serum albumins were recorded in the presence of SDS (red spectra), SDBS (green spectra) and AOT (blue spectra) and absence (black spectra) at pH 3.5. In (F) Hunman serum albumin at pH 7.4 (cyan spectra), at pH 3.5 (black spectra), presence of 3.0 mM SDS and AOT at pH 3.5 (yellow and magenta spectra).

Table 4.2. % secondary structure calculated by K2d method at different conditions.

S.No.	Proteins	Surfactants [μM]	SDS			SDBS			AOT		
			% α	% β	% Random Coil	% α	% β	% Random Coil	% α	% β	% Random Coil
1	HSA	0	75	2	23	75	2	23	75	2	75
		250	80	0	20	81	0	19	80	2	20
		1500	23	40	36	79	0	21	23	49	37
		2000	22	38	41	9	49	43	24	40	36
		2500	24	38	38	15	45	40	23	40	36
2	BSA	0	79	0	21	79	0	21	79	0	21
		250	81	0	19	23	40	46	80	0	20
		1500	4	48	48	8	48	44	23	40	36
		2000	20	38	42	22	40	38	23	40	36
		2500	31	11	58	10	35	56	23	41	36
3	PSA	0	78	0	22	78	0	22	78	0	22
		250	79	0	20	80	0	20	79	0	21
		1500	19	34	47	9	47	44	23	40	36
		2000	23	41	36	10	49	41	20	37	42
		2500	22	39	39	10	48	42	18	34	46
4	SSA	0	78	0	22	78	0	22	78	0	22
		250	81	0	19	79	0	21	80	0	20
		1500	20	42	38	15	45	40	20	42	38
		2000	18	45	37	18	48	34	23	40	36
		2500	21	42	37	12	40	48	23	40	36
5	RSA	0	74	0	26	74	0	26	74	0	26
		250	78	0	22	79	0	21	80	0	20
		1500	20	43	37	12	43	45	21	42	37
		2000	24	40	36	10	44	46	18	44	32
		2500	22	42	36	9	46	45	23	40	36

3.3.9. Transmission Electron Microscopy (TEM):

The morphology of surfactant induced aggregation of albumins was further examined by TEM. The TEM was used to check the morphology of aggregates whether fibrillar or amorphous (Pallares et al., 2004, Hettiarachchi et al., 2012). The protein sample at pH 7.4 and at pH 3.5 did not show any fibrillar structure, while in the presence of 2.0 mM SDS, SDBS and AOT at pH 3.5 mature fibrils were formed which is shown in Figure 3.8. From the TEM image it can be concluded that the aggregates are formed by SDS, SDBS and AOT is having fibrilar morphology which is also supported by ThT, CR and CD results..

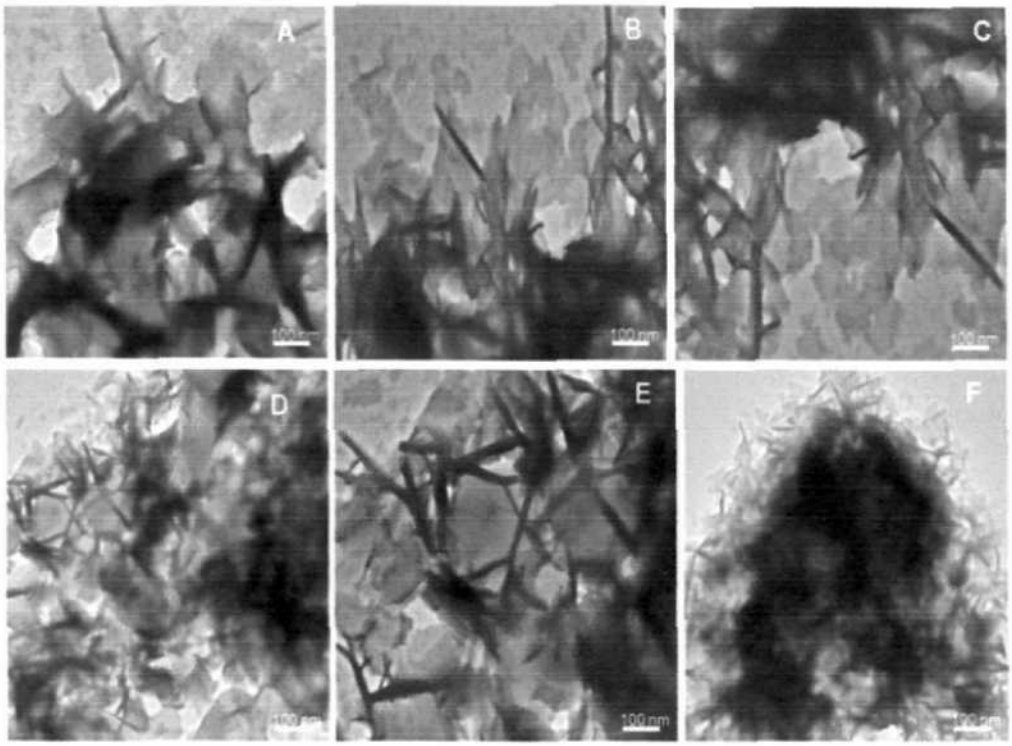

Figure 3.8. Morphology of aggregates was detected by TEM. TEM images of human serum albumins in the presence of 2000 μM SDS (A), SDBS (B) and AOT (C), bovine serum albumins in the presence of 2000 μM SDS (D), SDBS (E) and AOT (F) . Before taking the image sample were incubated for 12 hrs.

3.3.10. Isothermal titration calorimetry (ITC) measurements:

Isothermal titration calorimetry (ITC) is routinely used to allocate the stoichiometry of the association between ligand and protein. ITC also gives information about heat released or absorbed when ligand is bound to macromolecules and reveal the nature of interactions whether electrostatic or hydrobhobic. We studied the interaction of negatively charge surfactants (SDS, SDBS and AOT) with human serum albumins at pH 3.5. In Figure 3.9, the enthalpogram shows that heat changes accompanying binding of HSA with SDS, SDBS and AOT were exothermic as also evident from enthalpic values while higher concentrations of SDS was required for complete saturation, SDBS and AOT showed complete saturation at a far lesser concentration owing to their increased hydrophobicity. The heat released (enthalpy change ΔH) during binding of SDS is -2.179±0.083, SDBS -2.339 ±0.061 and AOT -4.14±0.499 $Kcal.mol^{-1}$ respectively with the human serum albumins.

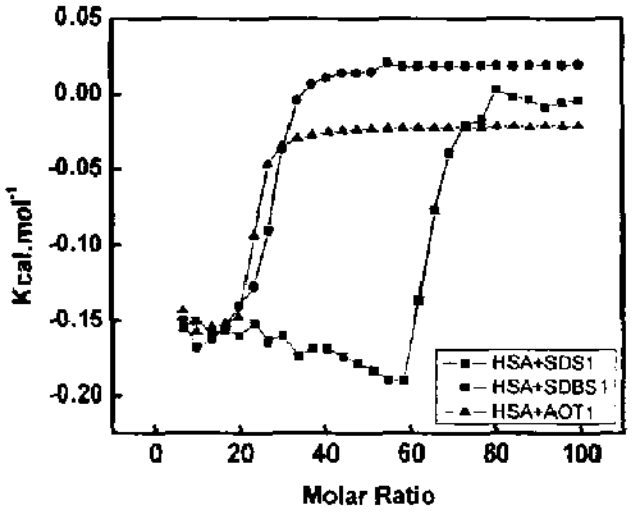

Figure 3.9. The heat released was measured by ITC. Enthalpograms of SDS, SDBS and AOT titration into human serum albumins solutions with concentration of (15.0 μM) at pH 3.5. The enthalpy change for each injection has been plotted versus the molar ratio scale [surfactant] : [albumins] of SDS (-■-), SDBS (-●-) and AOT (-▲-) at pH 3.5.

3.4. Discussion:

The negatively charged surfactants and lipids have a strong propensity to induce the amyloid fibrils in both amyloidogenic as well as non-amyloidogenic proteins (Butterfield and Lashuel, 2010, Sambasivam et al., 2011, Friedman and Caflisch, 2011, Sasahara et al., 2012). However the detail mechanism of surfactant/lipid induced aggregation still remain unclear. In our previous publication, 25 diverse proteins were subjected to pH below two units of their respective pI which led to the development of positive charges on the protein (Khan et al., 2012). This positive charge was neutralized by negatively charged SDS which resulted in aggregation of all the 25 proteins. From this study it was concluded that the electrostatic interaction is playing very important role. The role of ionic interaction was discussed in our previous communication. In the present study, our aim is to explore the role played by hydrophobic tail of the surfactant in the formation of aggregates in serum albumins by taking three negatively charged surfactant having variable chain length viz SDS (12C), SDBS (18C) and AOT (20C). The turbidity and light scattering measurements showed that the extent of aggregation increased with increasing chain length of the surfactant and followed the order: AOT>SDBS>SDS. We also showed the rate of

aggregation is time dependent change on RLS for all the albumins. It was observed that the rate of aggregation was dependent upon the negative charge of the head and length of hydrophobic tail of surfactants. Maximum aggregation was obtained in the presence of AOT followed by SDBS and then SDS. Also, the reaction is very fast such that no lag phase could be detected which suggests that fibrillation of albumins by their anionic surfactants was nucleus independent. Similar type of reaction kinetics was also reported in many proteins (Kad et al., 2001, Ookoshi et al., 2008, Motamedi-Shad et al., 2009b, Motamedi-Shad et al., 2012, Ruzafa et al., 2012). The change in hydrodynamic radii of the aggregated species was monitored by DLS as it is well known that during amyloid formation, the size of protein molecules increased due to complex formation (Liu et al., 2010). In our study, it was observed that both hydrodynamic radii of protein sample (pH 3.5) increased dramatically when incubated with SDS, SDBS and AOT upto certain concentration. After that aggregation was suppressed and hydrodynamic radii were more or less same as that of hydrodynamic radii of native albumins (data not shown). Interestingly the hydrodynamic radii of the aggregated species were more in the presence of AOT than that of SDBS and AOT which could be due to the fact that AOT is more hydrophobic as compared to SDBS and SDS. The tobacco mosaic virus coat protein also formed bigger size aggregates in the presence of cationic surfactant i.e. CTAB in comparison to its thermally induced aggregate (Panyukov et al., 2006). In order to confirm the nature of aggregates whether fibrilar or amorphous, we performed ThT as well as a CR dye binding assay. Both ThT and CR are specifically used to detect the presence of amyloid fibrils (Klunk et al., 1999, Carrotta et al., 2001, Hoyer et al., 2002). ThT binding assay revealed that all the five albumins yielded significantly enhanced ThT fluorescence intensity in the presence of (0.5-3.5 mM) SDBS and SDS at pH 3.5, whereas the ThT fluorescence of native albumin as well as control sample (containing only surfactant and ThT) was quite insignificant. Further the ThT fluorescence of the AOT containing protein sample did not decline up to 11 mM of surfactant. In case of SDBS, ThT fluorescence intensity is high compared to SDS and AOT because SDBS induced to mature fibril than AOT and SDS. The Congo Red binding assay showed a prominent red shift in the absorbance of albumins in the presence of AOT, SDBS and SDS as compared to control. From these two dyes binding experiments, it was confirmed that aggregate formed by the anionic surfactants in albumins at pH 3.5 were fibrillar in structure. The change in secondary structure of the five albumins upon fibrillation was

checked via far-UV CD. Vast literatures are available showing the conversion of α-helical protein into β-sheet structure upon fibrillation (Sen et al., 2009, Juarez et al., 2009). Similar conformational transitions were observed in our case also. The α-helical structure of all the five albumins were converted into β-sheets in the presence of AOT, SDBS and SDS at pH 3.5 which suggested that the fibrils have well defined β-sheet structures. The morphology of fibrils was further examined by TEM which revealed the presence of thick unbranched fibrils formed by albumins upon incubation with all the three anionic surfactants. After that we further explored ITC to know the nature of interaction between surfactants and albumins. ITC data revealed that binding of surfactants to albumin involved large enthalpic change which suggests the involvement of electrostatic interaction. The binding of SDS with α-synuclein (αSN), was also investigated by other group and they found similar type of enthalpic change as we got in our case (Giehm et al., 2010).

3.5. Mechanism of aggregation by negatively charged surfactants:

In this study, we studied the effect of negative charged surfactant (SDS, SDBS and AOT) with varying hydrophobic chain length on serum albumins at pH 3.5. At pH 3.5, native conformation of serum albumins undergo a transition into 'F' form which is a fast moving isomer of the protein. Further all the selected albumins exhibit a net positive charge at pH 3.5 (pI~5.5). The estimated charge on each albumin at pH 3.5 is given in Table 3.3. Negatively charged surfactants and lipids are used for amyloid induction in many proteins and it is reported that SDS interacts with Arg & Lys residues for inducing amyloid fibril formation. Serum albumins contain several basic and acidic residues. Below pI, the Arg, Lys & His which are positively charged residues become protonated while negatively charged residues were uncharged or vice versa. We incubated the serum albumins with negatively charged surfactant both below (pH 3.5) and above (pH 7.4) two units of pI of the proteins. It is believed that negatively charged head group of surfactant interacts with positive charge centers of the proteins (at pH 3.5) while the hydrophobic tail strongly repel water molecules leading to disruption of solute-solvent interactions. This causes enhanced solute-solute interaction. However, lack of fibril formation above pI of proteins suggest that strong electrostatic repulsion among the interacting molecules. This indicates that negatively charged surfactant have strong propencity to induce amyloid formation in proteins with basic residues (Arg, Lys & His) is ionized form i.e at pH below two

units of pI. Whereas hydrophobicity alone may not induce fibril formation, confirmed by studies performed above two units of pI. In this study, SDS and SDBS are showing dual behavior i.e fibril formation at lower concentrations and solubilization of aggregates at higher concentration. This is due to the fact that at the low concentration monomer of negatively charged surfactant interacted to the oppositely charged center of serum albumins and lead to amyloid fibril formation but at higher concentration the only hydrophobic part of surfactants playing important role in solubilization of aggregates. In contrast AOT was found to form fibril in micellar concentration also. It seems that one micelle interacts with more than one protein molecules and form amyloid. A proposed mechanism of SDS, SDBS and AOT is illustrated in Figure 3.10.

Table 4.3. Estimated charge of all albumins at pH 3.5 by "PROTEIN CALCULATOR v3.3" software.

S.No.	Protein Name	Charge at pH 3.5
1	HSA	80.7
2	BSA	79.2
3	PSA	82.3
4	RSA	94.2
5	SSA	92.2

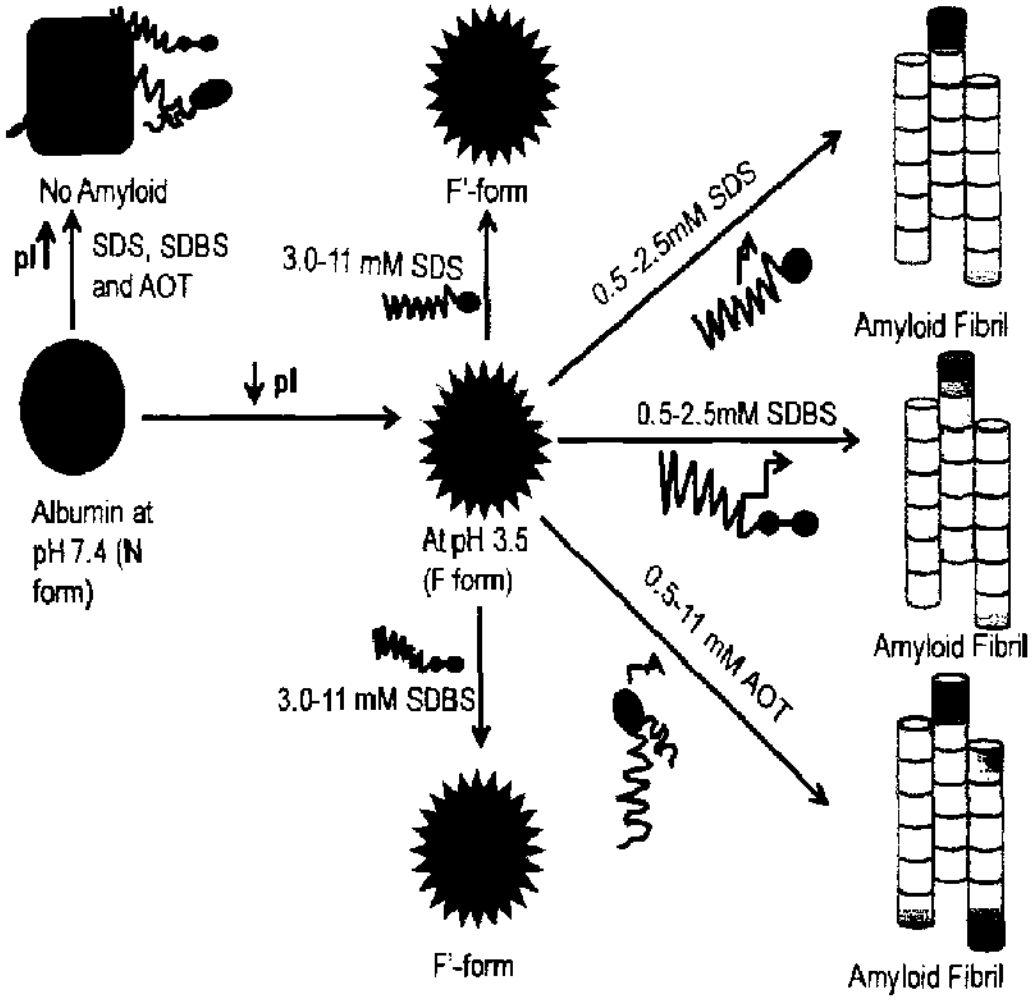

Figure 3.10. The proposed mechanism of aggregation by SDS, SDBS and AOT are illustrated.

3.6. Conclusion:

From this study it can be concluded that SDS, SDBS and AOT induces aggregation in all mammalian serum albumins at pH 3.5. At pH 3.5 albumins acquire net positive charge on the surface and the negative charge head of SDS, SDBS and AOT interacts electrostatically with the oppositely charged surface of serum albumins and leads to assembly of protein into characteristic amyloid fibrils. But the fibril formation propensity is also dependent on the chain length of these surfactants as evident from the results. The AOT has a very strong propensity to induce amyloid than SDBS and SDS because the overall hyderophobicity is higher in the AOT. Similarly we also have concluded that the hydrophobicity of surfactants is not playing a prominent role in amyloid fibril formation independently because charge neutralization is the most important factors. In simple word charge neutralization works first then hydrophobicity.

CHAPTER 4

Elucidating the Protective Effect of Sodium Dodecyl Sulphate on Serum Albumins Against Urea and Temperature at Low pH

4.1. Introduction:

Serum albumins play an important role in transportation and distribution of exogenous and endogenous ligands in the blood such as fatty acids, drugs, steroids, also maintain the physiological pH and osmotic pressure of the blood (Peters, 1985). Human serum albumin (HSA), bovine serum albumin (BSA), porcine serum albumin (PSA), sheep serum albumin (SSA) and rabbit serum albumin (RSA) are globular protein consisting of a single polypeptide chain. HSA and RSA contain one tryptophan while BSA, PSA and SSA contain two tryptophans which are located in hydrophobic cavities of IB and IIA sub domains respectively. All these albumins have high sequence similarity at the gene and protein sequence level, so it become important to know their structural and functional stability. As we have reported earlier that all the albumins, particularly HSA, BSA, PSA and RSA are having a similar aggregation propensity in the presence of acetonitrile (Sen et al., 2009). For understanding the structural and functional relationship of proteins under various stress condition is important for applicative aspects. The stability of serum albumins has been studied in many in-vitro studies (Farruggia and Pico, 1999, Farruggia et al., 2003, Brahma et al., 2005, Galantini et al., 2010). Several methods are used to examine the protein stability such as chemical denaturantion. Urea is a chemical denaturant which is widely exploited for investigating the conformational stability of proteins (Auton et al., 2007, Das and Zhou, 2010). The molecular mechanism of urea induced protein unfolding is still a controversial issue; because it is not complitely known what type of forces are responsible in unfolding? There are two types of mechanism proposed on the basis of experimental and theoretical observations. The first is an indirect mechanism, which propose that the urea disrupt the water molecules and help in salvation of hydrophobic groups (Bennion and Daggett, 2003). According to the second mechanism, the urea directly interacted with protein by electrostatic or Van der Waals forces (Lim et al., 2009). The thermal denaturation is another important method to test the conformational stability of proteins. Vast literatures is available on thermal denaturation (Rezaei Tavirani et al., 2006,

Kawamura et al., 2006, Fan et al., 2007). Various strategies have been proposed to achieve stabilization of proteins including chemical modification, protein engineering, use of surfactants and ploy hydrnxy compounds (Simon et al., 2002). Using these methods, the half-life, water solubility is also increased and self-aggregation property of proteins is reduced (Bailon et al., 2001, Marshall et al., 2003). Stabilizers are very extensively used to store the proteins for longer time. In the area of protein expression and purification, inclusion bodies formation is a major problem. Many additives are routinely used for the solubilization of inclusion bodies and surfactant is one of them. The surfactant-protein interaction creates much interest for many physiochemical as well as conformational phenomena. Sodium dodecyl sulphate (SDS) is the most repeatedly studied surfactant. It is well documented that SDS is used for both stabilization and destabilization of proteins (Nielsen et al., 2007). Hnwever, it is not clearly known how SDS interacts with proteins. Available literature reveals that SDS interactes with proteins via ionic as well as hydrophobic interactions (Gitlin et al., 2006). SDS also increases the enzymatic activity and conformational stability of many proteins (Kricka and De Luca, 1982, el-Sayed and Roberts, 1985). Protein stabilization property of SDS is not extensively studied so far in details. It is also reported that SDS is having great capacity to unfold the proteins (Otzen et al., 2009, Bhuyan, 2010). In this study we have taken five serum albumins from different source and studied the effect of SDS at pH 3.5 on the conformation nf albumin. Further, we have seen the effect of urea and temperature in the presence of 4.0 mM SDS. Other objectives of this work were to investigate the mechanism of urea action.

4.2. Material and Methods:

4.2.1. Materials:

Essentially fatty acid free human serum albumin (068K7538V), bovine serum albumin (110M1661V), porcine serum albumin (094K7636), sheep serum albumin (117K7540) and rabbit serum albumin (117K7565), urea and sodium dodecyl sulphate (SDS), were purchased from Sigma Chemical Co. (St. Louis, Mo, USA). All other reagents used were of analytical grade.

4.2.2. Methods:

4.2.3. Protein concentration determination:

The protein concentrations was determined spectrophotometrically using molar extinction coefficients; ε_m 35700 M^{-1} cm^{-1} (HSA), 43827 M^{-1} cm^{-1} (BSA), 43385 M^{-1} cm^{-1} (PSA and RSA) and 42925 M^{-1} cm^{-1} (SSA) at 280 nm on Perkin Elmer (Lambda 25) double beam spectrophotometer. The stock solutions of all proteins were prepared in 20.0 mM Tris-HCl buffer pH 7.4. The stock was diluted to the respective buffer for further uses.

4.2.4. pH measurements:

pH measurements were carried out on Metler Tolado pH meter (seven easy S 20-K) using Exper "Pro3 in 1" type electrode. The least count of the pH meter was 0.01 pH unit. The working protein samples were prepared in 20.0 mM sodium acetate buffer pH 3.5. The buffers were filtered through PVDF 0.45 μm syringe filter (Millipore Milex-HV).

4.2.5. Circular Dichroism

CD measurements were performed with a Jasco spectropolarimeter (J-815), equipped with a Jasco Peltier-type temperature controller (PTC–424S/15). The instrument was calibrated with D-10-camphorsulfonic acid. The measurements were carried out at 25 °C. Far-UV CD spectra were collected with a protein concentration of 5.0 μM with 0.1 cm path length in the range of 200-250 nm. Each spectrum was the average of 2 scans. The results were expressed as mean residual ellipticity (MRE) in deg cm^2 $dmol^{-1}$ which is defined as:

$$MRE = \theta_{obs}(mdeg) / 10 \times n \times Cp \times l \qquad (1)$$

where θ_{obs} is the CD in millidegree, n is the number of amino acid residues, l is the path length of the cell in centimeters and Cp is the molar fraction of proteins.

4.2.6. Fluorescence measurements:

Fluorescence measurements were performed on Hitachi spectrofluorometer (F-4500) equipped with a PC. The fluorescence spectra were collected at the 25 °C with a 1 cm path length cell. The intrinsic fluorescence spectra were recorded between 300 to 400 nm with excitation wavelength of 295 nm. The excitation and emission slit width were set at 5 nm. 5.0 μM of protein concentration were taken in all the conditions.

4.2.7. Dynamic light scattering:

DLS measurements were performed with protein concentration of 15 μM using DynaPro–TC–04 dynamic light scattering equipment (Protein Solutions, Wyatt Technology, Santa Barbara, CA) equipped with temperature-controlled microsampler. Before the measurements, all the samples were kept for overnight (24 hrs) incubation. Prior to scanning, all the solutions were spun at 10,000 rpm for 10 mins and filtered through microfilter (Millipore Millex-HV hydrophilic PVDF) having a pore size of 0.45 μm followed by further filtration using 0.22 μm pore sized filter (Whatman International, Maidstone, UK). Measured size was presented as the average value of 50 runs. Data were analyzed by using Dynamics 6.10.0.10 software at optimized resolution. The mean hydrodynamic radius (R_h) and polydispersity (P_d) were estimated on the basis of an autocorrelation analysis of scattered light intensity based on the translational diffusion coefficient, by Stokes–Einstein equation:

$$R_h = \frac{kT}{6\pi\eta D_W^{25^\circ C}} \qquad (3)$$

where R_h is the hydrodynamic radius, k is the Boltzman's constant, T is the absolute temperature, η is the viscosity of water and $D_W^{25^\circ C}$ is the translational diffusion coefficient.

4.3. Results:

4.3.1. Effect of urea on secondary structure of serum albumins:

Far-UV CD spectroscopy is greatly used to observe the changes in secondary structure, conformation and stability of proteins in solutions (Santra et al., 2005, Moriyama and Takeda, 2005). The far-UV CD is also used to estimate the fraction of secondary structure i.e. α-helix, β-sheet and random coil. Far-UV CD spectra of all the five albumins at pH 3.5 exhibited two minima, one at 208 nm and other at 222 nm which is characteristic of α-helical structure. Similar spectral features of serum albumins were also found at pH 7.4 (Mir et al., 2010b). Urea induced secondary structural change has been frequently observed in many proteins including serum albumins also (Tripathi et al., 2009, Galantini et al., 2010). As shown in Figure 4.1, in the presence of 4.0 mM of SDS ellipticity of spectra in all the albumins were same as that of spectra at pH 3.5. From this observation it was concluded that SDS is not

affecting the secondary structures of serum albumins. We further checked the effect of urea on albumins in the absence and presence of 4.0 mM SDS at pH 3.5. for sake of clarity only 4 representative spectra are shown i.e. at 0, 2.0, 8.0 and 9.0 M urea. Up to 2.0 M urea the ellipticity of all albumins did not change but beyond this concentration ellipticity decreased continuously till 9.0 M. However in the presence of 4.0 mM SDS, the ellipticity of spectra was not changed even up to 9.0 M urea. The Figure 4.2, shows urea induced unfolding of serum albumins in the absence and presence of 4.0 mM SDS as monitored the change in CD (mdeg) at 222 nm. Urea unfolds the serum albumins without SDS at pH 3.5 with *Cm* values 3.44 M, 2.28 M, 2.49 M, 2.58 M, 3.41 M in an HSA, BSA, PSA, RSA and SSA respectively. However in the presence of 4.0 mM SDS urea was unable to unfold albumins even at higher concentration. From CD measurements it can be concluded that in the presence of 4.0 mM SDS the secondary structures of serum albumins was stable against urea denaturation even up to 9.0 M.

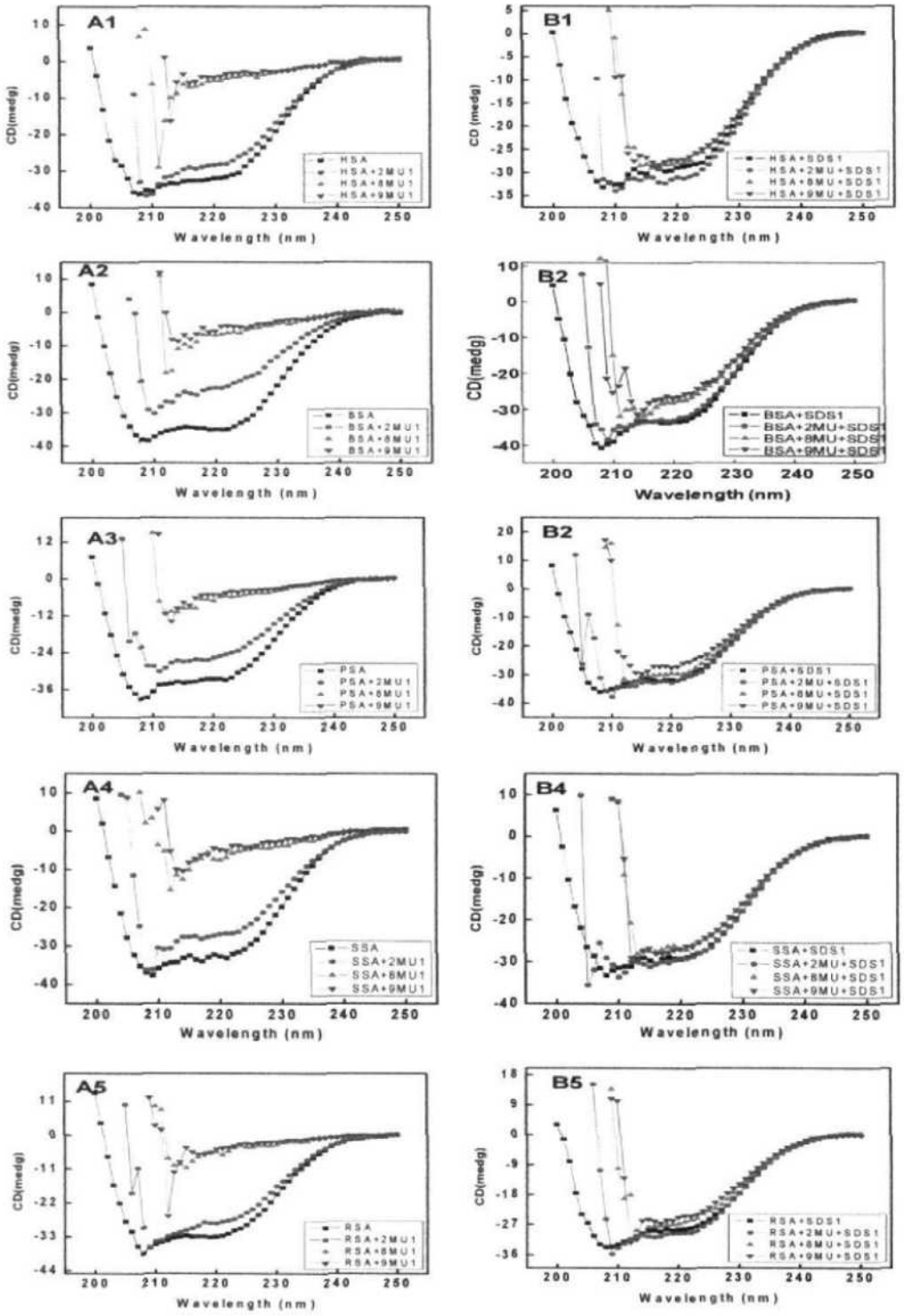

Figure 4.1. Secondary Structural change of albumins was monitored by Far-UV CD. Effect of increasing concentration of urea in the absence and presence of 4.0 mM SDS on (A) HSA (B) BSA (C) PSA (D) SSA and (E) RSA at pH 3.5. In all the measurements albumin concentration was fixed 5.0 μM and sample were incubated 12 hrs before measurements.

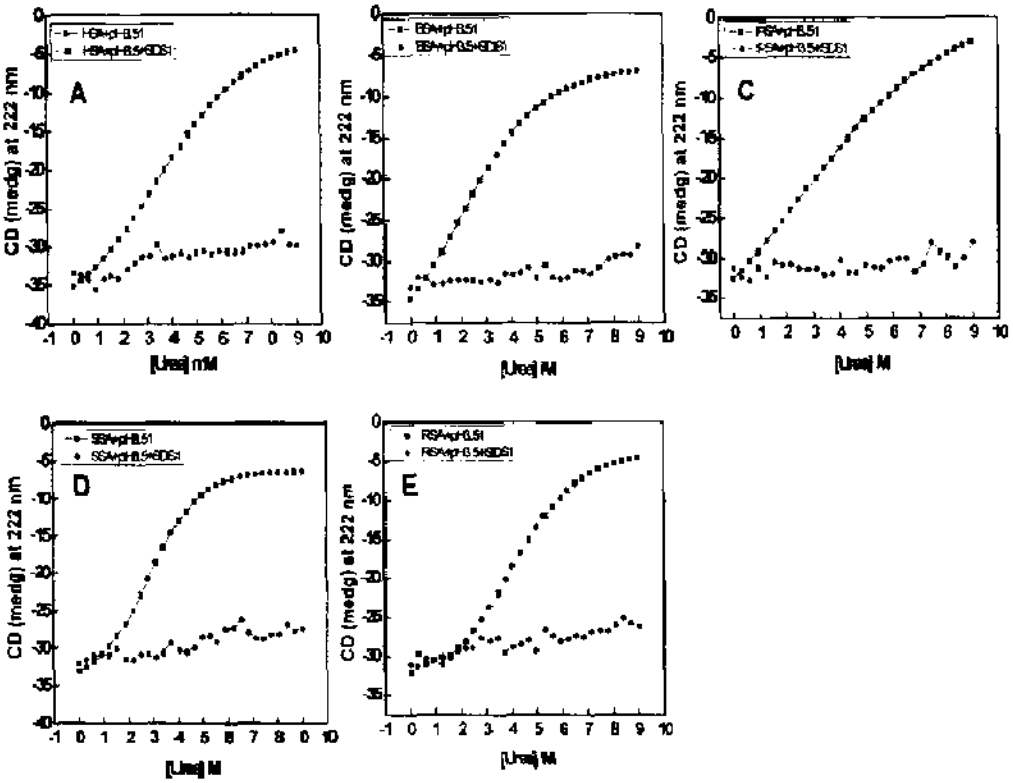

Figure 4.2. Change in α-helicity of albumins were demonsterated by urea in the absence and presence of 4.0 mM SDS at pH 3.5. The overall helicity of (A) human, (B) bovine, (C) porcine, (D) sheep and (E) rabbit serum albumins at 222 nm in the absence and presence of 4.0 mM SDS as a function of varying urea concentration. The albumins concentration was taken 5.0 μM.

4.3.2. Intrinsic fluorescence measurements:

Intrinsic fluorescence measurement gives information about the polarity of envimino acids and residues. Proteins contain three type of aromatic amino acid residues (Trp, Tyr and Phe) which may contribute to their intrinsic fluorescence but only tyrosine and tryptophan is used experimentally because their quantum yields is high enough to give a good fluorescence signal. The intrinsic fluorescence of proteins reveals the environment-dependent solvent exposure of the Trp indole ring and the tyrosine aromatic side chains. HSA RSA contains one Trp, while BSA, PSA and SSA contain two Trp which are buried in the hydrophobic core of the albumins at physiological pH. In Figure 4.3, shows the fluorescence emission spectra The maximum emission of fluorescence intensity was observed at 333 nm (HSA), 332 nm (BSA), 336 nm (PSA), 338 nm (SSA) and 336 nm (RSA). It is reported that if wavelength maximum is in the

range of 330-340 nm, the protein is well folded and tryptophan is buried in a hydrophobic core (Lakowicz, (1983)). After addition of 4.0 mM SDS in all albumins incubated at pH 3.5, a drastic change in the fluorescence emission spectrum was noticed and wavelength maximum showed a blue shift on an average of 8 nm. We studied the effect of increasing concentration of urea on albumins in the absence and presence of 4.0 mM SDS. As shown in Figure 4.3, in the absence of SDS the fluorrscence emission spectrum exhibited a slight red shift upon incubation with 2.0 M urea while maximum red shift was notice (8.0 nm). The fluorescence emission spectrum was slightly red shifting in the presence of 2.0 M urea and maximum red shift was noticed at 9.0 M urea with low fluorescence intensity. However in the presence of 4.0 mM SDS the emission maxima was very minutely shifted even in the presence of 9.0 M urea with slight increase in fluorescence intensity. The shift in wavelength maximum of five albumins in the absence and presence 4.0 mM SDS are plotted at varying concentration of urea as shown in Figure 4.4. Albumins incubated at pH 3.5 reveled a sigmoidal change in emission maxima with increasing concentration of urea (Figure 4.4A) but in the presence of 4.0 mM SDS (Figure 4.4B) no sigmoidal change was noticed even at 9.0 M urea. The change observed in emission maxima values are given in Table 4.1.

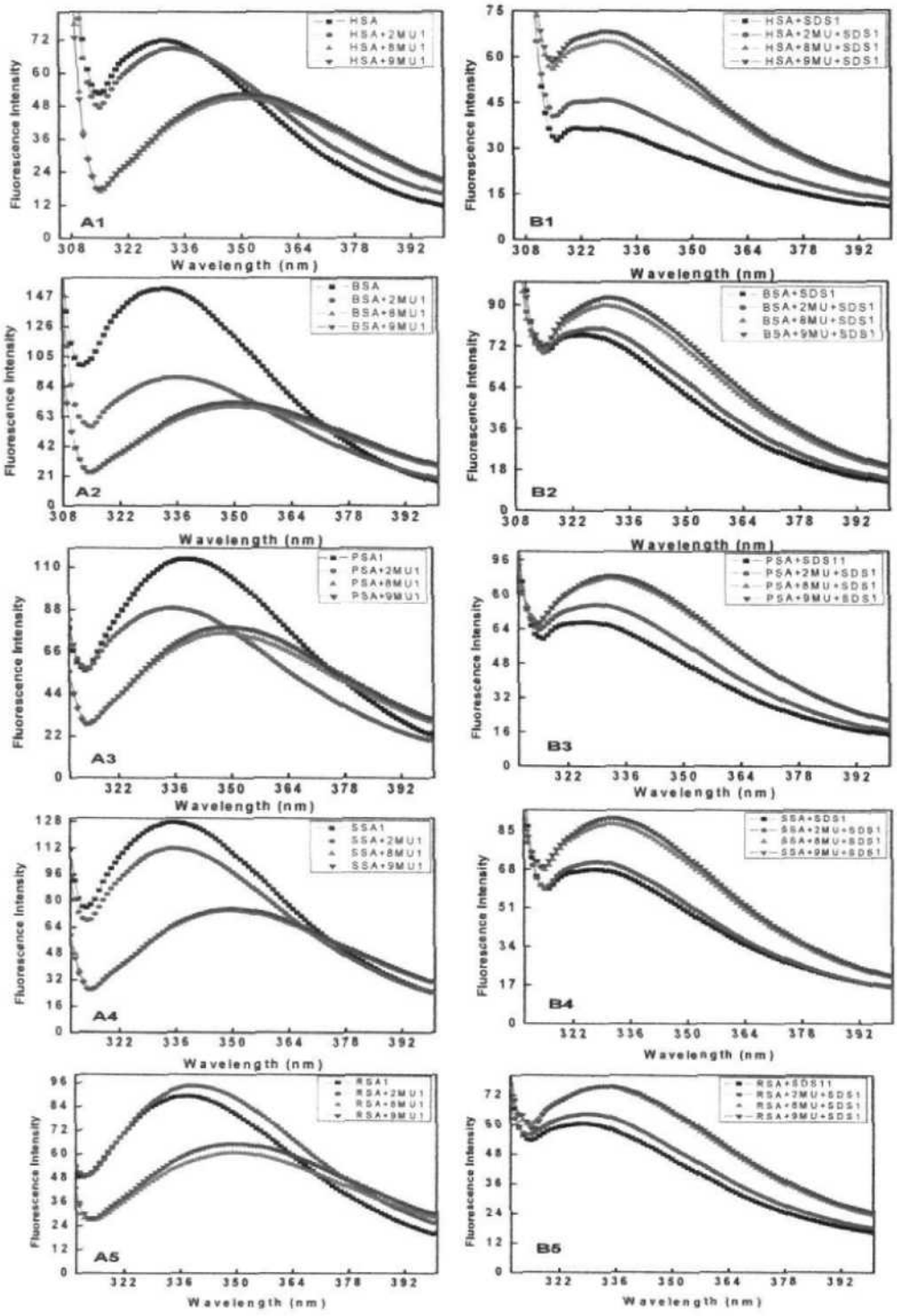

Figure 4.3. Effect of urea on 4.0 mM SDS-incubated serum albumins. Fluorescence emission spectra of (1) human, (2) bovine, (3) porcine, (4) sheep and (5) rabbit serum albumins at increasing concentration of urea in the (A) absence and (B) presence of 4.0 mM SDS at pH 3.5. The samples containing protein, SDS and urea were incubated overnight and protein concentration were 5.0 μM.

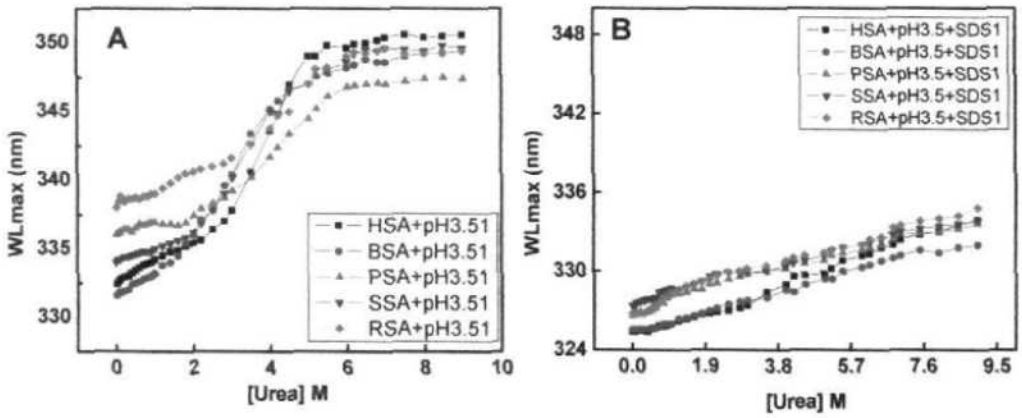

Figure 4.4. Effect of Urea on albumins in the absence and presence of 4.0 mM SDS at pH 3.5. Change in wavelength maximum of HSA (-■-), BSA (-●-), PSA (-▲-), RSA (-▼-) and SSA (-♦-) in the (A) absence and (B) presence of 4.0 mM SDS with respect to increasing concentration of urea. Before performing the experiments samples were incubated overnight with 5.0 μM of serum albumin concentration throughout the study.

Table 4.1. Shift in wavelength maximum of albumins at different conditions and a transition mid point by CD (mdeg) at 222 nm.

S. No.	Protein name	Wavelength maximum (nm)				Transition midpoint (*Cm*)
		pH 3.5	pH 3.5+SDS	Urea 10 M	Urea 10 M + 4.0 mM SDS	CD at 222 nm
1	HSA	332.4	325.4	350.6	333.9	3.44 M
2	BSA	331.6	325.6	349.4	332	2.28 M
3	PSA	336	326.6	347.4	333.6	2.49 M
4	SSA	338	326.8	349.4	334.8	3.41 M
5	RSA	334	327.4	349.6	333.8	2.58 M

4.3.3. Hydrodynamic Radii measurements:

DLS is used to characterize the hydrodynamic radii (R_h) of particles as well as to detect the conformational change of proteins. The change in hydrodynamic radii of five albumins at pH 7.4 alone and at pH 3.5 in the absence and presence of 4.0 mM SDS are shown in Figure 4.5. The effect of urea was also seen under both the conditions (pH 3.5 and pH 3.5 + 4.0 mM SDS). The R_h of albumins at pH 7.4 was found to be 3.4 nm (HSA), 3.7 nm (BSA), 3.9 (PSA) and 3.4 (RSA, SSA). At pH 3.5,

a slight increase in R_h was observed i.e 4.0 nm (HSA), 4.5 nm (BSA), 4.4 nm (PSA), 4.0 nm (RSA) and 4.4 nm (SSA) probably due to the partial unfolding of protein under acidic condition. The addition of 4.0 mM SDS at pH 3.5 caused decrease in R_h of partially unfolded albumins to 3.2 nm (HSA), 3.1 nm (BSA), 3.6 nm (RSA) and 3.9 nm (PSA, SSA) respectively owing to compaction of structure induced by SDS. The effect of urea was also seen on albumins at pH 3.5. The urea unfolds the albumins in the absence of SDS and hydrodynamic radii increases accordingly is shown in Table 4.2. However in the presence of 4.0 mm SDS, urea was incapable of unfolding protein as the hydrodynamic radii did not increase and is more or less like native albumins. The hydrodynamic radii at different conditions are summarized in a Table 4.2.

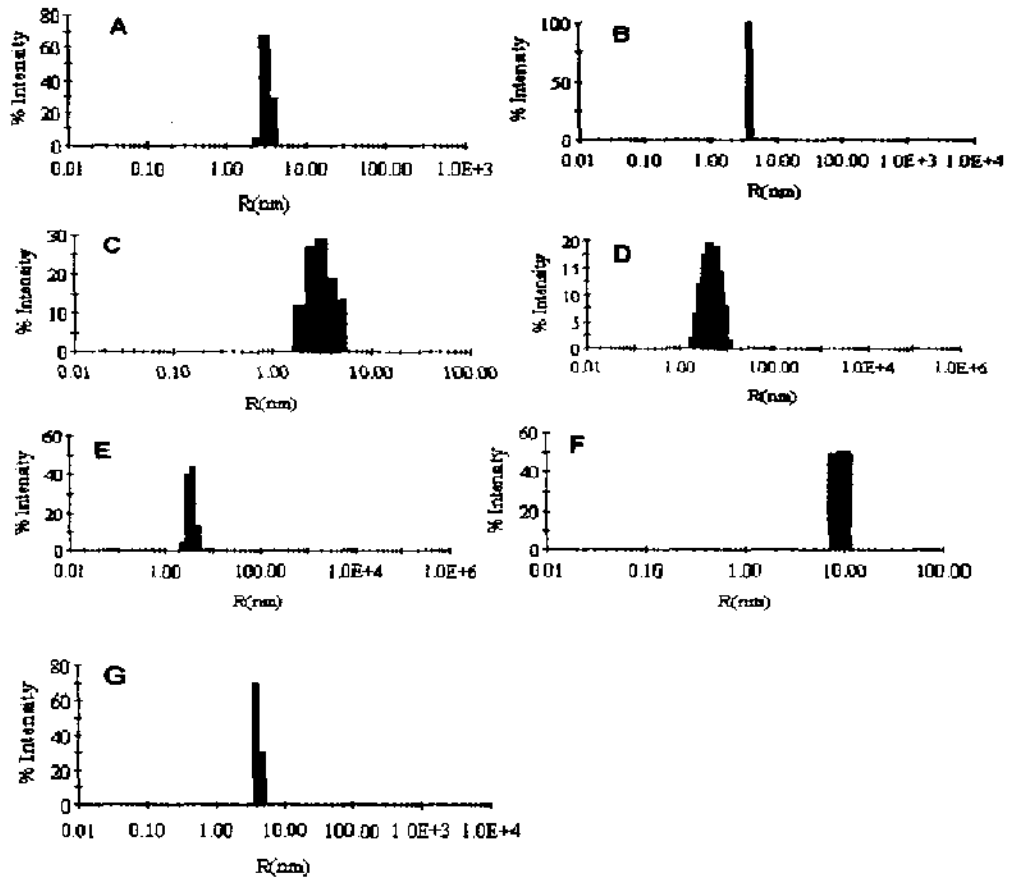

Figure 4.5. Change in hydrodynamic radii monitored by DLS. Change in hydrodynamic radii of HSA were monitored (A) at pH 7.4, (B) pH 3.5, (C) pH 3.5 + 4.0 mM SDS, (D) pH 3.5 + 5 M urea, (E) pH 3.5 + 4.0 mM SDS + 5 M urea, (F) pH 3.5 + 9.0 M urea and (G) pH 3.5 + 4.0 mM SDS + 9.0 M urea in HSA.

Table 4.2. Hydrodynamic radii of serum albumins at different condition.

S. No.	Proteins	R_h (nm)						
		pH 7.4	pH 3.5	pH 3.5 +SDS	pH3.5 +5MU	pH3.5+ 5MU+ 4.0mMSDS	pH3.5 +9MU	pH3.5+ 9MU +4.0mMSDS
1	HSA	3.4	4.0	3.2	5.1	3.7	9.3	4.3
2	BSA	3.7	4.5	3.1	6.2	3.9	11.3	4.8
3	PSA	3.9	4.4	3.9	5.2	4.5	14.3	5.0
4	SSA	3.4	4.4	3.9	5.8	3.9	12.4	4.5
5	RSA	3.4	4.0	3.6	6.0	4.1	10.8	4.6

4.3.4. Thermal Denaturation:

We also checked stabilizing effect of SDS on albumins against temperature changes. We incubated albumins at pH 7.4 and 3.5 and in the absence and presence of 4.0 mM SDS. Thermal unfolding of albumins in all above conditions were determined by observing the change in θ_{222} nm with respect to temperature. Figure 4.6, summarizes the changes in CD ellipticity at 222 nm of native albumins and in the absence/presence of 4.0 mM SDS at pH 3.5. The native albumins show broad sigmoidal change with respect to temperature and the transition temperature (T_m) were 76 °C (HSA), 79 °C (BSA), 70 °C (PSA), 75 °C (SSA) and 70 °C (RSA) while at pH 3.5 the *Tm* was decreased significantly to 54 °C (HSA), 57 °C (BSA, PSA), 59 °C (SSA) and 63 °C (RSA) which suggest that secondary structure of albumins at pH 3.5 is very labile due to partial unfolding. We further incubated the albumins with 4.0 mM SDS at pH 3.5 and monitored the changes in secondary structure as a function of temperature. A sigmoidal change was found and T_m increased significantly to 74 °C (HSA), 75 °C (BSA), 70 °C (PSA, SSA) and 75 °C (RSA) which is close to native albumins. The *Tm* values of albumins under different conditions are shown in Table 4.3. From the thermal denaturation profile it can be concluded that SDS is protecting the secondary structure of all albumins at pH 3.5.

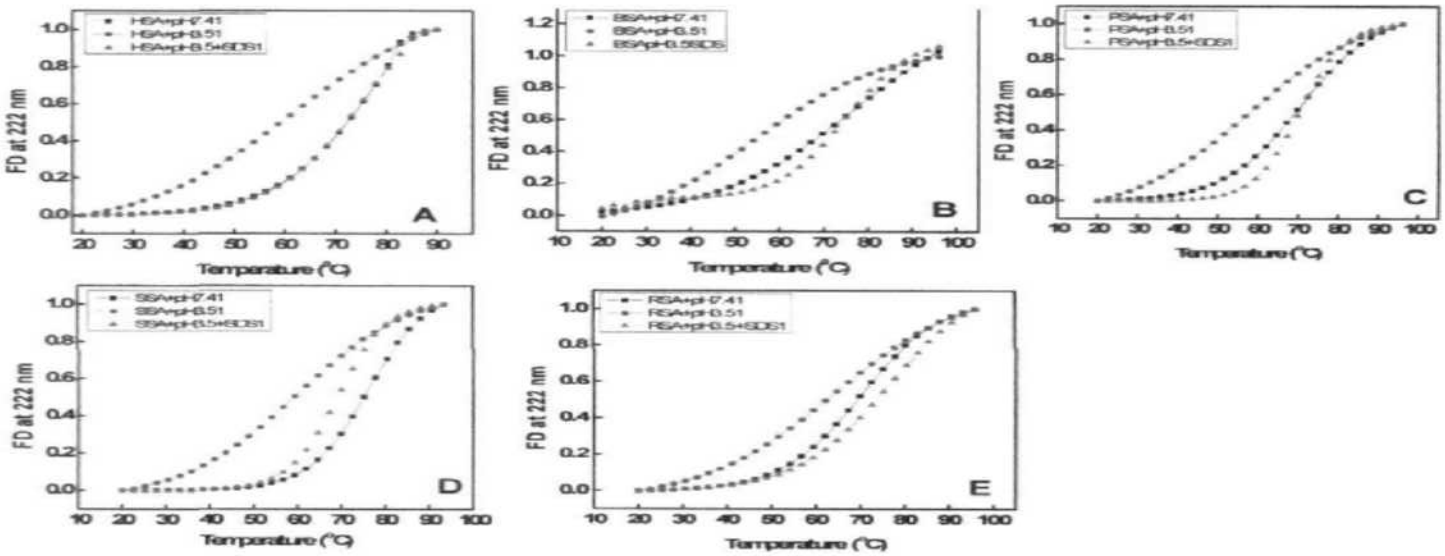

Figure 4.6. Thermal denaturation of albumins. Thermal denaturation of (A) human, (B) bovine, (C) porcine, (D) sheep and (E) rabbit serum albumins at pH 7.4 (-■-), pH 3.5 (-●-) and in the presence of 4.0 mM SDS at pH 3.5 (-▲-)measured by change in ellipticity at 222 nm. Albumin concentration was 5.0 μM.

Table 4.3. Tm were measured in all albumins at different condition

S.No.	Condition	T_m (°C)				
		HAS	BSA	PSA	SSA	RSA
1	pH 7.4	76	79	70	75	70
2	pH 3.5	54	57	57	59	63
3	pH 3.5 + 4.0 mM SDS	74	75	70	70	75

4.5. Discussion:

Protein denaturation and stabilization is very emerging topic in molecular biology due to its large application in the industry. Various methods and additives are used for protein stabilization and denaturation (Dobson, 2003, Paschek and Garcia, 2004). The surfactants, particularly SDS is frequently used in the stabilization and destabilization of proteins. SDS mimics the lipid of biological membrane so its interaction with protein gives important clues to understand the effect of the lipid on protein in vivo. In this study we have taken five serum albumins from different sources and observed the effect of SDS, urea and temperature at pH 3.5. First we investigated the effect of pH on all albumins. It is reported that at neutral pH all the albumins exist in a compact form native or 'N' form while at low pH (pH 3.5) it is less compact i. e. 'F' form and this form comes due to conformational isomerization (Nakamura et al., 1997). 'F' form is very fast moving and is less stable than the 'N' form because at lower pH the positively charge residues become protonated, due to this protein turn out to be partially unfolded state. Further we observed the effect of SDS on the fast moving ('F') state of serum albumins. The secondary structures of fast moving serum albumins remained unchanged in the presence of 4.0 mM SDS while the tertiary structure shows some alteration with shift in wavelength maximum by 8.0 nm. The blue shifting behavior of proteins signifies that aromatic chromophores are shifting into the more non-polar environment. Similar results were also found in case of HSA where around 16 nm blue shift was noticed in the presence of 7.0 mM SDS at pH 7.0 (Anand et al., 2010). From these results it appears that SDS is stabilizing the proteins at acidic pH because the negative head of SDS interact with e positive part of albumins while the hydrophobic tail interacts with with non-polar part of proteins. Lysozyme also showed similar patterns in the presence of SDS (Yonath et al., 1977). We further explored the effect of urea and temperature on albumins conformation in the absence and presence of 4.0 mM SDS at pH 3.5. Urea unfolds the albumins in the absence of SDS at a little bit lower concentration (2.0 M) while in the presence of 4.0 mM SDS the urea is unable to unfold both secondary as well as tertiary structures of albumins even up to 9.0 M concentration. Urea unfold albumin at pH 7.4 and helicity of proteins is almost lost but at low concentration with the added SDS the helicity of proteins is again recovered which is very close to the native state of albumins. These results indicate that small amount of SDS refolded the unfolded

protein (Takeda K, 1987). Hydrodynamic radii of albumins were monitored by DLS. The albumins at pH 7.4 have compact structure and hydrodynamic radii (Table 2) which is inconsistent with other reports (Gull et al., 2011). But at acidic pH, the hydrodynamic radii was found to increases due to partial unfolding. In the presence of 4.0 mM of SDS the hydrodynamic radii was decreased. The hydrodynamic radii of partially unfolded albumins were markedly increases in the presence of 9.0 M urea but in the presence of 4.0 mM SDS the urea is not capable of unfold and changing the hydrodynamic radii as also supported our CD data. The protective behavior of SDS was also observed in earlier reports and it is reported that SDS is wrapped around proteins with the help of hydrophilic head and a hydrophobic tail. This wrapping provides enough strength to proteins. At above CMC, SDS-protein interaction is based on two type of models one is a necklace and other is bead model. According to these two models the SDS is stabilizing the protein (Guo et al., 1990, Turro, 1995). From above results it is concluded that urea is uable to unfold the albumins in the presence of SDS. It is reported that urea has two types of denaturing property either directly or indirectly. From the above observation we can say that initially urea is favorably interacting with albumins electrostaticaly and through hydrogen bonding because albumins are positively charged at pH 3.5. But in the presence of 4.0 mM SDS at same pH the urea is unable to interact directly, the reason is hydrophobicity of environments is high and protein charge is masked with the head of SDS monomer. The similar protective behavior of SDS was also reported in cytochrome C. At pH 4.0 urea were unable to unfold the cytochrome C when it was incubated with 2.0 mM SDS and its secondary as well as tertiary structures was not altered (Chattopadhyay and Mazumdar, 2003). CD, fluorescence and DLS data reveled that if proteins are having charge on the surface, then urea interacts with protein directly and unfolding will occur on the another hand if the protein is in hydrophobic environment the urea is unable to interact directly with protein, but it will interact with environmental hydrophobicity. This lead us to conclude that urea interact with proteins directly if protein is having a charge on the surface while it interactes indirectly if the protein is in hydrophobic environments. Apart from urea denaturation we also performed thermal denaturation for better understanding of the protective effect of SDS. Anionic surfactants are capable of protecting the proteins also by the thermal denaturation (Moriyama et al., 2008, Chodankar et al., 2008). The thermal denaturations of albumins was studied in the presence and absence of 4.0 mM SDS at pH 3.5 and also

at neutral pH. The albumins, whether at neutral or acidic pH, in the presence of 4.0 mM SDS showed sigmoidal transition with respect to increasing temperature. One thing is important to note that the albumins at pH 3.5 have very less thermal stability than at pH 7.4. While in case of SDS stabilized albumins, stability is similar to that at pH 7.4 as evident from *Tm* values. Similar results were also found when BSA; was incubated with SDS the secondary structure of BSA was not disrupted even at 130 °C (Moriyama et al., 2008). Earlier we have reported that RSA is very heat tolerable in the presence of 20.0 mM CTAB and RSA is not unfolded in the presence of CTAB (Ali et al., 2010). From these observation we can concluded that the SDS is having strong protective effects against urea and thermal denaturation. Overall results are summarized in (Figure 4.7) as graphical presentation.

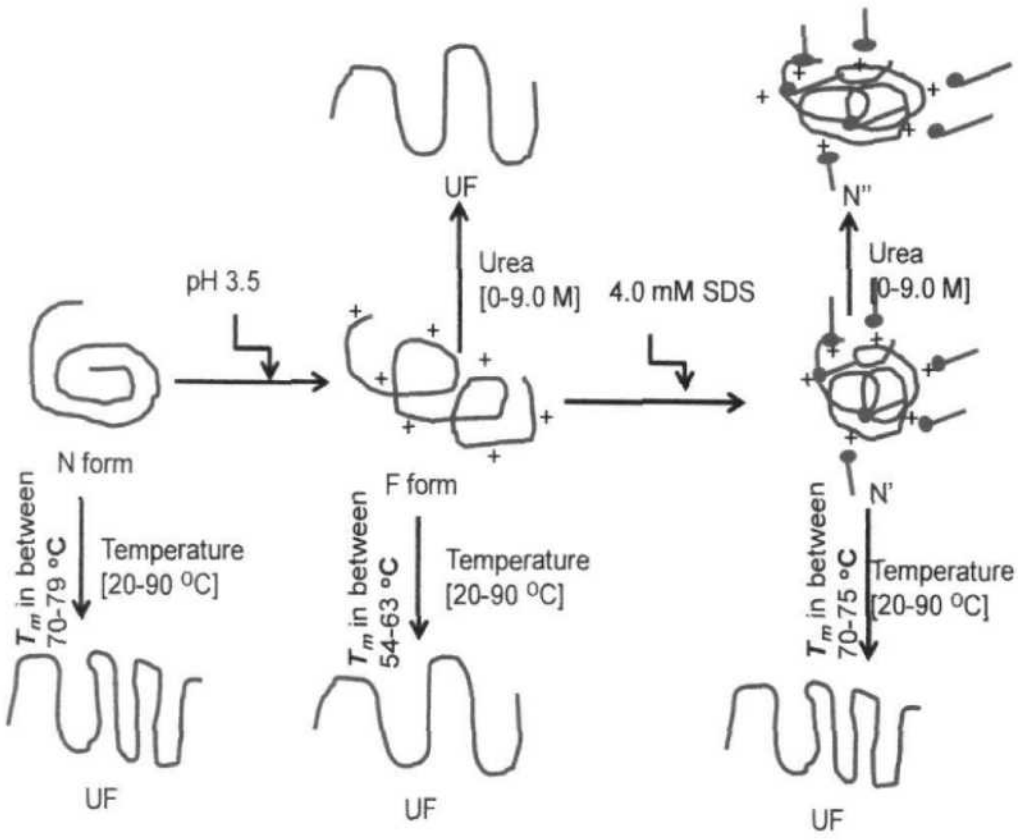

Figure 4.7. Schematic presentation of SDS-stabilized albumins and their unfolding by urea and temperature.

4.6. Conclusion:

Effect of SDS, urea and temperature in 'F' form of serum albumins was investigated. We found that 4.0 mM SDS concentration has great potential to protect the albumins from unfolding by urea (0-9.0 M). SDS is also showing a protective effect against temperature changes (20-90 °C). In the presence of 4.0 mM SDS, the urea was unable to unfold the serum albumins because SDS interact with albumins via electrostatic as well hydrophobic interactions. From this study we have also proposed the mechanism of interaction of urea. Urea will interact with protein directly if the protein is in charged state otherwise indirect interaction will take place. Thermal stability is also provide by SDS due to electrostatic as well as hydrophobic interaction.

Stability of protein is a major concern in industries because some proteins are very unstable at physiological pH. This study will satisfy the stability problem.

CHAPTER 5

Adapted from: **PLoS ONE (2013)**

Monomeric Banana Lectin at Acidic pH Overrules Conformational Stability of Its Native Dimeric Form

5.1. Introduction:

Understanding the factors that decide how a linear polypeptide chain folds into its unique three-dimensional structure relic one of the fundamental questions in biology. Several models for the mechanism of protein folding have been proposed and there is ample argument concerning competing hypothesis. Current sources of content consist of whether there are on-pathway intermediates in the folding and if so, what the nature of such partially folded intermediates is. There are substantial evidences which indicate that proteins of smaller molecular weight under appropriate conditions fold to the native state within a few milliseconds with no detectable intermediate (Privalov, 1996, Dill and Chan, 1997). Such folding is consistent with smooth-funnel energy landscape models. On the other hand, for many proteins there are extensive experimental data for transient intermediate, including the molten globule (Ptitsyn, 1987, Radford and Dobson, 1995). The molten globule is an intermediate state of protein stabilized by acidic/alkaline pH, moderate concentration of strong chemical denaturants at a certain temperature. The general properties of this intermediate state are the presence of marked secondary structures, massive or significant loss of tertiary structures together with exposed hydrophobic clusters (Kuwajima, 1989, Christensen and Pain, 1991, Ptitsyn, 1995). The available literatures support that the molten globule state (and other nonnative states of protein molecule) can stay in living cells and can be mixed up in a number of physiological processes owing to the fact that the negative electrostatic potential of the cell surface may attract protons from the immensity of solution leading to a local drop in pH, thus resulting in partial denaturation of proteins (Prats, 1986, Bychkova et al., 1988). There is now abundant data available regarding molten globule state of monomeric protein, which has greatly improved our knowledge about protein folding problem and folding intermediates (Griko, 2000, Park, 2004, Kelkar et al., 2010).

Lectins are (glyco) proteins which specifically bind to mono or oligosaccharide reversibly. Lectins are found in every kingdom of life. They perform various biological functions ranging from host-pathogenic interaction, cancer metastasis, cell–cell communication, embryogenesis, mitogenic stimulation as well as

the tissue development (Lis and Sharon, 1998, Drickamer, 1999, Chandra et al., 1999, Loris, 2002). Their high affinity and specificity for glycoconjugates have found many applications in biological and biomedical research (Sharon and Lis, 1990). Banana lectin (BL) is a member of jacalin-related superfaimly of lectins and explicitly binds to mannose and glucose containing oligosaccharides (Peumans et al., 2000, Meagher et al., 2005). It is a homodimeric protein where each subunit has a molecular weight of 14.5 kDa and consists of 141 amino acid residues with a single Trp at position 10 (Figure 5.1). Also each subunit has twelve β-strands arranged in a β-prism-I fold. BL is known to act as a potent inhibitor of HIV replication which is main perpetrator in the list of fatal diseases (Swanson et al., 2010). In this work, we investigated the unfolding of BL at acidic pH using several spectroscopic as well as hydrodynamic techniques. The stability of the protein was compared under different conditions using temperature and chemical denaturants. In several instances, the individual subunits of dimeric/oligomeric proteins are reported to be less stable than native and biologically functional state of protein as it is believed that interchain interactions that bind the subunits impart additional stability to the dimer/oligomer. However, to the best of our knowledge, this is the first report on the monomeric state of protein being more stable than its native dimeric state.

Figure 5.1. Ribbon structure of banana lectin (2BMY) generated from PyMol. Trp residues are shown in both subunits.

5.2. Material and Methods:

5.2.1. Materials:

Bananas were purchased from local shops. Urea, 1-analino-8-naphthalene sulfonate (ANS) Sephadex-75 was purchased from Sigma Chemicals Co. USA. All other chemicals used were of analytical grade.

5.2.2. Protein purification:

BL was purified by the procedure of Koshte et. al. (Koshte et al., 1990). 250 g of banana pulp was soaked in 1 L distilled water containing 250.0 mM NaCl, 5.0 mM $MgCl_2$ and 5.0 mM $CaCl_2$. The mixture was subjected to homogenization followed by drop wise addition of 4.0 M NaOH to maintain pH at 7.4. The homogenate was incubated for 15.0 min after that 0.1M Glucose was added to the final volume and stirred for 2.0 h at room temperature. The solution was centrifuged at 18000 rpm for 30 mins. The pellet was discarded, 85% ammonium sulphate was added to the supernatant and kept overnight for precipitation followed by centrifugation at 18000 rpm for 45 mins. The pellet was collected and redissolved in Tris-HCl buffer of pH 7.4 and dialyzed for overnight. The clear suspension was loaded onto Sephadex-G75 affinity column. The elution was carried out using 0.5 M glucose dissolved in buffer pH 7.4. The eluent was again dialyzed to remove the glucose and lyophilized for further use. The purity of lectin was checked by SDS-PAGE and the concentration was determined by Lowry and BCA methods.

5.2.3. Buffer Preparation:

pH measurements were carried out on Mettler Toledo pH meter (Seven Easy S20–K) using Expert ''Pro3 in 1'' type electrode having the least count of the pH meter of 0.01 pH unit. The acid denaturation of BL was carried out in 20.0 mM of following buffers: Tris-HCl (pH 7.0-7.4), sodium phosphate (pH 6.0), sodium acetate (pH 3.5–5.0), glycine-HCl (pH1.6–3.0) and KCl-HCl (pH 0.8–1.4). All the buffers were filtered through 0.45μm syringe filter. Before all of the spectrophotometric measurements the protein samples were incubated for overnight at room temperature.

5.2.4. Circular Dichroism:

CD measurements were performed with a Jasco spectropolarimeter (J-815), equipped with a Jasco Peltier-type temperature controller (PTC–424S/15). The instrument was

calibrated with D-10-camphorsulfonic acid. The measurements were carried out at 25 °C. Spectra were collected with a protein concentration of 0.15 mg ml^{-1} with 0.1 cm path length and 1.0 mg ml^{-1} with 1 cm path length for far-UV and near-UV CD respectively. Each spectrum was the average of 2.0 scans. The results were expressed as mean residual ellipticity (MRE) in deg cm^2 $dmol^{-1}$ which is defined as:

$$MRE = \theta_{obs}\,(mdeg)\,/10 \times n \times Cp \times l \qquad (1)$$

where θ_{obs} is the CD in millidegree, n is the number of amino acid residues in one subunit (141 for BL), l is the path length of the cell in centimeters and Cp is the molar fraction of proteins.

5.2.5. Thermal and Chemical Denaturations:

The thermal unfolding of BL was carried out by heating the samples and measuring the temperature-dependent CD response at 218 nm from 25 °C to 95 °C using a temperature rise of 1 °C/min in a water-jacketed cell attached to the Multitech M-H-03 water circulator. For chemical denaturation experiments, protein samples (0.15 mg ml^{-1}) were allowed to equilibrate overnight with 0–10 M urea at desired pH.

5.2.6. Fluorescence measurements:

Fluorescence measurements were performed on Hitachi spectrofluorometer (F-4500). For acif and chemical denaturation the fluorescence spectra were measured with a protein concentration of 0.15 mg ml^{-1}. The intrinsic spectra were recorded between 300 to 400 nm with excitation wavelength of 295 nm. For light scattering measurements, the excitation and emission wavelength was set at 350 nm as we have used this method in our previous report (Ahmad et al., 2009b). Both the excitation and emission slit widths were set at 5 nm. For extrinsic fluorescence measurement, the protein samples were incubated with 50-fold molar excess of ANS at room temperature in dark. The samples were excited at 380 nm and emission spectra were recorded between 400–600 nm.

5.2.7. Acrylamide quenching experiments:

For arcylamide quenching experiments, aliquots of 5 M acrylamide (quencher) stock solution were added to the protein samples (0.15 mg ml^{-1}) to achieve the desired range of quencher concentration (0–0.12 M). Excitation wavelength was set at 295 nm in order to excite Trp residues only and the emission spectrum was recorded in the range

300–400 nm. The decrease in fluorescence intensity at λ_{max} was analyzed according to the Stern–Volmer equation:

$$F_o/F = 1 + K_{sv}[Q] \qquad (2)$$

where F_o and F are the fluorescence intensities at an appropriate wavelength in the absence and presence of quencher respectively, K_{sv} is the Stern–Volmer constant and [Q] is concentration of the quencher.

5.2.8. Dynamic Light Scattering (DLS):

DLS measurements were performed with protein concentration of 1.0 mg ml^{-1} using DynaPro–TC–04 dynamic light scattering equipment (Protein Solutions, Wyatt Technology, Santa Barbara, CA) equipped with temperature-controlled microsampler. Before the measurements, all the samples were kept for overnight (12 hrs) incubation. Prior to scanning, all the solutions were spun at 10,000 rpm for 15 min and filtered through microfilter (Millipore Millex-HV hydrophilic PVDF) having a pore size of 0.45 μm followed by further filteration using 0.22 μm pore sized filter (Whatman International, Maidstone, UK). Measured size was presented as the average value of 50 runs. Data were analyzed by using Dynamics 6.10.0.10 software at optimized resolution. The mean hydrodynamic radius (R_h) and polydispersity (P_d) were estimated on the basis of an autocorrelation analysis of scattered light intensity based on the translational diffusion coefficient, by Stokes–Einstein equation:

$$R_h = \frac{kT}{6\pi\eta D_W^{25°C}} \qquad (3)$$

where R_h is the hydrodynamic radius, k is the Boltzman's constant, T is the absolute temperature, η is the viscosity of water and $D_W^{25°C}$ is the translational diffusion coefficient.

5.2.9. Size Exclusion Chromatography (SEC):

Size exclusion chromatography of BL was performed at pH 7.4 and pH 2.0 on the 120 ml column from the Äkta Purifier (Amersham Bioscience AB, Uppsala, Sweden) using a Sephadex G-75 matrix. The column was equilibrated with desired buffers containing 0.8 M Glucose and 0.15 N NaCl. The elution was carried out at a flow rate of 60 ml h^{-1} and the absorbance of eluted fractions was read at 280 nm. Blue dextran was used to determine the void volume of column.

5.2.10. Data Analysis:

Chemical and thermal denaturation data from CD and fluorescence spectroscopy were analyzed on the basis of two-state unfolding model. For a single step unfolding process, N⇌U, where N is the native state and U is the unfolded state, the equilibrium constant K_u is defined as

$$K_u = \frac{f_u}{f_n} \qquad (4)$$

With f_u and f_n being the molar fraction of U and N, respectively.

$$f_d = \frac{(Y_{obs} - Y_n)}{(Y_u - Y_{obs})} \qquad (5)$$

Where Y_{obs}, Y_n and Y_u represent the observed property, property of the native state and that of unfolded state respectively while f_d corresponds to the fraction of denatured protein. The change in free energy of unfolding in water ΔG_u° is obtained by the linear extrapolation method (Shirley et al., 1989). The relationship between the temperature and concentration of denaturant ΔG_u° is approximated by the following equation:

$$\Delta G_u = -RT \ln K_u \qquad (6)$$

and

$$\Delta G_u = \Delta G_u^\circ + m\,(D) \qquad (7)$$

where m is the experimental measure of the dependence of ΔG_u on temperature, R is the gas constant (1.987 cal K^{-1} mol^{-1}) and T is 298 K. The concentration of denaturant at which the protein is half denatured (when $\Delta G_U = 0$) is given by $D_{1/2}$ and derived from equation 7 as follows:

$$\Delta G_u^\circ = -\,m\,D_{1/2} \qquad (8)$$

5.3. Results:

5.3.1. Acid induced unfolding of BL:

5.3.2. Far-UV CD measurements:

Far-UV CD is one of the most sensitive spectroscopic techniques for analyzing secondary structure of the protein (Yang et al., 1986, Fast et al., 2009). A comparative change in far-UV CD spectra of BL at different pH is shown in Figure 5.2A. Native state of BL (pH 7.4) exhibited a single negative peak at 218 nm giving an indication for the presence of β-conformation, a feature typical for several lectins (Ahmad et al., 2007). The spectra of BL at pH 2.0 were quite similar to that of the native state (pH 7.4) a sign for considerable secondary structures being retained under acidic environment but in case of pH 0.8 a significant decrease in elipticity was found while the denatured state (6 M GdnHCl) appeared to have lost all the conformational elements. pH induced alteration in secondary structure of BL were further evaluated through changes in MRE at 218 nm as shown in Figure 5.2B. No change in ellipticity values was noticed in the pH range 1.4 to 7.4 indicating pronounced stability of BL against acidification. Further lowering of pH resulted in a noticeable decrease in ellipticity which suggested some loss of secondary structure driven possibly by the charge-charge repulsions occurring at extremely low pH.

5.3.3. Near UV-CD measurements:

The CD spectra in near-UV (250- 310 nm) range provides valuable information regarding changes in the environment of aromatic residues. The near-UV CD spectra of BL (Figure 5.2C) in native state revealed minima around 279 nm and 285 nm, a characteristic of buried aromatic chromophores particularly Trp (Naseem and Khan, 2005). The intensity of the signals was considerably diminished following incubation at pH 2.0. These data taken together with far-UV CD results suggested that BL retained significant secondary structure content with loose tertiary contacts at pH 2.0 and thus indicated the existence of molten globule state at this pH.

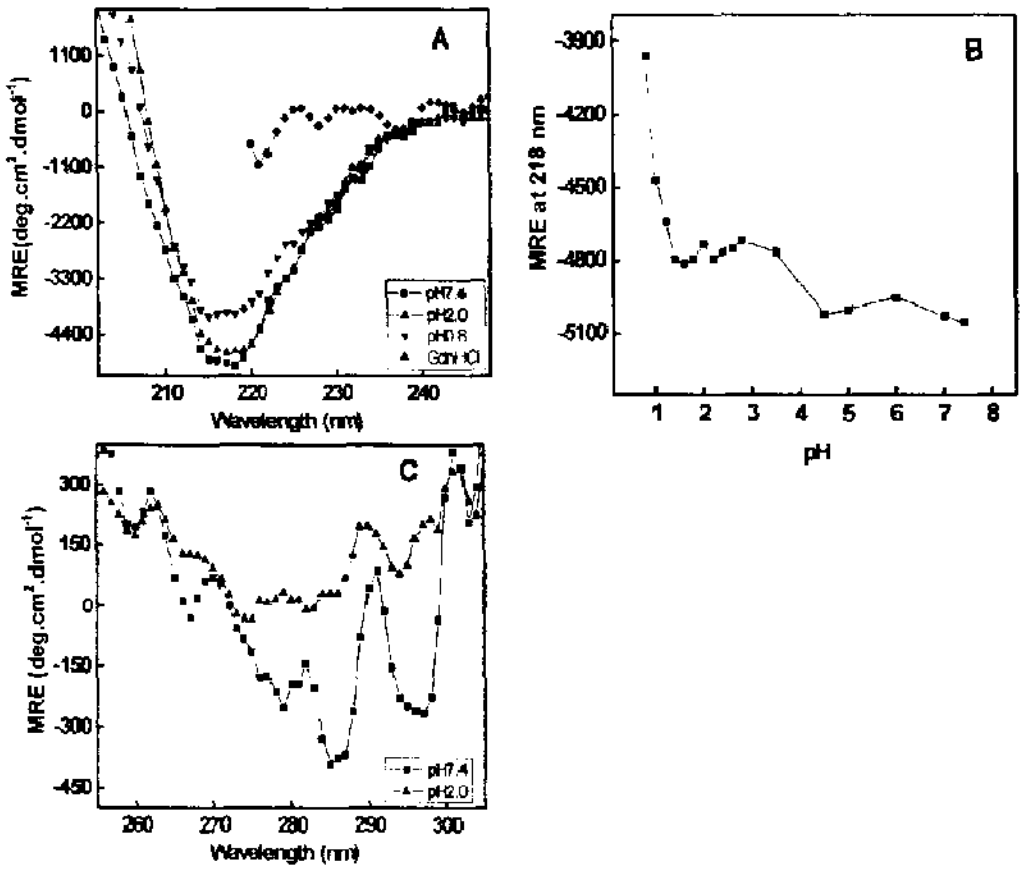

Figure 5.2. pH induced secondary structural change of BL. (A) Far-UV CD spectra of BL at pH 7.4 (-■-), pH 2.0 (-▲-), pH 0.8 (-▼-) and 6 M GdnHCl (-♦-). (B) The change in mean residual elipticity (MRE) of BL at 218 nm was plotted with respect to pH. (C) Near-UV CD spectrum of BL at pH 7.4 (-■-), and at pH 2.0 (-▲-). For far-UV CD and Near-UV CD measurements protein concentration was taken 0.15 and 1.0 mg ml^{-1}. BL was incubated at different pH overnight prior to measurements.

5.3.4. Intrinsic fluorescence:

Intrinsic fluorescence is an important method to study protein conformation because it reveals the environment-dependent solvent exposure of the Trp indole ring and the tyrosine aromatic side chains (Eftink, 1994, Eftink and Shastry, 1997). The main intrinsic fluorescence probes of protein conformation, dynamics and intermolecular interactions are Trp, Tyr, and Phe. Out of these three, Trp is the most important probe because the indole ring is highly sensitive to its neighboring environment making it an ideal choice for reporting protein conformational changes and interactions with other molecules. The emission spectrum with excitation wavelength of 295 nm is mainly

dominated by Trp fluorescence. As shown in Figure 3A, the native state of BL exhibited low fluorescence intensity (FI) and maximum fluorescence emission (λ_{max}) at 326 nm indicating that the Trp residues are buried in the core of the protein. One possible explanation for the lower FI value of native pH is that the Trp fluorescence could be quenched by neighboring amino acid side chains such as Met76 of BL, which is in close proximity (~4 Å, PDB: 2BMY) with the only Trp10 side chain (Ballew et al., 1996, Yuan et al., 1998). At pH 2.0, the emission maxima (λ_{max}) of protein was red shifted by 3 nm along with significant increases in FI similar change were also reported for diphtheria toxin (Blewitt et al., 1985). For denatured state (6 M GdnHCl), λ_{max} was shifted to 353 nm, indicating that Trp were maximally exposed to the solvent (Ahmad et al., 2010, Shukla et al., 2005). The pH dependant changes in FI of BL at 326 nm are shown in Figure 5.3B. A gradual increase the FI was noticed following acidification up to pH 2.0 which together with significant red shift (from 326 to 329 nm) indicates that Trp residues were in a non polar environment (Sedlak and Antalik, 1999, Boscolo et al., 2009). Due to the partial loosening of structure, Met76 and Trp10 residues might have displaced far apart to inhibit the quenching. The decrease in FI below pH 2.0 could be intrinsic quenching of Trp residues caused by conformational changes upon extreme acidification.

5.3.5. Rayleigh Scattering measurements:

To check the possibility of pH dependent aggregation, we performed light scattering measurements. It is reported that if extent of light scattering is fivefold more in comparison to the native state so the solution is having aggregates (Santiago et al., 2010). The results are shown in Figure 5.3C. As evident, the extent of light scattering at pH 2.0 was insignificant to that of native state and hence the chances of aggregation can be safely ruled out. As in our previous report we have found 12 times more scattering in the BL when it is incubated with SDS pH below two units of pI (Khan et al., 2012) .

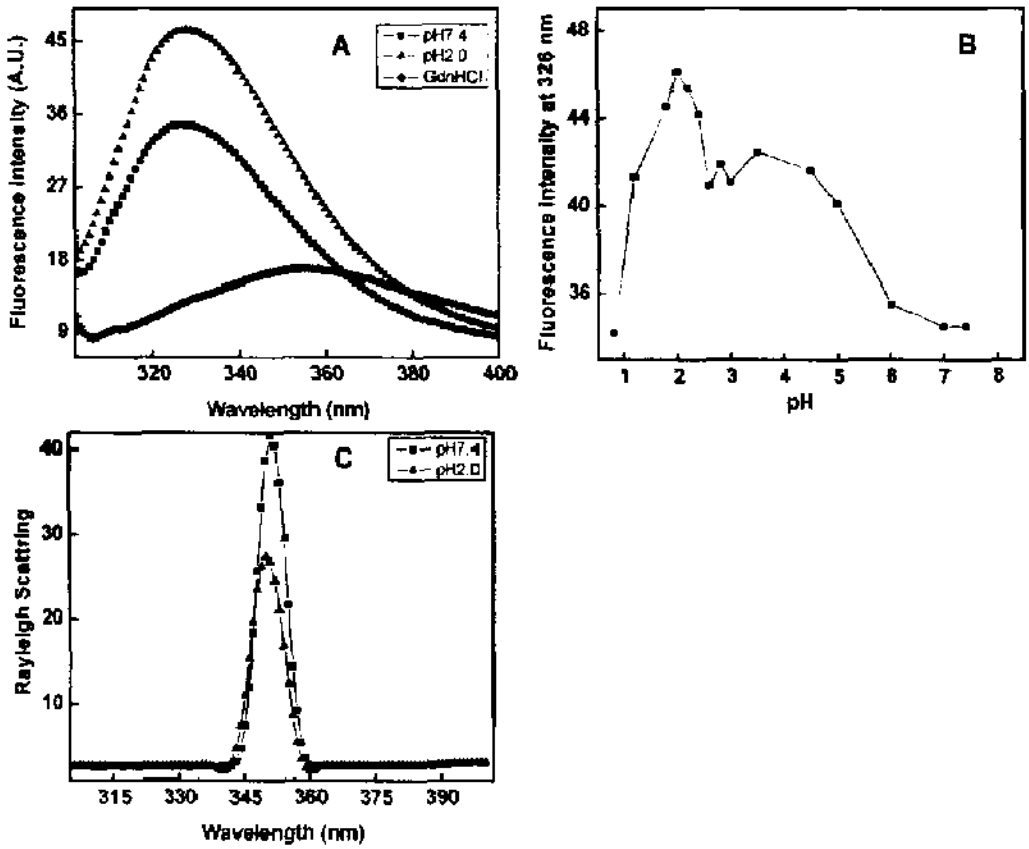

Figure 5.3. Effect of pH on the tertiary structure of BL was investigated by intrinsic fluorescence spectrosenpy. (A) Intrinsic fluorescence spectra of BL at pH 7.4 (-■-), pH 2.0 (-▲-) and 6 M GdnHCl (-♦-) after excitation at 295 nm. (B) Change in fluorescence intensity at 326 nm of BL was plotted against pH. (C) Rayleigh Scattering measurements of BL at pH 7.4 (-■-) and pH 2.0 (-▲-) after excitation at 350 and spectra was measured in the range of 300-400 nm. All the measurements were performed after 12 hrs incubation in 20.0 mM of respective buffer and final protein concentration was taken 0.15 mg ml^{-1}.

5.3.6. Extrinsic fluorescence (ANS binding) measurements:

ANS is a widely used hydrophobic dye for detecting the non-native states such as molten globule (MG) states in proteins (Ramboarina and Redfield, 2003, Safarian et al., 2006). Fluorescence spectra of BL with ANS at pH 7.4 and 2.0 (Figure 5.4.A) revealed that binding of ANS to hydrophobic patches resulted in a prominent blue shift along with a significant increase in fluorescence intensity at pH 2.0 while at pH 7.4 the ANS is unable to bind BL because hydrophobic residues are buried in the core

of the proteins. A plot of ANS fluorescence intensity at 480 nm as a function of pH is also shown in Figure 5.4B. ANS fluorescence was maximum at pH 2.0 suggesting considerable exposure of hydrophobic clusters that either remain inaccessible in native state (pH 7.4) or were minutely accessible in the denatured state of protein (6M GdnHCl). Native state of BL exhibited maximum emission of ANS fluorescence at 519 nm which decreased to 501 nm at pH 2.0 Figure 5.4C. Taken together, the above results confirm the existence of the MG - state of BL at pH 2.0 having pronounced secondary structure along with significantly disrupted tertiary contacts and hydrophobic clusters considerably exposed to the solvent.

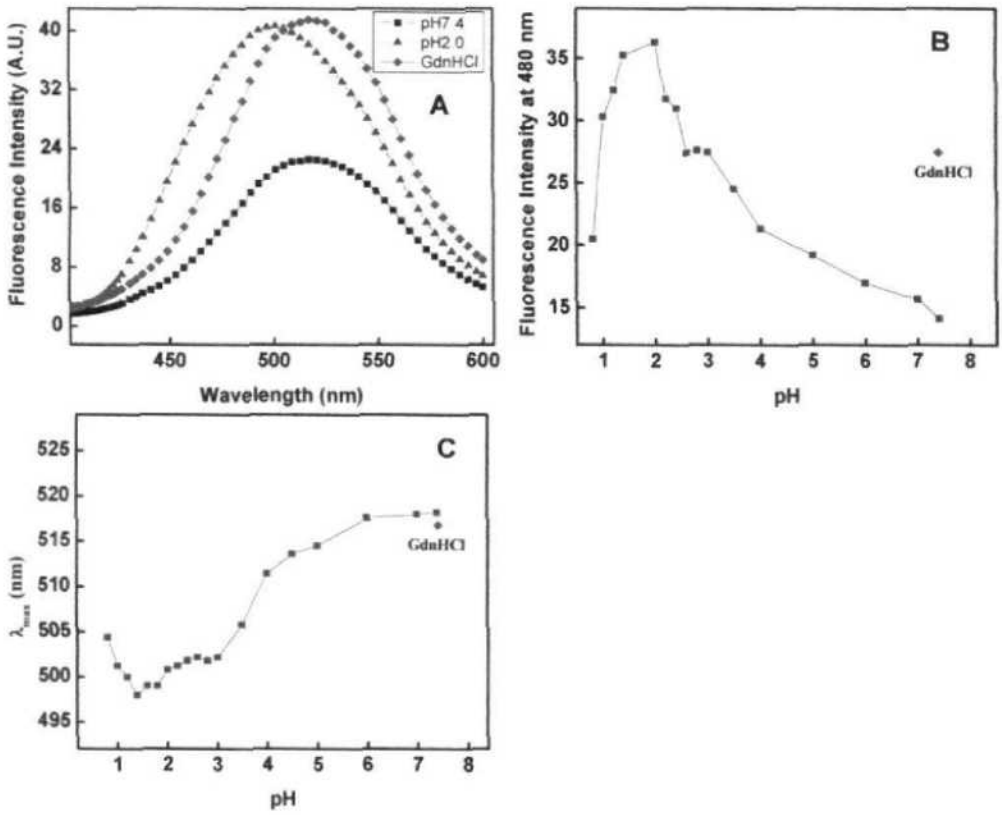

Figure 5.4. Change in Trp position was monitored by ANS dye binding. (A) Extrinsic fluorescence spectra of BL at pH 7.4 (-■-), pH 2.0 (-▲-) and 6 M GdnHCl (-♦-). (B) pH dependant changes in ANS fluorescence intensity of BL at 480 nm. (C) Change in wavelength maximum of BL was plotted verses pH. Prior to measurements all the samples were incubated for 12 hrs in a 20.0 mM respective buffer with 0.15 mg ml^{-1} protein concentration and 50 times more ANS (265.0 μM) were added in all samples.

5.3.7. Dynamic Light Scattering (DLS):

The pH dependent changes in hydrodynamic radii (R_h) were studied by DLS measurements. The R_h of folded BL (pH 7.4) was obtained 2.9 ± 1 nm (Figure 5.5A) with 7.8% polydispersity (Table 5.1), which is less than 30%, thus confirm that solution has a homogenous molecules. At pH 2.0, R_h values were obtained 1.7 nm and 3.7 nm is pointing towards incomplete monomerization (Figure 5.5B). Besides, the increase in R_h of the two species at pH 2.0 as compared to at pH 7.4 can be attributed to the perturbation of tertiary structure, thus supporting the existence of MG-state at this pH.

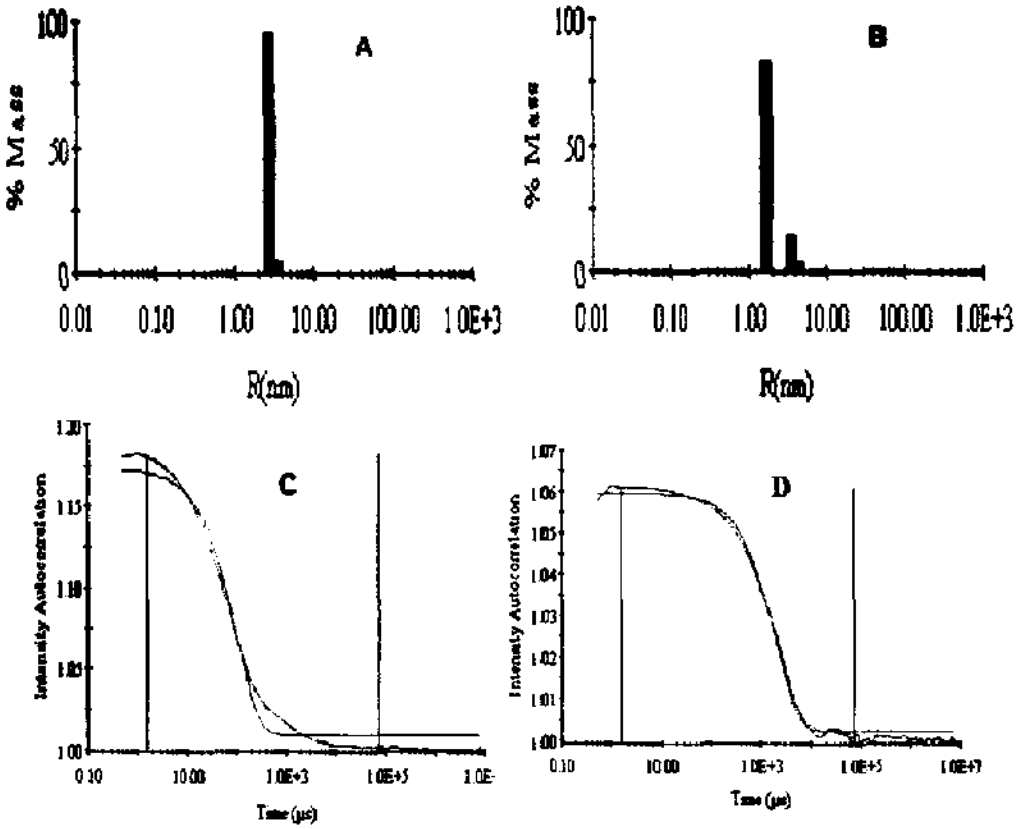

Figure 5.5. Change in hydrodynamic radii of BL at different pH were monitored by DLS. Hydrodynamic radii (R_h) of BL at (A) pH7.4 and (B) pH 2.0 and autocorrelation graph of BL (C) at pH 7.4 and (D) at pH 2.0. BL (1.0 mg ml^{-1}) were incubated at pH 7.4 and 2.0 for 12 hrs incubation.

Table 5.1. pH induced changes in hydrodynamic radii (R_h) of BL.

Conditions	R_h (nm)	[%] PD
pH 7.4	2.9	7.8
pH 2.0	1.7,3.6	10.08, 12.05

5.3.8. Size Exclusion Chromatography (SEC):

The elution profile of BL was obtained at pH 7.4 and pH 2.0 is depicted in (Figure 5.6) from size exclusion chromatography. A single peak around 61.45 ml was observed at pH 7.4 while the elution profile of protein at pH 2.0 revealed two peaks that were centered around 59.65 ml and 87.98 ml, although the later peak was not so sharp. The progressive monomerization of protein at pH 2.0 might have caused this peak to diminish resulting in only two peaks corresponding to the dimeric (59.65 ml) and relatively greater number of monomeric (87.98 ml) species. The distorted shape and lower elution volume of the later peak at pH 2.0 compared to at pH 7.4 can be attributed to the loss of tertiary structure (Bose and Clark, 2005). The results establish that monomer of BL was found at pH 2.0 although complete monomerization was not found.

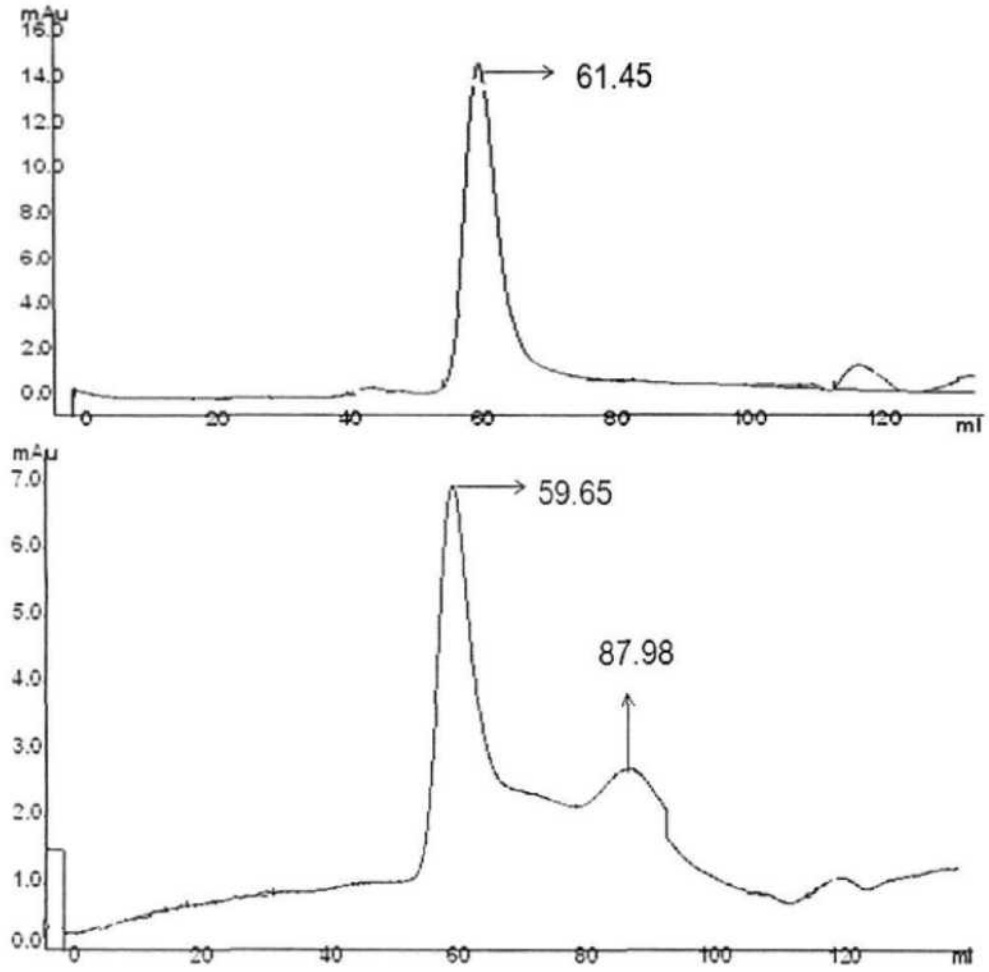

Figure 5.6. pH dependent monomerisation of BL. Size exclusion profile of BL at pH 7.4 and pH 2.0. Before performing the experiments the BL (1.0 mg ml^{-1})was incubated at respective pH for overnight.

5.3.9. Acrylamide quenching experiments:

To verify the environment of Trp residues, a fluorescence - quenching experiment was performed using the uncharged molecules of acrylamide as explained (Eftink and Ghiron, 1981). Figure 5.7, shows Stern–Volmer plot of BL at pH 7.4, 2.0 and in the presence of 6 M GdnHCl while Table 5.2, summarizes the K_{sv} obtained under respective conditions. The values for K_{sv} were in the order 4.48 M^{-1} (6 M GdnHCl) > 2.01 M^{-1} (pH 2.0) > 1.95 M^{-1} (pH 7.4). The data implied that Trp residues were maximally exposed in the presence of 6M GdnHCl, relatively less exposed at pH 2.0, even lesser in case of pH 7.4, indicating that exposure of hydrophobic residues at pH

2.0 and in turn authenticated the destabilization of tertiary structure at pH 2.0, which validate the presence of a molten globule like state (Khan et al., 2007).

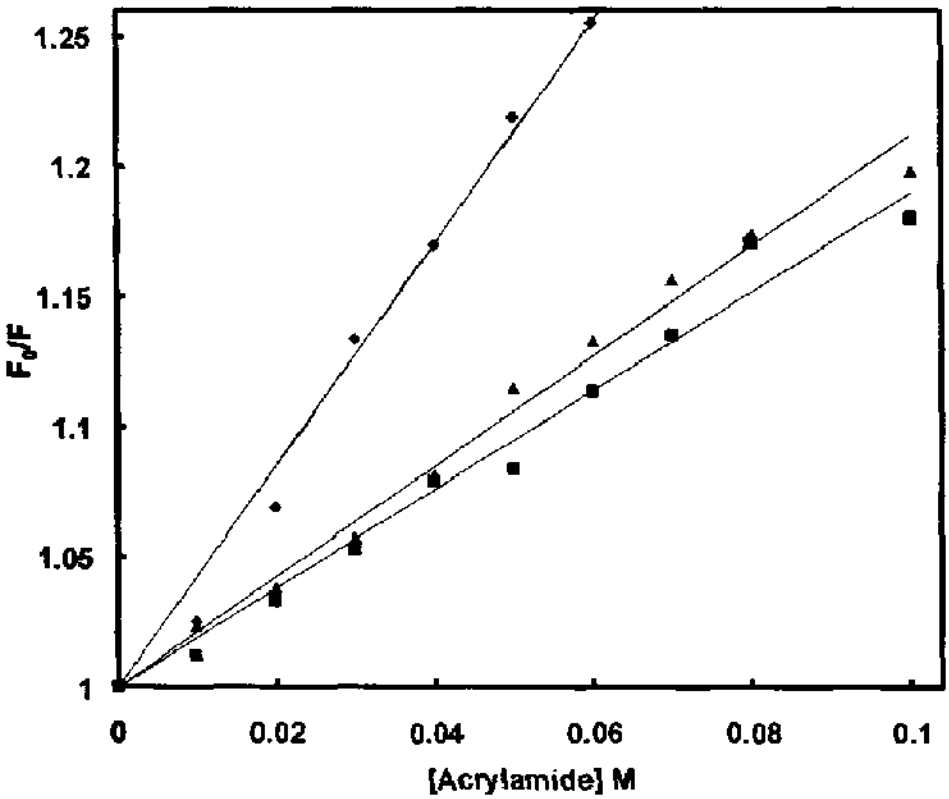

Figure 5.7. Exposure of Trp was monitored by acrylamide quenching. Stern–Volmer plot obtained from acrylamide quenching of BL at pH 7.4 (-■-), pH 2.0 (–▲–) and in the presence of 6.0 M GdnHCl (–♦–).

Table 5.2. Acrylamide quenching constant (K_{sv}) values of BL obtained at different pH values.

Conditions	$K_{sv[M^{-1}]}$	R^2
pH 7.4	1.95	0.98
pH 2.0	2.01	0.98
6 M GdnHCl	4.48	0.99

5.3.10. Chemical and thermal denaturation of BL:

The interesting results obtained from spectroscopic and hydrodynamic studies prompted us to compare the stability status of BL under native condition (pH 7.4) where protein existed as a homodimer and at molten globule state (pH 2.0) where

monomeric BL predominated. The stability was checked using temperature unfolding in addition to urea as denaturants.

5.3.11. Urea induced Conformational Changes of BL at Native and Molten globule State:

Urea induced structural transitions of BL were monitored by far-UV CD and intrinsic fluorescence spectroscopic techniques.

5.3.12. Secondary structure alterations:

Far-UV CD studies were carried out to study the effect of urea on the secondary structure of the BL at two different pH i.e 7.4 and 2.0 respectively. Figure 5.8A, recapitulates the effect of increasing urea concentration on loss of ellipticity at 218 nm of BL. At pH 7.4, no significant change in ellipticity was observed up to 5 M. However, a large sigmoidal change was observed from 5 to 8 M urea. In case of pH 2.0, BL showed relatively more resistance and no secondary structure change was observed up to 6 M urea, followed by a large sigmoidal change that reached a plateau around 10 M Urea. The midpoint of sigmoidal denaturation (C_m), an index to determine the stability of protein, was found to be 6.2 M for BL at pH 7.4. In case of pH 2.0, the C_m value increased to 7.4 M which indicated that the secondary structure of BL acquired more stability after minomerization. The transition midpoint and free energy change (ΔG) of urea induced unfolding of BL at two pH values were determined by far-UV CD and fluorescence data are summarized in Table 5.3.

6.3.13. Tertiary structure alterations:

The urea induced tertiary conformational changes in BL at pH 7.4 and 2.0 were also studied through changes in FI at 326 and 329 nm as a function of increasing concentration of urea. As shown in Figure 5.8B, urea denaturation profile of BL at both condition followed a two-state transition. At pH 7.4, the tertiary structure of protein remained unaffected by 2 M urea while complete loss of structure was observed with 6 M urea resulting in a midpoint of transition at 4.1 M. At pH 2.0, the molecular unfolding initiated beyond 3.0 M urea and complete unfolding was achieved with 9.0 M of chaotrop. The C_m value shoots up to 6.1 M which clearly pointed towards a more stable state of BL being attained at pH 2.0 with respect to at native state. The wavelength maximum of BL at pH 7.4 in the absence of urea was found around 326 NM. The wavelength maximum of BL at pH 7.4 was started red

shifing above 3 M urea concentration and maximum red shift were observed in the presence of 9 M urea with a difference of 22 nm. However at pH 2.0, the wavelength shift started at higher urea concentration but a shift in wavelength is not much more significant even at 9 M urea. The fluorescence spectra of BL at both pH 7.4 and 2.0 is shown in Figure 5.8C and 5.8D. The above results clearly suggested that monomeric BL (pH 2.0) is chemically more stable than its dimeric form (pH 7.4).

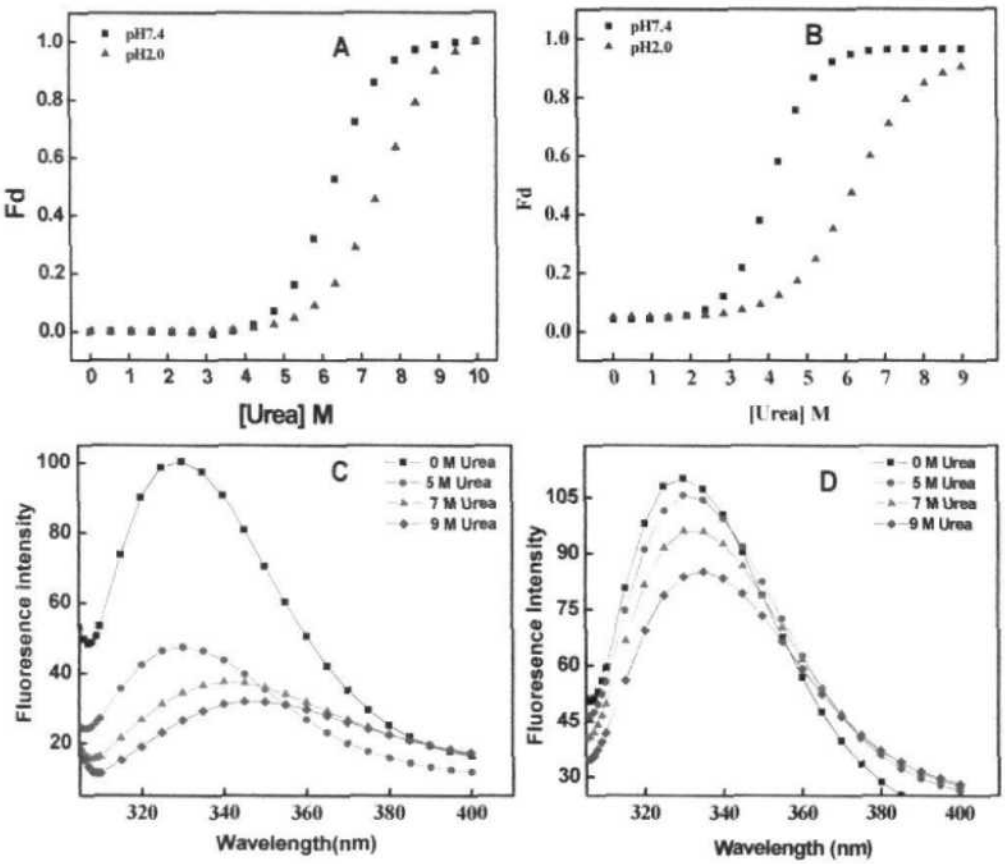

Figure 5.8. Urea-induced denaturation of BL was monitored by changes in secondary and tertiary structure. (A) Urea induced unfolding transition curves of BL at pH 7.4 (-■-) and pH 2.0 (–▲–) monitored through ellipticity measurement at 218 nm by far-UV CD. (B) Urea induced unfolding of BL at pH7.4 (-■-) and pH 2.0 (–▲–) monitored by a change in fluorescence emission intensity at 326 nm plotted as a function of urea concentration after excitation at 295 nm. (C) Fluorescence emission spectra of BL at pH 7.4 (8 C) and (D) at pH 2.0, at 0 M urea (-■-), 5 M urea (-●-), 7 M urea (-▲-) and 9 M urea (-♦-).

Table 5.3. Urea-induced unfolding parameters of BL at different conditions.

Conditions	Methods	Transition midpoint (C_m)	ΔG_u° (kcal/mol)
	FI at 326nm	4.1	3.13±0.20
pH 7.4, 25 °C	MRE at 218nm	6.2	3.85±0.085
	FI at 329nm	6.1	3.43±0.088
pH 2.0, 25 °C	MRE at 218nm	7.4	5.44±0.133

5.3.14. Thermal Denaturation:

The chemical stability of BL was also complimented by thermal stability. Far-UV CD spectra of BL at pH 7.4 were taken at different temperatures (Figure 5.9A). No changes in spectra could be noticed up to 75.0 °C beyond which a regular decrease in ellipticity was observed and spectra shifted towards higher wavelength due unfolding. Interestingly at pH 2.0 the spectra peak shifted towards shorter wavelength with increase in temperature (Figure 5.9B). Besides, no significant loss of ellipticity was observed even at 95.0 °C. Further, the temperature dependant changes in ellipticity at 218 nm of BL were monitored and shown in Figure 5.9C. The thermal denaturation profile of BL at pH 7.4 revealed sigmoidal transitions with midpoint of transition (T_m) at 77 °C. However at pH 2.0, no sigmoidal change was noticed over the entire temperature range(20-90 °C) although a considerable increase in ellipticity was recorded up to 70 °C suggesting induction rather than loss of secondary structure (Figure 5.9D). Thus, induction of secondary structure at pH 2.0 indicated uninterrupted gain of stability following monomerization. The results obtained from these experiments further strengthened the fact that acid-induced monomeric state, and not native dimeric form, of BL has more stability against temperature. Taken together, all these data further confirmed that BL acquires more chemical as well as thermal stability in its monomeric form than its native dimeric form. The overall results obtained in the present study are summarized in Figure 5.10.

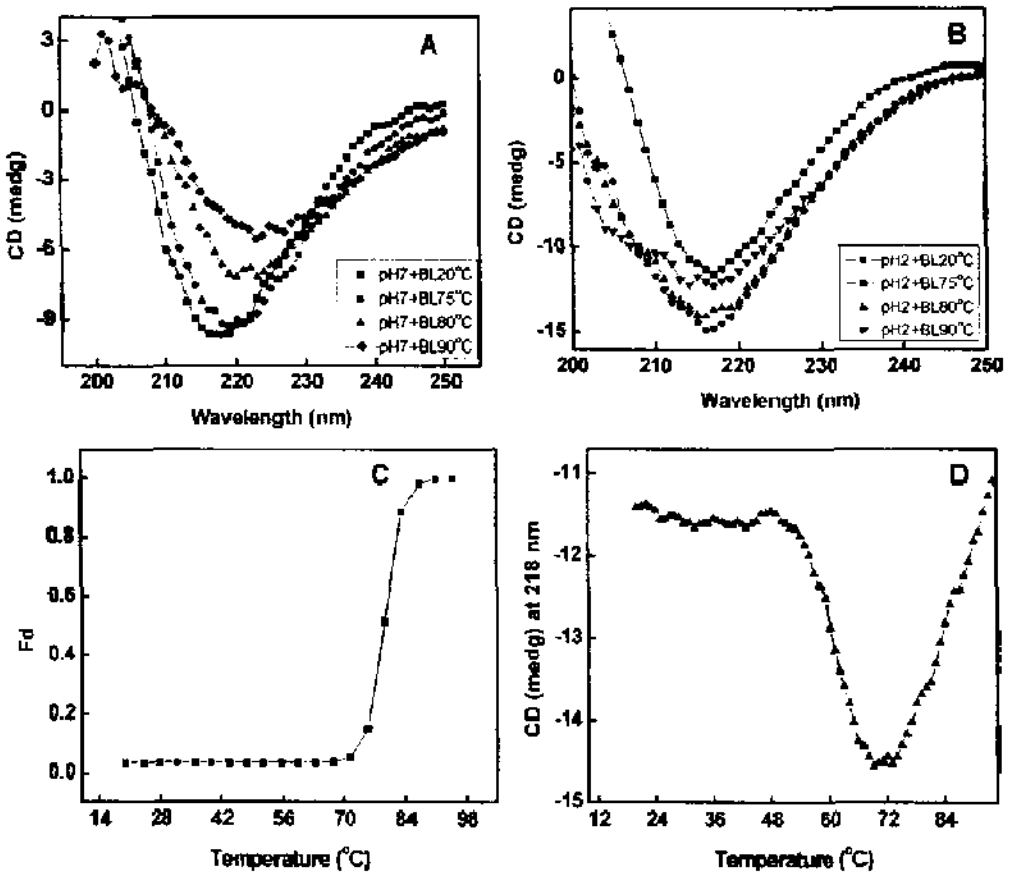

Figure 5.9. Effect of temperature on monomeric as well as dimeric form of BL. (A) temperature dependent change in far-UV CD spectra of BL at (A) pH 7.4, 20 °C (-■-) and (B) pH 2.0. 20 °C (-■-), 75 °C (•·), 80 °C (·▲-) and 90 °C (-♦-) (C) thermal denaturation profile of BL at pH 7.4 and (-■-) (D) pH 2.0 (-■-) obtained from changes in elipticity at 218 nm.

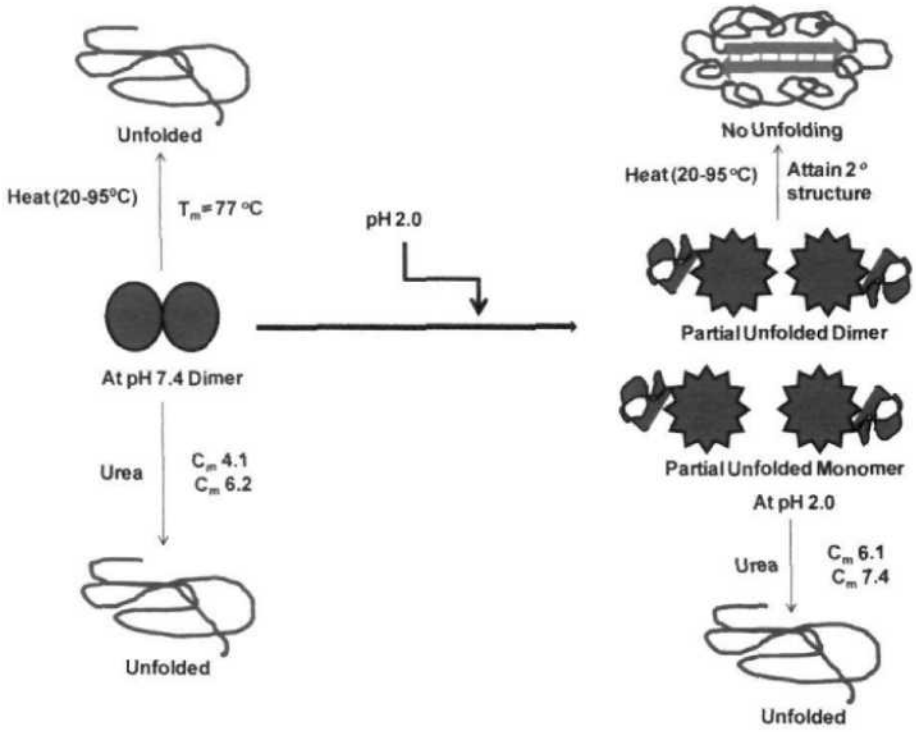

Figure 5.10. Schematic representations of the pH dependent conformational changes in BL as well as its urea and thermal induced unfolding. C_m values of BL obtained from fluorescence (▲) as well as far-UV CD (■) measurements.

5.4. Discussion:

Newly synthesized proteins are unfolded and do not have any structure. Over a short span of time, they attain various typical structures including secondary, tertiary and quaternary. The conformational elements acquired by polypeptides are stabilized by various non-covalent and covalent interactions. Breaking these interactions result in denaturation of the protein with either partial or complete loss of structure and its biological activity, that facilitates understanding the protein folding mechanism. The present study was divided into three parts: (i) pH denaturation (ii) chemical denaturation and (iii) thermal denaturation. The first part covers the pH dependent conformational change of BL to trace out any intermediate state that might encompass the folding pathway of protein. An intermediate state with characteristic features of a molten globule state was found to be populated at pH 2.0 as analyzed by CD, intrinsic as well extrinsic fluorescence methods. Size exclusion chromatography as well as DLS data confirmed that acid pH the dimeric BL was accompanied by monomerization. A single peak corresponding to native BL was observed at pH 7.4.

The signal intensity as well as elution volume was more for monomeric species of protein at pH 2.0. Besides, the R_h value of both monomeric as well as dimeric species increased to 1.7 nm and 3.7 nm respectively owing to the conformation transition induced by extreme low pH as observed during the CD and fluorescence analysis. The intramolecular charge-charge repulsion at extreme pH might have resulted in relatively extended conformation at low pH and similar explanation was also found in case beta-lactamase, cytochrome c, and apomyoglobin (Goto et al., 1990). Besides, the polydispersity value indicated that the number of monomeric species were considerably high with respect to dimeric species at pH 2.0 suggested that acid-induced MG state of BL exist possibly in the former state. The pH dependant change in subunit status has been reported earlier for several multimeric proteins. The several noncovalent interactions that held the subunit of multimeric proteins are likely to be dissociated with change in pH (Sinha and Surolia, 2005). The second part of this study was to compare the chemical stability of of BL at two different pH. Chemical stability of BL determined at neutral pH using guanidine hydrochloride has already been reported showing that BL is quite stable (Gupta et al., 2008). In the present study, chemical stability of BL was examined at both monomeric (pH 2.0) as well as dimeric (pH 7.4) state using urea as a denaturant. Urea is widely exploited as chaotrops for checking the stability of proteins at neutral as well as acidic pH (Rosner and Redfield, 2009, Dar et al., 2007, Pace et al., 1992). The equilibrium unfolding of BL in the presence of urea was found to be a cooperative process in which the protein molecule undergoes unfolding without a stabilization of intermediate at both pH values (7.4 and 2.0) similarly no intermediates were found as in the case of GdnHCl denaturation of same lectin at pH 7.4 (Gupta et al., 2008). Oligomeric proteins have usually more chemical stability than its monomer form because of additional non-covalent and covalent interactions (Mitra et al., 2002). In case of BL, however, it was noticed that monomeric state (pH 2.0) of protein was more stable in comparison to dimeric native state which was evident from C_m values as well as free energy changes (Table 5.3). C_m values for BL at pH 7.4 as determined by far-UV CD and intrinsic fluorescence analysis were found to be 4.1 M and 6.2 M respectively. The difference in the two C_m value reflects the perturbation of two different conformational elements (secondary and tertiary structure). In case of monomeric BL, the C_m values increased to 6.1 M and 7.4 M respectively. Similarly, free energy change for unfolding of monomeric BL was more than dimeric protein which is quite an unusual finding this

may be due to the development of positive charge on the protein and exposure of hydrophobic patches, urea is probably not able to interact at its lower concentration because urea is a neutral molecule with negligible hydrophobic moiety. However, at the higher concentration of urea might have disturbed the overall charge on BL, consequently resulting in unfolding of the molecule. Previously it is reported that urea interact with proteins nonspecifically at sub-global level by hydrogen bonding and Van der Waals interaction with main chain and side chain groups of protein (Bhuyan, 2002, Kumar et al., 2004). Concanavalin A, Cramoll 1 and SBA are legume lectins which mononerize and form MG states up to 3.0 M urea (Varejao et al., 2011 , Chatterjee and Mandal, 2003, Sinha and Surolia, 2007) but this non-leguminous BL shows the tertiary structural changes from 4.0M and secondary structural changes from 5 M urea which might be due to monomerization of native dimeric state of BL. This signifies that BL is more stable than other leguminous lectins. Urea concentrations up to 3-4 M affect BL in similar fashion at pH 2.0 or 7.4, after that the species formed on-pathway (possible monomers) are more stable in acidic conditions than at pH 7.4. Third part of this study was to check the stability of BL by employing temperature scan in the range of 20-95 °C. Thermal denaturation of BL was monitored by far-UV CD spectroscopic techniques aimed to follow secondary structural changes of the protein. Thermal denaturation of BL was a cooperative process without any intermediate at pH 7.4 but an intermediate state was found at pH 2.0. T_m value of BL was quite high at pH 7.4 (77 °C) indicating considerable stability against temperature change. Interestingly, the thermal denaturation profile was quite different at pH 2.0 where an intermediate state was acquired near 70 °C which did not denature completely even when heated beyond 95 °C, again confirming the significant increase in stability of BL in monomeric conditions.

5.5. Conclusions:

Acid denaturation of BL yielded an intermediate state at pH 2.0 and the monomerization of homodimeric BL was also found. Besides, the monomeric state of BL had more chemistry and thermal stability which, to the best of our knowledge, is the first report on significant stability exhibited by an individual subunit of an otherwise dimeric protein than the native state. An increase in intrasubunit interactions in monomeric level than in dimeric condition may be the possible reason for such finding.

BIBLIOGRAPHY

Bibliography

Ahmad A, Muzaffar M, Ingram VM (2009) Ca(2+), within the physiological concentrations, selectively accelerates Abeta42 fibril formation and not Abeta40 in vitro. *Biochim Biophys Acta,* **1794,** 1537-48.

Ahmad B, Ahmed MZ, Haq SK, Khan RH (2005) Guanidine hydrochloride denaturation of human serum albumin originates by local unfolding of some stable loops in domain III. *Biochim Biophys Acta,* **1750,** 93-102.

Ahmad B, Shamim TA, Haq SK, Khan RH (2007) Identification and characterization of functional intermediates of stem bromelain during urea and guanidine hydrochloride unfolding. *J Biochem,* **141,** 251-9.

Ahmad E, Fatima S, Khan MM, Khan RH (2010) More stable structure of wheat germ lipase at low pH than its native state. *Biochimie,* **92,** 885-93.

Ahmad E, Rahman SK, Khan JM, Varshney A, Khan RH (2009b) Phytolacca americana lectin (Pa-2; pokeweed mitogen): an intrinsically unordered protein and its conversion into partial order at low pH. *Biosci Rep,* **30,** 125-34.

Ahmad E, Sen P, Khan RH (2011) Structural stability as a probe for molecular evolution of homologous albumins studied by spectroscopy and bioinformatics. *Cell Biochem Biophys,* **61,** 313-25.

Ahmad MF, Ramakrishna T, Raman B, Rao ChM (2006) Fibrillogenic and non-fibrillogenic ensembles of SDS-bound human alpha-synuclein. *J Mol Biol,* **364,** 1061-72.

Ahn M, De GE, Kaminski Schierle GS, Erdelyi M, Kaminski CF, Dobson CM, Kumita JR (2012) Analysis of the native structure, stability and aggregation of biotinylated human lysozyme. *PLoS One.* 7, e50192.

Ahrer K, Buchacher A, Iberer G, Josic D, Jungbauer A (2003) Analysis of aggregates of human immunoglobulin G using size-exclusion chromatography, static and dynamic light scattering. *J Chromatogr A,* **1009,** 89-96.

Ali MS, Khan JM, Aswal VK, Khan RH, Kabir-ud D (2010) Multi-technique approach on the effect of surfactant concentrations on the thermal unfolding of rabbit

serum albumin: formation and solubilization of the protein aggregates. *Colloids Surf B Biointerfaces,* **80,** 169-75.

Anand U, Jash C, Mukherjee S (2010) Spectroscopic probing of the microenvironment in a protein-surfactant assembly. *J Phys Chem B,* **114,** 15839-45.

Andersen KK, Oliveira CL, Larsen KL, Poulsen FM, Callisen TH, Westh P, Pedersen JS, Otzen D (2009) The role of decorated SDS micelles in sub-CMC protein denaturation and association. *J Mol Biol,* **391,** 207-26.

Andersson E, Hellman L, Gullberg U, Olsson I (1998) The role of the propeptide for processing and sorting of human myeloperoxidase. *J Biol Chem,* **273,** 4747-53.

Anelli T, Sitia R (2008) Protein quality control in the early secretory pathway. *EMBO J,* **27,** 315-27.

Anfinsen CB (1972) The formation and stabilization of protein structure. *Biochem J,* **128,** 737-49.

Anfinsen CB (1973) Principles that govern the folding of protein chains. *Science,* **181,** 223-30.

Arnaudov LN, de Vries R (2005) Thermally induced fibrillar aggregation of hen egg white lysozyme. *Biophys J,* **88,** 515-26.

Arora A, Ha C, Park CB (2004) Insulin amyloid fibrillation at above 100 degrees C: new insights into protein folding under extreme temperatures. *Protein Sci,* **13,** 2429-36.

Auton M, Holthauzen LM, Bolen DW (2007) Anatomy of energetic changes accompanying urea-induced protein denaturation. *Proc Natl Acad Sci U S A,* **104,** 15317-22.

Bailon P, Palleroni A, Schaffer CA, Spence CL, Fung WJ, Porter JE, Ehrlich GK, Pan W, Xu ZX, Modi MW, Farid A, Berthold W, Graves M (2001) Rational design of a potent, long-lasting form of interferon: a 40 kDa branched polyethylene glycol-conjugated interferon alpha-2a for the treatment of hepatitis C. *Bioconjug Chem,* **12,** 195-202.

Baker EN, Hubbard RE (1984) Hydrogen bonding in globular proteins. *Prog Biophys Mol Biol,* **44,** 97-179.

Baldwin RL, Rose GD (1999) Is protein folding hierarchic? II. Folding intermediates and transition states. *Trends Biochem Sci,* **24,** 77-83.

Ballew RM, Sabelko J, Gruebele M (1996) Direct observation of fast protein folding: the initial collapse of apomyoglobin. *Proc Natl Acad Sci U S A,* **93,** 5759-64.

Barghorn S, Nimmrich V, Striebinger A, Krantz C, Keller P, Janson B, Bahr M, Schmidt M, Bitner RS, Harlan J, Barlow E, Ebert U, Hillen H (2005) Globular Abeta(1-40) oligomer-a homogenous and stable neuropathological protein in Alzheimer's disease. *J Neurochem,* **95,** 834-47.

Bathaie SZ, Moosavi-Movahedi AA, Saboury AA (1999) Energetic and binding properties of DNA upon interaction with dodecyl trimethylammonium bromide. *Nucleic Acids Res,* **27,** 1001-5.

Bennion BJ, Daggett V (2003) The molecular basis for the chemical denaturation of proteins by urea. *Proc Natl Acad Sci U S A,* **100,** 5142-7.

Berteotti A, Barducci A, Parrinello M (2011) Effect of urea on the beta-hairpin conformational ensemble and protein denaturation mechanism. *J Am Chem Soc,* **133,** 17200-6.

Bhak G, Choe YJ, Paik SR (2009) Mechanism of amyloidogenesis: nucleation-dependent fibrillation versus double-concerted fibrillation. *BMB Rep,* **42,** 541-51.

Bhattacharya M, Jain N, Mukhopadhyay S (2011) Insights into the mechanism of aggregation and fibril formation from bovine serum albumin. *J Phys Chem B,* **115,** 4195-205.

Bhunia A, Domadia PN, Xu X, Gingras R, Ni F, Bhattacharjya S (2008) Equilibrium unfolding of the dimeric SAM domain of MAPKKK Ste11 from the budding yeast: role of the interfacial residues in structural stability and binding. *Biochemistry,* **47,** 651-9.

Bhuyan AK (2002) Protein stabilization by urea and guanidine hydrochloride. *Biochemistry,* **41,** 13386-94.

Bhuyan AK (2010) On the mechanism of SDS-induced protein denaturation. *Biopolymers,* **93,** 186-99.

Biancalana M, Koide S (2010) Molecular mechanism of Thioflavin-T binding to amyloid fibrils. *Biochim Biophys Acta,* **1804,** 1405-12.

Biancalana M, Makabe K, Koide A, Koide S (2008) Aromatic cross-strand ladders control the structure and stability of beta-rich peptide self-assembly mimics. *J Mol Biol,* **383,** 205-13.

Biancalana M, Makabe K, Koide A, Koide S (2009) Molecular mechanism of thioflavin-T binding to the surface of beta-rich peptide self-assemblies. *J Mol Biol,* **385,** 1052-63.

Blewitt MG, Chung LA, London E (1985) Effect of pH on the conformation of diphtheria toxin and its implications for membrane penetration. *Biochemistry,* **24,** 5458-64.

Booth DR, Sunde M, Bellotti V, Robinson CV, Hutchinson WL, Fraser PE, Hawkins PN, Dobson CM, Radford SE, Blake CC, Pepys MB (1997) Instability, unfolding and aggregation of human lysozyme variants underlying amyloid fibrillogenesis. *Nature,* **385,** 787-93.

Boscolo B, Leal SS, Salgueiro CA, Ghibaudi EM, Gomes CM (2009) The prominent conformational plasticity of lactoperoxidase: a chemical and pH stability analysis. *Biochim Biophys Acta,* **1794,** 1041-8.

Bose K, Clark AC (2005) pI1 effects on the stability and dimerization of procaspase-3. *Protein Sci,* **14,** 24-36.

Bourgault S, Solomon JP, Reixach N, Kelly JW (2011) Sulfated glycosaminoglycans accelerate transthyretin amyloidogenesis by quaternary structural conversion. *Biochemistry,* **50,** 1001-15.

Braakman I, Hoover-Litty H, Wagner KR, Helenius A (1991) Folding of influenza hemagglutinin in the endoplasmic reticulum. *J Cell Biol,* **114,** 401-11.

Brahma A, Mandal C, Bhattacharyya D (2005) Characterization of a dimeric unfolding intermediate of bovine serum albumin under mildly acidic condition. *Biochim Biophys Acta,* **1751,** 159-69.

Brooks CL, 3rd (2002) Protein and peptide folding explored with molecular simulations. *Acc Chem Res,* **35,** 447-54.

Butterfield SM, Lashuel HA (2010) Amyloidogenic protein-membrane interactions: mechanistic insight from model systems. *Angew Chem Int Ed Engl,* **49,** 5628-54.

Bychkova VE, Pain RH, Ptitsyn OB (1988) The molten globule state is involved in the translocation of proteins across membranes? *FEBS Lett,* **238,** 231-4.

Carrotta R, Bauer R, Waninge R, Rischel C (2001) Conformational characterization of oligomeric intermediates and aggregates in beta-lactoglobulin heat aggregation. *Protein Sci,* **10,** 1312-8.

Carter DB, Chou KC (1998) A model for structure-dependent binding of Congo Red to Alzheimer beta-amyloid fibrils. *Neurobiol Aging,* **19,** 37-40.

Carter DC, Ho JX (1994) Structure of serum albumin. *Adv Protein Chem,* **45,** 153-203.

Chandra NR, Ramachandraiah G, Bachhawat K, Dam TK, Surolia A, Vijayan M (1999) Crystal structure of a dimeric mannose-specific agglutinin from garlic: quaternary association and carbohydrate specificity. *J Mol Biol,* **285,** 1157-68.

Chatterjee A, Mandal DK (2003) Denaturant-induced equilibrium unfolding of concanavalin A is expressed by a three-state mechanism and provides an estimate of its protein stability. *Biochim Biophys Acta,* **1648,** 174-83.

Chattopadhyay K, Mazumdar S (2003) Stabilization of partially folded states of cytochrome c in aqueous surfactant: effects of ionic and hydrophobic interactions. *Biochemistry,* **42,** 14606-13.

Chauhan A, Ray I, Chauhan VP (2000) Interaction of Abeta-protein with anionic phospholipids: possible involvement of Lys28 and C-terminus aliphatic amino acids. *Neurochem Res,* **25,** 423-9.

Chen W, Helenius J, Braakman I, Helenius A (1995) Cotranslational folding and calnexin binding during glycoprotein synthesis. *Proc Natl Acad Sci U S A,* **92,** 6229-33.

Chen X, Sagle LB, Cremer PS (2007) Urea orientation at protein surfaces. *J Am Chem Soc,* **129,** 15104-5.

Chen YJ, Inouye M (2008) The intramolecular chaperone-mediated protein folding. *Curr Opin Struct Biol,* **18,** 765-70.

Chi EY, Ege C, Winans A, Majewski J, Wu G, Kjaer K, Lee KY (2008) Lipid membrane templates the ordering and induces the fibrillogenesis of Alzheimer's disease amyloid-beta peptide. *Proteins,* **72,** 1-24.

Chi EY, Frey SL, Lee KY (2007) Ganglioside G(M1)-mediated amyloid-beta fibrillogenesis and membrane disruption. *Biochemistry,* **46,** 1913-24.

Chi EY, Krishnan S, Kendrick BS, Chang BS, Carpenter JF, Randolph TW (2003a) Roles of conformational stability and colloidal stability in the aggregation of recombinant human granulocyte colony-stimulating factor. *Protein Sci,* **12,** 903-13.

Chi EY, Krishnan S, Randolph TW, Carpenter JF (2003b) Physical stability of proteins in aqueous solution: mechanism and driving forces in nonnative protein aggregation. *Pharm Res,* **20,** 1325-36.

Chi EY, Weickmann J, Carpenter JF, Manning MC, Randolph TW (2005) Heterogeneous nucleation-controlled particulate formation of recombinant human platelet-activating factor acetylhydrolase in pharmaceutical formulation. *J Pharm Sci,* **94,** 256-74.

Chiti F, Dobson CM (2006) Protein misfolding, functional amyloid, and human disease. *Annu Rev Biochem,* **75,** 333-66.

Chiti F, Dobson CM (2009) Amyloid formation by globular proteins under native conditions. *Nat Chem Biol,* **5,** 15-22.

Chiti F, Stefani M, Taddei N, Ramponi G, Dobson CM (2003) Rationalization of the effects of mutations on peptide and protein aggregation rates. *Nature,* **424,** 805-8.

Chiti F, Taddei N, Baroni F, Capanni C, Stefani M, Ramponi G, Dobson CM (2002) Kinetic partitioning of protein folding and aggregation. *Nat Struct Biol,* **9,** 137-43.

Chiti F, Taddei N, Bucciantini M, White P, Ramponi G, Dobson CM (2000) Mutational analysis of the propensity for amyloid formation by a globular protein. *EMBO J,* **19,** 1441-9.

Chiti F, Webster P, Taddei N, Clark A, Stefani M, Ramponi G, Dobson CM (1999) Designing conditions for in vitro formation of amyloid protofilaments and fibrils. *Proc Natl Acad Sci U S A,* **96,** 3590-4.

Chodankar S, Aswal VK, Kohlbrecher J, Vavrin R, Wagh AG (2008) Structural evolution during protein denaturation as induced by different methods. *Phys Rev E Stat Nonlin Soft Matter Phys,* **77,** 031901.

Choo-Smith LP, Surewicz WK (1997) The interaction between Alzheimer Abeta(1-40) peptide and ganglioside GM1-containing membranes. *FEBS Lett,* **402,** 95-8.

Christensen H, Pain RH (1991) Molten globule intermediates and protein folding. *Eur Biophys J,* **19,** 221-9.

Correa DH, Ramos CH (2011) Amyloid fibril formation by circularly permuted and C-terminally deleted mutants. *Int J Biol Macromol,* **48,** 583-8.

Croguennec TK, B.TMehra, R (2004) Heat-induced denaturation/aggregation of β-lactoglobulin A and B: kinetics of the first intermediates formed. *Int. Dairy. J.,* **14,** 399–409.

Cromwell ME, Hilario E, Jacobson F (2006) Protein aggregation and bioprocessing. *AAPS J,* **8,** E572-9.

Daggett V, Fersht AR (2003) Is there a unifying mechanism for protein folding? *Trends Biochem Sci,* **28,** 18-25.

Dar TA, Singh LR, Islam A, Anjum F, Moosavi-Movahedi AA, Ahmad F (2007) Guanidinium chloride and urea denaturations of beta-lactoglobulin A at pH 2.0 and 25 degrees C: the equilibrium intermediate contains non-native structures (helix, tryptophan and hydrophobic patches). *Biophys Chem,* **127,** 140-8.

Das A, Mukhopadhyay C (2008) Atomistic mechanism of protein denaturation by urea. *J Phys Chem B,* **112,** 7903-8.

Das A, Mukhopadhyay C (2009) Urea-mediated protein denaturation: a consensus view. *J Phys Chem B,* **113,** 12816-24.

Das P, Zhou R (2010) Urea-induced drying of carbon nanotubes suggests existence of a dry globule-like transient state during chemical denaturation of proteins. *J Phys Chem B,* **114,** 5427-30.

De Ferrari GV, Mallender WD, Inestrosa NC, Rosenberry TL (2001) Thioflavin T is a fluorescent probe of the acetylcholinesterase peripheral site that reveals

conformational interactions between the peripheral and acylation sites. *J Biol Chem,* **276,** 23282-7.

De S, Girigoswami A, Das S (2005) Fluorescence probing of albumin-surfactant interaction. *J Colloid Interface Sci,* **285,** 562-73.

Dill KA (1990) Dominant forces in protein folding. *Biochemistry,* **29,** 7133-55.

Dill KA, Chan HS (1997) From Levinthal to pathways to funnels. *Nat Struct Biol,* **4,** 10-9.

Dill KA, Ozkan SB, Shell MS, Weikl TR (2008) The protein folding problem. *Annu Rev Biophys,* **37,** 289-316.

Dobson CM (2001) The structural basis of protein folding and its links with human disease. *Philos Trans R Soc Lond B Biol Sci,* **356,** 133-45.

Dobson CM (2003) Protein folding and misfolding. *Nature,* **426,** 884-90.

Dobson CM (2004) Principles of protein folding, misfolding and aggregation. *Semin Cell Dev Biol,* **15,** 3-16.

Dobson CM, Sali, A. & Karplus, M (1998) Protein folding: A perspective from theory and experiment. *Angew. Chem. Int. Ed. Engl.,* **37,** 868–893.

Drickamer K (1999) C-type lectin-like domains. *Curr Opin Struct Biol,* **9,** 585-90.

Eftink MR (1994) The use of fluorescence methods to monitor unfolding transitions in proteins. *Biophys J,* **66,** 482-501.

Eftink MR, Ghiron CA (1981) Fluorescence quenching studies with proteins. *Anal Biochem,* **114,** 199-227.

Eftink MR, Shastry MC (1997) Fluorescence methods for studying kinetics of protein-folding reactions. *Methods Enzymol,* **278,** 258-86.

el-Sayed MY, Roberts MF (1985) Charged detergents enhance the activity of phospholipase C (Bacillus cereus) towards micellar short-chain phosphatidylcholine. *Biochim Biophys Acta,* **831,** 133-41.

Elam JS, Taylor AB, Strange R, Antonyuk S, Doucette PA, Rodriguez JA, Hasnain SS, Hayward LJ, Valentine JS, Yeates TO, Hart PJ (2003) Amyloid-like filaments and

water-filled nanotubes formed by SOD1 mutant proteins linked to familial ALS. *Nat Struct Biol,* **10,** 461-7.

Ellis RJ (1997) Molecular chaperones: avoiding the crowd. *Curr Biol,* **7,** R531-3.

England JL, Pande VS, Haran G (2008) Chemical denaturants inhibit the onset of dewetting. *J Am Chem Soc,* **130,** 11854-5.

Englander SW (2000) Protein folding intermediates and pathways studied by hydrogen exchange. *Annu Rev Biophys Biomol Struct,* **29,** 213-38.

Esler WP, Stimson ER, Ghilardi JR, Felix AM, Lu YA, Vinters HV, Mantyh PW, Maggio JE (1997) A beta deposition inhibitor screen using synthetic amyloid. *Nat Biotechnol,* **15,** 258-63.

Eyles SJ, Radford SE, Robinson CV, Dobson CM (1994) Kinetic consequences of the removal of a disulfide bridge on the folding of hen lysozyme. *Biochemistry,* **33,** 13038-48.

Fan H, Vitharana SN, Chen T, O'Keefe D, Middaugh CR (2007) Effects of pH and polyanions on the thermal stability of fibroblast growth factor 20. *Mol Pharm,* **4,** 232-40.

Fandrich M, Fletcher MA, Dobson CM (2001) Amyloid fibrils from muscle myoglobin. *Nature,* **410,** 165-6.

Farruggia B, Nerli B, Pico G (2003) Study of the serum albumin-polyethyleneglycol interaction to predict the protein partitioning in aqueous two-phase systems. *J Chromatogr B Analyt Technol Biomed Life Sci,* **798,** 25-33.

Farruggia B, Pico GA (1999) Thermodynamic features of the chemical and thermal denaturations of human serum albumin. *Int J Biol Macromol,* **26,** 317-23.

Fast JL, Cordes AA, Carpenter JF, Randolph TW (2009) Physical instability of a therapeutic Fc fusion protein: domain contributions to conformational and colloidal stability. *Biochemistry,* **48,** 11724-36.

Feige MJ BJ (2010) The role of disulfide bonds in protein folding and stability. Oxidative Folding of Peptides and Proteins.

Fernandes F, Loura LM, Prieto M, Koehorst R, Spruijt RB, Hemminga MA (2003) Dependence of M13 major coat protein oligomerization and lateral segregation on bilayer composition. *Biophys J,* **85,** 2430-41.

Fernandez A, Berry RS (2003) Proteins with H-bond packing defects are highly interactive with lipid bilayers: Implications for amyloidogenesis. *Proc Natl Acad Sci U S A,* **100,** 2391-6.

Ferrao-Gonzales AD, Souto SO, Silva JL, Foguel D (2000) The preaggregated state of an amyloidogenic protein: hydrostatic pressure converts native transthyretin into the amyloidogenic state. *Proc Natl Acad Sci U S A,* **97,** 6445-50.

Ferreon AC, Deniz AA (2011) Protein folding at single-molecule resolution. *Biochim Biophys Acta,* **1814,** 1021-9.

Fersht AR (1995) Optimization of rates of protein folding: the nucleation-condensation mechanism and its implications. *Proc Natl Acad Sci U S A,* **92,** 10869-73.

Fersht AR (1997) Nucleation mechanisms in protein folding. *Curr Opin Struct Biol,* **7,** 3-9.

Fersht AR (2008) From the first protein structures to our current knowledge of protein folding: delights and scepticisms. *Nat Rev Mol Cell Biol,* **9,** 650-4.

Fezoui Y, Teplow DB (2002) Kinetic studies of Abeta-protein fibril assembly. Differential effects of alpha-helix stabilization. *J Biol Chem,* **277,** 36948-54.

Findeis MA (2000) Approaches to discovery and characterization of inhibitors of Abeta-peptide polymerization. *Biochim Biophys Acta,* **1502,** 76-84.

Fink AL, Calciano LJ, Goto Y, Kurotsu T, Palleros DR (1994) Classification of acid denaturation of proteins: intermediates and unfolded states. *Biochemistry,* **33,** 12504-11.

Finkelstein AV (1997) Can protein unfolding simulate protein folding? *Protein Eng,* **10,** 843-5.

Fowler DM, Koulov AV, Alory-Jost C, Marks MS, Balch WE, Kelly JW (2006) Functional amyloid formation within mammalian tissue. *PLoS Biol,* **4,** e6.

Frare E, Polverino De Laureto P, Zurdo J, Dobson CM, Fontana A (2004) A highly amyloidogenic region of hen lysozyme. *J Mol Biol,* **340,** 1153-65.

Friedman R, Caflisch A (2011) Surfactant effects on amyloid aggregation kinetics. *J Mol Biol,* **414,** 303-12.

Frydman J (2001) Folding of newly translated proteins in vivo: the role of molecular chaperones. *Annu Rev Biochem,* **70,** 603-47.

Fucinos Gonzalez JP, Bassani G, Farruggia B, Pico GA, Pastrana Castro L, Rua ML (2011) Conformational flexibility of lipase Lip1 from Candida rugosa studied by electronic spectroscopies and thermodynamic approaches. *Protein J,* **30,** 77-83.

Fukunaga S, Ueno H, Yamaguchi T, Yano Y, Hoshino M, Matsuzaki K (2012) GM1 Cluster Mediates Formation of Toxic Abeta Fibrils by Providing Hydrophobic Environments. *Biochemistry,* **51,** 8125-31.

Galantini L, Leggio C, Konarev PV, Pavel NV (2010) Human serum albumin binding ibuprofen: a 3D description of the unfolding pathway in urea. *Biophys Chem,* **147,** 111-22.

Garwicz D, Lindmark A, Persson AM, Gullberg U (1998) On the role of the proform-conformation for processing and intracellular sorting of human cathepsin G. *Blood,* **92,** 1415-22.

Gessel MM, Wu C, Li H, Bitan G, Shea JE, Bowers MT (2012) Abeta(39-42) modulates Abeta oligomerization but not fibril formation. *Biochemistry,* **51,** 108-17.

Gething MJ, Sambrook J (1992) Protein folding in the cell. *Nature,* **355,** 33-45.

Gitlin I, Gudiksen KL, Whitesides GM (2006) Peracetylated bovine carbonic anhydrase (BCA-Ac18) is kinetically more stable than native BCA to sodium dodecyl sulfate. *J Phys Chem B,* **110,** 2372-7.

Goto Y, Calciano LJ, Fink AL (1990) Acid-induced folding of proteins. *Proc Natl Acad Sci U S A,* **87,** 573-7.

Greenspan P, Mayer EP, Fowler SD (1985) Nile red: a selective fluorescent stain for intracellular lipid droplets. *J Cell Biol,* **100,** 965-73.

Griko YV (2000) Energetic basis of structural stability in the molten globule state: alpha-lactalbumin. *J Mol Biol,* **297,** 1259-68.

Groenning M (2009) Binding mode of Thioflavin T and other molecular probes in the context of amyloid fibrils-current status. *J Chem Biol,* **3,** 1-18.

Groenning M (2010) Binding mode of Thioflavin T and other molecular probes in the context of amyloid fibrils-current status. *J Chem Biol,* **3,** 1-18.

Groenning M, Norrman M, Flink JM, van de Weert M, Bukrinsky JT, Schluckebier G, Frokjaer S (2007) Binding mode of Thioflavin T in insulin amyloid fibrils. *J Struct Biol,* **159,** 483-97.

Groves MR, Taylor MA, Scott M, Cummings NJ, Pickersgill RW, Jenkins JA (1996) The prosequence of procaricain forms an alpha-helical domain that prevents access to the substrate-binding cleft. *Structure,* **4,** 1193-203.

Gull N, Mir MA, Khan JM, Khan RH, Rather GM, Dar AA (2011) Refolding of bovine serum albumin via artificial chaperone protocol using gemini surfactants. *J Colloid Interface Sci,* **364,** 157-62.

Guo XH, Zhao NM, Chen SH, Teixeira J (1990) Small-angle neutron scattering study of the structure of protein/detergent complexes. *Biopolymers,* **29,** 335-46.

Gupta G, Sinha S, Surolia A (2008) Unfolding energetics and stability of banana lectin. *Proteins,* **72,** 754-60.

Hadley KC, Borrelli MJ, Lepock JR, McLaurin J, Croul SE, Guha A, Chakrabartty A (2011) Multiphoton ANS fluorescence microscopy as an in vivo sensor for protein misfolding stress. *Cell Stress Chaperones,* **16,** 549-61.

Hagen SJ (2010) Solvent viscosity and friction in protein folding dynamics. *Curr Protein Pept Sci,* **11,** 385-95.

Hagihara Y, Hong DP, Hoshino M, Enjyoji K, Kato H, Goto Y (2002) Aggregation of beta(2)-glycoprotein I induced by sodium lauryl sulfate and lysophospholipids. *Biochemistry,* **41,** 1020-6.

Hansted JG, Wejse PL, Bertelsen H, Otzen DE (2011) Effect of protein-surfactant interactions on aggregation of beta-lactoglobulin. *Biochim Biophys Acta,* **1814,** 713-23.

Harel M, Sonoda LK, Silman I, Sussman JL, Rosenberry TL (2008) Crystal structure of thioflavin T bound to the peripheral site of Torpedo californica acetylcholinesterase

reveals how thioflavin T acts as a sensitive fluorescent reporter of ligand binding to the acylation site. *J Am Chem Soc,* **130,** 7856-61.

Harper JD, Lansbury PT, Jr. (1997) Models of amyloid seeding in Alzheimer's disease and scrapie: mechanistic truths and physiological consequences of the time-dependent solubility of amyloid proteins. *Annu Rev Biochem,* **66,** 385-407.

Harper JD, Wong SS, Lieber CM, Lansbury PT, Jr. (1999) Assembly of A beta amyloid protofibrils: an in vitro model for a possible early event in Alzheimer's disease. *Biochemistry,* **38,** 8972-80.

Hartl FU, Hayer-Hartl M (2002) Molecular chaperones in the cytosol: from nascent chain to folded protein. *Science,* **295,** 1852-8.

Hebert DN, Molinari M (2007) In and out of the ER: protein folding, quality control, degradation, and related human diseases. *Physiol Rev,* **87,** 1377-408.

Heegaard NH, Sen JW, Nissen MH (2000) Congophilicity (Congo Red affinity) of different beta2-microglobulin conformations characterized by dye affinity capillary electrophoresis. *J Chromatogr A,* **894,** 319-27.

Hermeling S, Schellekens H, Maas C, Gebbink MF, Crommelin DJ, Jiskoot W (2006) Antibody response to aggregated human interferon alpha2b in wild-type and transgenic immune tolerant mice depends on type and level of aggregation. *J Pharm Sci,* **95,** 1084-96.

Hettiarachchi CA, Melton LD, Gerrard JA, Loveday SM (2012) Formation of beta-lactoglobulin nanofibrils by microwave heating gives a peptide composition different from conventional heating. *Biomacromolecules,* **13,** 2868-80.

Higurashi T, Yagi H, Mizobata T, Kawata Y (2005) Amyloid-like fibril formation of co-chaperonin GroES: nucleation and extension prefer different degrees of molecular compactness. *J Mol Biol,* **351,** 1057-69.

Hobart SA, Meinhold DW, Osuna R, Colon W (2002) From two-state to three-state: the effect of the P61A mutation on the dynamics and stability of the factor for inversion stimulation results in an altered equilibrium denaturation mechanism. *Biochemistry,* **41,** 13744-54.

Holley M, Eginton C, Schaefer D, Brown LR (2008) Characterization of amyloidogenesis of hen egg lysozyme in concentrated ethanol solution. *Biochem Biophys Res Commun,* **373,** 164-8.

Hoyer W, Antony T, Cherny D, Heim G, Jovin TM, Subramaniam V (2002) Dependence of alpha-synuclein aggregate morphology on solution conditions. *J Mol Biol,* **322,** 383-93.

Hua L, Zhou R, Thirumalai D, Berne BJ (2008) Urea denaturation by stronger dispersion interactions with proteins than water implies a 2-stage unfolding. *Proc Natl Acad Sci U S A,* **105,** 16928-33.

Hünenberger PHB, U. Lins, R. D. (2001) Electrostatic Interactions in Biomolecular Systems. *Chimia,* **55** 861–866.

Hung YT, Lin MS, Chen WY, Wang SS (2010) Investigating the effects of sodium dodecyl sulfate on the aggregative behavior of hen egg-white lysozyme at acidic pH. *Colloids Surf B Biointerfaces,* **81,** 141-51.

Ibarra-Molero B, Loladze VV, Makhatadze GI, Sanchez-Ruiz JM (1999) Thermal versus guanidine-induced unfolding of ubiquitin. An analysis in terms of the contributions from charge-charge interactions to protein stability. *Biochemistry,* **38,** 8138-49.

Inouye H, Nguyen JT, Fraser PE, Shinchuk LM, Packard AB, Kirschner DA (2000) Histidine residues underlie Congo Red binding to A beta analogs. *Amyloid,* **7,** 179-88.

Itzhaki LS, Otzen DE, Fersht AR (1995) The structure of the transition state for folding of chymotrypsin inhibitor 2 analysed by protein engineering methods: evidence for a nucleation-condensation mechanism for protein folding. *J Mol Biol,* **254,** 260-88.

Izawa Y, Tateno H, Kameda H, Hirakawa K, Hato K, Yagi H, Hongo K, Mizobata T, Kawata Y (2012) Role of C-terminal negative charges and tyrosine residues in fibril formation of alpha-synuclein. *Brain Behav,* **2,** 595-605.

Jaenicke R, Lilie H (2000) Folding and association of oligomeric and multimeric proteins. *Adv Protein Chem,* **53,** 329-401.

Jain N, Bhattacharya M, Mukhopadhyay S (2011) Kinetics of surfactant-induced aggregation of lysozyme studied by fluorescence spectroscopy. *J Fluoresc,* **21,** 615-25.

Jain S, Udgaonkar JB (2010) Salt-induced modulation of the pathway of amyloid fibril formation by the mouse prion protein. *Biochemistry,* **49,** 7615-24.

Jaroniec CP, MacPhee CE, Astrof NS, Dobson CM, Griffin RG (2002) Molecular conformation of a peptide fragment of transthyretin in an amyloid fibril. *Proc Natl Acad Sci U S A,* **99,** 16748-53.

Jensen MO, Mouritsen OG (2004) Lipids do influence protein function-the hydrophobic matching hypothesis revisited. *Biochim Biophys Acta,* **1666,** 205-26.

Jimenez JL, Guijarro JI, Orlova E, Zurdo J, Dobson CM, Sunde M, Saibil HR (1999) Cryo-electron microscopy structure of an SH3 amyloid fibril and model of the molecular packing. *EMBO J,* **18,** 815-21.

Jimenez JL, Nettleton EJ, Bouchard M, Robinson CV, Dobson CM, Saibil HR (2002) The protofilament structure of insulin amyloid fibrils. *Proc Natl Acad Sci U S A,* **99,** 9196-201.

Johnson AE, van Waes MA (1999) The translocon: a dynamic gateway at the ER membrane. *Annu Rev Cell Dev Biol,* **15,** 799-842.

Johnston MJ, Nemr K, Hefford MA (2010) Influence of bovine serum albumin on the secondary structure of interferon alpha 2b as determined by far UV circular dichroism spectropolarimetry. *Biologicals,* **38,** 314-20.

Juarez J, Taboada P, Mosquera V (2009) Existence of different structural intermediates on the fibrillation pathway of human serum albumin. *Biophys J,* **96,** 2353-70.

Kad NM, Thomson NH, Smith DP, Smith DA, Radford SE (2001) Beta(2)-microglobulin and its deamidated variant, N17D form amyloid fibrils with a range of morphologies in vitro. *J Mol Biol,* **313,** 559-71.

Kardos J, Micsonai A, Pal-Gabor H, Petrik E, Graf L, Kovacs J, Lee YH, Naiki H, Goto Y. (2011) Reversible heat-induced dissociation of beta2-microglobulin amyloid fibrils. *Biochemistry,* **50,** 3211-20.

Karplus M, Weaver DL (1976) Protein-folding dynamics. *Nature,* **260,** 404-6.

Kauzmann W (1959) Some factors in the interpretation of protein denaturation. *Adv Protein Chem,* **14,** 1-63.

Kawamura S, Ohno K, Ohkuma M, Chijiiwa Y, Torikata T (2006) Experimental verification of the crucial roles of Glu73 in the catalytic activity and structural stability of goose type lysozyme. *J Biochem,* **140,** 75-85.

Kelkar DA, Chaudhuri A, Haldar S, Chattopadhyay A (2010) Exploring tryptophan dynamics in acid-induced molten globule state of bovine alpha-lactalbumin: a wavelength-selective fluorescence approach. *Eur Biophys J,* **39,** 1453-63.

Kelly JW (2000) Mechanisms of amyloidogenesis. *Nat Struct Biol,* **7,** 824-6.

Kervinen J, Tobin GJ, Costa J, Waugh DS, Wlodawer A, Zdanov A (1999) Crystal structure of plant aspartic proteinase prophytepsin: inactivation and vacuolar targeting. *EMBO J,* **18,** 3947-55.

Khan F, Ahmad A, Khan MI (2007) Chemical, thermal and pH-induced equilibrium unfolding studies of Fusarium solani lectin. *IUBMB Life,* **59,** 34-43.

Khan JM, Qadeer A, Chaturvedi SK, Ahmad E, Rehman SA, Gourinath S, Khan RH (2012) SDS can be utilized as an amyloid inducer: a case study on diverse proteins. *PLoS One,* **7,** e29694.

Khazaei S, Yousefi R, Alavian-Mehr MM (2012) Aggregation and fibrillation of eye lens crystallins by homocysteinylation; implication in the eye pathological disorders. *Protein J,* **31,** 717-27.

Khurana R, Coleman C, Ionescu-Zanetti C, Carter SA, Krishna V, Grover RK, Roy R, Singh S (2005) Mechanism of thioflavin T binding to amyloid fibrils. *J Struct Biol,* **151,** 229-38.

Khurana R, Uversky VN, Nielsen L, Fink AL (2001) Is Congo Red an amyloid-specific dye? *J Biol Chem,* **276,** 22715-21.

Kihara M, Chatani E, Sakai M, Hasegawa K, Naiki H, Goto Y (2005) Seeding-dependent maturation of beta2-microglobulin amyloid fibrils at neutral pH. *J Biol Chem,* **280,** 12012-8.

Kim YS, Randolph TW, Manning MC, Stevens FJ, Carpenter JF (2003) Congo Red populates partially unfolded states of an amyloidogenic protein to enhance aggregation and amyloid fibril formation. *J Biol Chem,* **278,** 10842-50.

Klunk WE, Debnath ML, Pettegrew JW (1994) Development of small molecule probes for the beta-amyloid protein of Alzheimer's disease. *Neurobiol Aging,* **15,** 691-8.

Klunk WE, Jacob RF, Mason RP (1999) Quantifying amyloid by Congo Red spectral shift assay. *Methods Enzymol,* **309,** 285-305.

Klunk WE, Pettegrew JW, Abraham DJ (1989) Quantitative evaluation of Congo Red binding to amyloid-like proteins with a beta-pleated sheet conformation. *J Histochem Cytochem,* **37,** 1273-81.

Koshte VL, van Dijk W, van der Stelt ME, Aalberse RC (1990) Isolation and characterization of BanLec-I, a mannoside-binding lectin from Musa paradisiac (banana). *Biochem J,* **272,** 721-6.

Krebs MR, Wilkins DK, Chung EW, Pitkeathly MC, Chamberlain AK, Zurdo J, Robinson CV, Dobson CM (2000) Formation and seeding of amyloid fibrils from wild-type hen lysozyme and a peptide fragment from the beta-domain. *J Mol Biol,* **300,** 541-9.

Kricka LJ, De Luca M (1982) Effect of solvents on the catalytic activity of firefly luciferase. *Arch Biochem Biophys,* **217,** 674-81.

Krishnan R, Lindquist SL (2005) Structural insights into a yeast prion illuminate nucleation and strain diversity. *Nature,* **435,** 765-72.

Krobath H, Estacio SG, Faisca PF, Shakhnovich EI (2012) Identification of a conserved aggregation-prone intermediate state in the folding pathways of Spc-SH3 amyloidogenic variants. *J Mol Biol,* **422,** 705-22.

Kumar GR, Sharma A, Kumari M, Jagannadham MV, Debnath M (2011) Equilibrium unfolding of A. niger RNase: pH dependence of chemical and thermal denaturation. *Eur Biophys J,* **40,** 923-35.

Kumar M, Mommer MS, Sourjik V (2010) Mobility of cytoplasmic, membrane, and DNA-binding proteins in Escherichia coli. *Biophys J,* **98,** 552-9.

Kumar R, Prabhu NP, Yadaiah M, Bhuyan AK (2004) Protein stiffening and entropic stabilization in the subdenaturing limit of guanidine hydrochloride. *Biophys J,* **87,** 2656-62.

Kumar S, Nussinov R (2002) Close-range electrostatic interactions in proteins. *Chembiochem,* **3,** 604-17.

Kumar S, Ravi VK, Swaminathan R (2008) How do surfactants and DTT affect the size, dynamics, activity and growth of soluble lysozyme aggregates? *Biochem J,* **415,** 275-88.

Kumar S, Udgaonkar JB (2009) Conformational conversion may precede or follow aggregate elongation on alternative pathways of amyloid protofibril formation. *J Mol Biol,* **385,** 1266-76.

Kumar TK, Yang PW, Lin SH, Wu CY, Lei B, Lo SJ, Tu SC, Yu C (1996) Cloning, direct expression, and purification of a snake venom cardiotoxin in Escherichia coli. *Biochem Biophys Res Commun,* **219,** 450-6.

Kumaran R, Ramamurthy P (2011) Denaturation mechanism of BSA by urea derivatives: evidence for hydrogen-bonding mode from fluorescence tools. *J Fluoresc,* **21,** 1499-508.

Kuwajima K (1989) The molten globule state as a clue for understanding the folding and cooperativity of globular-protein structure. *Proteins,* **6,** 87-103.

La Mesa C (2005) Polymer-surfactant and protein-surfactant interactions. *J Colloid Interface Sci,* **286,** 148-57.

Lakowicz JR (1983)) Principle of fluorescence spectroscopy. *Plenum Press, new York.*

Lansbury PT, Jr. (1999) Evolution of amyloid: what normal protein folding may tell us about fibrillogenesis and disease. *Proc Natl Acad Sci U S A,* **96,** 3342-4.

Laughlin RB, Pines D, Schmalian J, Stojkovic BP, Wolynes P (2000) The middle way. *Proc Natl Acad Sci U S A,* **97,** 32-7.

Lee AG (2004) How lipids affect the activities of integral membrane proteins. *Biochim Biophys Acta,* **1666,** 62-87.

Legg-E'silva D, Achilonu I, Fanucchi S, Stoychev S, Fernandes M, Dirr HW (2012) Role of arginine 29 and glutamic acid 81 interactions in the conformational stability of human chloride intracellular channel 1. *Biochemistry,* **51,** 7854-62.

Li W, Zhou R, Mu Y (2012) Salting effects on protein components in aqueous NaCl and urea solutions: toward understanding of urea-induced protein denaturation. *J Phys Chem B,* **116,** 1446-51.

Li Y, Cao M, Wang Y (2006) Alzheimer Abeta(1-40) peptide: interactions with cationic gemini and single-chain surfactants. *J Phys Chem B,* **110,** 18040-5.

Lim WK, Rosgen J, Englander SW (2009) Urea, but not guanidinium, destabilizes proteins by forming hydrogen bonds to the peptide group. *Proc Natl Acad Sci U S A,* **106,** 2595-600.

Lindgren M, Sorgjerd K, Hammarstrom P (2005) Detection and characterization of aggregates, prefibrillar amyloidogenic oligomers, and protofibrils using fluorescence spectroscopy. *Biophys J.* **88,** 4200-12.

Lindorff-Larsen K, Rogen P, Paci E, Vendruscolo M, Dobson CM (2005) Protein folding and the organization of the protein topology universe. *Trends Biochem Sci,* **30,** 13-9.

Lis H, Sharon N (1998) Lectins: carbohydrate-specific proteins that mediate cellular recognition. *Chem Rev,* **98,** 637-674.

Liu KN, Lai CM, Lee YT, Wang SN, Chen RP, Jan JS, Liu HS, Wang SS (2012) Curcumin's pre-incubation temperature affects its inhibitory potency toward amyloid fibrillation and fibril-induced cytotoxicity of lysozyme. *Biochim Biophys Acta,* **1820,** 1774-86.

Liu KN, Wang HY, Chen CY, Wang SS (2010) L-Arginine reduces thioflavin T fluorescence but not fibrillation of bovine serum albumin. *Amino Acids,* **39,** 821-9.

Liu W, Cellmer T, Keerl D, Prausnitz JM, Blanch HW (2005) Interactions of lysozyme in guanidinium chloride solutions from static and dynamic light-scattering measurements. *Biotechnol Bioeng,* **90,** 482-90.

Loris R (2002) Principles of structures of animal and plant lectins. *Biochim Biophys Acta,* **1572,** 198-208.

Lu RC, Cao AN, Lai LH, Zhu BY, Zhao GX, Xiao JX (2005) Interaction between bovine serum albumin and equimolarly mixed cationic-anionic surfactants decyltriethylammonium bromide-sodium decyl sulfonate. *Colloids Surf B Biointerfaces,* **41,** 139-43.

Luheshi LM, Crowther DC, Dobson CM (2008) Protein misfolding and disease: from the test tube to the organism. *Curr Opin Chem Biol,* **12,** 25-31.

Luo JC, Wang SC, Jian WB, Chen CH, Tang JL, Lee CI (2012) Formation of amyloid fibrils from beta-amylase. *FEBS Lett,* **586,** 680-5.

MacPhee CE, Dobson CM (2000) Chemical dissection and reassembly of amyloid fibrils formed by a peptide fragment of transthyretin. *J Mol Biol,* **297,** 1203-15.

Mahanta S, Singh RB, Guchhait N (2009) Study of protein-probe interaction and protective action of surfactant sodium dodecyl sulphate in urea-denatured HSA using charge transfer fluorescence probe methyl ester of N,N-dimethylamino naphthyl acrylic acid. *J Fluoresc,* **19,** 291-302.

Makin OS, Atkins E, Sikorski P, Johansson J, Serpell LC (2005) Molecular basis for amyloid fibril formation and stability. *Proc Natl Acad Sci U S A,* **102,** 315-20.

Makin OS, Serpell LC (2005) Structures for amyloid fibrils. *FEBS J,* **272,** 5950-61.

Malisauskas M, Zamotin V, Jass J, Noppe W, Dobson CM, Morozova-Roche LA (2003) Amyloid protofilaments from the calcium-binding protein equine lysozyme: formation of ring and linear structures depends on pH and metal ion concentration. *J Mol Biol,* **330,** 879-90.

Markossian KA, Kurganov BI (2004) Protein folding, misfolding and aggregation. Formation of inclusion bodies and aggresomes. *Biochemistry (Mosc),* **69,** 971-84.

Marshall SA, Lazar GA, Chirino AJ, Desjarlais JR (2003) Rational design and engineering of therapeutic proteins. *Drug Discov Today,* **8,** 212-21.

Marti DN, Bosshard HR (2003) Electrostatic interactions in leucine zippers: thermodynamic analysis of the contributions of Glu and His residues and the effect of mutating salt bridges. *J Mol Biol,* **330,** 621-37.

Mayr LM, Schmid FX (1993) Stabilization of a protein by guanidinium chloride. *Biochemistry,* **32,** 7994-8.

McClellan AJ, Frydman J (2001) Molecular chaperones and the art of recognizing a lost cause. *Nat Cell Biol,* **3,** E51-3.

McLaurin J, Franklin T, Chakrabartty A, Fraser PE (1998) Phosphatidylinositol and inositol involvement in Alzheimer amyloid-beta fibril growth and arrest. *J Mol Biol,* **278,** 183-94.

McParland VJ, Kad NM, Kalverda AP, Brown A, Kirwin-Jones P, Hunter MG, Sunde M, Radford SE (2000) Partially unfolded states of beta(2)-microglobulin and amyloid formation in vitro. *Biochemistry,* **39,** 8735-46.

Meagher JL, Winter HC, Ezell P, Goldstein IJ, Stuckey JA (2005) Crystal structure of banana lectin reveals a novel second sugar binding site. *Glycobiology,* **15,** 1033-42.

Meng X, Fink AL, Uversky VN (2008) The effect of membranes on the in vitro fibrillation of an amyloidogenic light-chain variable-domain SMA. *J Mol Biol,* **381,** 989-99.

Mir MA, Gull N, Khan JM, Khan RH, Dar AA, Rather GM (2010a) Interaction of bovine serum albumin with cationic single chain+nonionic and cationic gemini+nonionic binary surfactant mixtures. *J Phys Chem B,* **114,** 3197-204.

Mir MA, Khan JM, Khan RH, Dar AA, Rather GM (2012) Interaction of Cetyltrimethylammonium Bromide and Its Gemini Homologue Bis(cetyldimethylammonium)butane Dibromide with Xanthine Oxidase. *J Phys Chem B.*

Mir MA, Khan JM, Khan RH, Rather GM, Dar AA (2010b) Effect of spacer length of alkanediyl-alpha,omega-bis(dimethylcetylammonium bromide) gemini homologues on the interfacial and physicochemical properties of BSA. *Colloids Surf B Biointerfaces,* **77,** 54-9.

Mishra R, Sjulander D, Hammarstrom P (2011a) Spectroscopic characterization of diverse amyloid fibrils in vitro by the fluorescent dye Nile red. *Mol Biosyst,* **7,** 1232-40.

Mishra R, Sorgjerd K, Nystrom S, Nordigarden A, Yu YC, Hammarstrom P (2007) Lysozyme amyloidogenesis is accelerated by specific nicking and fragmentation but decelerated by intact protein binding and conversion. *J Mol Biol,* **366,** 1029-44.

Mishra V, Ali V, Nozaki T, Bhakuni V (2011b) Biophysical characterization of Entamoeba histolytica phosphoserine aminotransferase (EhPSAT): role of cofactor and domains in stability and subunit assembly. *Eur Biophys J,* **40,** 599-610.

Mitaben D. Lad VML, Barbara Briggs, Rebecca J. Green and Richard A. Frazier (2003) Analysis of the SDS−Lysozyme Binding Isotherm. *Langmuir,* **19,** 5098–5103.

Mitra J, Tang X, Almo SC, Shields D (1998) Temperature-induced conformational changes in prosomatostatin-II: implications for processing. *Biochem J,* **334 (Pt 1),** 275-82.

Mitra N, Srinivas VR, Ramya TN, Ahmad N, Reddy GB, Surolia A (2002) Conformational stability of legume lectins reflect their different modes of quaternary association: solvent denaturation studies on concanavalin A and winged bean acidic agglutinin. *Biochemistry,* **41,** 9256-63.

Modler AJ, Gast K, Lutsch G, Damaschun G (2003) Assembly of amyloid protofibrils via critical oligomers--a novel pathway of amyloid formation. *J Mol Biol,* **325,** 135-48.

Moosavi-Movahedi AA, Pirzadeh P, Hashemnia S, Ahmadian S, Hemmateenejad B, Amani M, Saboury AA, Ahmad F, Shamsipur M, Hakimelahi GH, Tsai FY, Alijanvand HH, Yousefi R (2007) Fibril formation of lysozyme upon interaction with sodium dodecyl sulfate at pH 9.2. *Colloids Surf B Biointerfaces,* **60,** 55-61.

Morell M, Bravo R, Espargaro A, Sisquella X, Aviles FX, Fernàndez-Busquets X, Ventura S (2008) Inclusion bodies: specificity in their aggregation process and amyloid-like structure. *Biochim Biophys Acta,* **1783,** 1815-25.

Moriyama Y, Takeda K (2005) Protective effects of small amounts of bis(2-ethylhexyl)sulfosuccinate on the helical structures of human and bovine serum albumins in their thermal denaturations. *Langmuir,* **21,** 5524-8.

Moriyama Y, Watanabe E, Kobayashi K, Harano H, Inui E, Takeda K (2008) Secondary structural change of bovine serum albumin in thermal denaturation up to 130 degrees C and protective effect of sodium dodecyl sulfate on the change. *J Phys Chem B,* **112,** 16585-9.

Morshedi D, Ebrahim-Habibi A, Moosavi-Movahedi AA, Nemat-Gorgani M (2010) Chemical modification of lysine residues in lysozyme may dramatically influence its amyloid fibrillation. *Biochim Biophys Acta,* **1804,** 714-22.

Motamedi-Shad N, Garfagnini T, Penco A, Relini A, Fogolari F, Corazza A, Esposito G, Bemporad F, Chiti F (2012) Rapid oligomer formation of human muscle acylphosphatase induced by heparan sulfate. *Nat Struct Mol Biol,* **19,** 547-54, S1-2.

Motamedi-Shad N, Monsellier E, Chiti F (2009a) Amyloid formation by the model protein muscle acylphosphatase is accelerated by heparin and heparan sulphate through a scaffolding-based mechanism. *J Biochem,* **146,** 805-14.

Motamedi-Shad N, Monsellier E, Torrassa S, Relini A, Chiti F (2009b) Kinetic analysis of amyloid formation in the presence of heparan sulfate: faster unfolding and change of pathway. *J Biol Chem,* **284,** 29921-34.

Mukherjee S, Kombrabail M, Krishnamoorthy G, Chattopadhyay A (2007) Dynamics and heterogeneity of bovine hippocampal membranes: role of cholesterol and proteins. *Biochim Biophys Acta,* **1768,** 2130-44.

Muzammil S, Kumar Y, Tayyab S (2000) Anion-induced stabilization of human serum albumin prevents the formation of intermediate during urea denaturation. *Proteins,* **40,** 29-38.

Naidoo N (2009) ER and aging-Protein folding and the ER stress response. *Ageing Res Rev,* **8,** 150-9.

Naidu KT, Prabhu NP (2011) Protein-surfactant interaction: sodium dodecyl sulfate-induced unfolding of ribonuclease A. *J Phys Chem B,* **115,** 14760-7.

Naiki H, Gejyo F (1999) Kinetic analysis of amyloid fibril formation. *Methods Enzymol,* **309,** 305-18.

Nakamura K, Era S, Ozaki Y, Sogami M, Hayashi T, Murakami M (1997) Conformational changes in seventeen cystine disulfide bridges of bovine serum albumin proved by Raman spectroscopy. *FEBS Lett,* **417,** 375-8.

Naseem F, Khan RH (2005) Characterization of a common intermediate of pea lectin in the folding pathway induced by TFE and HFIP. *Biochim Biophys Acta,* **1723,** 192-200.

Necula M, Chirita CN, Kuret J (2003) Rapid anionic micelle-mediated alpha-synuclein fibrillization in vitro. *J Biol Chem,* **278,** 46674-80.

Nelson R, Eisenberg D (2006) Structural models of amyloid-like fibrils. *Adv Protein Chem,* **73,** 235-82.

Nenninger A, Mastroianni G, Mullineaux CW (2010) Size dependence of protein diffusion in the cytoplasm of Escherichia coli. *J Bacteriol,* **192,** 4535-40.

Nicholson EM, Scholtz JM (1996) Conformational stability of the Escherichia coli HPr protein: test of the linear extrapolation method and a thermodynamic characterization of cold denaturation. *Biochemistry,* **35,** 11369-78.

Nicola AV, McEvoy AM, Straus SE (2003) Roles for endocytosis and low pH in herpes simplex virus entry into HeLa and Chinese hamster ovary cells. *J Virol,* 77, 5324-32.

Nielsen AD, Borch K, Westh P (2007) Thermal stability of Humicola insolens cutinase in aqueous SDS. *J Phys Chem B,* **111,** 2941-7.

Nielsen L, Frokjaer S, Brange J, Uversky VN, Fink AL (2001a) Probing the mechanism of insulin fibril formation with insulin mutants. *Biochemistry,* **40,** 8397-409.

Nielsen L, Khurana R, Coats A, Frokjaer S, Brange J, Vyas S, Uversky VN, Fink AL (2001b) Effect of environmental factors on the kinetics of insulin fibril formation: elucidation of the molecular mechanism. *Biochemistry,* **40,** 6036-46.

Nilsson MR (2004) Techniques to study amyloid fibril formation in vitro. *Methods,* **34,** 151-60.

O'Brien EP, Dima RI, Brooks B, Thirumalai D (2007) Interactions between hydrophobic and ionic solutes in aqueous guanidinium chloride and urea solutions: lessons for protein denaturation mechanism. *J Am Chem Soc,* **129,** 7346-53.

Oellerich S, Wackerbarth H, Hildebrandt P (2003) Conformational equilibria and dynamics of cytochrome c induced by binding of sodium dodecyl sulfate monomers and micelles. *Eur Biophys J,* **32,** 599-613.

Ohhashi Y, Kihara M, Naiki H, Goto Y (2005) Ultrasonication-induced amyloid fibril formation of beta2-microglobulin. *J Biol Chem,* **280,** 32843-8.

Ohnishi S, Kameyama K, Takagi T (1998) Characterization of a heat modifiable protein, Escherichia coli outer membrane protein OmpA in binary surfactant system of sodium dodecyl sulfate and octylglucoside. *Biochim Biophys Acta,* **1375,** 101-9.

Ookoshi T, Hasegawa K, Ohhashi Y, Kimura H, Takahashi N, Yoshida H, Miyazaki R, Goto Y, Naiki H (2008) Lysophospholipids induce the nucleation and extension of beta2-microglobulin-related amyloid fibrils at a neutral pH. *Nephrol Dial Transplant,* **23,** 3247-55.

Otzen DE (2002) Protein unfolding in detergents: effect of micelle structure, ionic strength, pH, and temperature. *Biophys J,* **83,** 2219-30.

Otzen DE, Sehgal P, Westh P (2009) Alpha-Lactalbumin is unfolded by all classes of surfactants but by different mechanisms. *J Colloid Interface Sci,* **329,** 273-83.

Pace CN (2001) Polar group burial contributes more to protein stability than nonpolar group burial. *Biochemistry,* **40,** 310-3.

Pace CN, Fu H, Fryar KL, Landua J, Trevino SR, Shirley BA, Hendricks MM, Iimura S, Gajiwala K, Scholtz JM, Grimsley GR (2011) Contribution of hydrophobic interactions to protein stability. *J Mol Biol,* **408,** 514-28.

Pace CN, Laurents DV, Erickson RE (1992) Urea denaturation of barnase: pH dependence and characterization of the unfolded state. *Biochemistry,* **31,** 2728-34.

Pallares I, Vendrell J, Aviles FX, Ventura S (2004) Amyloid fibril formation by a partially structured intermediate state of alpha-chymotrypsin. *J Mol Biol,* **342,** 321-31.

Palsdottir H, Hunte C (2004) Lipids in membrane protein structures. *Biochim Biophys Acta,* **1666,** 2-18.

Panyukov YV, Nemykh MA, Rafikova ER, Kurganov BI, Yaguzhinsky LS, Arutyunyan AM, Drachev VA, Dobrov EN (2006) Low cetyltrimethylammonium bromide concentrations induce reversible amorphous aggregation of tobacco mosaic virus and its coat protein at room temperature. *Int J Biochem Cell Biol,* **38,** 533-43.

Panza G, Luers L, Stöhr J, Nagel-Steger L, Weiss J, Riesner D, Willbold D, Birkmann E (2010) Molecular interactions between prions as seeds and recombinant prion proteins as substrates resemble the biological interspecies barrier in vitro. *PLoS One,* **5,** e14283.

Park SH (2004) Hydrophobic core variant ubiquitin forms a molten globule conformation at acidic pH. *J Biochem Mol Biol,* **37,** 676-83.

Paschek D, Garcia AE (2004) Reversible temperature and pressure denaturation of a protein fragment: a replica exchange molecular dynamics simulation study. *Phys Rev Lett,* **93,** 238105.

Patel MM, Sgourakis NG, Garcia AE, Makhatadze GI (2010) Experimental test of the thermodynamic model of protein cooperativity using temperature-induced unfolding of a Ubq-UIM fusion protein. *Biochemistry,* **49,** 8455-67.

Pedersen JS, Christensen G, Otzen DE (2004) Modulation of S6 fibrillation by unfolding rates and gatekeeper residues. *J Mol Biol,* **341,** 575-88.

Pertinhez TA, Bouchard M, Smith RA, Dobson CM, Smith LJ (2002) Stimulation and inhibition of fibril formation by a peptide in the presence of different concentrations of SDS. *FEBS Lett,* **529,** 193-7.

Peters T, Jr. (1985) Serum albumin. *Adv Protein Chem,* **37,** 161-245.

Peters TJ (1996) All about albumin: Biochemistry, genetics and medical applications. *California: Academic Press.*

Peumans WJ, Zhang W, Barre A, Houlès Astoul C, Balint-Kurti PJ, Rovira P, Rougé P, May GD, Van Leuven F, Truffa-Bachi P, Van Damme EJ (2000) Fruit-specific lectins from banana and plantain. *Planta,* **211,** 546-54.

Pica A, Russo Krauss I, Castellano I, La Cara F, Graziano G, Sica F, Merlino A (2013) Effect of NaCl on the conformational stability of the thermophilic gamma-glutamyltranspeptidase from Geobacillus thermodenitrificans: Implication for globular protein halotolerance. *Biochim Biophys Acta,* **1834,** 149-57.

Pickarska B, Konieczny L, Rybarska J, Stopa B, Zemanek G, Szneler E, Król M, Nowak M, Roterman I (2001) Heat-induced formation of a specific binding site for self-assembled Congo Red in the V domain of immunoglobulin L chain lambda. *Biopolymers,* **59,** 446-56.

Pirzadeh P, Moosavi-Movahedi AA, Hemmateenejad B, Ahmad F, Shamsipur M, Saboury AA (2006) Chemometric studies of lysozyme upon interaction with sodium dodecyl sulfate and beta-cyclodextrin. *Colloids Surf B Biointerfaces,* **52,** 31-8.

Prasanna Kumari NK, Jagannadham MV (2011) SDS induced molten globule state of heynein; a new thiol protease: Evidence of domains and their sequential unfolding. *Colloids Surf B Biointerfaces,* **82,** 609-15.

Prats M, Teissie, J and Tocanne JF (1986) Lateral proton conduction at lipid–water interfaces and its implication for the chemiosmotic-coupling hypothesis. *Nature,* **322,** 756–758.

Privalov PL (1996) Intermediate states in protein folding. *J Mol Biol,* **258,** 707-25.

Ptitsyn OB (1987) Protein folding: hypothesis and experiment. *J. Protein Chem,* **6,** 273-293.

Ptitsyn OB (1994) Kinetic and equilibrium intermediates in protein folding. *Protein Eng,* **7,** 593-6.

Ptitsyn OB (1995) Molten globule and protein folding. *Adv Protein Chem,* **47,** 83-229.

Radford SE, Dobson CM (1995) Insights into protein folding using physical techniques: studies of lysozyme and alpha-lactalbumin. *Philos Trans R Soc Lond B Biol Sci,* **348,** 17-25.

Ramachandran G, Udgaonkar JB (2012) Evidence for the existence of a secondary pathway for fibril growth during the aggregation of tau. *J Mol Biol,* **421,** 296-314.

Ramakrishna D, Prasad MD, Bhuyan AK (2012) Hydrophobic collapse overrides Coulombic repulsion in ferricytochrome c fibrillation under extremely alkaline condition. *Arch Biochem Biophys,* **528,** 67-71.

Ramboarina S, Redfield C (2003) Structural characterisation of the human alpha-lactalbumin molten globule at high temperature. *J Mol Biol,* **330,** 1177-88.

Ramirez-Alvarado M, Merkel JS, Regan L (2000) A systematic exploration of the influence of the protein stability on amyloid fibril formation in vitro. *Proc Natl Acad Sci U S A,* **97,** 8979-84.

Raso SW, Abel J, Barnes JM, Maloney KM, Pipes G, Treuheit MJ, King J, Brems DN (2005) Aggregation of granulocyte-colony stimulating factor in vitro involves a conformationally altered monomeric state. *Protein Sci,* **14,** 2246-57.

Reynolds JA, Tanford C (1970) The gross conformation of protein-sodium dodecyl sulfate complexes. *J Biol Chem,* **245,** 5161-5.

Rezaei Tavirani M, Moghaddamnia SH, Ranjbar B, Amani M, Marashi SA (2006) Conformational study of human serum albumin in pre-denaturation temperatures by differential scanning calorimetry, circular dichroism and UV spectroscopy. *J Biochem Mol Biol,* **39,** 530-6.

Ritter C, Maddelein ML, Siemer AB, Lührs T, Ernst M, Meier BH, Saupe SJ, Riek R (2005) Correlation of structural elements and infectivity of the HET-s prion. *Nature,* **435,** 844-8.

Rizo J, Blanco FJ, Kobe B, Bruch MD, Gierasch LM (1993) Conformational behavior of Escherichia coli OmpA signal peptides in membrane mimetic environments. *Biochemistry,* **32,** 4881-94.

Robbins KJ, Liu G, Selmani V, Lazo ND (2012) Conformational analysis of thioflavin T bound to the surface of amyloid fibrils. *Langmuir,* **28,** 16490-5.

Rochet JC, Lansbury PT, Jr. (2000) Amyloid fibrillogenesis: themes and variations. *Curr Opin Struct Biol,* **10,** 60-8.

Roller DG, Dollery SJ, Doyle JL, Nicola AV (2008) Structure-function analysis of herpes simplex virus glycoprotein B with fusion-from-without activity. *Virology,* **382,** 207-16.

Rosner HI, Redfield C (2009) The human alpha-lactalbumin molten globule: comparison of structural preferences at pH 2 and pH 7. *J Mol Biol,* **394,** 351-62.

Roterman I, KrUl M, Nowak M, Konieczny L, Rybarska J, Stopa B, Piekarska B, Zemanek G (2001) Why Congo Red binding is specific for amyloid proteins - model studies and a computer analysis approach. *Med Sci Monit,* **7,** 771-84.

Rudyk H, Vasiljevic S, Hennion RM, Birkett CR, Hope J, Gilbert IH (2000) Screening Congo Red and its analogues for their ability to prevent the formation of PrP-res in scrapie-infected cells. *J Gen Virol,* **81,** 1155-64.

Rumbley J, Hoang L, Mayne L, Englander SW (2001) An amino acid code for protein folding. *Proc Natl Acad Sci U S A,* **98,** 105-12.

Rumfeldt JA, Galvagnion C, Vassall KA, Meiering EM (2008) Conformational stability and folding mechanisms of dimeric proteins. *Prog Biophys Mol Biol,* **98,** 61-84.

Rutkevich LA, Williams DB (2011) Participation of lectin chaperones and thiol oxidoreductases in protein folding within the endoplasmic reticulum. *Curr Opin Cell Biol,* **23,** 157-66.

Ruzafa D, Morel B, Varela L, Azuaga AI, Conejero-Lara F (2012) Characterization of oligomers of heterogeneous size as precursors of amyloid fibril nucleation of an SH3 domain: An experimental kinetics study. *PLoS One,* **7,** e49690.

Ryan TM, Griffin MD, Teoh CL, Ooi J, Howlett GJ (2011) High-affinity amphipathic modulators of amyloid fibril nucleation and elongation. *J Mol Biol,* **406,** 416-29.

Sabate R, Gallardo M, Estelrich J (2003) An autocatalytic reaction as a model for the kinetics of the aggregation of beta-amyloid. *Biopolymers,* **71,** 190-5.

Sachse C, Fandrich M, Grigorieff N (2008) Paired beta-sheet structure of an Abeta(1-40) amyloid fibril revealed by electron microscopy. *Proc Natl Acad Sci U S A,* **105,** 7462-6.

Sackett DL, Wolff J (1987) Nile red as a polarity-sensitive fluorescent probe of hydrophobic protein surfaces. *Anal Biochem,* **167,** 228-34.

Safarian S, Saffarzadeh M, Zargar SJ, Moosavi-Movahedi AA (2006) Molten globule-like state of bovine carbonic anhydrase in the presence of acetonitrile. *J Biochem,* **139,** 1025-33.

Sagle LB, Zhang Y, Litosh VA, Chen X, Cho Y, Cremer PS (2009) Investigating the hydrogen-bonding model of urea denaturation. *J Am Chem Soc,* **131,** 9304-10.

Sambasivam D, Sivanesan S, Ashok BS, Rajadas J (2011) Structural preferences of Abeta fragments in different micellar environments. *Neuropeptides,* **45,** 369-76.

Samuel D, Kumar TK, Balamurugan K, Lin WY, Chin DH, Yu C (2001) Structural events during the refolding of an all beta-sheet protein. *J Biol Chem,* **276,** 4134-41.

Santiago PS, Carvalho FA, Domingues MM, Carvalho JW, Santos NC, Tabak M Isoelectric point determination for Glossoscolex paulistus extracellular hemoglobin: oligomeric stability in acidic pH and relevance to protein-surfactant interactions. *Langmuir,* **26,** 9794-801.

Santiago PS, Carvalho FA, Domingues MM, Carvalho JW, Santos NC, Tabak M (2010) Isoelectric point determination for Glossoscolex paulistus extracellular

hemoglobin: oligomeric stability in acidic pH and relevance to protein-surfactant interactions. *Langmuir,* **26,** 9794-801.

Santos SF, Zanette D, Fischer H, Itri R (2003) A systematic study of bovine serum albumin and sodium dodecyl sulfate interactions by surface tension and small angle X-ray scattering. *J Colloid Interface Sci,* **262,** 400-8.

Santra MK, Banerjee A, Rahaman O, Panda D (2005) Unfolding pathways of human serum albumin: evidence for sequential unfolding and folding of its three domains. *Int J Biol Macromol,* **37,** 200-4.

Sasahara K, Hall D, Hamada D (2010) Effect of lipid type on the binding of lipid vesicles to islet amyloid polypeptide amyloid fibrils. *Biochemistry,* **49,** 3040-8.

Sasahara K, Morigaki K, Okazaki T, Hamada D (2012) Binding of islet amyloid polypeptide to supported lipid bilayers and amyloid aggregation at the membranes. *Biochemistry,* **51,** 6908-19.

Sawaya MR, Sambashivan S, Nelson R, Ivanova MI, Sievers SA, Apostol MI, Thompson MJ, Balbirnie M, Wiltzius JJ, McFarlane HT, Madsen AØ, Riekel C, Eisenberg D (2007) Atomic structures of amyloid cross-beta spines reveal varied steric zippers. *Nature,* **447,** 453-7.

Schmittschmitt JP, Scholtz JM (2003) The role of protein stability, solubility and net charge in amyloid fibril formation. *Protein Sci.* **12,** 2374-8.

Schokker E, Singh, H., & Creamer, LK. (2000) Heat-induced aggregation of beta-lactoglobulin A and B with alpha-lactalbumin. *Int. Dairy. J.* , **10,** 843-853.

Sedlak E, Antalik M (1999) Molten globule-like state of cytochrome c induced by polyanion poly(vinylsulfate) in slightly acidic pH. *Biochim Biophys Acta,* **1434,** 347-55.

Semisotnov GV, Rodionova NA, Razgulyaev OI, Uversky VN, Gripas AF, Gilmanshin RI (1991) Study of the molten globule intermediate state in protein folding by a hydrophobic fluorescent probe. *Biopolymers,* **31,** 119-28.

Sen P, Fatima S, Khan JM, Khan RH (2009) How methyl cyanide induces aggregation in all-alpha proteins: a case study in four albumins. *Int J Biol Macromol,* **44,** 163-9.

Sereikaite J, Bumelis VA (2006) Congo Red interaction with alpha-proteins. *Acta Biochim Pol,* **53,** 87-92.

Serio TR, Cashikar AG, Kowal AS, Sawicki GJ, Moslehi JJ, Serpell L, Arnsdorf MF, Lindquist SL (2000) Nucleated conformational conversion and the replication of conformational information by a prion determinant. *Science,* **289,** 1317-21.

Sharon N, Lis H (1990) Legume lectins--a large family of homologous proteins. *FASEB J,* **4,** 3198-208.

Sheinerman FB, Norel R, Honig B (2000) Electrostatic aspects of protein-protein interactions. *Curr Opin Struct Biol,* **10,** 153-9.

Shinde UP, Liu JJ, Inouye M (1997) Protein memory through altered folding mediated by intramolecular chaperones. *Nature,* **389,** 520-2.

Shirley BA, Stanssens P, Steyaert J, Pace CN (1989) Conformational stability and activity of ribonuclease T1 and mutants. Gln25----Lys, Glu58----Ala and the double mutant. *J Biol Chem,* **264,** 11621-5.

Shukla N, Bhatt AN, Aliverti A, Zanetti G, Bhakuni V (2005) Guanidinium chloride and urea-induced unfolding of FprA, a mycobacterium NADPH-ferredoxin reductase: stabilization of an apo-protein by GdmCl. *FEBS J,* **272,** 2216-24.

Sigler PB, Xu Z, Rye HS, Burston SG, Fenton WA, Horwich AL (1998) Structure and function in GroEL-mediated protein folding. *Annu Rev Biochem,* **67,** 581-608.

Simon LM, Kotorman M, Garab G, Laczko I (2002) Effects of polyhydroxy compounds on the structure and activity of alpha-chymotrypsin. *Biochem Biophys Res Commun,* **293,** 416-20.

Loveday SM, Su J, Rao MA, Anema SG, Singh H (2011) Effect of Calcium on the Morphology and Functionality of Whey Protein Nanofibrils *Biomacromolecules,* **12,** 3780 -3788.

Simpanya MF, Ansari RR, Leverenz V, Giblin FJ (2008) Measurement of lens protein aggregation in vivo using dynamic light scattering in a guinea pig/UVA model for nuclear cataract. *Photochem Photobiol,* **84,** 1589-95.

Sinha S, Surolia A (2005) Oligomerization endows enormous stability to soybean agglutinin: a comparison of the stability of monomer and tetramer of soybean agglutinin. *Biophys J,* **88,** 4243-51.

Sinha S, Surolia A (2007) Attributes of glycosylation in the establishment of the unfolding pathway of soybean agglutinin. *Biophys J,* **92,** 208-16.

Sparr E, Engel MF, Sakharov DV, Sprong M, Jacobs J, de Kruijff B, Hoppener JW, Killian JA (2004) Islet amyloid polypeptide-induced membrane leakage involves uptake of lipids by forming amyloid fibers. *FEBS Lett,* **577,** 117-20.

Srinivasan R, Jones EM, Liu K, Ghiso J, Marchant RE, Zagorski MG (2003) pH-dependent amyloid and protofibril formation by the ABri peptide of familial British dementia. *J Mol Biol,* **333,** 1003-23.

Stefani M, Dobson CM (2003a) Protein aggregation and aggregate toxicity: new insights into protein folding, misfolding diseases and biological evolution. *J Mol Med* **81,** 678-99.

Stefani M, Dobson CM (2003b) Protein aggregation and aggregate toxicity: new insights into protein folding, misfolding diseases and biological evolution. *J Mol Med (Berl),* **81,** 678-99.

Stenstam A KA, Wennerström H (2001) The lysozyme-dodecyl sulfate system. An example of protein-surfactant aggregation. *Langmuir,* **17,** 7513-7520.

Stickle DF, Presta LG, Dill KA, Rose GD (1992) Hydrogen bonding in globular proteins. *J Mol Biol,* **226,** 1143-59.

Sugio S, Kashima A, Mochizuki S, Noda M, Kobayashi K (1999) Crystal structure of human serum albumin at 2.5 A resolution. *Protein Eng,* **12,** 439-46.

Sukenik S, Politi R, Ziserman L, Danino D, Friedler A, Harries D (2011) Crowding alone cannot account for cosolute effect on amyloid aggregation. *PLoS One,* **6,** e15608.

Sulatskaya AI, Kuznetsova IM, Turoverov KK (2012) Interaction of thioflavin T with amyloid fibrils: fluorescence quantum yield of bound dye. *J Phys Chem B,* **116,** 2538-44.

Sureshbabu N, Kirubagaran R, Jayakumar R (2009) Surfactant-induced conformational transition of Abeta-peptide. *Eur Biophys J,* **38,** 355-67.

Sutter M, Oliveira S, Sanders NN, Lucas B, van Hoek A, Hink MA, Visser AJ, De Smedt SC, Hennink WE, Jiskoot W (2007) Sensitive spectroscopic detection of large and denatured protein aggregates in solution by use of the fluorescent dye Nile red. *J Fluoresc,* **17,** 181-92.

Suzuki M, Yokoyama K, Lee YH, Ginto Y (2011) A two-step refolding of acid-denatured microbial transglutaminase escaping from the aggregation-prone intermediate. *Biochemistry,* **50,** 10390-8.

Swanson MD, Winter HC, Goldstein IJ, Markovitz DM (2010) A lectin isolated from bananas is a potent inhibitor of HIV replication. *J Biol Chem,* **285,** 8646-55.

Taboada P, Barbosa S, Castro E, Mosquera V (2006) Amyloid fibril formation and other aggregate species formed by human serum albumin association. *J Phys Chem B,* **110,** 20733-6.

Taheri-Kafrani A, Asgari-Mobarakeh E, Bordbar AK, Haertle T (2010) Structure-function relationship of beta-lactoglobulin in the presence of dodecyltrimethyl ammonium bromide. *Colloids Surf B Biointerfaces,* **75,** 268-74.

Takeda K SM, Aoki K (1987) Secondary structures of bovine serum albumin in anionic and cationic surfactant solutions. *J Colloid Interface Sci,* **117,** 120–126.

Temussi PA, Masino L, Pastore A (2003) From Alzheimer to Huntington: why is a structural understanding so difficult? *EMBO J,* **22,** 355-61.

Tian M, Fan Y, Ji G, Wang Y (2012) Spontaneous aggregate transition in mixtures of a cationic gemini surfactant with a double-chain cationic surfactant. *Langmuir,* **28,** 12005-14.

Tjernberg L, Hosia W, Bark N, Thyberg J, Johansson J (2002) Charge attraction and beta propensity are necessary for amyloid fibril formation from tetrapeptides. *J Biol Chem,* **277,** 43243-6.

Touchette JC, Williams LL, Ajit D, Gallazzi F, Nichols MR (2010) Probing the amyloid-beta(1-40) fibril environment with substituted tryptophan residues. *Arch Biochem Biophys,* **494,** 192-7.

Tougu V, Karafin A, Zovo K, Chung RS, Howells C, West AK, Palumaa P (2009) Zn(II) and Cu(II)-induced non-fibrillar aggregates of amyloid-beta (1-42) peptide are transformed to amyloid fibrils, both spontaneously and under the influence of metal chelators. *J Neurochem,* **110,** 1784-95.

Toyama BH, Weissman JS (2011) Amyloid structure: conformational diversity and consequences. *Annu Rev Biochem,* **80,** 557-85.

Tripathi T, Na BK, Sohn WM, Becker K, Bhakuni V (2009) Structural, functional and unfolding characteristics of glutathione S-transferase of Plasmodium vivax. *Arch Biochem Biophys,* **487,** 115-22.

Turnell WG, Finch JT (1992) Binding of the dye Congo Red to the amyloid protein pig insulin reveals a novel homology amongst amyloid-forming peptide sequences. *J Mol Biol,* **227,** 1205-23.

Turro NJ, Lei X, Ananthapadmanabhan KP and Aronson M (1995) Spectroacopic probe analysis of protein–surfactant interactions: The BSA/SDS system. *Langmuir* **11,** 2525–2533.

Tycko R (2006) Molecular structure of amyloid fibrils: insights from solid-state NMR. *Q Rev Biophys,* **39,** 1-55.

Uversky VN (2008) Alpha-synuclein misfolding and neurodegenerative diseases. *Curr Protein Pept Sci,* **9,** 507-40.

Uversky VN, Fink AL (2004) Conformational constraints for amyloid fibrillation: the importance of being unfolded. *Biochim Biophys Acta,* **1698,** 131-53.

Valpuesta JM, Martin-Benito J, Gomez-Puertas P, Carrascosa JL, Willison KR (2002) Structure and function of a protein folding machine: the eukaryotic cytosolic chaperonin CCT. *FEBS Lett,* **529,** 11-6.

Valstar A AM, Brown W, Vasilescu M (2000) The interaction of bovine serum albumin with surfactants studied by light scattering. *Langmuir,* **16,** 922-927.

Varejao N, Correia MT, Foguel D (2011) Characterization of the unfolding process of the tetrameric and dimeric forms of Cratylia mollis seed lectin (CRAMOLL 1): effects of natural fragmentation on protein stability. *Biochemistry,* **50,** 7330-40.

Vasilescu M AD, Almgren M, Valstar A (1999) Interactions of globular proteins with surfactants studied with fluorescence probe methods *Langmuir* **15,** 2635-2643.

Vetri V, Canale C, Relini A, Librizzi F, Militello V, Gliozzi A, Leone M (2007a) Amyloid fibrils formation and amorphous aggregation in concanavalin A. *Biophys Chem,* **125,** 184-90.

Vetri V, Librizzi F, Leone M, Militello V (2007b) Thermal aggregation of bovine serum albumin at different pH: comparison with human serum albumin. *Eur Biophys J,* **36,** 717-25.

Vetri V, Militello V (2005) Thermal induced conformational changes involved in the aggregation pathways of beta-lactoglobulin. *Biophys Chem,* **113,** 83-91.

Vilasi S, Sarcina R, Maritato R, De Simone A, Irace G, Sirangelo I (2011) Heparin induces harmless fibril formation in amyloidogenic W7FW14F apomyoglobin and amyloid aggregation in wild-type protein in vitro. *PLoS One,* **6,** e22076.

Villegas V, Zurdo J, Filimonov VV, Aviles FX, Dobson CM, Serrano L (2000) Protein engineering as a strategy to avoid formation of amyloid fibrils. *Protein Sci,* **9,** 1700-8.

Volkova KD, Kovalska VB, Balanda AO, Vermeij RJ, Subramaniam V, Slominskii YL, Yarmoluk SM (2007) Cyanine dye-protein interactions: looking for fluorescent probes for amyloid structures. *J Biochem Biophys Methods,* **70,** 727-33.

Vus KT, V. Gorbenko, G. Kirilova, E. Kirilov, G. Kalnina, I.Kinnunen, P (2012) Novel aminobenzanthrone dyes for amyloid fibril detection. *Chemical Physics Letters,* **532,** 110–115.

Wang L, Maji SK, Sawaya MR, Eisenberg D, Riek R (2008) Bacterial inclusion bodies contain amyloid-like structure. *PLoS Biol,* **6,** e195.

Wang SS, Hung YT, Wen WS, Lin KC, Chen GY (2011) Exploring the inhibitory activity of short-chain phospholipids against amyloid fibrillogenesis of hen egg-white lysozyme. *Biochim Biophys Acta,* **1811,** 301-13.

Wang W (1999) Instability, stabilization and formulation of liquid protein pharmaceuticals. *Int J Pharm,* **185,** 129-88.

Wang W (2005) Protein aggregation and its inhibition in biopharmaceutics. *Int J Pharm,* **289,** 1-30.

Wojciak P, Mazurkiewicz A, Bakalova A, Kuciel R (2003) Equilibrium unfolding of dimeric human prostatic acid phosphatase involves an inactive monomeric intermediate. *Int J Biol Macromol,* **32,** 43-54.

Wolynes PG, Onuchic JN, Thirumalai D (1995) Navigating the folding routes. *Science,* **267,** 1619-20.

Wu C, Biancalana M, Koide S, Shea JE (2009) Binding modes of thioflavin-T to the single-layer beta-sheet of the peptide self-assembly mimics. *J Mol Biol,* **394,** 627-33.

Wu C, Wang Z, Lei H, Duan Y, Bowers MT, Shea JE (2008) The binding of thioflavin T and its neutral analog BTA-1 to protofibrils of the Alzheimer's disease Abeta(16-22) peptide probed by molecular dynamics simulations. *J Mol Biol,* **384,** 718-29.

Wu C, Wang Z, Lei H, Zhang W, Duan Y (2007) Dual binding modes of Congo Red to amyloid protofibril surface observed in molecular dynamics simulations. *J Am Chem Soc,* **129,** 1225-32.

Xu Y, Seeman D, Yan Y, Sun L, Post J, Dubin PL (2012) Effect of heparin on protein aggregation: inhibition versus promotion. *Biomacromolecules,* **13,** 1642-51.

Yagi H, Ban T, Morigaki K, Naiki H, Goto Y (2007) Visualization and classification of Abeta supramolecular assemblies. *Biochemistry,* **46,** 15009-17.

Yamamoto K, Yagi H, Ozawa D, Sasahara K, Naiki H, Goto Y (2008) Thiol compounds inhibit the formation of amyloid fibrils by beta 2-microglobulin at neutral pH. *J Mol Biol,* **376,** 258-68.

Yamamoto S, Hasegawa K, Yamaguchi I, Tsutsumi S, Kardos J, Goto Y, Gejyo F, Naiki H (2004) Low concentrations of sodium dodecyl sulfate induce the extension of beta 2-microglobulin-related amyloid fibrils at a neutral pH. *Biochemistry,* **43,** 11075-82.

Yanagi K, Sakurai K, Yoshimura Y, Koouma T, Lee YH, Sugase K, Ikegami T, Naiki H, Goto Y (2012) The monomer-seed interaction mechanism in the formation of the beta2-microglobulin amyloid fibril clarified by solution NMR techniques. *J Mol Biol,* **422,** 390-402.

Yang JT, Wu CS, Martinez HM (1986) Calculation of protein conformation from circular dichroism. *Methods Enzymol,* **130,** 208-69.

Yang L, Gao YQ (2010) Effects of cosolvents on the hydration of carbon nanotubes. *J Am Chem Soc,* **132,** 842-8.

Yang ZC, Yang L, Zhang YX, Yu HF, An W (2007) Effect of heat and pH denaturation on the structure and conformation of recombinant human hepatic stimulator substance. *Protein J,* **26,** 303-13.

Yonath A, Podjarny A, Honig B, Sielecki A, Traub W (1977) Crystallographic studies of protein denaturation and renaturation. 2. Sodium dodecyl sulfate induced structural changes in triclinic lysozyme. *Biochemistry,* **16,** 1418-24.

Yuan T, Weljie AM, Vogel HJ (1998) Tryptophan fluorescence quenching by methionine and selenomethionine residues of calmodulin: orientation of peptide and protein binding. *Biochemistry,* **37,** 3187-95.

Zako T, Sakono M, Hashimoto N, Ihara M, Maeda M (2009) Bovine insulin filaments induced by reducing disulfide bonds show a different morphology, secondary structure and cell toxicity from intact insulin amyloid fibrils. *Biophys J,* **96,** 3331-40.

Zerovnik E (2002) Amyloid-fibril formation. Proposed mechanisms and relevance to conformational disease. *Eur J Biochem,* **269,** 3362-71.

Zhao H, Tuominen EK, Kinnunen PK (2004) Formation of amyloid fibers triggered by phosphatidylserine-containing membranes. *Biochemistry,* **43,** 10302-7.

Zhou HX, Rivas G, Minton AP (2008) Macromolecular crowding and confinement: biochemical, biophysical and potential physiological consequences. *Annu Rev Biophys,* **37,** 375-97.

Zhou R, Li J, Hua L, Yang Z, Berne BJ (2011) Comment on "urea-mediated protein denaturation: a consensus view". *J Phys Chem B,* **115,** 1323-6.

Zou Q, Habermann-Rottinghaus SM, Murphy KP (1998) Urea effects on protein stability: hydrogen bonding and the hydrophobic effect. *Proteins,* **31,** 107-15.

Zuhl F, Seemuller E, Golbik R, Baumeister W (1997) Dissecting the assembly pathway of the 20S proteasome. *FEBS Lett,* **418,** 189-94.

APPENDIX – A

List of Publications

PUBLICATIONS:

Published:

1 **Khan JM;** Qadeer A; Ahmad E; Ashraf R; Bhushan B; Chaturvedi S K; Rabbani G; Khan RH. Monomeric banana lectin at acidic pH overrules conformational stability of its native dimeric form. ***PLoS One*** (Accepted PONE-D-13-03070).

2 Rub MA; **Khan JM;** Yaseen Z; Khan RH; Kabir-ud-Din. Conformational change of serum albumin upon complexation with amphiphilic drug imipramine hydrochloride. ***Journal of Proteins and Proteomics***, 2012, 3 (3):207-215.

3 Qadeer A; Rabbani G; Zaidi N; Ahmad E; **Khan JM**; Khan RH. 1-Anilino-8-Naphthalene Sulfonate (ANS) Is Not a Desirable Probe for Determining the Molten Globule State of Chymopapain. ***PLoS One.*** 2012; 7(11):e50633. [impact factor= 4.41]

4 Khan AB; **Khan JM;** Ali MS; Khan RH; Kabir-Ud-Din. interaction of amphiphilic drugs with human and bovine serum albumins. ***Spectrochimica Acta Part A: Molecular and Biomolecular Spectroscopy***. 2012, 7 (97C):119-124. [impact factor=2.09]

5 Mir MA; **Khan JM;** Khan RH; Dar AA; Rather GM. Interaction of cetyltrimethylammonium Bromide and Its Gemini Homologue Bis(cetyldimethylammonium)butane Dibromide with Xanthine Oxidase. ***Journal of Physical Chemistry B,*** 2012, 116 (19): 5711–5718. [impact factor= 3.69]

6 **Khan JM;** Qadeer A; Chaturvedi SK; Ahmad E; Rehman SA; Gourinath S; Khan RH. SDS Can Be Utilized as an Amyloid Inducer: A Case Study on Diverse Proteins. ***PLoS One***. 7(1) (2012): e29694. [impact factor=4.41].

7 Gull N; Mir MA; **Khan JM**; Khan RH; Rather GM; Dar AA. Refolding of bovine serum albumin via artificial chaperone protocol using gemini surfactants. ***Journal of Colloid and Interface Science*** 364(1) (2011): 157-62. [impact factor=3.07].

8 Khan AB; **Khan JM;** Ali MS; **Khan RH;** Kabir-ud Din. Spectroscopic approach of the interaction study of amphiphilic drugs with the serum albumins ***Colloids and Surfaces B: Biointerfaces***. 87 (2) (2011): 447-53. [impact factor=3.45].

9 Ali MS; Anjum K; **Khan JM;** Khan RH; Kabir-ud-Din. Complexation behavior of gelatin with amphiphilic drug imipramine hydrochloride as studied by conductimetry, surface tensiometry and circular dichroism studies. ***Colloids and Surfaces B: Biointerfaces***. 82(1) (2011): 258-62. [impact factor=3.45]

10 Ali MS; Gull N; **Khan JM;** Aswal VK; Khan RH; Kabir-ud-Din. Unfolding of rabbit serum albumin by cationic surfactants: surface tensiometry, small-angle neutron scattering, intrinsic fluorescence, resonance Rayleigh scattering and circular dichroism studies. ***Journal of Colloid and Interface Science.*** 352 (2) (2010). 436-43. [Impact factor=3.07].

11 Ali MS; **Khan JM;** Aswal VK; Khan RH; Kabir-ud-Din. Multi-technique approach on the effect of surfactant concentrations on the thermal unfolding of rabbit serum albumin: Formation and solubilization of the protein aggregates. ***Colloids and Surfaces B: Biointerfaces***. 80 (2010) 169–175. (impact Factor =3.45].

12 Mir MA; Gull N; **Khan JM;** Khan RH; Dar AA; Rather GM. Interaction of bovine serum albumin with cationic single chain + nonionic and cationic + nonionic binary surfactants mixtures. ***Jurnal of Physical Chemistry B***. 114 (2010) 3197-3204. (impact Factor = 3.69).

13 Mir MA; **Khan JM;** Khan RH; Rather GM; Dar AA. Effect of spacer length of alkanediyl-α,ω-bis (dimethylcetylammunium bromide) gemini homologues on the interfacial and physicochemical properties of BSA. ***Colloids and Surfaces B: Biointerfaces.*** 77 (2010) 54–59. (Impact Factor = 3.45)

14 Sen P; Fatima S; **Khan JM;** Khan RH. How methyl cynide induces aggregation in all-alpha proteins: A case study in four albumins. ***International Journal of Biological Macramolecule.*** 44 (2009) 163-169. (impact Factor = 2.266)

15 Ahmad E; Rahman SK; **Khan JM;** Varshney A; Khan RH. *Phytolacca americana* lectin (Pa-2; pokeweed mitogen): an intrinsically unordered protein and its conversion into partial order at low pH. ***Bioscience Reports***, 30 (2009) 125-134.(impact Factor = 2.37)

Paper Under Review:

1. **Javed Masood Khan;** Sumit kumar Chaturvedi; Atiyatul Qadeer; Ejaz Ahmad; Shah Kamranur Rahman; Mohd Ishtikhar; Rizwan Hasan Khan. The influence of sodium dodecyl sulphate in promoting amyloid fibril formation in hen egg white lysozyme as pH lowered from 11.0 to 1.0. **(FEBS Journal)**
2. **Javed Masood Khan;** Atiyatul Qadeer, Sumit Kumar Chaturvedi and Rizwan Hasan Khan. Hydophobicity alone can not trigger aggregation in protonated mammalian serum albumins **(Biochemistry).**
3. **Javed Masood Khan;** Rizwan Hasan Khan. Elucidating the protective effect of SDS on serum albumins against temperature and urea at low pH **(BBA).**
4. Afshin Iram; Md Tauqeer Alam; **Javed Masood Khan;** Taqi A Khan; Rizwan H Khan; Aabgeena Naeem. Molten globule of hemoglobin proceeds into aggregates and Advanced Glycated End products (AGEs) **(PLOS ONE).**
5. Nuzhat Gull; **Javed Masood Khan;** Atiyatul Qadeer and Rizwan Hassan Khan. Refolding of Sheep (SSA), Rat (RSA) and Porcine (PSA) serum albumins via artificial chaperone protocol using gemini surfactant pentanediyl-α,ω-bis(cetyldimethylammonium bromide **(Langmuir)**
6. Samreen amani; Faisal Naseem, Taqi Ahmad Khan; Mohammad Furkan; **Javed Masood Khan;** Rizwan Hasan Khan and Aabgeena Naeem. Assessment of detergents in the formation of IGg aggregates: A multimethodoligical approach **(IJBM).**
7. Atiyatul qadeer; Masihuzzaman; Mohd Wasif Khan; Javed Masood Khan; Gulam Rabbani; Mohd Faisal; Gaurav Sharma; Samudrala Gaurinath; and Rizwan Hasan Khan. Surfactant-induced fibrillation in stem bromlin and possible mechanism of its inhibition by ANS and bis-ANS **(Biochemistry)**

Manuscript Under preparation:

1. Ejaz Ahmad; **Javed Masood Khan;** Fatima Kamal Zaidi and Rizwan Hasan Khan. Differential leucoverin binding to human serum albumin in physiological and disease mimetic condition.
2. Ejaz Ahmad; **Javed Masood Khan;** Fatima Kamal Zaidi and Rizwan Hasan Khan. Binding of leucoverin and 5-Fu to α-1 acid glycoprotein in the presence of glucose and urea at physiological pH.

3. Ejaz Ahmad; **Javed Masood Khan;** Gulam Rabbani and Rizwan Hasan Khan. Effect of co-solvent on four different proteins (lysozyme, IgG, Cytochrome C, Myoglobin).

4. Ejaz Ahmad; **Javed Masood Khan;** Gulam Rabbani and Rizwan Hasan Khan. Effect of Guanidine hydrochloride and urea on fetuin at neutral pH.

5. Afshin Iram; Minhal Adidi; **Javed Masood Khan;** Rizwan Hasan Khan and Aabgeena Naeem. Organic solvent induced detection of aggregates of glucoamylase.

6. Sumit Kumar Chaturvedi; **Javed Masood Khan;** Khursheed Alam and Rizwan Hasan Khan. Effect of cationic and anionic surfactant on hen egg white lysozyme at moderate and extreme alkaline condition.

Autobiography

I Javed Masood Khan was born on 28 September 1982 in Pehar Bazar, district Balrampur. Pehar is situated 175 km away from Lucknow. I am the youngest son of Janab Masoodul Haq Khan. I took my primary education from my home school. I did my 10th and 12th (1997-1999) from Mohmmad Yusuf Usmani Inter college Utraula district Balrampur. Then, I moved to Lucknow for my higher education. I did B.Sc. from Lucknow University in 2003. I studied biology and chemistry that helped me to see biology in a technical way.

For this I choose Biochemistry as a subject in my Master (2004-2006). I completed master in biochemistry in 2006 from Jamia Hamdard, New Delhi. After this course I could find myself a good thinker over the subject of concern. This is the reason I continued biotechnology as a research carrier. I got admission in Ph.D. (2008) Interdisciplinary Biotechnology Unit, Aligarh Muslim University, Aligarh.

Javed Masood Khan
Village & Post Pehar
District Balrampur
UP-271604
Email: javedjmk@gmail.com
Mob No: +91-9760594596

SDS Can Be Utilized as an Amyloid Inducer: A Case Study on Diverse Proteins

Javed Masood Khan[1], Atiyatul Qadeer[1], Sumit Kumar Chaturvedi[1], Ejaz Ahmad[1], Syed Arif Abdul Rehman[2], Samudrala Gourinath[2], Rizwan Hasan Khan[1]*

1 Interdisciplinary Biotechnology Unit, Aligarh Muslim University, Aligarh, India, **2** School of Life Sciences, Jawaharlal Nehru University, New Delhi, India

Abstract

Sodium dodecyl sulphate (SDS), an anionic surfactant that mimics some characteristics of biological membrane has also been found to induce aggregation in proteins. The present study was carried out on 25 diverse proteins using circular dichroism, fluorescence spectroscopy, dye binding assay and electron microscopy. It was found that an appropriate molar ratio of protein to SDS readily induced amyloid formation in all proteins at a pH below two units of their respective isoelectric points (pI) while no aggregation was observed at a pH above two units of pI. We also observed that electrostatic interactions play a leading role in the induction of amyloid. This study can be used to design or hypothesize a molecule or drug, which may counter act the factor responsible for amyloid formation.

Citation: Khan JM, Qadeer A, Chaturvedi SK, Ahmad E, Abdul Rehman SA, et al. (2012) SDS Can Be Utilized as an Amyloid Inducer: A Case Study on Diverse Proteins. PLoS ONE 7(1): e29694. doi:10.1371/journal.pone.0029694

Editor: Vladimir N. Uversky, University of South Florida College of Medicine, United States of America

Received September 23, 2011; **Accepted** December 2, 2011; **Published** January 12, 2012

Funding: The financial assistance to the authors was provided by Council of Scientific and Industrial Research (http://csirhrdg.res.in/), New Delhi, India in the form of Senior Research Fellowship and Junior Research Fellowship. The funders had no role in study design, data collection and analysis, decision to publish, or preparation of the manuscript.

Competing Interests: The authors have declared that no competing interests exist.

* E-mail: rizwanhkhan@hotmail.com

Introduction

While the majority of the proteins may acquire completely folded and functional conformation under *in-vivo* conditions, some of these undergo misfolding due to several reasons. It still remains unclear whether amyloid development is commenced by native state of proteins, partially or totally unfolded states. The amyloid formation is often linked with genetic mutations that can efficiently destabilize the native state suggesting that a conformational change is the first essential step in amyloidogenesis [1 2]. The partially unfolded states of a protein produced under high temperature, high pressure, low pH or moderate concentrations of organic solvents exhibit more propensity to aggregate. Due to several biological and environmental factors, the partially folded intermediates of proteins undergo α/β or β-sheet transition, a characteristic feature of amyloidosis. Amyloid formation is usually a pathogenic process where proteins undergo a conformational change and self-assemble into nonfunctional but toxic fibrils [3]. This process is linked with wide range of human disorders such as Alzheimer's and Creutz-feldt-Jacob disease, senile systemic amyloidosis, type 2 diabetes and dialysis amyloidosis, etc. Amyloid fibrils are also formed in endogenous proteins where they perform normal functions. Hence amyloid formation is not always harmful as evidenced from the simplest to complex organisms [4 5]. Sodium dodecyl sulfate (SDS), an anionic surfactant having negatively charged head group and hydrophobic tail, mimics the structure of lipid molecules of biological membranes. SDS is often used as a denaturant that destroys protein's native conformation; it provides an anionic micellar interface that has been shown to accelerate the aggregation of Aβ (1 40) over a limited range of (low SDS) concentrations [6]. Understanding the nature of protein surfactant interaction is of vital interest and allows us to gain insight into the binding mechanism between the two components and its consequence effect on protein structure and functions in the complex [7 8]. Since the conditions required to induce aggregation vary from protein to protein, the objective of this study was to provide a simple legislative to induce protein aggregation or amyloid formation with SDS by choosing appropriate pH conditions based on isoelectric point (pI). The aggregates so formed were studied using various spectroscopic as well as microscopic methods including circular dichroism, turbidity measurements, intrinsic fluorescence, Thioflavin T (ThT) binding and transmission electronic microscopy.

Materials and Methods

Materials

Human serum albumin [HSA] (5.67), porcine serum albumin [PSA] (5.89), bovine serum albumin [BSA] (5.65), sheep serum albumin [SSA] (5.63), rabbit serum albumin [RSA] (5.70), ovalbumin [Oval] (4.5), *Mucor javanicus* lipase [M. Java] (5.90), lysozyme [Lyso] (11.2), invertase [Invert] (3.4), hemoglobin [Hb] (7.1), glucose oxidase [GOD] (4.94), Gelatin (4.7), fetuin (5.21), concanavalin A [ConA] (5.43), α-lactalbumin [ALA] (4.4), cobra toxin [Cobra] (7.69), *Candida rugosa* lipase [Cand] (4.7), β-lactoglobulin [BLG] (5.2), bovine liver catalase [BLC] (5.4), α-amylase [Alp Amy] (5.9), conalbumin [CA] (6.69), chymopapain [Chymo] (10.4), rat IgG [RIgG] (7.8), asialofetuin [AFT] (5.1), banana lectin [BL] (6.26) and SDS were purchased from Sigma Chemical Co. (St. Louis, MO, USA). All other reagents used were of analytical grade. Abbreviations used for particular proteins are

Monomeric Banana Lectin at Acidic pH Overrules Conformational Stability of Its Native Dimeric Form

Javed M. Khan, Atiyatul Qadeer, Ejaz Ahmad, Raghib Ashraf, Bharat Bhushan, Sumit K. Chaturvedi, Gulam Rabbani, and Rizwan H. Khan*.

Interdisciplinary Biotechnology Unit, Aligarh Muslim University, Aligarh 202002, India

* To whom correspondence should be addressed: Tel.: +91 571 2720388; Fax: +91 571 2721776; E-mail: rizwanhkhan@hotmail.com

Keywords: Banana lectin; urea; molten globule; circular dichroism; stability; pH.

PLOS ONE

1-Anilino-8-Naphthalene Sulfonate (ANS) Is Not a Desirable Probe for Determining the Molten Globule State of Chymopapain

Atiyatul Qadeer, Gulam Rabbani, Nida Zaidi, Ejaz Ahmad, Javed M. Khan, Rizwan H. Khan*

Interdisciplinary Biotechnology Unit, Aligarh Muslim University, Aligarh, India

Abstract

The molten globule (MG) state of proteins is widely detected through binding with 1-anilino-8-naphthalene sulphonate (ANS), a fluorescent dye. This strategy is based upon the assumption that when in molten globule state, the exposed hydrophobic clusters of protein are readily bound by the nonpolar anilino-naphthalene moiety of ANS molecules which then produce brilliant fluorescence. In this work, we explored the acid-induced unfolding pathway of chymopapain, a cysteine proteases from *Carica papaya*, by monitoring the conformational changes over a pH range 1.0–7.4 by circular dichroism, intrinsic fluorescence, ANS binding, acrylamide quenching, isothermal titration calorimetry (ITC) and dynamic light scattering (DLS). The spectroscopic measurements showed that although maximum ANS fluorescence intensity was observed at pH 1.0, however protein exhibited ~80% loss of secondary structure which does not comply with the characteristics of a typical MG-state. In contrast at pH 1.5, chymopapain retains substantial amount of secondary structure, disrupted side chain interactions, increased hydrodynamic radii and nearly 30-fold increase in ANS fluorescence with respect to the native state, indicating that MG-state exists at pH 1.5 and not at pH 1.0. ITC measurements revealed that ANS molecules bound to chymopapain *via* hydrophobic interaction were more at pH 1.5 than at pH 1.0. However, a large number of ANS molecules were also involved in electrostatic interaction with protein at pH 1.0 which, together with hydrophobically interacted molecules, may be responsible for maximum ANS fluorescence. We conclude that maximum ANS-fluorescence alone may not be the criteria for determining the MG of chymopapain. Hence a comprehensive structural analysis of the intermediate is essentially required.

Citation: Qadeer A, Rabbani G, Zaidi N, Ahmad E, Khan JM, et al. (2012) 1-Anilino-8-Naphthalene Sulfonate (ANS) Is Not a Desirable Probe for Determining the Molten Globule State of Chymopapain. PLoS ONE 7(11): e50633. doi:10.1371/journal.pone.0050633

Editor: Eugene A. Permyakov, Russian Academy of Sciences, Institute for Biological Instrumentation, Russian Federation

Received September 6, 2012; **Accepted** October 23, 2012; **Published** November 29, 2012

Funding: Financial assistance to A. Qadeer, G. Rabbani, N. Zaidi, J.M. Khan and E. Ahmad in the form of a Senior Research Fellowship was supported by the Council of Scientific and Industrial Research (CSIR), New Delhi, India. R.H. Khan is an Associate Professor in A.M.U., Aligarh. No additional external funding was received for this study. The funders had no role in study design, data collection and analysis, decision to publish, or preparation of the manuscript.

Competing Interests: The authors have declared that no competing interests exist.

* E-mail: rizwanhkhan@hotmail.com

Introduction

The process of protein folding, despite being one of the most intensely investigated areas, remains obscure in terms of its detailed molecular mechanism. The spontaneity and extreme cooperativity of this process makes it a challenging task to unravel the entire mechanism mainly because of the inability to populate the distinct intermediate states that encompass the folding pathway of a nascent polypeptide [1–3]. Characterization of these intermediates is the key to unlock the step by step mechanism and to extend our knowledge on the principles governing protein folding [4,5].

In past, a lot of attention has been paid to molten globule (MG), an intermediate with feasible occurrence as a general physical state in the folding pathway of globular proteins [6–8]. The MG state generally corresponds to late folding intermediate and has been obtained for many proteins under different solvent conditions [9–12]. In order to be defined as a typical molten globule, an intermediate requires being a compact collapsed state with substantial amount of secondary structure, loose tertiary contacts without tight side chain packing and a solvent accessible hydrophobic core [13]. Conventionally, the exposed hydrophobic clusters of folding intermediates are detected through 1-anilino-8-naphthalene sulfonate (ANS) binding, a much utilized fluorescence probe for detecting the non-polar character of proteins and membranes [14]. In fact, the available literature reveals that molten globule state is mostly pinpointed from its maximum ANS binding ability under the conditions studied since the other typical features *viz* pronounced secondary structure and disrupted tertiary contacts often seem to merge with intermediates lying in the vicinity of MG-state [12,15–20]. Such utilization of ANS which is based upon the principle that ANS is practically non fluorescent in water but produces brilliant fluorescence upon binding to hydrophobic sites of protein [21] generally ignores the contribution of sulfonate group that was earlier considered as a mere solublizing agent for otherwise almost water-insoluble anilino-naphthalene moiety. However, the role of electrostatic interactions in ANS-protein interaction was highlighted later in the findings that ANS binding to proteins depends upon protein cationic charge and pH of the solution and occurs precisely through ion-pair formation between sulfonate group of ANS and side chains of Arg/Lys/His residues of polypeptide chain [22,23]. A more recent study has revealed that interaction of sulfonate group of ANS with charged centers of Arg and Lys residues resulted in enhanced

Interaction of Bovine Serum Albumin with Cationic Single Chain+Nonionic and Cationic Gemini+Nonionic Binary Surfactant Mixtures

Mohammad Amin Mir,[†] Nuzhat Gull,[†] Javeed Masood Khan,[‡] Rizwan Hasan Khan,[‡] Aijaz Ahmad Dar,[†] and Ghulam Mohammad Rather*[,†]

Department of Chemistry, University of Kashmir, Srinagar-190006, J&K, India, Interdisciplinary Biotechnology Unit, Aligarh Muslim University, Aligarh 202002, India

Received: September 17, 2009; Revised Manuscript Received: January 25, 2010

The interaction of bovine serum albumin (BSA) with cetyltrimethylammonium bromide (CTAB), $C_{16}C_4C_{16}Br_2$, Brij58, and their binary mixtures has been studied using tensiometry, spectrofluorometry, and circular dichroism at physiological pH and 25 °C. The tensiometric profiles of CTAB and $C_{16}C_4C_{16}Br_2$ in the presence of BSA exhibit a single break at a lower surfactant concentration termed as C_1 (concentration corresponding to saturation of the interface) compared to their critical micelle concentration (CMC) in the buffered solution. However, for Brij58, CTAB+Brij58, and $C_{16}C_4C_{16}Br_2$+Brij58, two breaks were observed, first at the critical aggregation concentraion (CAC), corresponding to onset of interaction with BSA and the second at C_1 corresponding to saturation of the interface. The interaction of CTAB+Brij58 and $C_{16}C_4C_{16}Br_2$+Brij58 mixtures with the BSA solution is discussed in terms of competition between surfactant−surfactant and surfactant−BSA interactions. CTAB+Brij58 and $C_{16}C_4C_{16}Br_2$+Brij58 mixtures show nonideality with respect to mixed micelle formation, which is reflected in their interaction with the BSA. The interaction of CTAB+Brij58 with BSA decreases with increase in the mole fraction of CTAB in the mixture, whereas in $C_{16}C_4C_{16}Br_2$+Brij58 the reverse is the case. The results of the present study may prove fruitful in optimizing the properties of surfactant−protein mixtures relevant for many formulations.

Introduction

Protein−surfactant interactions have been a subject of extensive studies because of their relevance to the field of pharmaceutics, paints and coatings, adhesives, oil recovery, and so forth.[1−4] Moreover, such studies can provide insight relevant to the solubilizing and denaturing[1,2,5] /renaturing[6−10] action of surfactants on proteins. Protein−surfactant interactions are usually dependent on the surfactant features. Compared to the anionics, cationic surfactants weakly interact with the proteins as a consequence of smaller relevance of electrostatic interactions at the pH of interest.[11] However, the binding isotherms of both types of surfactants have been found to be similar.[11,12] At low surfactant concentrations, ionic surfactants bind to the oppositely charged sites of proteins, causing them to unfold and expose more binding sites. As the surfactant concentration is increased, the binding becomes cooperative, and ultimately the protein is saturated by the surfactant and its aggregates.[2] Compared to ionics, nonionic surfactants bind weakly to the proteins due to the absence of electrostatic interactions, thus making micelle formation in bulk more favorable.[1,13] For general aspects of interactions between ionic surfactants and water-soluble proteins, sodium dodecyl sulfate (SDS) and bovine serum albumin (BSA) have been oftenly used as a representative system.[14] The interaction of proteins with the surfactant molecules can change the conformation of proteins in the bulk[1,2,15,16] and at the interface.[17−20] Therefore, understanding of interaction between the surfactants and proteins in the bulk and at the interface, formation of protein−surfactant complexes and displacement of protein molecules from the interface by surfactant molecules is important from scientific as well as practical viewpoints. A number of papers deal with the theoretical and experimental studies on the adsorption behavior of protein surfactant mixtures,[17−38] and different mechanisms for the displacement of protein molecules from the interface by the surfactants have been suggested such as orogenic displacement[35] or competitive adsorption.[38]

Recent investigations[39−44] on the interaction of cationic gemini surfactants with proteins have revealed that such surfactants interact more efficiently with proteins as compared to conventional single chain surfactants because of their unique aggregation properties such as lower critical micelle concentration (CMC) and kraft temperature, special aggregation morphology, strong hydrophobic microdomains, and so forth.[45−48] Cationic surfactants, being antimicrobial, have attracted attention with respect to their interaction with deoxyribonucleic acid (DNA) and lipids.[49] Surfactant mixtures exhibit a wide range of properties and are known to perform better than their individual components[50,51] making them important for technological, pharmaceutical, and biological fields. However, little attention[52] has been paid toward their interaction with proteins. Recently, Lu et al.[52] reported very weak interaction of mixed cationic−anionic (decyltriethylammonium bromide + sodium decylsulfonate) surfactants with the BSA due to the strong synergism in mixed micelle formation between the cationic and anionic surfactants in aqueous solutions.

In this paper, we report the results of interaction of BSA with some cationic+nonionic mixed surfactants at 25 °C and physiological pH, employing tensiometry, spectrofluorometry, and circular dichroism (CD). A conventional cationic single chain surfactant, cetyltrimethylammonium bromide (CTAB), its gemini homologue, bis(cetyldimethylammonium)butane dibromide

* To whom correspondence should be addressed. E-mail: gmrather2002@yahoo.com.
† University of Kashmir.
‡ Aligarh Muslim University.

10.1021/jp908985v
Published on Web 02/11/2010

THE JOURNAL OF PHYSICAL CHEMISTRY B

Article

pubs.acs.org/JPCB

Interaction of Cetyltrimethylammonium Bromide and Its Gemini Homologue Bis(cetyldimethylammonium)butane Dibromide with Xanthine Oxidase

Mohammad Amin Mir,[†,§] Javed Masood Khan,[‡] Rizwan Hasan Khan,[‡] Aijaz Ahmad Dar,*[,†] and Ghulam Mohammad Rather*[,†]

[†]Department of Chemistry, University of Kashmir, Srinagar 190006, J&K, India

[‡]Interdisciplinary Biotechnology Unit, Aligarh Muslim University, Aligarh 202002, India

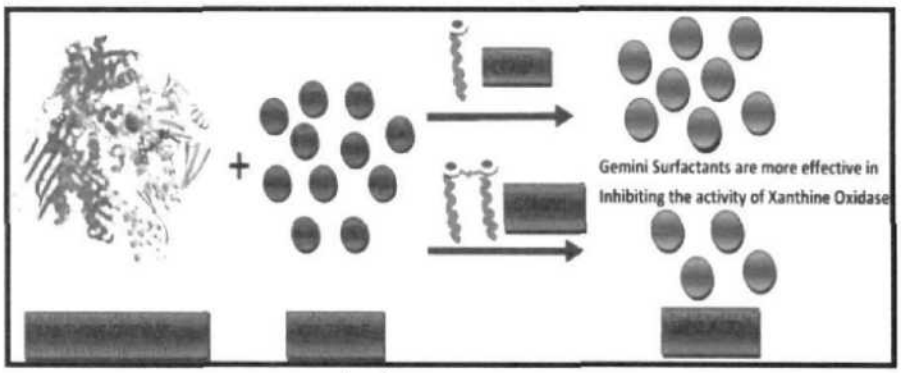

ABSTRACT: The interaction of xanthine oxidase (XO), a key enzyme in purine metabolism, with cetyltrimethylammonium bromide (CTAB) and bis(cetyldimethylammonium)butane dibromide ($C_{16}C_4C_{16}Br_2$) has been studied using tensiometry, spectrofluorometry, spectrophotometry, and circular dichroism at pH 7.4 and 25 °C. The tensiometric profiles of CTAB and $C_{16}C_4C_{16}Br_2$ in the presence of XO exhibit a single break at a lower surfactant concentration termed as C_1 compared to their CMC in the buffered solution and show the existence of interaction between the surfactants and the enzyme. The results of the multitechnique approach showed that, although both CTAB as well as $C_{16}C_4C_{16}Br_2$ interact with the XO, $C_{16}C_4C_{16}Br_2$ interacts more strongly than its conventional single chain counterpart. Fluorescence and absorption measurements revealed that, compared to CTAB, $C_{16}C_4C_{16}Br_2$ is more effective in unfolding the enzyme. Change in XO activity by the surfactants was in concurrence with the structural alterations monitored by circular dichroism and showed structural stabilization of XO at higher surfactant concentrations, consistent with the aggregation results. This stabilization has been explained in light of strong tendency of $C_{16}C_4C_{16}Br_2$ for micellar growth and membrane/water stabilization of proteins by membrane-like fragments provided by higher concentrations of $C_{16}C_4C_{16}Br_2$. The results are related to the stronger electrostatic and hydrophobic forces in $C_{16}C_4C_{16}Br_2$, owing to the presence of two charged headgroups and two hydrophobic tails.

■ INTRODUCTION

The interaction of proteins with surfactants has received a great deal of interest for many years due to its application in a variety of industrial, biological, cosmetic, pharmaceutical, and food processing systems.[1−4] The binding of surfactants with proteins is usually determined by the surfactant features. It is known in general that, compared to anionic surfactants, cationic surfactants interact weakly with the proteins as a consequence of smaller relevance of electrostatic interactions at the pHs of interest.[5] However, the shapes of binding isotherms of these two kinds of surfactants with the same protein have been found to be similar[5,6] and are well studied.[7] Initially, at low surfactant concentrations, ionic surfactants bind noncooperatively to the oppositely charged high energy sites of proteins thereby unfolding the protein. As the surfactant concentration is increased, the binding becomes cooperative, and ultimately, the protein is saturated by the surfactant and its aggregates.[2]

Xanthine oxidase (XO), a complex molybdoflavo protein, is a key enzyme in purine metabolism that has attracted lots of attention because of its potential role in tissue and vascular injuries, as well as in inflammatory diseases and chronic heart failure.[8,9] It catalyzes the oxidation of hypoxanthine to xanthine and that of xanthine to uric acid with concomitant reduction of molecular oxygen.[10] This last step results in the production of superoxide anion and hydrogen peroxide, two reactive oxygen species that have been associated with the potential damaging role of the enzyme.[9−11] The enzyme is a homodimer, each monomer is composed of an N-terminal domain containing two iron−sulfur centers (Fe/S I and Fe/S II), a central flavin adenine dinucleotide (FAD) domain, and a C-terminal

Received: August 14, 2011
Revised: April 23, 2012
Published: April 24, 2012

dx.doi.org/10.1021/jp207803c | J. Phys. Chem. B 2012, 116, 5711−5718

Journal of Colloid and Interface Science 364 (2011) 157–162

Contents lists available at SciVerse ScienceDirect

Journal of Colloid and Interface Science

www.elsevier.com/locate/jcis

Refolding of bovine serum albumin via artificial chaperone protocol using gemini surfactants

Nuzhat Gull [a], Mohammad Amin Mir [a], Javed Masood Khan [b], Rizwan Hassan Khan [b], Ghulam Mohammad Rather [a,*], Aijaz Ahmad Dar [a,*]

[a] Department of Chemistry, University of Kashmir, Hazratbal, J&K, Srinagar 190 006, India
[b] Interdisciplinary Biotechnology Unit, Aligarh Muslim University, Aligarh 202 002, India

ARTICLE INFO

Article history:
Received 21 April 2011
Accepted 3 August 2011
Available online 11 August 2011

Keywords:
Gemini surfactant
Artificial chaperone
Bovine serum albumin
Circular dichroism
Dynamic light scattering
Intrinsic fluorescence
Extrinsic fluorescence

ABSTRACT

Surfactants prevent the irreversible aggregation of partially refolded proteins, and they are also known to assist in protein refolding. A novel approach to protein refolding that utilizes a pair of low molecular weight folding assistants, a detergent and cyclodextrin, was proposed by Rozema and Gellman (D. Rozema, S.H. Gellman, J. Am. Chem. Soc. 117 (1995) 2373). We report the refolding of bovine serum albumin (BSA) assisted by these artificial chaperones, utilizing gemini surfactants for the first time. A combination of cationic gemini surfactants, bis(cetyldimethylammonium)pentane dibromide ($C_{16}H_{33}(CH_3)_2N^+$–$(CH_2)_5$–$N^+(CH_3)_2C_{16}H_{33}\cdot 2Br^-$ designated as G5 and bis(cetyldimethylammonium)hexane dibromide ($C_{16}H_{33}(CH_3)_2N^+$–$(CH_2)_6$–$N^+(CH_3)_2C_{16}H_{33}\cdot 2Br^-$ designated as G6 and cyclodextrins, was used to refold guanidinium chloride (GdCl) denatured BSA in the artificial chaperone assisted two step method. The single chain cationic surfactant cetyltrimethylammonium bromide (CTAB) was used for comparative studies. The studies were carried out in an aqueous medium at pH 7.0 using circular dichroism, dynamic light scattering and ANS binding studies. The denatured BSA was found to get refolded by very small concentrations of gemini surfactant at which the single chain counterpart was found to be ineffective. Different from the single chain surfactant, the gemini surfactants exhibit much stronger electrostatic and hydrophobic interactions with the protein and are thus effective at much lower concentrations. Based on the present study it is expected that gemini surfactants may prove useful in the protein refolding operations and may thus be effectively employed to circumvent the problem of misfolding and aggregation.

1. Introduction

Refolding of the denatured proteins has been an important issue at the fundamental as well as the biotechnological level. The rising interest in the protein refolding process stems from the fact that the proteins overproduced by genetically engineered cells are often obtained in non-native forms, and the use of such proteins for basic research and biotechnological applications require that the native conformation be achieved [1,2].

Misfolding and aggregation pose a serious problem in the industrial production of recombinant proteins [3,4]. Aggregation may be due to the association of hydrophobic surfaces that are exposed during refolding process [5,6]. An approach for controlling the competition between renaturation and aggregation, using "Artificial chaperones" involving the sequential addition of a detergent and cyclodextrin to the denatured protein was described by Rozema and Gellman [7,8]. Chaperone proteins help to keep a protein in proper conformation by complex formation with folded protein [9–14].

Though the cationic single-chain surfactants have been tested as the refolding agents in the artificial chaperone protocol [7], there is no report of the use of gemini surfactants [15] which consist of two identical amphiphilic moieties covalently linked by a spacer group at or near the ionic head group. Gemini surfactants have stimulated considerable interest because of their unique aggregation properties like low Kraft temperature, low cmc, strong hydrophobic microdomain [16,17]. Referred to as second-generation surfactants, the geminis have shown promise in various potential areas of surfactant application showing stronger surface activity and better solubility, wetting, foaming, and lime soap dispersion capability. They can be orders of magnitude more surface active than the conventional single chain counterparts [18].

Abbreviations: BSA, bovine serum albumin; CTAB, cetyltrimethylammonium bromide; G5, bis(cetyldimethylammonium)pentane dibromide; G6, bis(cetyldimethylammonium)hexane dibromide; ANS, 1-anilino-8-naphthalenesulphonate; CD, *circular dichroism; DLS, dynamic light scattering.*

* Corresponding authors.
E-mail addresses: gmrather2002@yahoo.com (G.M. Rather), aijaz_n5@yahoo.co.in (A.A. Dar).

0021-9797/$ - see front matter © 2011 Elsevier Inc. All rights reserved.
doi:10.1016/j.jcis.2011.08.015

Journal of Colloid and Interface Science 352 (2010) 436–443

Contents lists available at ScienceDirect

Journal of Colloid and Interface Science

www.elsevier.com/locate/jcis

Unfolding of rabbit serum albumin by cationic surfactants: Surface tensiometry, small-angle neutron scattering, intrinsic fluorescence, resonance Rayleigh scattering and circular dichroism studies

Mohd. Sajid Ali [a], Nuzhat Gull [b], Javed M. Khan [c], Vinod K. Aswal [d], Rizwan H. Khan [c], Kabir-ud-Din [a,*]

[a] Department of Chemistry, Aligarh Muslim University, Aligarh 202 002, India
[b] Department of Chemistry, Kashmir University, Hazratbal, Srinagar 190 006, India
[c] Interdisciplinary Biotechnology Unit, Aligarh Muslim University, Aligarh 202 002, India
[d] Solid State Physics Division, Bhabha Atomic Research Centre, Mumbai 400 085, India

ARTICLE INFO

Article history:
Received 22 May 2010
Accepted 27 August 2010
Available online 22 September 2010

Keywords:
Rabbit serum albumin
Surfactant
Protein–surfactant interaction
Rayleigh scattering
SANS
CD
Fluorescence

ABSTRACT

Unfolding of rabbit serum albumin (RSA) by cationic surfactants cetyltrimethylammonium bromide (CTAB) and tetradecyltrimethylammonium bromide (TTAB) was studied by exploiting surface tensiometry, small-angle neutron scattering (SANS), intrinsic fluorescence, resonance Rayleigh scattering (RRS) (also referred as turbidity at 350/350), and circular dichroism (CD) techniques. Surface tension measurements revealed the formation of highly surface-active complexes occurring as a consequence of RSA–surfactants interactions. SANS measurements show that, in the low surfactant concentration regime (0–10 mM), increase in the dimension of the ellipsoidal protein occurs. Conversely, at higher concentrations (20–80 mM), the surfactant molecules result in the formation of a fractal structure representing a 'necklace model' of micelle-like clusters randomly distributed along the polypeptide chain. The overall size of the complex increases and the fractal dimension decreases on increasing the surfactant concentration. The size of the micelle-like clusters decreases while the number of such clusters and their aggregation number increase with increasing CTAB concentration. Taken all observant together, the fluorescence, RRS, and CD studies were found to be consistent with the SANS measurements. Both CTAB and TTAB were found to behave likewise and the effect of hydrophobicity was clearly visible in the CD, RRS, and intrinsic fluorescence results. The Rayleigh scattering study shows that TTAB was more skilled to solubilize the serum albumin and may be more convenient than CTAB to isolate proteins from inclusion bodies.

1. Introduction

Serum albumins are the most widely investigated globular proteins. The albumin molecule is made of three homologous, predominantly helical evolutionary related domains. Each domain is made up of two sub-domains [1] and the sub-domains share a number of common features, like a hydrophobic face, a cluster of basic amino acid residues, and protein residues at tops of long loops. Also, each sub-domain is unique and exhibits a certain degree of binding specificity [2–4]. Due to the hydrophobic and hydrophilic properties of the amino acids, a protein exhibits dualism that makes small amphiphilic molecules interact with proteins. The amphiphilic molecules chosen to study the protein–surfactant complexes, in general, are the ionic surfactants in view of their application in the area of membrane studies [5,6]. Further, protein–surfactant interactions are of importance in a wide variety of industrial, biological, pharmaceutical, drug delivery and cosmetic systems too [7–10].

Usually, surfactant binding with proteins depends on the features of the former. Both the ionic surfactants and proteins in aqueous solution share the common property of having charged groups and hydrophobic portions. It is believed that in a system consisting of these two components, surfactant molecules at low concentrations undergo electrostatic binding to the protein, whereas above critical aggregation concentration hydrophobic interaction amongst surfactant molecules takes over the binding process [10]. Understanding the behavior of such protein-surfactant complexes is of vital interest and allows to gain insight into the binding mechanism between the two components and its effect on the protein structure and function in the complex. In most of such studies, the surfactants have typically been anionic (because their interactions with proteins are stronger as compared to the cationic ones) [10,11]. In a recent study [12] we had reported the interaction of a cationic gemini and its monomeric counterpart CTAB at low surfactant concentrations (which is a common practice for studying protein–surfactant interactions) wherein the conformational changes and saturation

* Corresponding author. Fax: +91 571 2708336.
E-mail address: kabir7@rediffmail.com (Kabir-ud-Din).

0021-9797/$ - see front matter © 2010 Elsevier Inc. All rights reserved.
doi:10.1016/j.jcis.2010.08.073

International Journal of Biological Macromolecules 44 (2009) 163–169

Contents lists available at ScienceDirect

International Journal of Biological Macromolecules

journal homepage: www.elsevier.com/locate/ijbiomac

How methyl cyanide induces aggregation in all-alpha proteins: A case study in four albumins

Priyankar Sen, Sadaf Fatima, Javed Masood Khan, Rizwan Hasan Khan*

Interdisciplinary Biotechnology Unit, Aligarh Muslim University, Aligarh 202002, India

ARTICLE INFO

Article history:
Received 20 August 2008
Received in revised form
22 November 2008
Accepted 24 November 2008
Available online 30 November 2008

Keywords:
Aggregation
Circular dichroism
Infrared spectroscopy
Tryptophan fluorescence
Serum albumins

ABSTRACT

Serum albumins are chief carrier of ligands in blood, hence important in clinical biotechnology. The effects of methyl cyanide (MeCN), a chief solvent of reverse phase chromatography, on four mammalian serum albumins (human, bovine, porcine and rabbit sources) were studied at neutral pH with the help of scattering, circular dichroism, IR and fluorescence spectroscopy. We have detected an intermediate state in the presence of 20% (v/v) MeCN, having 8–9% higher α-helical structure than that of their native states. In the presence of 60% (v/v) MeCN another intermediate was observed with non-native β-sheet structure and high tendency to form aggregates.

1. Introduction

The alpha helix to beta sheet transition of proteins is a key issue for understanding the folding and biological function of a number of proteins [1–7]. For example, α to β transitions have been suggested in various conformational diseases, such as prion disease or Alzheimer's where normal protein turn from alpha helix to beta sheet to be amyloidogenic [3–5]. Aggregation is thought to be a reversible process of self association of several identical protein molecules driven by stereo-specific intermolecular contacts [8]. Proteins with different types of structures; like, α-helical (apolipoprotein A1 [9,10], prion (PrP^C) [11]) β-sheet (crystallins [12], transthyretin [9,10]), α + β (lysozyme and gelsolin [9,10]), α/β (cystic fibrosis trans-membrane regulator [13]) or natively unfolded (Aβ peptide and tau [14]); single-domain or multi-domain, etc., can aggregate [15].

In several pathological disorders and in various *in vitro* experiments, proteins also turn into "amorphous aggregates", without local order [16]. Protein aggregation mechanism and their extent depend on the physical and chemical environment such as pH, ionic strength, denaturant addition, etc. For stabilizing non-native states of protein, it is modulated either by site directed mutagenesis or by solvent engineering. Non-polar solvents like alcohols and MeCN exert several distinct effects on protein. Alcohols denature the tertiary and quaternary structures of several proteins while enhancing their helicity [17]. On the other hand, MeCN induces or enhances beta sheet in some proteins [18]. In alcohols and other cosolvents, the non-polar groups of proteins tend to get interact with hydrophobic regions of the cosolvents, thus decreasing the environmental polarity around the polypeptide which in turn favors the formation of hydrogen bonds resulting in helical structure [19,20]. In contrast, MeCN induces beta sheet, due to its higher polarity than alcohols in water, which provides a favorable environment for the formation of intermolecular beta sheets [21–24].

Serum albumins (~66.5 kDa), the most abundant carrier proteins in blood, are single chain polypeptides, having three homologous domains. They are amongst the most studied proteins and have a typical physiological concentration of 5 g/100 ml in human. It is the principle carrier of fatty acids, which are otherwise insoluble in circulating plasma. Albumins are predominantly alpha helical with the remaining polypeptide occurring in turns and extended or flexible regions between sub-domains, with no beta sheet.

A lot of work has been done to understand the effect of alcohols on various proteins and the degree of formation of alpha helix in them [25,26]. However, relatively much less work has been done to understand the effect of MeCN on a predominantly alpha helical model protein, like albumin. We have taken serum albumins from four different mammalian sources, i.e., human, bovine, porcine and

Abbreviations: a.u., arbitrary unit; BSA, bovine serum albumin; HSA, human serum albumin; IR, infra-red; MeCN, methyl cyanide; MRE, mean residue ellipticity; PSA, porcine serum albumin; RFI, relative fluorescence intensity; RSA, rabbit serum albumin; UV-CD, ultra-violet circular dichroism.

* Corresponding author. Tel.: +91 571 2720388; fax: +91 571 2721776.
E-mail addresses: rizwanhkhan@hotmail.com, rizwanhkhan1@yahoo.com (R.H. Khan).

0141-8130/$ – see front matter © 2008 Elsevier B.V. All rights reserved.
doi:10.1016/j.ijbiomac.2008.11.008

Colloids and Surfaces B: Biointerfaces 77 (2010) 54–59

Contents lists available at ScienceDirect

Colloids and Surfaces B: Biointerfaces

journal homepage: www.elsevier.com/locate/colsurfb

Effect of spacer length of alkanediyl-α,ω-bis(dimethylcetylammonium bromide) gemini homologues on the interfacial and physicochemical properties of BSA

Mohammad Amin Mir[a], Javeed Masood Khan[b], Rizwan Hasan Khan[b], Ghulam Mohammad Rather[a], Aijaz Ahmad Dar[a,*]

[a] Department of Chemistry, University of Kashmir, Srinagar 190006, J&K, India
[b] Interdisciplinary Biotechnology Unit, Aligarh Muslim University, Aligarh 202002, India

ARTICLE INFO

Article history:
Received 26 September 2009
Received in revised form 4 January 2010
Accepted 7 January 2010
Available online 14 January 2010

Keywords:
BSA
Interfacial tension
Circular dichroism
Gemini surfactant
Denaturation

ABSTRACT

The interactions of bovine serum albumin (BSA) with cationic gemini surfactants alkanediyl-α,ω-bis(dimethylcetylammonium bromide) (designated as $C_{16}C_sC_{16}Br_2$, s=4, 5, and 6) and single chain surfactant cetyltrimethylammonium bromide (CTAB) have been investigated with tensiometry, Rayleigh's scattering, fluorescence spectroscopy, and circular dichroism at physiological pH and 25 °C. The results of the multi-technique approach showed that the gemini surfactants interact more efficiently with the proteins than their conventional single chain counterparts and their efficiency increases with decrease in the length of the spacer. The saturation in interfacial tension occurred at a lower concentration in presence of BSA compared to CMC of the surfactants in absence of BSA and the concentration of gemini surfactants corresponding to interfacial saturation decreases with decrease in the spacer length. Fluorescence and circular dichroism spectroscopy results revealed increase in unfolding of BSA with decrease in spacer length of gemini surfactants.

1. Introduction

Protein–surfactant interactions have been a subject of extensive studies because of its relevance to the field of pharmaceutics, paints and coatings, adhesives, oil recovery, etc. [1–8]. Moreover, such studies can provide insight relevant to the solubilizing and denaturing/renaturing action of surfactants on proteins. Protein–surfactant interactions are usually dependent on the surfactant features. Compared to anionic surfactants, cationic surfactants weakly interact with the proteins as a consequence of smaller relevance of electrostatic interactions at the pHs of the interest [9–14]. However, the binding isotherms of both types of surfactants have been found to be similar [14,15]. At low surfactant concentrations ionic surfactants bound to the oppositely charged sites of proteins which cause the protein to unfold resulting in the exposure of more binding sites. As the surfactant concentration is increased the binding becomes cooperative and ultimately the protein is saturated by the surfactants and their aggregates [16].

Cationic gemini surfactants are made up of two hydrophobic chains and two polar head groups covalently linked through a spacer group [17–20]. These kinds of surfactants have number of unique aggregation properties such as lower CMC and kraft temperature, special aggregation morphology, strong hydrophobic microdomains, etc. [21–24]. Because of these unique properties gemini surfactants strongly interact with the proteins [25–30] compared to conventional ones. The unusual properties of aggregates of gemini surfactants are related to spacer structure because it influences the distances between head groups in the aggregate [31]. In aggregates formed by conventional surfactants, the only distance is the thermodynamic distance between polar head groups, whereas in aggregates formed by gemini, two head group distance control the aggregation properties (bimodal distribution), one corresponding to the single chain surfactant equilibrium distance and one corresponding to the length and nature of the spacer [32]. Various applications of the gemini surfactants relevant to the surfactant–protein interactions viz., antimicrobial, hair conditioning, skin and eye care, etc., are important over the other conventional surfactants [33,34]. The effectiveness of gemini surfactants depends upon the length and type of spacer, and the hydrophobic counterpart. In spite of that, the effect of spacer length of the gemini surfactant on the surfactant–protein interaction has not been given the due attention. Although, Li et al. [25] studied the interaction of BSA with short alkyl chain DTAB and its gemini homologues ($C_{12}C_sC_{12}Br_2$, where s=3, 6, 12) but due to the large differences and lack of continuity in the spacer lengths, a critical analysis escaped.

We hereby report the interaction of BSA with long alkyl chain CTAB and its gemini homologues ($C_{16}C_sC_{16}Br_2$, where s=4, 5, 6)

* Corresponding author.
E-mail address: aijaz.n5@yahoo.co.in (A.A. Dar).

0927-7765/$ – see front matter © 2010 Elsevier B.V. All rights reserved.
doi:10.1016/j.colsurfb.2010.01.005

Colloids and Surfaces B: Biointerfaces 80 (2010) 169–175

Contents lists available at ScienceDirect

Colloids and Surfaces B: Biointerfaces

journal homepage: www.elsevier.com/locate/colsurfb

Multi-technique approach on the effect of surfactant concentrations on the thermal unfolding of rabbit serum albumin: Formation and solubilization of the protein aggregates

Mohd. Sajid Ali[a], Javed M. Khan[b], Vinod K. Aswal[c], Rizwan H. Khan[b], Kabir-ud-Din[a,*]

[a] Department of Chemistry, Aligarh Muslim University, Aligarh 202002, Uttar Pradesh, India
[b] Interdisciplinary Biotechnology Unit, Aligarh Muslim University, Aligarh 202002, Uttar Pradesh, India
[c] Solid State Physics Division, Bhabha Atomic Research Centre, Mumbai 400085, India

ARTICLE INFO

Article history:
Received 30 January 2010
Received in revised form 28 May 2010
Accepted 28 May 2010
Available online 15 June 2010

Keywords:
Serum albumin
Surfactant
Thermal denaturation
Protein aggregation

ABSTRACT

Effect of cationic surfactant, cetyltrimethylammonium bromide (CTAB) addition on the thermal denaturation of rabbit serum albumin (RSA) has been studied by employing small-angle neutron scattering (SANS), circular dichroism (CD), intrinsic fluorescence and ultra violet (UV) spectroscopy. The studies were performed at three different temperatures viz., 30, 50 and 70 °C and at two different concentrations of CTAB: the low concentration of CTAB used was 1 mM and the higher concentration was 80 mM (for SANS) and 20 mM (for CD, fluorescence and UV). A collective effect of high temperature and low concentration of CTAB led to the protein aggregation followed by solubilization of these aggregates at higher concentration of surfactant. At 1 mM CTAB and 30 °C, the protein–surfactant complex has a prolate ellipsoidal shape with semi-major axis of 88.9 Å and semi-minor axis of 19.6 Å which are slightly greater than the values of the native RSA. At 50 °C, the size of the semi-major axis increases while at 70 °C an increase in the size of both axes was found. The thermal outcome at higher concentration of CTAB (80 mM) was rather different. Higher concentration of CTAB unfolds the protein by the formation of micelle-like aggregates along the polypeptide chains of the protein and the complex was stabilized at higher temperatures, which was not found with lower concentration of CTAB. The CD results were found to be consistent with the SANS results, i.e., decrease in α-helicity of RSA was more when less amount of surfactant was present as compared to the system with higher surfactant concentration. In a similar fashion, results of relative fluorescence intensity (RFI) reveal that increase in temperature causes decrease in λ_{max} of native RSA as well as RSA + 1 mM CTAB, whereas the λ_{max} remains unchanged for RSA + 20 mM CTAB systems. That means the structure remains compact in presence of 20 mM CTAB while the structure becomes loose when low or zero amount of surfactant was present. The UV results indicate that the protein aggregation takes place in presence of low amount of CTAB and these aggregates become soluble at high concentration of CTAB.

1. Introduction

Proteins arrange themselves with astonishing exactitude to carry out various biological functions with other molecules. Proteins acquire and preserve a particular well-defined three dimensional structure to perform specific biological tasks [1,2]. This ordered state of the protein is called as the native or folded state. The delicate balance of forces between the protein's interactions with itself and its interactions with its environment keeps the protein folded [2]. When this environment becomes denaturing, this stability is disrupted and the protein unfolds. Protein denaturation is sometimes useful as it plays an important role in conferring specificity to protein translocation and degradation in the cell [3]. However, the unfolding of a protein may lead to terrible effects on biological functions. Protein unfolding or denaturation may be defined as a process whereby the spatial arrangement of the polypeptide chains within the molecule change from that of the native protein to a more disordered one [3]. Unfolding can be provoked by a range of external stimulants such as alteration in pH, temperature and pressure or even through the addition of a denaturing agent. Protein unfolding results in the disruption of H-bonds, disulphide bonds, and hydrophobic interactions, directing to its consecutive modification of quaternary, tertiary, and secondary structures.

Temperature is regarded as a perturbing agent of the equilibrium between different conformational species in proteins [4,5].

* Corresponding author. Tel.: +91 5712703515.
E-mail address: kabir7@rediffmail.com (Kabir-ud-Din).

0927-7765/$ – see front matter © 2010 Elsevier B.V. All rights reserved.
doi:10.1016/j.colsurfb.2010.05.044

Colloids and Surfaces B: Biointerfaces 82 (2011) 258–262

Contents lists available at ScienceDirect

Colloids and Surfaces B: Biointerfaces

journal homepage: www.elsevier.com/locate/colsurfb

Short communication

Complexation behavior of gelatin with amphiphilic drug imipramine hydrochloride as studied by conductimetry, surface tensiometry and circular dichroism studies

Mohd. Sajid Ali[a], Kahkashan Anjum[a], Javed M. Khan[b], Rizwan H. Khan[b], Kabir-ud-Din[a,*]

[a] Department of Chemistry, Aligarh Muslim University, Aligarh 202002, India
[b] Interdisciplinary Biotechnology Unit, Aligarh Muslim University, Aligarh 202002, India

ARTICLE INFO

Article history:
Received 28 May 2010
Accepted 28 August 2010
Available online 8 September 2010

Keywords:
Gelatin
Imipramine hydrochloride
Critical aggregation concentration
Polymer saturation point

ABSTRACT

Herein we report our studies carried out on the interaction between IMP and gelatin in aqueous medium at 25 C using conductimetry, surface tensiometry and circular dichroism (CD) techniques. Both surface tensiometry and conductimetry results indicate that the drug interacts with the gelatin in a surfactant-like manner, i.e., both critical aggregation (cac) and polymer saturation points (psp) were observed. The interaction starts with the formation of a highly surface-active complex as revealed by the lowering of surface tension on the addition of drug to the macromolecule. The decrease in cac on increasing gelatin concentration is an indication of the strong interaction between gelatin and IMP. However, at low concentration of gelatin the interaction was not much strong as exposed by surface tension study, i.e., the cac was not very clear (as with higher gelatin concentrations). As usual, the psp increased on increasing the gelatin concentration and was always higher than the critical micelle concentration of the drug in pure aqueous medium. Using CD measurements the influence of IMP on the secondary structure of gelatin in aqueous solutions was also investigated. CD studies (performed at very low drug concentrations) illustrated that the random coil content of gelatin increases with increasing drug concentration. Free energies of aggregation (ΔG_{agg}) and micellization (ΔG_{mic}) were computed with the help of degrees of micelle ionization obtained from the specific conductivity – [IMP] plots.

1. Introduction

Macromolecules at interfaces are vital because of both their useful applications and fundamental properties. For example, the adsorption of polymers onto colloid surfaces plays a critical task in the stabilization of emulsions in various industries [1]. Furthermore, biopolymers frequently have disordered hydrophobic and hydrophilic sequences that make them quite interesting [2]. Gelatin is a polypeptide that is obtained from collagen by breaking the triple-helix structure of collagen and comprising all 20 amino acid residues such as glycine, proline, glutamic acid, aspartic acid, lysine, arginine, etc., in different proportions [3]. The lysine and arginine groups comprise about 7.5% of the residues and are positively charged. Glutamic and aspartic acids, constituting about 12.5% of the residues, gives the negative nature to the chain. Another 6% of the residues are strongly hydrophobic in nature leaving 58% of the chain to be neutral. Several pharmaceutical applications of gelatin have already been reported (either alone or in support of any other polymer) in the form of hydrogels in drug delivery technology [4–6]. Interactions of ionic surfactants with gelatin have been widely studied and are very much important for photographic and food industries and in drug delivery too [7–14]. Gelatin is a denatured protein and does not interact with surfactants as the folded proteins do [10]. Rather it interacts in a simple polymer-like manner, i.e., the existence of critical aggregation concentration (cac) and critical micelle concentration (cmc) or polymer saturation point (psp). cac, the onset of aggregation, is either near or well below the cmc of pure surfactant while the psp is assigned to the saturation of polymer domains by the monomers and/or micelle-like aggregates [15]. Above the psp, formation of normal micelles takes place. Both hydrophobic and electrostatic forces play an important role in the interaction of polymers and surfactants when both the entities are ionic in nature.

Like surfactants, a variety of drugs exhibit amphiphilic character and comprise a propensity to form aggregates above a critical concentration [16]. The drugs belonging to tricyclic antidepressant (TCA) category, such as imipramine hydrochloride (IMP) (Fig. 1), display such a behavior. Studies show that overdose of TCAs may be harmful; therefore, their controlled release is necessary [17]. A large number of polymers are being used in controlled release for-

* Corresponding author. Tel.: +91 571 2703515; fax: +91 571 2708336.
E-mail address: kabir7@rediffmail.com (Kabir-ud-Din).

0927-7765/$ – see front matter © 2010 Elsevier B.V. All rights reserved.
doi:10.1016/j.colsurfb.2010.08.043

Biosci. Rep. (2010) / 30 / 125–134 (Printed in Great Britain) / doi 10.1042/BSR20090035

Bioscience Reports

Phytolacca americana lectin (Pa-2; pokeweed mitogen): an intrinsically unordered protein and its conversion into partial order at low pH

Ejaz AHMAD, Shah KAMRANUR RAHMAN, Javed MASOOD KHAN, Ankita VARSHNEY and Rizwan HASAN KHAN[1]

Interdisciplinary Biotechnology Unit, Aligarh Muslim University, Aligarh 202002, India

Synopsis

This is the first report of its kind that well demonstrates that a lectin from *Phytolacca americana* [Pa-2 (*P. americana* lectin-2)] can also be intrinsically unordered, based on the results obtained by CD, tryptophan fluorescence, ANS (8-anilinonaphthalene-1-sulfonic acid) binding, acrylamide quenching, DLS (dynamic light scattering) and its amino acid composition database analyses. Pa-2 is an acidic monomeric lectin and acquires random coil conformation at neutral pH without any regular secondary structure. As confirmed by different spectroscopic techniques, on lowering the pH, some secondary structures, predominantly α-helices, are detected by far-UV CD that adopt a marginally stable partially folded collapsed conformation possessing the characteristics of a premolten globule state. It is in accordance with coil–helix transition that is commonly observed when these intrinsically unordered proteins interact with their partner molecules *in vivo*.

Key words: CD, dynamic light scattering, hydropathy, intrinsically unordered protein, premolten globule state

INTRODUCTION

The complete programme of native conformation is locked in the primary sequence of a polypeptide chain and native conformation of a protein is the structure with lowest total free energy state. The process of minimizing free energy may not be obligatory, as some portions of a molecule may be folded in such a manner as to be favoured kinetically, but actually not yielding the lowest free energy. Native protein or its functional regions can exist in any one of the four thermodynamic states: ordered forms, molten globules, premolten globules and unordered random coils. In this view, a particular function can depend on any one of these states [1]. Besides, it has already been discovered that in protein some non-structured segments play an important role in its crucial function. Therefore those proteins that are functional and natively have any other conformation than the regular ordered one are known as IUP [intrinsically unordered protein; also known as IDP (intrinsically disordered protein) or NUP (natively unfolded protein)].

In recapitulation, absolute denaturation of an ordered protein leads to an unordered random coil. Moreover, during this denaturation pathway, a transient intermediate or a partially unfolded state, between ordered and denatured random coil states, is observed. This intermediate exhibits side chains with motional characteristics more like those of the random coil but with a backbone secondary structure like that of the ordered state. Ptitsyn and Uversky [2] termed it 'molten globule', which represents a third thermodynamically stable and functional state for proteins. Hence, the classical structure–function paradigm that protein should be ordered in order to be biologically active should go.

Broadly speaking, there are ten methods, in practice, to characterize intrinsic disorderness of a given sequence [3]. One is N^{15}-H^1 heteronuclear NOE (nuclear Overhauser effect) data analysis, where an amino acid sequence gives positive values for ordered regions due to slower tumbling and negative values for disordered regions because of more rapid tumbling [4]. Also from protein structures determined by X-ray crystallography, disorderness at any region in the sequence leads to missing

Abbreviations used: ANS, 8-anilinonaphthalene-1-sulfonic acid; DLS, dynamic light scattering; f_H, average fractional helicity; GdmCl, guanidinium chloride; GRAVY, grand average of hydropathicity; $<H>$, mean normalized hydrophobicity; $<H>_b$, boundary mean hydrophobicity; IDP, intrinsically disordered protein; I_{PMG}, premolten globule-like intermediate state; IUP, intrinsically unordered protein; MRE, mean residue ellipticity; N_{EC}, random coil native state; Pa-2, *Phytolacca americana* lectin-2; PWM, pokeweed mitogen; R_h, hydrodynamic radii; R_s, Stokes radius; RLS, Rayleigh light scattering; U_D, GdmCl-induced unfolded state.

[1] To whom any correspondence should be addressed (email rizwanhkhan@hotmail.com and rizwanhkhan1@yahoo.com).